

*University of Misan*  
*College of Science*  
*Department of Chemistry*



***Synthesis, Molecular Docking and Biological Activity***  
***Evaluation of some Novel Indole-Bearing Triazoles***

*A thesis*

*Presented to the College of Science\University of Misan*  
*in fulfillment of the thesis Requirement for the Degree of Master of Science*  
*in*  
*Chemistry*

***By***

***Zainab Mohammad Khalid***

*B. Sc. Chemistry / University of Misan (2018-2019)*

***Supervisor***

***Asst. Prof. Dr. Usama Ali Muhsen***

***2026***

بِسْمِ اللَّهِ الرَّحْمَنِ الرَّحِيمِ

﴿وَمَا يَعْقُبُهَا إِلَّا الْعَالَمُونَ﴾

(العنكبوت- الآية ٤٣)

## Supervisor Certificate

I am the supervisor of Zainab Mohammad Khalid. I certify that the thesis (**Synthesis, Molecular Docking and Biological Activity Evaluation of some Novel Indole-Bearing Triazoles**) was carried out and written under my supervision as a fulfillment of the requirement for the master's degree of science in chemistry.

Signature: \_\_\_\_\_

**Asst. Prof. Dr. Usama Ali Muhsen**

College of Science

University of Misan

Date: \_\_\_ / \_\_\_ / 2026

## Head of Chemistry Department Recommendation

According to the recommendation of the supervisor, this thesis is forwarded to the examination committee for approval.

Signature: \_\_\_\_\_

**Asst. Prof. Dr. Mohammed Abdul Raheem Saeed**

Head of Chemistry Department

College of Science

University of Misan

Date: \_\_\_ / \_\_\_ / 2026

## ***Acknowledgements***

*All praise is due to Allah, the Lord of the worlds. By His grace and guidance, I have completed this thesis. I ask Allah to make this work beneficial and a source of useful knowledge.*

*I would like to express my sincere gratitude and appreciation to my supervisor, Assistant Professor Dr. Usama Ali Muhsen, for the continuous guidance, encouragement, and support he provided throughout the duration of this research. His valuable advice and scientific expertise played a significant role in the successful completion of this work.*

*My sincere appreciation goes to my colleagues in the laboratory and everyone who provided scientific advice or technical assistance; their cooperation significantly contributed to the progress of this study.*

*Finally, I want to express my sincere gratitude and appreciation to my beloved family for their unwavering patience, encouragement, and ongoing support throughout my years of study. They have consistently been a source of strength and inspiration for me.*

# Contents

Acknowledgements.....	I
List of tables.....	IV
List of Schemes.....	IV
List of Figures.....	VI
Abbreviations.....	IX
Abstract.....	XI
<b>1. Introduction.....</b>	<b>1</b>
<b>1.1. Triazole.....</b>	<b>1</b>
<b>1.2. Triazole-3-thione.....</b>	<b>2</b>
<b>1.2.1. Synthesis of 4-amino-1,2,4-triazole-3-thiones.....</b>	<b>3</b>
<b>1.2.1.1. From thiocarbohydrazide.....</b>	<b>3</b>
<b>1.2.1.2. From carboxylic acid hydrazides.....</b>	<b>4</b>
<b>1.2.1.3. From 1,3,4-oxadiazol-5-thiones.....</b>	<b>5</b>
<b>1.2.2. Reactions of 4-amino-1,2,4-triazole-3-thiones.....</b>	<b>6</b>
<b>1.2.2.1. Synthesis of Schiff Bases.....</b>	<b>6</b>
<b>1.2.2.2. Alkylation of 4-amino-4H-1,2,4-triazol-3-thione.....</b>	<b>6</b>
<b>1.2.2.3. Synthesis of triazolothiadiazoles.....</b>	<b>7</b>
<b>1.2.2.4. The Synthesis of triazolothiadiazines.....</b>	<b>8</b>
<b>1.3. Biological importance of triazole and triazole-thione.....</b>	<b>9</b>
<b>1.4. Indole.....</b>	<b>11</b>
<b>1.4.1. Reactions of indole.....</b>	<b>15</b>
<b>1.4.1.1. Electrophilic substitution reaction.....</b>	<b>15</b>
<b>1.4.1.2. Oxidation of indole.....</b>	<b>18</b>
<b>1.4.1.3. Aminoalkylation (The Mannich Reaction).....</b>	<b>18</b>
<b>1.4.2. Biological importance of indole.....</b>	<b>19</b>
<b>1.4.2.1. Indole as anticancer.....</b>	<b>19</b>
<b>1.4.2.2. Indole as an antiviral agent.....</b>	<b>20</b>
<b>1.4.2.3. Indole as antimicrobial.....</b>	<b>21</b>
<b>1.4.2.4. Indole as an antioxidant.....</b>	<b>21</b>

1.4.2.5 Indole as an anti-diabetic agent.....	22
1.5. Schiff bases.....	23
1.5.1. Synthesis methods of Schiff bases .....	24
1.5.1.1. Reaction of aldehydes and ketones with primary amines.....	24
1.5.1.2. Reaction of organometallic compounds with nitriles .....	25
1.5.1.3. Reaction of phenols and phenol ethers with nitriles .....	25
1.5.2. Miscellaneous reactions of Schiff Bases.....	26
1.6. Molecular docking.....	28
1.6.1 Tryptophan 2,3-dioxygenase (TDO2) .....	29
1.7. Study aims.....	30
2. Experimental.....	31
2.1. Chemical Materials.....	31
2.2. Instruments.....	32
2.3. Synthetic Methods.....	33
2.3.1. Synthesis of thiocarbohydrazide (A).....	33
2.3.2. Synthesis of 4-amino-5-methyl-2,4-dihydro-3H-1,2,4-triazole-3-thione (B).....	34
2.3.3. Synthesis of Schiff Bases (C1-C11).....	34
2.4. Biological activity .....	37
2.4.1. Anticancer Activity .....	37
2.4.2. Antibacterial Activity .....	38
2.5. Molecular Docking Studies .....	39
3. Results and Discussion .....	40
3.1. Thiocarbohydrazide(A) .....	40
3.1.1. The synthetic strategy .....	40
3.1.2. The proposed mechanism.....	40
3.2. 4-amino-5-methyl-2,4-dihydro-1H-1,2,4-triazole-3-thione (B).....	41
3.2.1. The synthetic strategy .....	41
3.2.2. The proposed mechanism.....	42
3.2.3. Spectroscopic characterization of 4-amino-5-methyl-2,4-dihydro-3H-1,2,4-triazole-3-thione (B).....	43

<b>3.3. Schiff Bases (C1-C11)</b> .....	45
<b>3.3.1. The synthetic strategy</b> .....	45
<b>3.3.2. The proposed mechanism</b> .....	46
<b>3.3.3. Spectroscopic characterization of Schiff bases (C1-C11)</b> .....	48
<b>3.4. Attempted Synthesis of <math>\beta</math>-Lactam Derivative</b> .....	78
<b>3.4. Biological activity</b> .....	79
<b>3.4.1. The cytotoxic activity of the synthesized compounds (C1-C11)</b> .....	79
<b>3.4.2. Antibacterial activity</b> .....	91
<b>3.5. Molecular Docking Studies</b> .....	93
<b>3.6. Conclusions</b> .....	104
<b>3.7. Recommendations</b> .....	105
<b>REFERENCES</b> .....	106

## List of tables

<b>Table 2.1:</b> The chemicals used in the study.....	31
<b>Table 2.2:</b> Physical properties of thiocarbohydrazid (A) .....	33
<b>Table 2.3:</b> Physical properties of 4-amino-3-methyl-4,5-dihydro-1H-1,2,4-triazole-5-thione (B) .....	34
<b>Table 2.4:</b> Physical properties of Schiff bases(C1-C2).....	35
<b>Table 3.1:</b> In vitro anticancer screening of the compound(C1-C11) .....	79
<b>Table 3.2:</b> Growth inhibition (%) of HepG2 cells at different concentrations.....	80
<b>Table 3.3:</b> Molecular docking results of compounds (C1-C11) .....	94

## List of Schemes

<b>Scheme 1.1:</b> Tautomer forms of triazole. ....	2
<b>Scheme 1.2:</b> Thione-thiol tautomeric forms .....	3
<b>Scheme 1.3:</b> Synthesis of 4-amino 4H-1,2,4-trizole-3-thiones from carboxylic acids .....	3
<b>Scheme 1.4:</b> Reaction of thiocarbohydrazide with lactones.....	4
<b>Scheme 1.5:</b> Reaction of thiocarbohydrazide with esters .....	4
<b>Scheme 1.6:</b> Synthesis of triazole From Carboxylic Acid Hydrazides .....	5
<b>Scheme 1.7:</b> Synthesis of triazole from 1,3,4-Oxadiazol-3-thiones.....	5

<b>Scheme 1.8:</b> Synthesis of azomethine. ....	6
<b>Scheme 1.9:</b> Alkylation of the triazole .....	6
<b>Scheme 1.10:</b> Alkylation of the triazole .....	7
<b>Scheme 1.11:</b> N-acylation of the triazole. ....	7
<b>Scheme 1.12:</b> Synthesis of Triazolothiadiazoles .....	8
<b>Scheme 1.13:</b> Synthesis of Triazolothiadiazines .....	8
<b>Scheme 1.14:</b> The first synthesis of indole.....	13
<b>Scheme 1.15:</b> Tautomeric structures of the indole ring.....	13
<b>Scheme 1.16:</b> possible regioisomers in the electrophilic attack.....	14
<b>Scheme 1.17:</b> Nitration of the indole.....	16
<b>Scheme 1.18:</b> Sulfonation of indole. ....	16
<b>Scheme 1.19:</b> Friedel–Crafts Alkylation .....	16
<b>Scheme 1.20:</b> The Vilsmeier–Haack reaction. ....	17
<b>Scheme 1.21:</b> Fluorination of indole. ....	17
<b>Scheme 1.22:</b> Iodination and bromination of indole .....	17
<b>Scheme 1.23:</b> Oxidation of indole.....	18
<b>Scheme 1.24:</b> Oxidative cleavage of the indole. ....	18
<b>Scheme 1.25:</b> The Mannich Reaction of indole.. ....	19
<b>Scheme 1.26:</b> Synthesis of Schiff bases.. ....	24
<b>Scheme 1.27:</b> Addition of organometallic reagents to nitriles.. ....	25
<b>Scheme 1.28:</b> Reaction of phenol with nitriles.....	25
<b>Scheme 1.29:</b> Synthesis of azetidine .....	26
<b>Scheme 1.30:</b> Synthesis of thiazolidine.....	26
<b>Scheme 1.31:</b> synthesis of Hydroquinoline.....	27
<b>Scheme 3.1:</b> Synthesis of thiocarbohydrazide (A).. ....	40
<b>Scheme 3.2:</b> The proposed mechanism of the synthesis of thiocarbohydrazide (A) .....	41
<b>Scheme 3.3:</b> Synthesis of 4-amino-5-methyl-3 <i>H</i> -1,2,4-triazole-3-thione (B).....	41
<b>Scheme 3.4:</b> The proposed mechanism of Synthesis 4-amino-5-methyl-3 <i>H</i> -1,2,4- triazole-3-thione (B).....	42
<b>Scheme 3.5:</b> Synthesis of schiff bases (C1-C11).....	46
<b>Scheme 3.6:</b> The proposed mechanism of the Synthesis of Schiff bases.....	47
<b>Scheme 3.7:</b> Attempted Synthesis of $\beta$ -Lactam.....	77

## List of Figures

<b>Figure 1.1:</b> Two isomer forms of triazole..	1
<b>Figure 1.2:</b> Some of the triazole possessing drugs.	9
<b>Figure 1.3:</b> Ribavirin	10
<b>Figure 1.4:</b> Some of the triazole possessing aromatase inhibitors.	10
<b>Figure 1.5:</b> Prothioconazole	11
<b>Figure 1.6:</b> The chemical structure of the indole ring.	11
<b>Figure 1.7:</b> Structures of indole-containing natural products.	12
<b>Figure 1.8:</b> Numbering of the indole system.	15
<b>Figure 1.9:</b> Natural indole alkaloids used as anticancer agents.	20
<b>Figure 1.10:</b> Indole derivatives as antiviral agents.	20
<b>Figure 1.11:</b> Indole derivatives as Antimicrobial.	21
<b>Figure 1.12:</b> Indole Derivatives as Antioxidants.	22
<b>Figure 1.13:</b> Indole derivatives as anti-diabetic.	22
<b>Figure 1.14:</b> General structure of Schiff base.	23
<b>Figure 1.15:</b> Crystal Structure of human Tryptophan 2,3-dioxygenase.	29
<b>Figure 3.1:</b> IR Spectrum of the compound B.	44
<b>Figure 3.2:</b> <sup>1</sup> H NMR Spectrum of the compound B.	44
<b>Figure 3.3:</b> <sup>13</sup> C NMR Spectrum of the compound B.	45
<b>Figure 3.4:</b> IR Spectrum of the compound C1.	54
<b>Figure 3.5:</b> <sup>1</sup> H NMR Spectrum of the compound C1.	54
<b>Figure 3.6:</b> <sup>13</sup> C NMR Spectrum of the compound C1.	55
<b>Figure 3.7:</b> HSQC Spectrum of the compound C1	55
<b>Figure 3.8:</b> Mass Spectrum (ESI) of the compound C1	56
<b>Figure 3.9:</b> IR Spectrum of the compound C2.	56
<b>Figure 3.10:</b> <sup>1</sup> H NMR Spectrum of the compound C2.	57
<b>Figure 3.11:</b> <sup>13</sup> C NMR Spectrum of the compound C2.	57
<b>Figure 3.12:</b> Mass Spectrum (ESI) of the compound C2	58
<b>Figure 3.13:</b> IR Spectrum of the compound C3.	58
<b>Figure 3.14:</b> <sup>1</sup> H NMR Spectrum of the compound C3.	59
<b>Figure 3.15:</b> <sup>13</sup> C NMR Spectrum of the compound C3.	59
<b>Figure 3.16:</b> Mass Spectrum (ESI) of the compound C3	60
<b>Figure 3.17:</b> IR Spectrum of the compound C4.	60
<b>Figure 3.18:</b> <sup>1</sup> H NMR Spectrum of the compound C4.	61
<b>Figure 3.19:</b> <sup>13</sup> C NMR Spectrum of the compound C4.	61
<b>Figure 3.20:</b> Mass Spectrum (ESI) of the compound C4	62
<b>Figure 3.21:</b> IR Spectrum of the compound C5.	62
<b>Figure 3.22:</b> <sup>1</sup> H NMR Spectrum of the compound C5.	63

<b>Figure 3.23:</b> $^{13}\text{C}$ NMR Spectrum of the compound C5.....	63
<b>Figure 3.24:</b> Mass Spectrum (ESI) of the compound C5.....	64
<b>Figure 3.25:</b> IR Spectrum of the compound C6.....	64
<b>Figure 3.26:</b> $^1\text{H}$ NMR Spectrum of the compound C6.....	65
<b>Figure 3.27:</b> $^{13}\text{C}$ NMR Spectrum of the compound C6.....	65
<b>Figure 3.28:</b> Mass Spectrum (ESI) of the compound C6.....	66
<b>Figure 3.29:</b> IR Spectrum of the compound C7.....	66
<b>Figure 3.30:</b> $^1\text{H}$ NMR Spectrum of the compound C7.....	67
<b>Figure 3.31:</b> $^{13}\text{C}$ NMR Spectrum of the compound C7.....	67
<b>Figure 3.32:</b> Mass Spectrum (ESI) of the compound C7.....	68
<b>Figure 3.33:</b> IR Spectrum of the compound C8.....	68
<b>Figure 3.34:</b> $^1\text{H}$ NMR Spectrum of the compound C8.....	69
<b>Figure 3.35:</b> $^{13}\text{C}$ NMR Spectrum of the compound C8.....	69
<b>Figure 3.36:</b> Mass Spectrum (ESI) of the compound C8.....	70
<b>Figure 3.37:</b> IR Spectrum of the compound C9.....	70
<b>Figure 3.38:</b> $^1\text{H}$ NMR Spectrum of the compound C9.....	71
<b>Figure 3.39:</b> $^{13}\text{C}$ NMR Spectrum of the compound C9.....	71
<b>Figure 3.40:</b> HSQC Spectrum of the compound C9.....	72
<b>Figure 3.41:</b> Mass Spectrum (ESI) of the compound C9.....	72
<b>Figure 3.42:</b> IR Spectrum of the compound C10.....	73
<b>Figure 3.43:</b> $^1\text{H}$ NMR Spectrum of the compound C10.....	73
<b>Figure 3.44:</b> $^{13}\text{C}$ NMR Spectrum of the compound C10.....	74
<b>Figure 3.45:</b> Mass Spectrum (ESI) of the compound C10.....	74
<b>Figure 3.46:</b> IR Spectrum of the compound C11.....	75
<b>Figure 3.47:</b> $^1\text{H}$ NMR Spectrum of the compound C11.....	75
<b>Figure 3.48:</b> $^{13}\text{C}$ NMR Spectrum of the compound C11.....	76
<b>Figure 3.49:</b> Mass Spectrum (ESI) of the compound C11.....	76
<b>Figure 3.50:</b> MTT image of compound C1 against HepG2 cells.....	84
<b>Figure 3.51:</b> MTT image of compound C2 against HepG2 cells.....	84
<b>Figure 3.52:</b> MTT image of compound C3 against HepG2 cells.....	85
<b>Figure 3.53:</b> MTT image of compound C4 against HepG2 cells.....	85
<b>Figure 3.54:</b> MTT image of compound C5 against HepG2 cells.....	86
<b>Figure 3.55:</b> MTT image of compound C6 against HepG2 cells.....	86
<b>Figure 3.56:</b> MTT image of compound C7 against HepG2 cells.....	87
<b>Figure 3.57:</b> MTT image of compound C8 against HepG2 cells.....	87
<b>Figure 3.58:</b> MTT image of compound C9 against HepG2 cells.....	88
<b>Figure 3.59:</b> MTT image of compound C10 against HepG2 cells.....	88
<b>Figure 3.60:</b> MTT image of compound C11 against HepG2 cells.....	89
<b>Figure 3.61:</b> MTT image of compound doxorubicin against HepG2 cells.....	89

<b>Figure 3.62:</b> Graph illustrating the MIC values of (C1-C11) against <i>Escherichia coli</i> and <i>Staphylococcus aureus</i> .....	91
<b>Figure 3.63:</b> Images of MIC produced by C1-C11 against <i>Escherichia coli</i> and <i>Staphylococcus aureus</i> .....	92
<b>Figure 3.64:</b> Binding mode of compound C1 with TDO2 and its 2D schematic interaction.....	97
<b>Figure 3.65:</b> Binding mode of compound C2 with TDO2 and its 2D schematic interaction.....	97
<b>Figure 3.66:</b> Binding mode of compound C3 with TDO2 and its 2D schematic interaction.....	98
<b>Figure 3.67:</b> Binding mode of compound C4 with TDO2 and its 2D schematic interaction.....	98
<b>Figure 3.68:</b> Binding mode of compound C5 with TDO2 and its 2D schematic interaction.....	99
<b>Figure 3.69:</b> Binding mode of compound C6 with TDO2 and its 2D schematic interaction.....	99
<b>Figure 3.70:</b> Binding mode of compound C7 with TDO2 and its 2D schematic interaction.....	100
<b>Figure 3.71:</b> Binding mode of compound C8 with TDO2 and its 2D schematic interaction.....	100
<b>Figure 3.72:</b> Binding mode of compound C9 with TDO2 and its 2D schematic interaction.....	101
<b>Figure 3.73:</b> Binding mode of compound C10 with TDO2 and its 2D schematic interaction.....	101
<b>Figure 3.74:</b> Binding mode of compound C11 with TDO2 and its 2D schematic interaction.....	102
<b>Figure 3.75:</b> Binding mode of compound 3-(5-fluoro-1H-indol-3-yl)pyrrolidine-2,5-dione with TDO2 and its 2D schematic interaction .....	102

## Abbreviations

AcOH	Acetic acid
CS <sub>2</sub>	carbon disulfide
°C	Degrees Celsius
conc.	Concentrated
CLSI	Clinical Laboratory Standards Institute
DCM	Dichloromethane
DEPT	Distortionless Enhancement by polarization Transfer
DFT	Density Functional Theory
DMF	N, N-dimethylformamide
DMSO	Dimethyl sulfoxide
DIM	Diindolylmethane
<i>E.coli</i>	<i>Escherichia coli</i>
EtOAc	Ethyl acetate
Et <sub>3</sub> N	Triethylamine
EtOH	Ethanol
FTIR	Fourier Transform Infra-Red spectrophotometer
g	Gram
5-HT	5-hydroxytryptamine (serotonin)
h	Hour
Hz	Hertz
HRMS	High-Resolution Mass Spectra
HSQC	Heteronuclear single quantum coherence spectroscopy
J	Coupling constant
IC <sub>50</sub>	Half-maximal inhibitory concentration
IAA	Indole-3-acetic acid
MeOH	Methanol

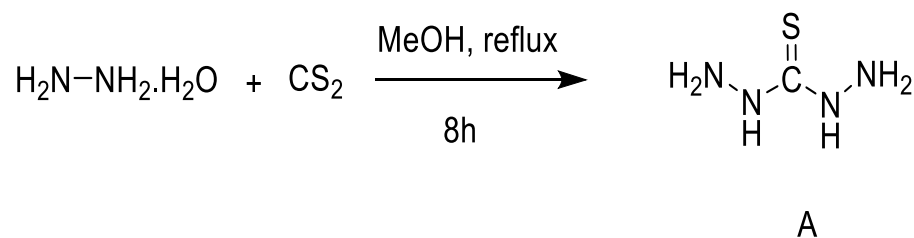
m.p	Melting point
min	Minute
MTT	3-(4,5-dimethylthiazol-2-yl)-2,5-diphenyltetrazolium bromide
MIC	Minimum inhibitory concentration
MHB	Mueller–Hinton broth
NMR	Nuclear Magnetic Resonance spectrometer
PDB	Protein Data Bank
PBS	phosphate- buffered saline
PPAR $\alpha$	Peroxisome proliferator-activated receptor
<i>S. aureus</i>	<i>Staphylococcus aureus</i>
TDO2	Tryptophan 2,3-dioxygenase
THF	Tetrahydrofuran
TLC	Thin-layer chromatography
r.t.	room temperature
$\delta$	Chemical shift

## Abstract

The study focuses on the synthesis, characterization, and biological evaluation of novel indole-bearing triazole-3-thione derivatives. The study is organized into five main parts as outlined below.

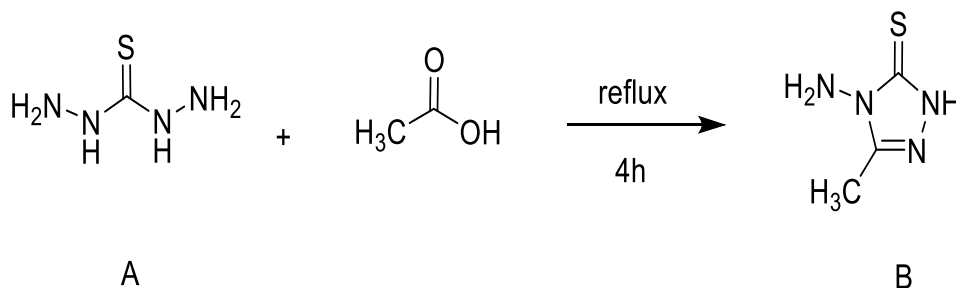
### Part One:

Included the preparation of thiocarbohydrazide (A), which was obtained through the reaction of hydrazine hydrate (80%) with carbon disulfide ( $\text{CS}_2$ ) in methanol under reflux conditions, followed by simple workup, affording a good yield (83%).



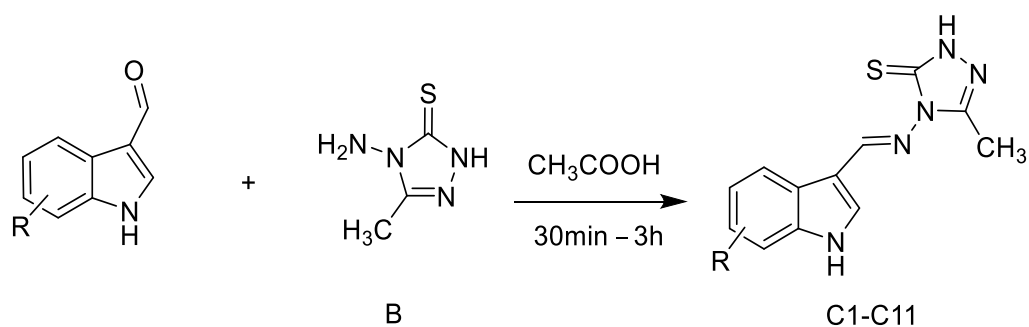
### Part Two:

This part involved the synthesis of 4-amino-5-methyl-1,2,4-dihydro-3H-1,2,4-triazole-3-thione (B) via cyclization of thiocarbohydrazide (A), which had been previously prepared in Part One, with glacial acetic acid under reflux conditions. The resulting product was then recrystallized, affording a moderate yield (44.8%). The structure of the compound was confirmed using FTIR,  $^1\text{H}$  NMR, and  $^{13}\text{C}$  NMR spectroscopy.



### Part Three:

This part included the reaction of 4-amino-5-methyl-2,4-dihydro-3H-1,2,4-triazole-3-thione (B) with various substituted indole-3-carboxaldehyde under reflux and acidic conditions by using glacial acetic acid as solvent to synthesize Schiff base compounds (C1-C11) in good yields (48-98%) for a short time. The structures of compounds were confirmed by FTIR, <sup>1</sup>HNMR, <sup>13</sup>CNMR and HRMS spectroscopy.



### Part Four

The synthesized compounds (C1-C11) were evaluated for their anticancer activity against hepatocellular carcinoma cells (hepG2) cell lines, where they exhibited weak activity compared to the standard anticancer drug (doxorubicin), which exhibited strong cytotoxic activity.

In addition, the antibacterial activity was evaluated using the MIC assay against *Staphylococcus aureus* and *Escherichia coli*. The tested compounds exhibited weak antibacterial effects, with MIC values ranging from 1000 to 2000  $\mu\text{M}$ .

## **Part Five**

Molecular docking studies were performed using PyRx software (version 0.8), which utilizes AutoDock Vina as the docking engine, and PyMOL software (version 3.1.6.1) was used for protein preparation and visualization.

To investigate the binding affinity of the synthesized compounds toward tryptophan 2,3-dioxygenase (TDO2), which is considered a key enzyme in the kynurenine pathway, primarily expressed in the liver, where it regulates tryptophan metabolism. It is also considered an important target for cancer therapy due to its role in tumor immune evasion and progression. The docking results demonstrated favorable binding scores and strong interactions consistent with the observed biological activity.

# CHAPTER ONE

# 1. Introduction

## 1.1. Triazole

Triazole is a heterocyclic organic compound consisting of two carbon atoms and three nitrogen atoms arranged in a five-member aromatic ring, with the formula  $C_2H_3N_3$ . Triazole rings are not found in nature yet, all known triazoles are synthetic.<sup>1</sup> Triazole ring systems are among the heterocycles that have drawn a lot of interest because of their uses as agrochemicals in industry, medicine, and agriculture.<sup>2-4</sup> There are two isomeric forms of the triazoles: 1,2,3-triazole (1) and the 1,2,4-triazole (2). 1,2,4-triazole rings derivatives play a significant role in chemistry and exhibit a wide range of applications<sup>5</sup> (Figure 1.1).

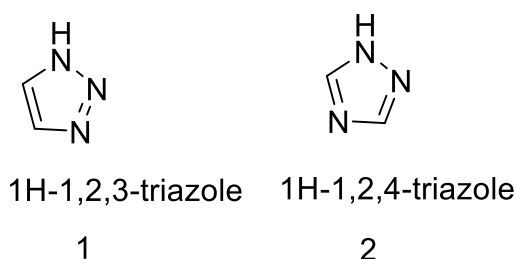
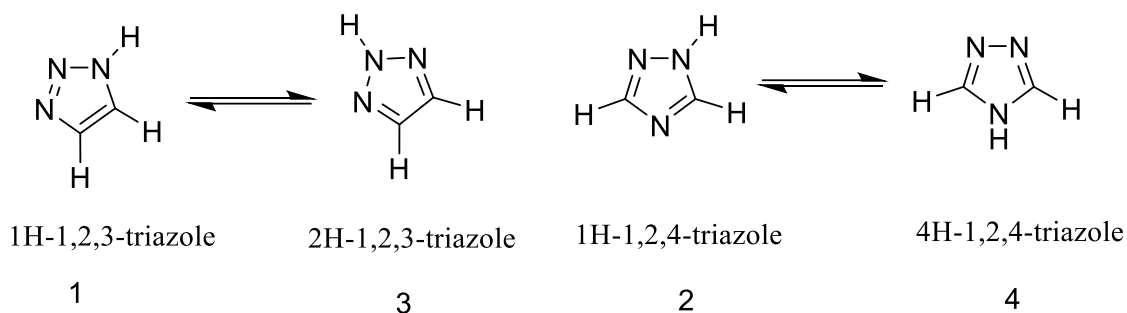


**Figure 1.1: Two isomer forms of triazole**

In 1885, Bladin first introduced the term (triazole) to describe the carbon-nitrogen ring structure ( $C_2N_3H_3$ ) and detailed its derivatives.<sup>6</sup> The stability of the triazole ring is mainly attributed to its aromaticity, which arises from the presence of six delocalized  $\pi$ -electrons satisfying Hückel's rule. These electrons are contributed by the atoms involved in the double bonds, along with a lone pair from one of the nitrogen atoms.<sup>7</sup> Furthermore, triazoles exhibit resonance, allowing them to exist in different tautomeric forms.<sup>8</sup> 1,2,3-Triazoles and 1,2,4-Triazoles have tautomeric structures, namely 1H-1,2,3-triazole (1) and 2H-1,2,3-triazole (3),<sup>9</sup> 1H-1,2,4-triazole (2) and 4H-1,2,4-triazole (4).<sup>10</sup> Numerous studies have shown that tautomer 1H-1,2,4-triazole (2) is more stable<sup>11</sup> (Scheme 1.1).



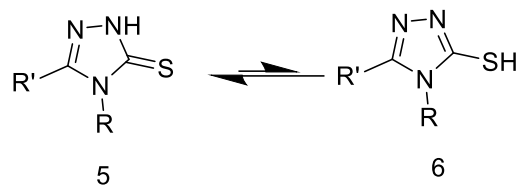
**Scheme 1.1: Tautomer forms of triazole**

1,2,4-triazole may impact hydrogen bonding and polarity of molecules, improving their toxicological and pharmacological properties. Physicochemical and pharmacokinetic characteristics of substances.<sup>12</sup> Triazole's three nitrogen atoms offer excellent coordination with metal ions.<sup>13</sup>

## 1.2. Triazole-3-thione

Triazole-thione derivatives represent an important class of heterocyclic compounds that have attracted considerable attention due to their diverse structural features and promising biological activities. Incorporation of a thione group at the 3- position of the triazole ring has been frequently reported to enhance the biological properties associated with the triazole scaffold.<sup>14</sup> Furthermore, the triazolethione system is considered a cyclic analogue of key functional groups such as thiosemicarbazides and thiocarbohydrazides, which are extensively employed as reactive building blocks in numerous organic transformations, leading to the formation of various heterocyclic frameworks with notable biological activities. The presence of three nucleophilic centers in 1,2,4-triazole-3-thione, the exocyclic sulfur atom and the endocyclic nitrogen atoms (N<sub>1</sub>, N<sub>2</sub>, and N<sub>4</sub>), is of considerable theoretical importance. This structural feature provides broad opportunities for designing new derivatives whose properties, including biological activity, vary depending on the nature of the substituents.<sup>15</sup> The mercapto-1,2,4-triazole core, in particular, is found in a variety of naturally occurring substances and pharmaceutical agents.<sup>16</sup>

Additionally, mercapto-1,2,4-triazole derivatives can be synthesized from natural products through specific chemical reactions aimed at obtaining the desired structures<sup>17</sup>(Scheme 1.2 ).



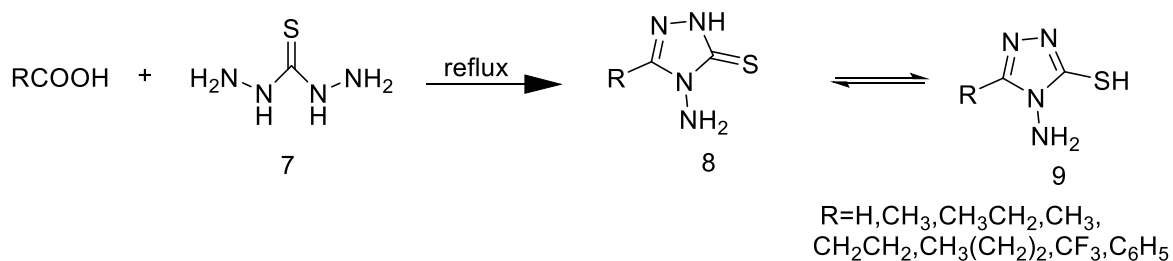
**Scheme 1.2: Thione-thiol tautomeric forms**

1,2,4-triazolethiones (5) have been prepared successfully by various methods. The most common classical method is the dehydrative cyclization of different hydrazinecarbothioamides in the presence of basic media, using various reagents such as sodium hydroxide,<sup>18-20</sup> potassium hydroxide,<sup>21,22</sup> sodium bicarbonate<sup>23</sup> or acidic ionic liquids.<sup>24</sup>

## 1.2.1. Synthesis of 4-amino-1,2,4-triazole-3-thiones

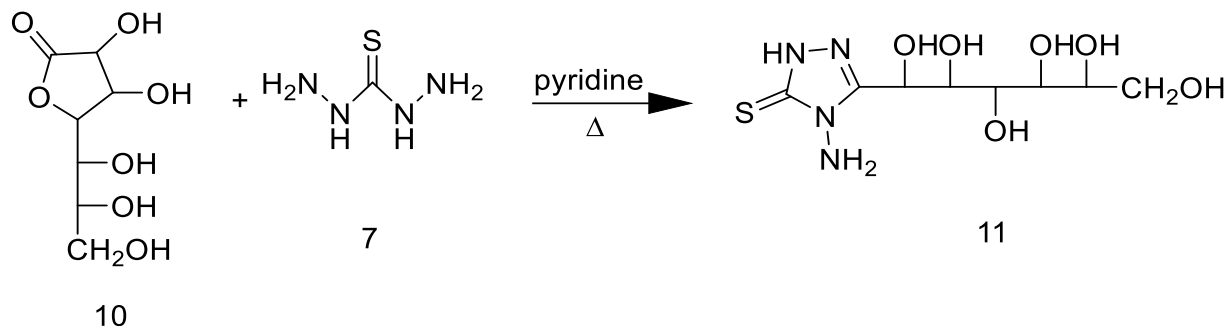
### 1.2.1.1. From thiocarbohydrazide

Substituted 4-amino-4H-1,2,4-triazole-3-thiones (8) were synthesized through the reaction of carboxylic acids with thiocarbohydrazide (7)<sup>25</sup> (Scheme 1.3).



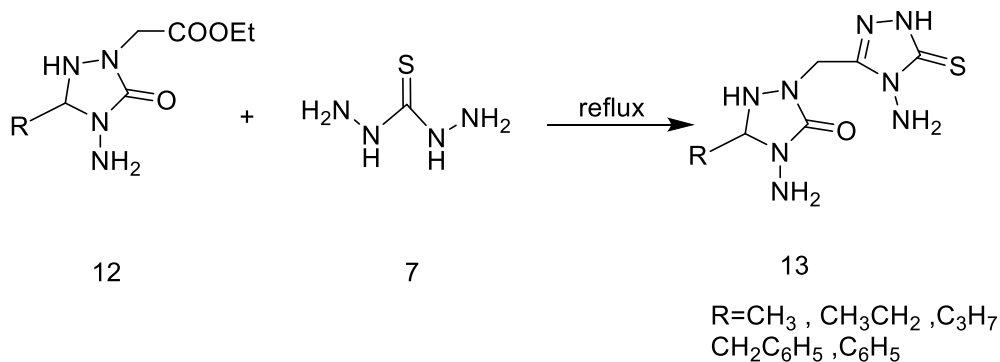
**Scheme 1.3: Synthesis of 4-amino 4H-1,2,4-triazole-3-thiones from carboxylic acids**

When 1,4-lactones (10) and thiocarbohydrazide (7) reacted, the result was (D-glycero-D-gulo-hexitol-1-yl)-1,2,4-triazol-3-thiones (11)<sup>26</sup> (Scheme 1.4).



**Scheme 1.4: Reaction of thiocarbohydrazide with lactones**

The alkyl-4-amino-2-((4-amino-5-thioxo-4,5-dihydro-1H-1,2,4-triazol-3-yl)methyl)-5-methyl-1,2,4-triazolidin-3-one (13) were prepared by refluxing thiocarbohydrazide (7) with ethyl (3-alkyl-4-amino-5-oxo-1,2,4-triazolidin-1-yl)acetate (12)<sup>27</sup> (Scheme 1.5).

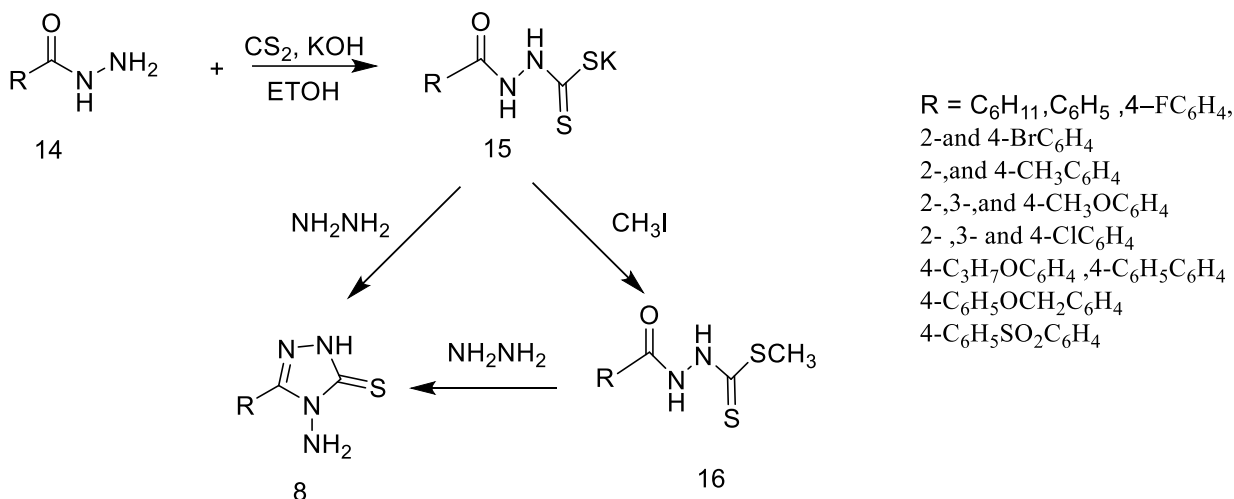


**Scheme 1.5: Reaction of thiocarbohydrazide with esters**

### 1.2.1.2. From carboxylic acid hydrazides

The Hoggarth synthesis of 5-substituted-4-amino-(4H)-1,2,4-triazol-3-thiones (8) begins with the reaction of carboxylic acid hydrazides (14), which are condensed with carbon disulfide in ethanolic potassium hydroxide to produce potassium 3-

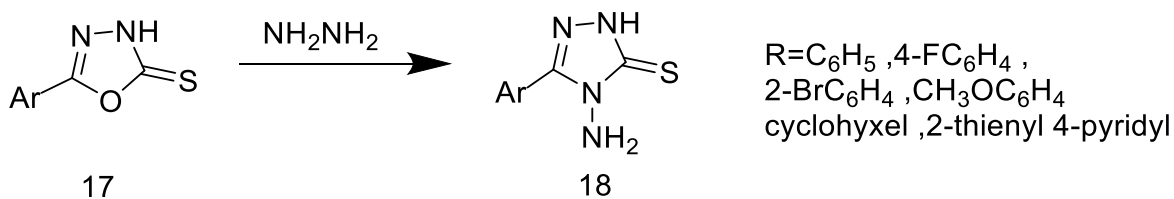
aroyldithiocarbazates (15). The methylation of these compounds with methyl iodide results in the formation of S-alkylated derivatives. These methyl 3-aryldithiocarbazates (16) undergo cyclization with hydrazine to form 4-amino-4H-1,2,4-triazol-3-thiones (8). Additionally, the salts can be directly converted to 4-amino-2,4-dihydro-1,2,4-triazol-3(3H)-thiones using an excess of hydrazine<sup>28</sup> (Scheme 1.6).



**Scheme 1.6: Synthesis of triazole From Carboxylic Acid Hydrazides.**

### 1.2.1.3. From 1,3,4-oxadiazol-5-thiones

In the quest for an effective method to convert 1,3,4-oxadiazol-3-thiones into 4-amino-1,2,4-triazol-3-thiones, it was found that this transformation could be accomplished through the reaction of the oxadiazole with hydrazine hydrate.<sup>29</sup> Reid and Heindel noted that the 5-aryl-1,3,4-oxadiazol-2(3H)-thiones (17) underwent a recyclization reaction with hydrazine hydrate, resulting in the formation of 4-amino-1,2,4-triazole-3-thiones (18)<sup>30</sup> (Scheme 1.7).

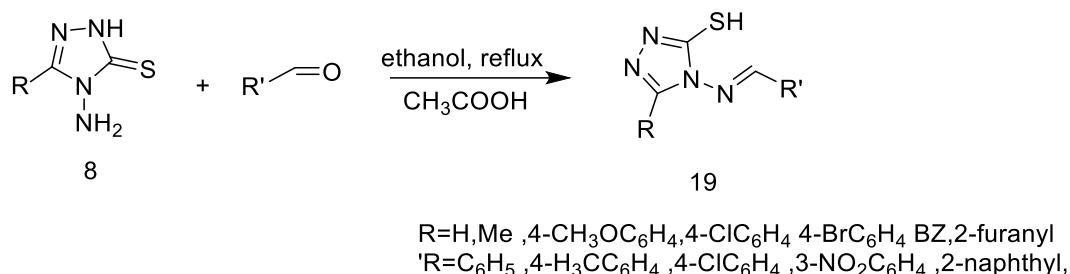


**Scheme 1.7: Synthesis of triazole from 1,3,4 -Oxadiazol-3-thiones.**

## 1.2.2. Reactions of 4-amino-1,2,4-triazole-3-thiones

### 1.2.2.1. Synthesis of Schiff Bases

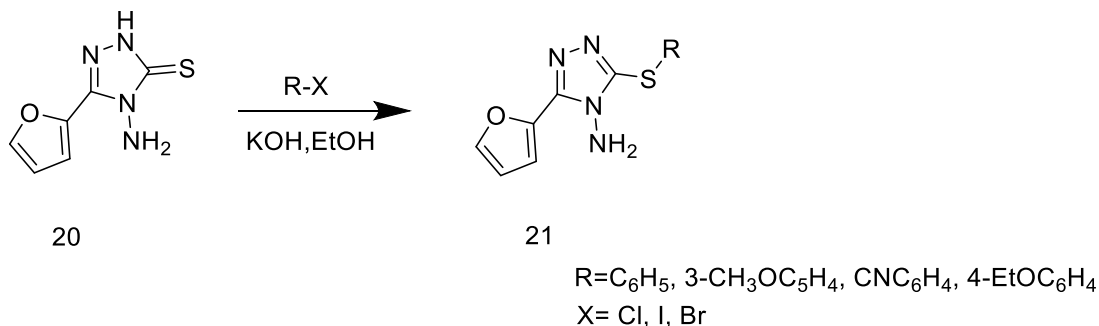
Several azomethine derivatives (19) were prepared by the condensation of 4-amino-1,2,4-triazole-3-thiones (8) with aldehydes<sup>31-33</sup> (Scheme 1.8).



**Scheme 1.8: Synthesis of azomethine**

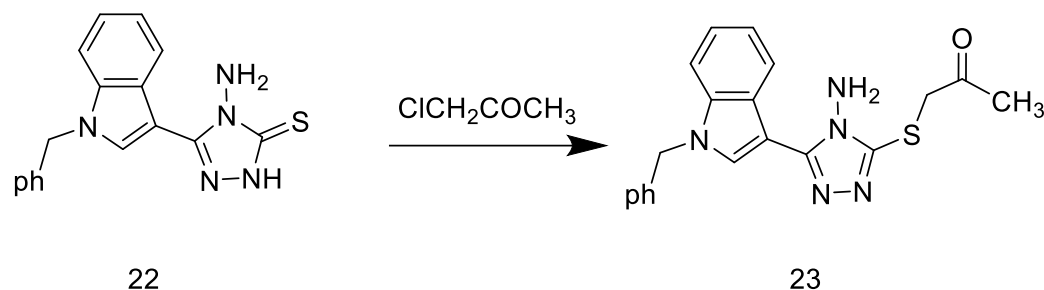
### 1.2.2.2. Alkylation of 4-amino-4H-1,2,4-triazol-3-thione

Alkylation of 4-amino-5-(furan-2-yl)-2,4-dihydro-3H-1,2,4-triazole-3-thione (20) was carried out using various alkyl halides in ethanolic potassium hydroxide solution to afford 3-alkylthio-5-(furan-2-yl)-4H-1,2,4-triazol-4-amine (21)<sup>34,35</sup> (Scheme 1.9).



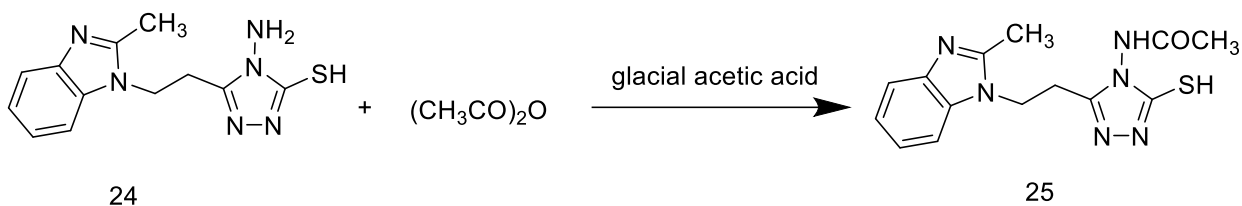
**Scheme 1.9: Alkylation of the triazole**

The reaction compound (22) with chloroacetone yielded the corresponding acetylthio derivative (23)<sup>36</sup> (Scheme 1.10).



**Scheme 1.10: Acylation of the triazole**

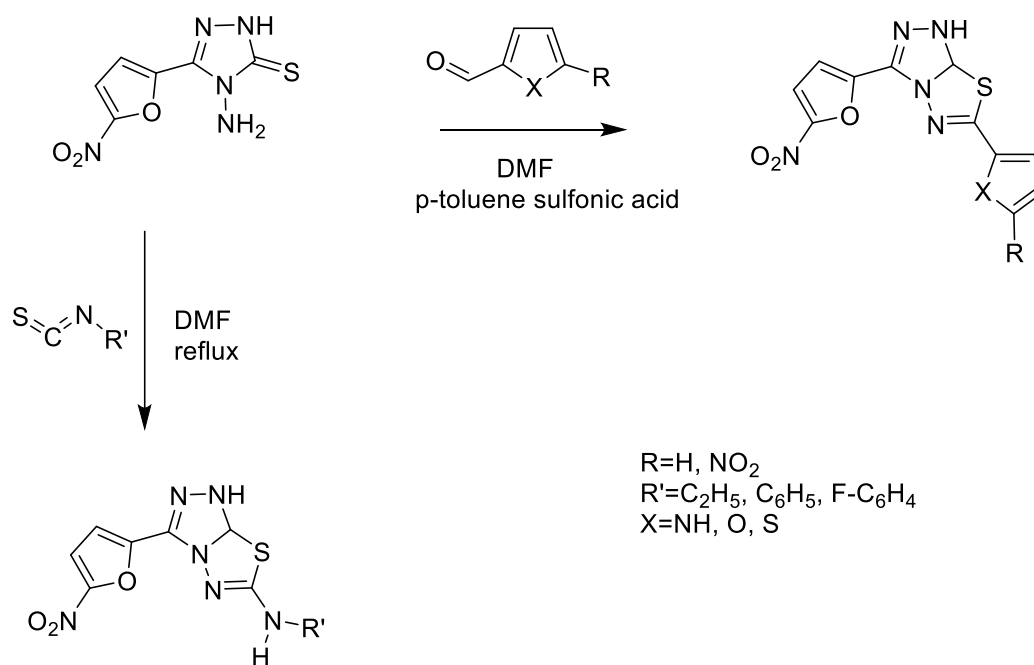
The acylation with acetic anhydride in the presence of glacial acetic acid afforded the N-acylated derivative (25)<sup>37</sup> (Scheme 1.11).



**Scheme 1.11: N-acylation of the triazole**

### 1.2.2.3. Synthesis of triazolothiadiazoles

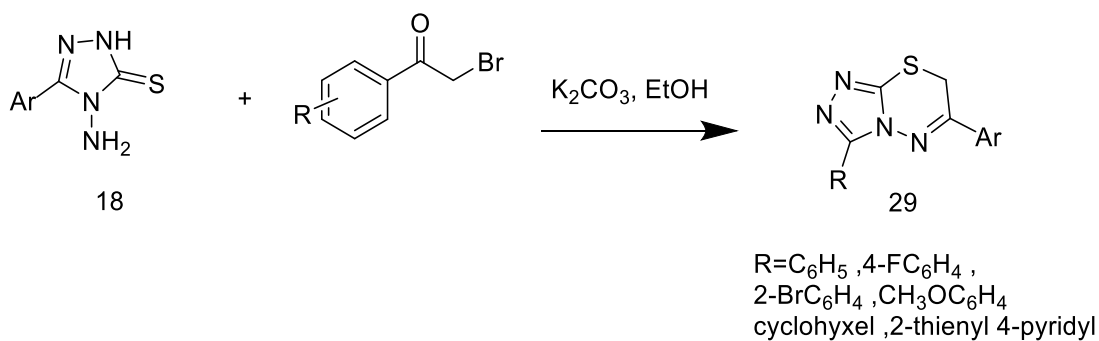
The reactivity of the triazole-thione system was further demonstrated through its condensation with heteroaromatic aldehydes and isothiocyanates. Thus, 4-amino-5-(5-nitrofur-2-yl)-2,4-dihydro-1,2,4-triazole-3(3H)-thiol (26) underwent refluxing with the appropriate heteroaromatic aldehyde in anhydrous DMF and a catalytic amount of p-toluenesulfonic acid to afford the corresponding triazolothiadiazole derivatives (27). Likewise, reaction of compound 25 with alkyl or aryl isothiocyanates in DMF under reflux to afford the corresponding triazolothiadiazole (28)<sup>38</sup> (Scheme 1.12).



**Scheme 1.12: Synthesis of triazolothiadiazoles**

#### 1.2.2.4. The Synthesis of triazolothiadiazines

It was reported on the preparation of triazolo[3,4-*b*]-1,3,4-thiadiazine (29) during the reaction of amino-triazolthione (18) with substituted phenacyl bromide<sup>39</sup> (Scheme 1.13).



**Scheme 1.13: Synthesis of triazolothiadiazines**

### 1.3. Biological importance of triazole and triazole-thione

Many 1,2,4-triazole-containing ring systems have been added to a wide range of therapeutically intriguing drug candidates, such as those with anti-inflammatory, central nervous system stimulant, sedative, antianxiety, antimicrobial, antimigraine (rizatriptan), and antimycotic properties. fluconazole, itraconazole, and voriconazole are examples of antimycotic active drugs that prevent  $14\alpha$ -demethylation, therefore inhibiting the formation of ergosterol. Additionally, certain medications, such as triazolam, alprazolam, and estazolam, are known to include the 1,2,4-triazole group. The anticonvulsant medication estazolam includes a triazolo benzodiazepine ring<sup>40</sup> (Figure 1.2).

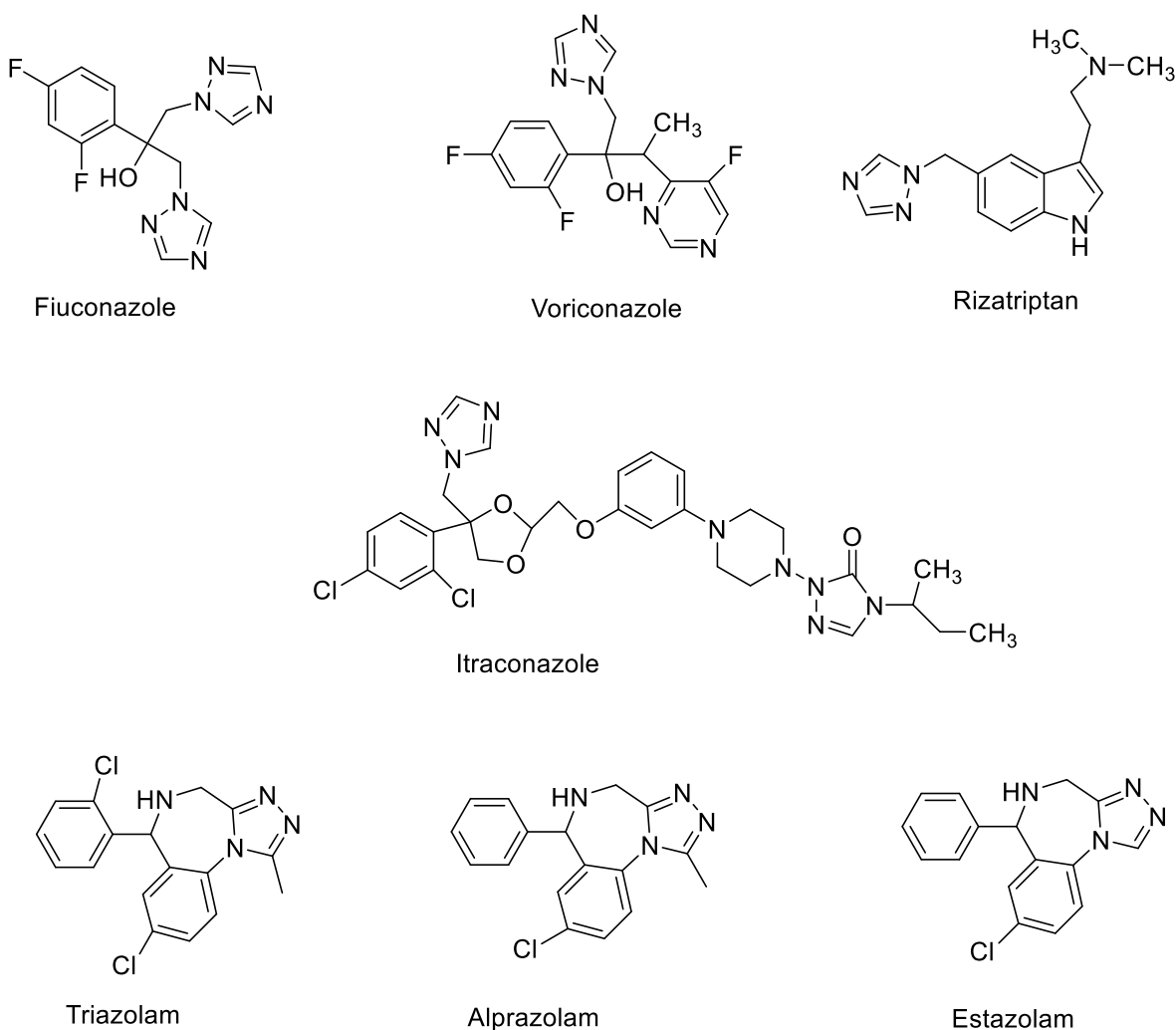


**Figure 1.2:** Some of the triazole-containing drugs.

A broad-spectrum antiviral drug with a 1,2,4-triazole ring is ribavirin (1-β-D-ribofuranosyl-1H-1,2,4-triazole-3-carboxamide). This substance is effective against viral diseases, including both DNA and RNA viruses. These days, hepatitis-C is treated with an interferon-ribavirin combination<sup>17</sup> (Figure 1.3).

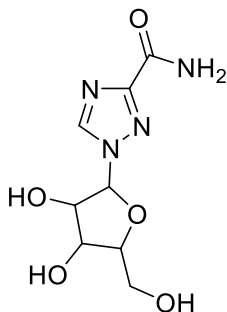


**Figure 1.3: Ribavirin**

The 1,2,4-triazole nucleus of letrozole, anastrozole, and vorozole makes them potent aromatase inhibitors<sup>41</sup> (Figure 1.4).

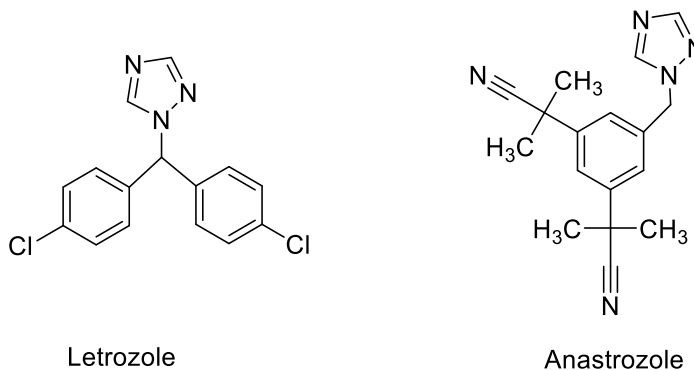


**Figure 1.4: Some of the triazole possessing aromatase inhibitors.**

In addition to these biologically important triazole derivatives, Prothioconazole represents a noteworthy example, as it is commercially available for the treatment of plant-pathogenic fungal infections<sup>42</sup> (Figure 1.5).

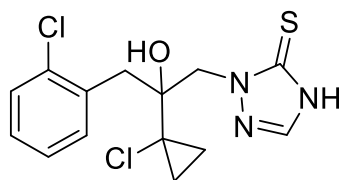
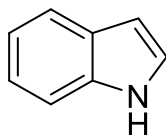


**Figure 1.5: Prothioconazole**

## 1.4. Indole

The study of heterocyclic compounds occupies a prominent place in chemistry due to their wide range of applications in medicinal chemistry, material chemistry, photochemistry, and many other fields,<sup>43</sup> and among these heterocyclic compounds, indole (30) stands out as one of the most important ring systems with broad biological significance. Indole is an organic compound with the molecular formula  $C_8H_7N$ . It comprises a six-membered benzene ring that is fused to a five-membered pyrrole ring. Containing a nitrogen atom, also known as benzo[b]pyrrole, this unique structure has established indole as a key building block in the field of medicinal chemistry due to its significant role in drug design and development<sup>44</sup> (Figure 1.6).



30

**Figure 1.6: The chemical structure of the indole ring.**

The indole core is a nearly ubiquitous structural motif in biologically active natural products. For instance, indole-3-acetic acid (IAA) is among the most prevalent naturally occurring derivatives of indole and functions as a plant hormone belonging to the auxin class.<sup>45</sup> Tryptophan, an essential amino acid, plays a crucial role in numerous biological processes.<sup>46</sup> Serotonin, commonly known as 5-hydroxy

tryptamine (5-HT), is a type of neurotransmitter. derived biochemically from tryptophan and is present in all bilaterally symmetrical animals.<sup>47</sup> Melatonin is a hormone found in animals, plants, and microorganisms; in animals, it helps regulate seasonal biological rhythms based on the duration of its daily production<sup>48</sup> (Figure 1.7).

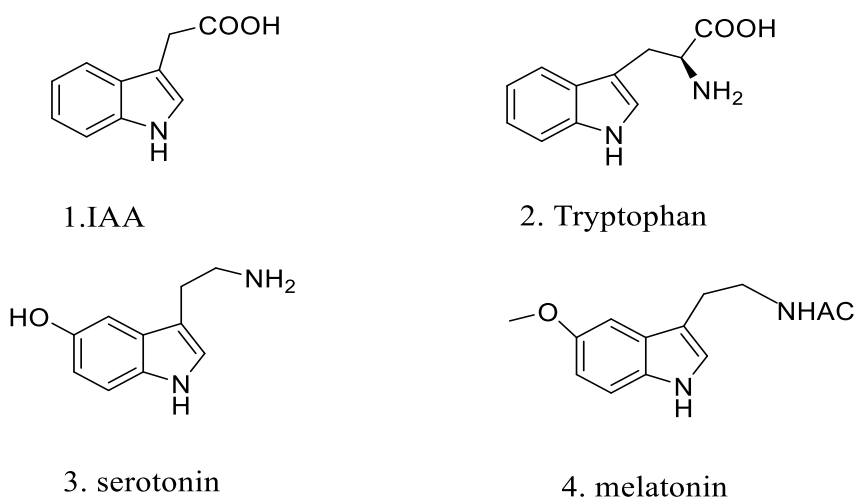
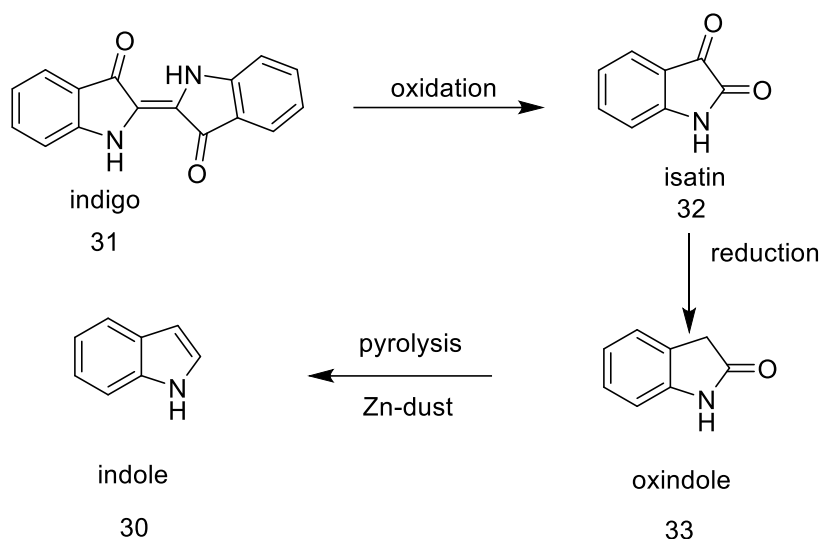


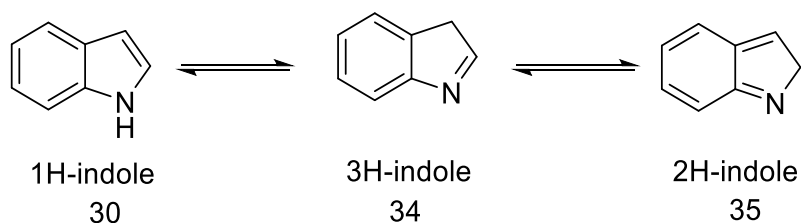
**Figure 1.7: Structures of indole-containing natural products.**

The term "indole" originates from the combination of "indigo" and "oleum," as the compound was first obtained by treating indigo dye with oleum.<sup>49</sup> Indole occurs naturally in certain floral oils, such as jasmine and orange blossom, and can also be found in coal tar. It is widely used in the perfume industry due to its distinctive aroma.<sup>50</sup> In 1886, Adolf von Baeyer successfully synthesized indole by reducing oxindole (33),<sup>51</sup> marking one of the earliest methods for obtaining this important heterocyclic compound. He began by oxidizing indigo (31) to form isatin (32), which he then reduced with zinc dust to produce dioxindole and oxindole (33). Finally, indole was obtained by passing the vapors of oxindole over heated zinc oxide, completing the multistep synthesis<sup>52</sup> (Scheme 1.14).



**Scheme 1.14: The first synthesis of indole**

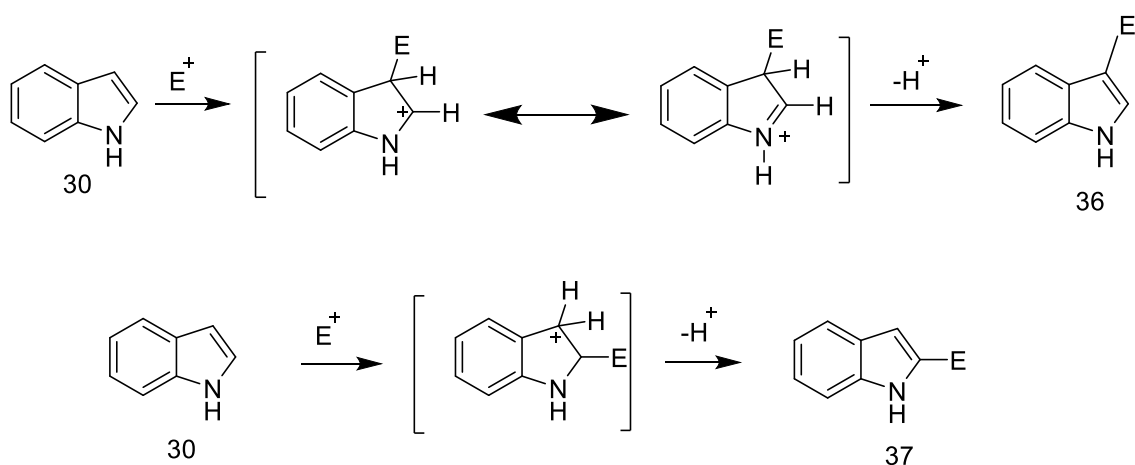
Indole is capable of existing in three different tautomeric forms 1H-indole (30), 2H-indole (35), and 3H-indole (34). These tautomeric variations can significantly affect the chemical behavior and biological activity of indole-based compounds.<sup>53</sup> high-level quantum chemical calculations based on Density Functional Theory (DFT) estimate that 1H-indole (30) is significantly more stable, with energy differences of approximately 5.20 kcal/mol compared to 3H-indole (34), and 24.1 kcal/mol relative to 2H-indole (35)<sup>54</sup> (Scheme 1.15).



**Scheme 1-15: Tautomeric structures of the indole ring.**

Indole, which contains 10  $\pi$ -electrons (8 from the double bonds and 2 from the nitrogen's lone pair), is considered aromatic according to Hückel's rule. This aromaticity arises from the delocalization of these  $\pi$ -electrons across the ring

system.<sup>55</sup> Indole is often described as an electron-rich system that exhibits significantly greater reactivity than benzene in electrophilic aromatic substitution reactions. This characteristic must always be considered when working with indole and its derivatives. While its high reactivity enables certain organic transformations that are not possible with benzene or similar arenes, careful control of reaction conditions and additives is essential to prevent unwanted poly substitution on the indole ring. Among the possible sites, the C3 position is the most reactive toward electrophilic substitution, approximately  $10^{13}$  times more reactive than benzene (Scheme 1.16).



**Scheme 1.16: Possible regioisomers in the electrophilic attack**

other positions such as N1 (with a pKa for the NH group ranging from 12.36 to 19.50 in water) and C2 should also be considered when evaluating the molecule's overall reactivity<sup>56</sup> (Figure 1.8).

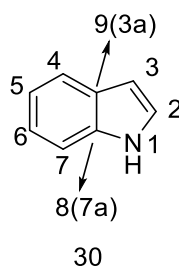


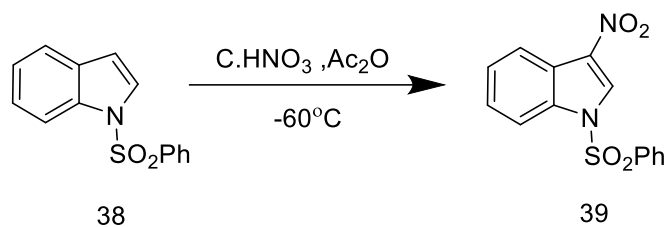
**Figure 1.8: Numbering of the indole system**

In addition to acting as a proton donor via the N–H group, the delocalized  $\pi$ -electron density across the indole scaffold contributes to an increase in its highest occupied molecular orbital (HOMO) energy level. This electronic property enhances interactions with nucleobases, especially protonated atoms, as well as with target proteins.<sup>57</sup> The indole ring can form hydrogen bonds through the N–H group and can also participate in  $\pi$ – $\pi$  stacking and cation– $\pi$  interactions due to its aromatic nature. In terms of hydrophobicity, the indole ring is comparable to a phenyl group, but less hydrophobic than similar aromatic systems like benzothiophene and benzofuran.<sup>58</sup>

## 1.4.1. Reactions of indole

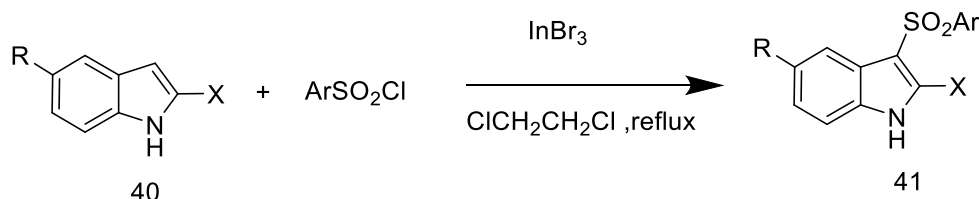
### 1.4.1.1. Electrophilic substitution reaction

**Indole nitration:** Indole can be nitrated using benzoyl nitrate as a non-acidic nitrating agent. The conventional mixed-acid nitration system typically produces intractable compounds, most likely due to acid-catalyzed polymerization. This can be avoided by performing the nitration at a low temperature with concentrated nitric acid and acetic anhydride; under these conditions, N-alkylindoles and indoles containing electron-withdrawing substituents on nitrogen can be successfully nitrated, whereas indole itself cannot<sup>59</sup> (Scheme 1.17).



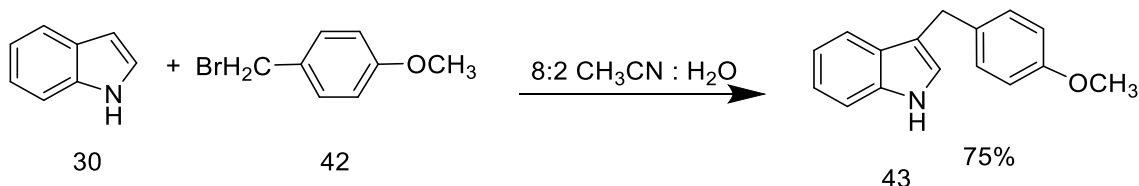
**Scheme 1.17: Nitration of the indole**

Sulfonation of indole, indoles reacted readily with sulfonyl chlorides in the presence of catalytic indium tribromide at room temperature, yielding 3-arylsulfonylindoles (41) with high regioselectivity<sup>60</sup> (Scheme 1.18).



**Scheme 1.18: Sulfonation of indole.**

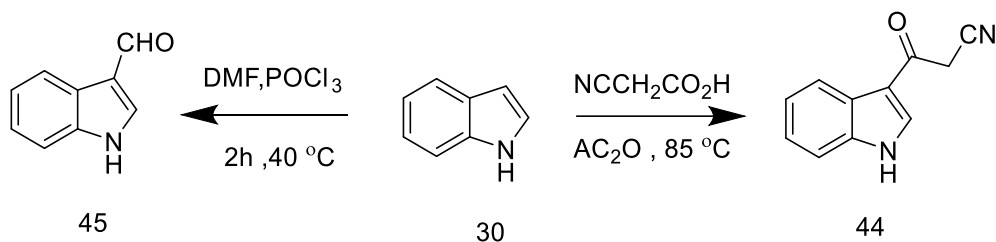
**Friedel–Crafts Alkylation:** An example of direct Alkylation (benzylation) under solvolytic conditions has been reported by Mayr and coworkers<sup>61</sup> (Scheme 1.19).



**Scheme 1.19: Friedel–Crafts Alkylation**

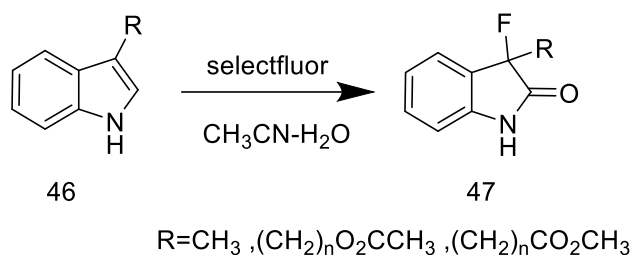
**Formylation and acylation:** The Vilsmeier–Haack reaction, which utilizes a combination of an amide and phosphorus oxychloride (POCl<sub>3</sub>), represents one of the most reliable methods for the acylation of indoles at the 3-position, the Vilsmeier–Haack conditions exhibit excellent regioselectivity toward substitution at the 3-

position, even in the presence of electron-withdrawing substituents at the C-2 position<sup>62</sup> (Scheme 1.20).



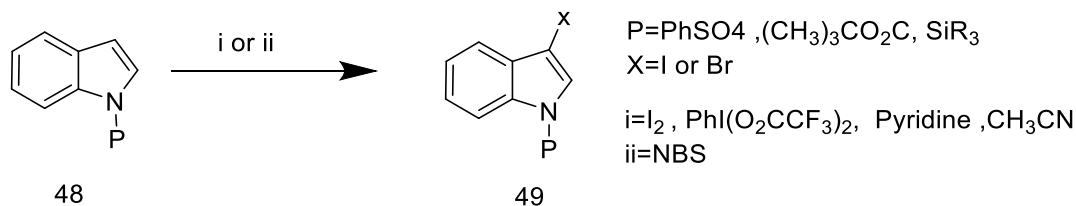
**Scheme 1.20: The Vilsmeier–Haack reaction**

**Halogenation:** Fluorination is the most recently investigated of the direct halogenation procedures, and it has become feasible with the advent of commercially accessible fluorinating chemicals such as Selectfluor<sup>63</sup> (Scheme 1.21).



**Scheme 1.21: Fluorination of indole.**

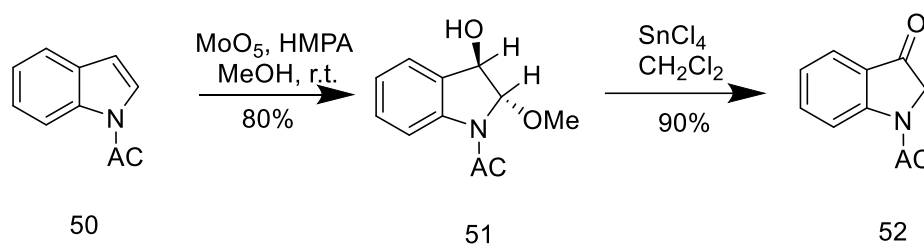
N-Protected indoles can be iodinated<sup>64</sup> and brominated by using phenyliodonium bis trifluoroacetate and brominating agents such as N-bromosuccinimide<sup>65</sup> and pyridinium bromide perbromide<sup>66</sup> (Scheme 1.22).



**Scheme 1.22: Iodination and bromination of indole.**

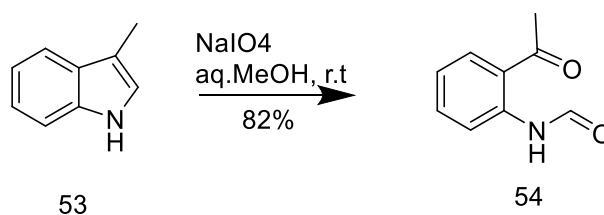
### 1.4.1.2. Oxidation of indole

The reagent  $\text{MoO}_5 \cdot \text{HMPA}$ , commonly referred to as MoOPH, facilitates the addition of methyl hydrogen peroxide to N-acylindoles (50). The resulting (51) can undergo methanol elimination, leading to the oxidative transformation of indoles into indoxyl derivatives (52). This reaction offers a convenient and efficient pathway for synthesizing indoxyl frameworks from indole precursors<sup>67</sup> (Scheme 1.23).



**Scheme 1.23: Oxidation of indole.**

Oxidative cleavage of the 2,3-double bond in indole can be accomplished using several oxidizing agents such as ozone, sodium periodate, potassium superoxide, oxygen in the presence of cuprous chloride, and photochemically in ethanolic solution<sup>68</sup> (Scheme 1.24).



**Scheme 1.24: Oxidative cleavage of the indole.**

### 1.4.1.3. Aminoalkylation (The Mannich Reaction)

The Mannich reaction, which involves the use of iminium ions as electrophiles in alkylation reactions, is a common method for the synthesis of various indole derivatives. The simple example is the reaction of indole with formaldehyde and dimethylamine to produce gramine (3-(dimethylaminomethyl)indole) (56), an essential synthetic intermediate. Depending on the reaction conditions, this method



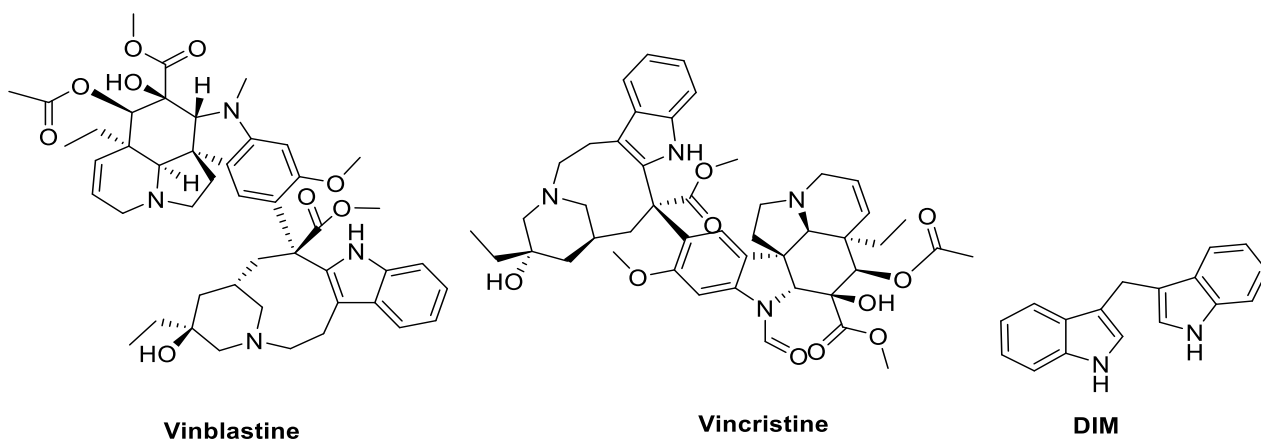


**Figure 1.9: Natural indole alkaloids used as anticancer agents**

### 1.4.2.2. Indole as an antiviral agent

Several indole-based compounds have demonstrated potent antiviral activity and have been approved for clinical use. For instance, Arbidol exhibits both immunomodulatory and antiviral effects against influenza A and B viruses, respiratory syncytial virus (RSV), and severe acute respiratory syndrome (SARS).<sup>77,78</sup> Another example is Delavirdine, a first-generation non-nucleoside reverse transcriptase inhibitor (NNRTI) approved by the FDA in 1997 for the treatment of HIV-1 infection as part of highly active antiretroviral therapy (HAART)<sup>79</sup> Similarly, Ateviridine, a heteroaryl piperazine-based NNRTI, has shown strong inhibitory effects on HIV-1 replication and syncytia formation in infected cell cultures. These findings highlight the versatility of the indole nucleus as a privileged scaffold for the<sup>80</sup> (Figure 1.10).

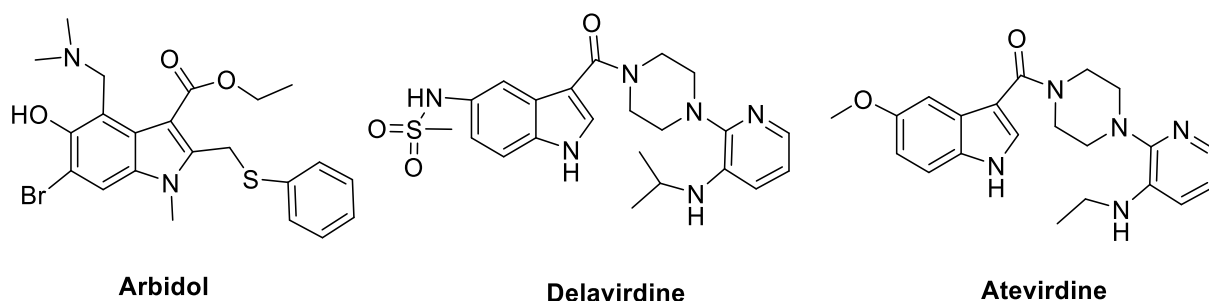


**Figure 1.10: Indole derivatives as antiviral agents.**

### 1.4.2.3. Indole as antimicrobial

New indole derivatives with different mechanisms are being investigated. Sanna et al. developed indole-thiourea hybrids that are effective against both Gram-positive and Gram-negative bacteria. Compound (57) (MIC < 12.5  $\mu\text{g/mL}$ ) showed significant efficacy compared to ciprofloxacin (MIC < 1.0  $\mu\text{g/mL}$ )<sup>81</sup>, and Compound (58) exhibited significant potency (MIC < 8  $\mu\text{g/mL}$ )<sup>82</sup> (Figure 1.11).

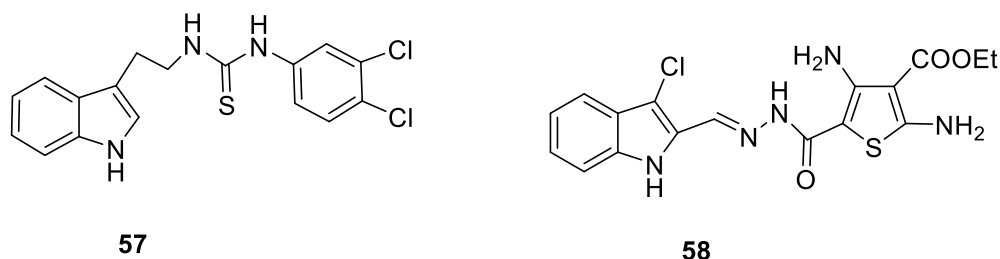


Figure 1.11: Indole derivatives as Antimicrobial

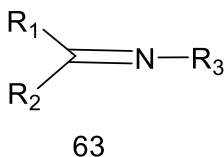
### 1.4.2.4. Indole as an antioxidant

Indole derivatives have strong antioxidant effects by protecting biomolecules from peroxidation.<sup>83,84</sup> Melatonin, which is present in almost all cells, increases antioxidant enzymes (e.g., superoxide dismutase, glutathione peroxidase) and scavenges reactive oxygen species such as peroxy radicals and peroxy nitrite. Orhan et al. (2016) produced melatonin-based indole derivatives (59).<sup>85</sup> Silveira et al. (2013) investigated C-3 sulfenyl indoles (60); SAR revealed that bis-indole systems connected by sulfide at C-3 enhanced antioxidant activity by stabilizing the ring and facilitating electron delocalization.<sup>86</sup> Baytas and colleagues prepared triazole-substituted indoles (61) and tested them against DPPH and superoxide radicals. SAR demonstrated that the unsubstituted 1,2,4-triazole-5(4H)-thione at the second indole position promoted activity<sup>87</sup> (Figure 1.12).



## 1.5. Schiff bases

Schiff bases (-C=N-) are compounds containing the imine or azomethine functional group.<sup>89</sup> They are formed when a primary amine reacts with a carbonyl compound.<sup>90,91</sup> Hugo Schiff, a German chemist, was the first to synthesize this chemical in 1864, which became known as the Schiff base.<sup>92-94</sup> They have the general structure (63) (Figure 1.14)



R<sub>1</sub>, R<sub>2</sub> and R<sub>3</sub> are Hydrogen or alkyl or (more often) aryl groups

**Figure 1. 14: General structure of Schiff base.**

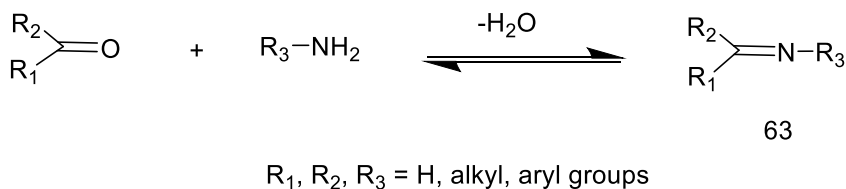
Aromatic Schiff bases exhibit greater stability compared to aliphatic Schiff bases, which are known to be unstable and can undergo polymerization.<sup>95</sup> The carbon-nitrogen double bond formed in Schiff bases, resulting from the reaction between primary amines and aldehydes is referred to as azomethine or aldimine, while the bond formed from the reaction with ketones is known as imine or ketimine. The chemical significance of Schiff bases stems from the unique electronic structure of the azomethine group, where a lone pair of electrons resides in an sp<sup>2</sup> hybridized orbital of the nitrogen atom.<sup>89</sup> This electronic configuration contributes to their versatile coordination chemistry and biological activities. The relative ease of synthesis, coupled with the ability to modulate their properties through structural modifications, has established Schiff bases as important synthetic intermediates and target molecules in organic and medicinal chemistry.<sup>96</sup> Schiff bases constitute a significant category of commonly utilized organic compounds and possess a wide range of applications across various domains, including analytical, biological, and inorganic chemistry. Their relevance in medicinal and pharmaceutical fields has increased due to their extensive range of biological effects such as anti-inflammatory,

analgesic<sup>97-101</sup> antimicrobial,<sup>102,103</sup> anticonvulsant,<sup>104</sup> antitubercular,<sup>105</sup> anticancer,<sup>106,107</sup> antioxidant,<sup>108</sup> anthelmintic,<sup>109</sup> and more. The nitrogen atom present in azomethine can participate in forming hydrogen bonds with the active sites of cell components, disrupting normal cellular operations.<sup>110,111</sup> Beyond their biological functions, Schiff bases are also employed as catalysts, intermediates in organic synthesis, dyes, pigments, polymer stabilizers, and corrosion inhibitors. Research has shown that metal complexes tend to exhibit enhanced biological activities compared to their free organic counterparts. The introduction of transition metals into Schiff bases has been linked to an increase in biological activity.<sup>112</sup> Schiff bases have been employed as building blocks in the synthesis of various industrial and biologically significant compounds, such as formazans, 4-thiazolidinines, and benzoxazines, through processes including ring closure, cycloaddition, and substitution reactions.<sup>113</sup>

### 1.5.1. Synthesis methods of Schiff bases

#### 1.5.1.1. Reaction of aldehydes and ketones with primary amines

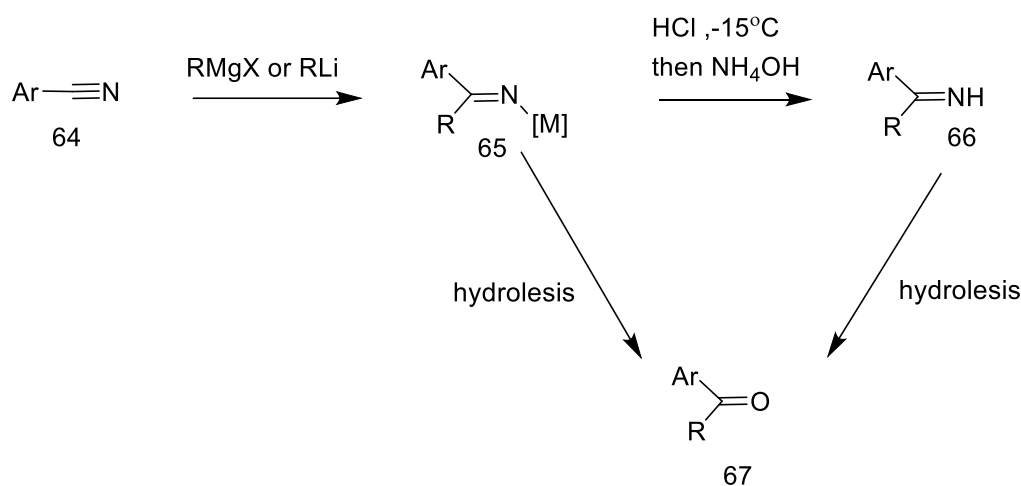
Aldehydes readily react with primary amines to produce Schiff bases, whereas this reaction is not as straightforward with ketones. To successfully create Schiff bases from ketones, it is crucial to consider factors such as the type of catalyst used, the suitable pH range, the choice of a solvent that can form an azeotropic mixture with the water generated during the reaction, and the correct reaction temperature<sup>114</sup> (Scheme 1.26).



**Scheme 1.26: Synthesis of Schiff bases.**

### 1.5.1.2. Reaction of organometallic compounds with nitriles

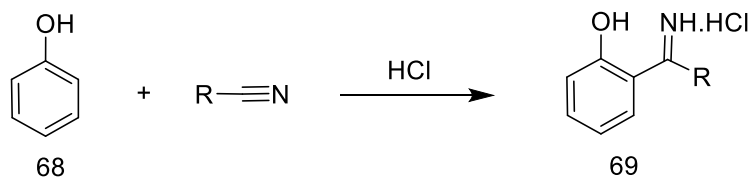
Grignard reagents are capable of reacting with nitriles to produce ketimines (66). To avoid hydrolysis of the intermediate products into ketones, anhydrous hydrogen chloride or anhydrous ammonia is introduced into the reaction mixture. Using this approach, intermediate products can be obtained with an efficiency ranging from 50% to 90% <sup>115</sup> (Scheme 1.27).



**Scheme 1.27: Addition of organometallic reagents to nitriles.**

### 1.5.1.3. Reaction of phenols and phenol ethers with nitriles

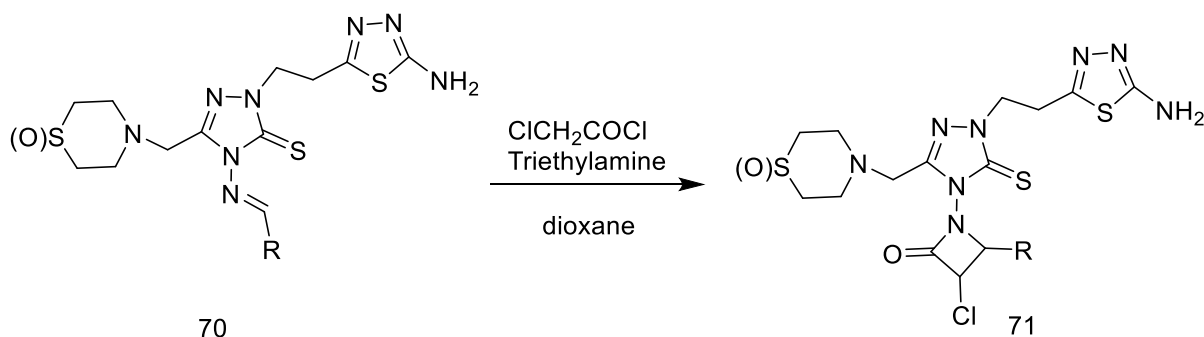
Alkyl or aryl nitriles interact effectively with phenol (68) and phenol ethers under acidic conditions to produce ketimines (69). This reaction is conducted by saturating a solution of nitrile and phenol in ether with hydrochloric acid gas. When working with phenols that have lower reactivity, Zinc Chloride ( $\text{ZnCl}_2$ ) should be utilized in the reactions <sup>116</sup> (Scheme 1.28).



**Scheme 1.28: Reaction of phenol with nitriles**

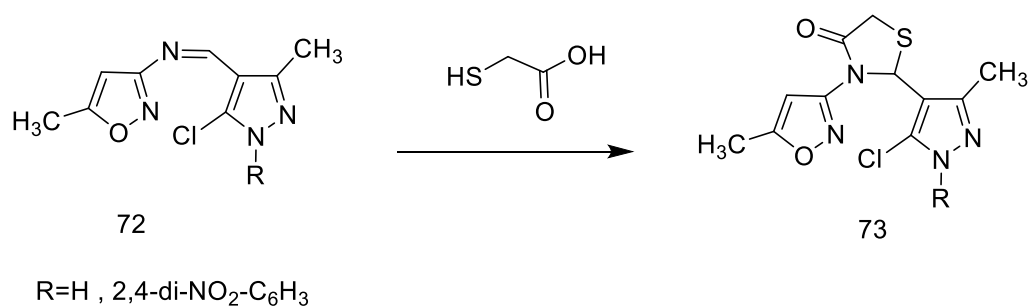
## 1.5.2. Miscellaneous reactions of Schiff Bases

Schiff bases are versatile intermediates in organic synthesis, participating in a wide variety of reactions. Among these, cyclization reactions are particularly important, as they enable the formation of diverse heterocyclic systems.<sup>117</sup> For instance, the imine group can react with  $\alpha$ -chloroacetyl chloride to yield azetidine ( $\beta$ -lactam) (71)<sup>118,119</sup> (Scheme 1.29)



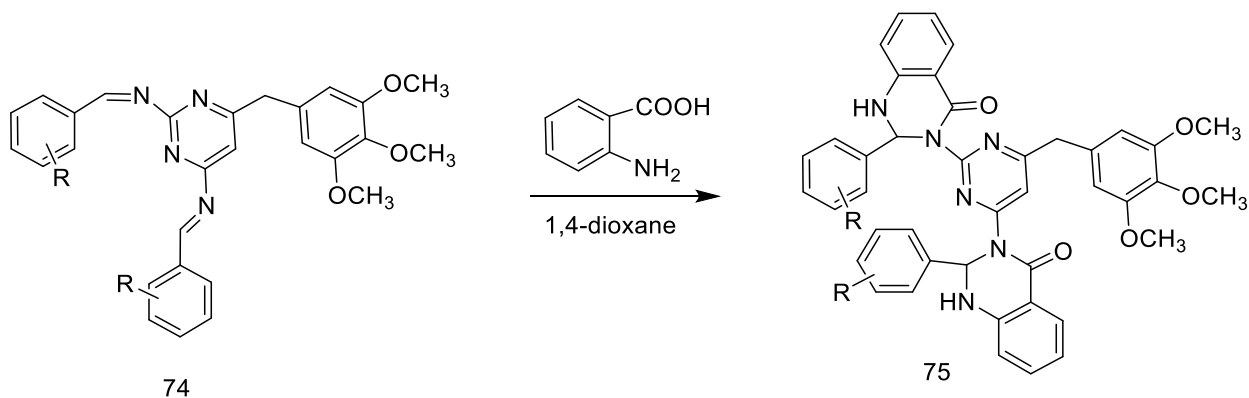
**Scheme 1.29: Synthesis of azetidine**

When isoxazol-pyrazole Schiff bases (72) were treated with thioglycolic acid, the reaction yielded the corresponding thiazolidine-4-one derivative (73)<sup>120</sup> (Scheme 1.30).



**Scheme 1.30: Synthesis of thiazolidine**

Schiff bases have been effectively utilized as key intermediates for the synthesis of hydroquinoline derivatives (75), highlighting their versatility in heterocyclic compound construction<sup>121</sup> (Scheme 1.31).



**Scheme 1.31: Synthesis of hydroquinoline**

The discovery of Schiff bases represented a significant advancement in the field of coordination chemistry. When coordinated with various transition metal ions, Schiff base ligands can form stable metal complexes with numerous applications. They are notable for their strong chelating properties. The availability of a lone pair of electrons on the azomethine nitrogen atom allows Schiff bases to form complexes with many metals. This lone pair facilitates the formation of monodentate complexes, while the inclusion of additional donor groups, such as (OH) and (SH) can produce bidentate chelates, which contribute to the significant chemical and biological properties of Schiff bases. Moreover, heterocyclic Schiff bases containing multiple donor atoms play an even more prominent role in coordination chemistry.<sup>122-124</sup>

## 1.6. Molecular docking

Molecular docking is considered one of the most commonly used and reliable structure-based in silico methods. It is widely applied to predict and analyze the interactions between small molecules and biological macromolecular targets. The docking process generally involves placing the ligand into the receptor binding pocket to determine its optimal pose and subsequently assessing the interaction through scoring functions.<sup>125</sup>

Since its introduction in the mid-1970s, molecular docking has become an essential tool for understanding ligand–target interactions and for supporting drug discovery and development. Over the years, there has been a substantial rise in studies focusing on both identifying the structural features required for efficient ligand–receptor binding and developing more accurate docking methodologies.<sup>126-129</sup>

Molecular docking continues to play a central role in structural molecular biology and computer-aided drug design, allowing virtual screening of large compound libraries, prioritization of results, and the formulation of structural hypotheses regarding how ligands interact with or inhibit their targets, making it indispensable for lead optimization. Proper preparation of input structures is as critical as the docking process itself, and analysis of results from stochastic search methods may sometimes be challenging. Overall, molecular docking has evolved into a powerful computational technique not only for predicting ligand–receptor interactions but also as a valuable tool in drug development.<sup>130</sup>

### 1.6.1 Tryptophan 2,3-dioxygenase (TDO2)

Tryptophan 2,3-dioxygenase (TDO) is a heme-containing enzymes that catalyze the initial and rate-limiting step of tryptophan catabolism through the kynurenine pathway. In this process, tryptophan is oxidized to tryptophan dioxide, which is subsequently converted into N-formylkynurenine and other kynurenine derivatives.<sup>131</sup> TDO has been reported to be overexpressed in various cancer cell types at different levels.<sup>132,133</sup> Within the tumor microenvironment, tryptophan depletion combined with the accumulation of kynurenine metabolites promotes the expansion and functional activity of regulatory T cells (Tregs) activity of regulatory T cells (Tregs),<sup>134</sup> while simultaneously inhibiting effector T-cell responses. These two mechanisms act synergistically to establish an immunosuppressive milieu, thereby enabling tumor cells to evade effective immune surveillance.<sup>135</sup> Such findings have stimulated considerable interest in exploring TDO as a therapeutic targets for cancer drug discovery. TDO is predominantly expressed in the liver, where it plays a key role in regulating blood tryptophan levels. Structurally, TDO functions as a homotetrameric enzyme, displaying high substrate specificity and preferentially catalyzing the oxidative cleavage of tryptophan (Figure 1.15)

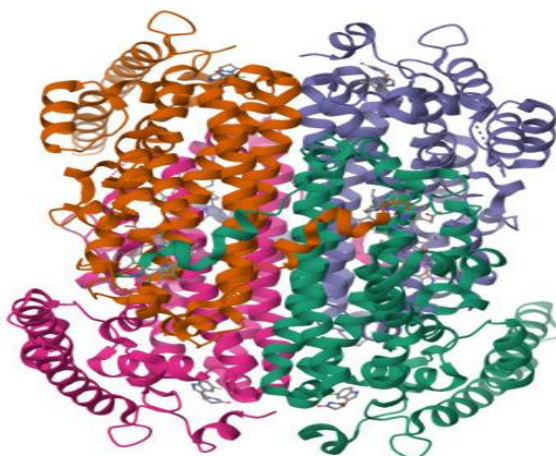


**Figure 1.15: Crystal Structure of human Tryptophan 2,3-dioxygenase**

## 1.7. Study aims

The research project aims to:

1- Synthesizing 4-amino-3-methyl-1*H*-1,2,4-triazole-3-thione and confirm its structure using FTIR, <sup>1</sup>HNMR and <sup>13</sup>CNMR spectrometry.

2- Synthesizing novel indole bearing 1,2,4-triazole-3-thione derivatives and confirm their structures using FTIR, <sup>1</sup>HNMR, <sup>13</sup>CNMR and HRMS spectrometry.

3- Evaluation of the biological activity of synthesized compounds, including their in vitro anticancer activity against HepG2 cell lines and their antibacterial activity against representative human pathogenic Gram-positive and Gram-negative bacteria.

4-Evaluation of the molecular docking interactions of the synthesized compounds with the human tryptophan 2,3-dioxygenase (TDO2) enzyme to predict their binding affinity and possible biological activity.

# CHAPTER TWO

## 2. Experimental

### 2.1. Chemical Materials

The chemicals used in this study were supplied by the companies shown in Table (2.1).

**Table 2.1: The chemicals used in the study**

<b>Chemicals</b>	<b>Company</b>
Hydrazine hydrate	CDH
Carbon disulfide	Fluka AG
Acetic acid glacial	SDFCL
Indole-3-carboxaldehyde	BLDpharm
6-Bromo-1H-Indole-3-carboxaldehyde	BLDpharm
5-Fluoro-1H-Indole-3-carboxaldehyde	BLDpharm
5-Chloro -1H-Indole-3-carboxaldehyde	BLDpharm
7-Nitro-1H-Indole-3-carboxaldehyde	BLDpharm
3-Formyl-1H-indole-5-carbonitrile	BLDpharm
5-methoxy-1H-Indole-3-carboxaldehyde	BLDpharm
4-Fluoro-1H-Indole-3-carboxaldehyde	HEOWNS
6-Fluoro-1H-Indole-3-carboxaldehyde	HEOWNS
5-Bromo-1H-Indole-3-carboxaldehyde	HEOWNS
6-Chloro -1H-Indole-3-carboxaldehyde	HEOWNS
Dichloromethane	SRL
Absolute ethanol	Honywell
Methanol	SRL

Acetone	J.T.Baker
Ethyl acetate	SRL
Petroleum ether 40-60	THOMAS BAKER

## 2.2. Instruments

### 2.2.1. Melting Point

All melting points are uncorrected and expressed in degree ( $^{\circ}\text{C}$ ). They were measured at the Department of Chemistry, College of Science, University of Misan, by using Stuart melting point apparatus (Cole-Parmer, UK).

### 2.2.2. Thin Layer Chromatography

TLC was performed using silica gel 60 F254 on Merck precoated aluminum sheet (0.2 mm thickness), with visualization by UV light.

### 2.2.3. Fourier Transform Infrared Spectrophotometer

FTIR spectra of all synthesized compounds were measured as KBr disc for solid samples for the region between (400-4000)  $\text{cm}^{-1}$  using SHIMADZU IRAffinity-1 (Japan) at BPC-Analysis Center in Baghdad, Iraq. Only principal absorption bands of interest were reported and expressed in  $\text{cm}^{-1}$ .

### 2.2.4. Nuclear Magnetic Resonance Spectrometer

All  $^1\text{H}$ -NMR,  $^{13}\text{C}$ -NMR, and HSQC experiments were recorded at the University of Basrah, Iraq, using a Bruker DRX-400 spectrometer (Germany), and chemical shifts are reported in ppm ( $\delta$ ). DMSO- $d_6$  was used as a solvent, while TMS was used as an internal standard. The coupling constants (J) are measured in Hertz and multiplicities

are quoted as singlet (s), doublet (d), triplet (t), doublet of doublets (dd), multiplet (m).

## 2.2.6. Mass Spectrometer

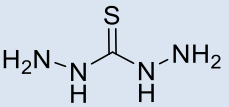
Electrospray ionization (ESI) high-resolution mass spectra (HRMS) were determined using Thermo Scientific Orbitrap Exploris 120 Mass Spectrometer (mass analyzer type: QTOF) at Mass Spectrometry Center operated by the College of Chemistry and Biochemistry, Auburn University, USA.

## 2.3. Synthetic Methods

### 2.3.1. Synthesis of thiocarbohydrazide (A)

Hydrazine hydrate 80% (20 g, 0.4 mol) was added to a round-bottom flask, followed by the slow addition of carbon disulfide (6.0 g, 0.08 mol) for about 60 min. with continuous stirring at room temperature. Subsequently, 120 mL of methanol was added, and the reaction mixture was heated under reflux for 8 h. Finally, the solution was permitted to cool to room temperature, and the resultant precipitate, thiocarbohydrazide, was separated by filtration. The precipitate was washed with methanol and dried. The crude product was purified by dissolving it in water at 40 °C and then cooling to room temperature before refrigeration at 0 °C for 12 h. The white needle crystals obtained were washed with methanol and dried, using TLC (DCM:MeOH; 3:0.2)<sup>136</sup>

Table 2.2: Physical properties of thiocarbohydrazid (A)

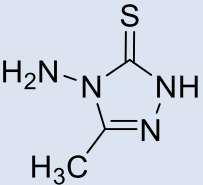
Comp. No	Structural formula	Molecular formula	M.P (°C)	R <sub>f</sub> *	Color	Yield (%)
A		CN <sub>4</sub> H <sub>6</sub> S	172-175	0.42	White	83%

\*R<sub>f</sub> values were determined by TLC (DCM : MeOH; 3:0.2)

### 2.3.2. Synthesis of 4-amino-5-methyl-2,4-dihydro-3H-1,2,4-triazole-3-thione (B)

Thiocarbohydrazide (A) (1 g, 0.0094 mol) was dissolved in 6 mL of glacial acetic acid, and the mixture was heated under reflux for 4 h. After completion of the reaction, the mixture was allowed to stand at room temperature overnight. The resulting product, 4-amino-5-methyl-2,4-dihydro-3H-1,2,4-triazole-3-thione, was isolated and purified by recrystallization from ethanol. The reaction progress was monitored by thin-layer chromatography (TLC) (DCM : MeOH; 5:0.3).<sup>137</sup>

Table 2.3: Physical properties of 4-amino-5-methyl-1,2,4-triazole-3-thione (B)

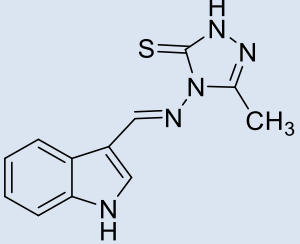
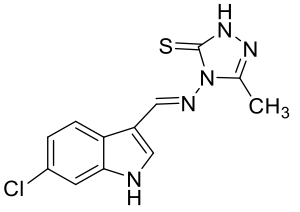
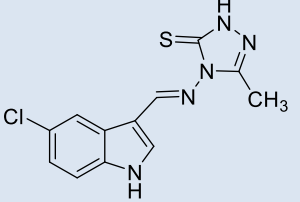
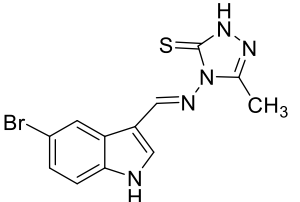
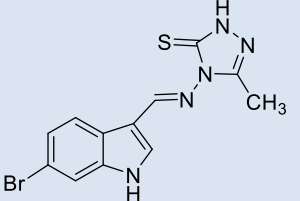
Comp. No	Structural formula	Molecular formula	M.P (°C)	R <sub>f</sub> *	color	Yield (%)
B		C <sub>3</sub> N <sub>4</sub> H <sub>6</sub> S	192-194	0.25	White	44.8

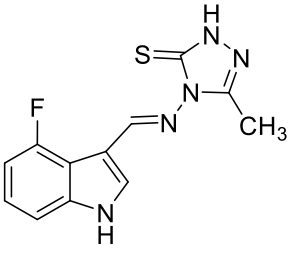
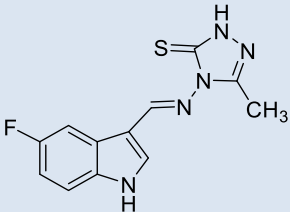
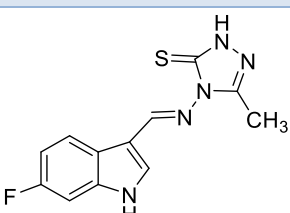
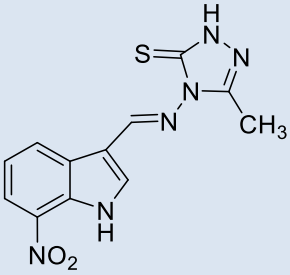
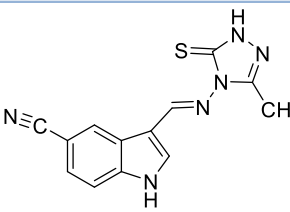
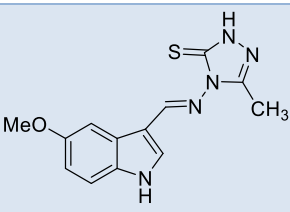
\*R<sub>f</sub> values were determined by TLC (DCM : MeOH; 5:0.3)

### 2.3.3. Synthesis of Schiff Bases (C1-C11)

4-Amino-5-methyl-1,2,4-triazole-3-thione (B) (0.004 mol) was treated with various substituted indole-3-carboxaldehyde (0.004 mol) in glacial acetic acid (22 mL). The mixture was heated under reflux for 30 minutes to 3 hours, then cooled, filtered, and washed with cold water. The reaction progress was monitored by thin-layer chromatography (TLC) (DCM : MeOH ; 5:0.2).<sup>138</sup>

**Table 2.4: Physical properties of Schiff bases (C1-C11)**

Comp. No	Structural formula	Molecular formula	M.P (°C)	R <sub>f</sub> *	color	Yield (%)
C1		C <sub>12</sub> H <sub>11</sub> N <sub>5</sub> S	280-282	0.42	White	92%
C2		C <sub>12</sub> H <sub>10</sub> ClN <sub>5</sub> S	303-305	0.33	Pale orange	84%
C3		C <sub>12</sub> H <sub>10</sub> ClN <sub>5</sub> S	300-302	0.73	Pale orange	97%
C4		C <sub>12</sub> H <sub>10</sub> BrN <sub>5</sub> S	288-292	0.5	Off white	86%
C5		C <sub>12</sub> H <sub>10</sub> BrN <sub>5</sub> S	300-304	0.64	Yellow	89%

C6		$C_{12}H_{10}FN_5S$	266-268	0.5	Pale yellow	48%
C7		$C_{12}H_{10}FN_5S$	302-306	0.32	Pale yellow	84%
C8		$C_{12}H_{10}FN_5S$	306-308	0.24	Pale yellow	67%
C9		$C_{12}H_{10}O_2N_6S$	288-291	0.67	yellow	80%
C10		$C_{13}H_{10}N_6S$	308-309	0.28	yellow	98%
C11		$C_{13}H_{13}N_5OS$	260-263	0.48	Pale yellow	53%

\* $R_f$  values were determined by TLC (DCM : MeOH; 5:0.2)

## **2.4. Biological activity**

### **2.4.1. Anticancer Activity**

HepG2 cell line (a human hepatocarcinoma cell line) was purchased from the National Cell Bank of Iran (Pasteur Institute, Iran). Cells were grown in RPMI-1640 (Gibco), with 10% FBS (Gibco) supplemented with antibiotics (100 U/ml penicillin and 100 µg/ml streptomycin). Cells were maintained at 37 °C under humidified air containing 5% CO<sub>2</sub> and were passaged using trypsin/EDTA (Gibco) and phosphate-buffered saline (PBS) solution. <sup>139</sup>

Cell growth and viability were assessed using the MTT [3-(4,5-dimethylthiazol-2-yl)-2,5-diphenyltetrazolium bromide] assay (Sigma-Aldrich). Briefly, cells were digested with trypsin, harvested, adjusted to a density of  $1.4 \times 10^4$  cells/well, and seeded into 96-well plates containing 200 µl of fresh medium per well for 24 h. Once the cells formed a monolayer, they were treated with compounds dissolved in DMSO at concentrations ranging from 7.4 to 600 µg/ml for 24 h at 37 °C in a 5% CO<sub>2</sub> atmosphere. At the end of the treatment, the culture medium was removed, and 200 µl/well of MTT solution (0.5 mg/ml in phosphate-buffered saline, PBS) was added. The plates were incubated at 37 °C for 4 h. After incubation, the MTT solution was removed, and 100 µl/well of dimethyl sulfoxide (DMSO) was added to dissolve the formazan crystals completely on a shaker at 37 °C. Cell viability was quantified by measuring absorbance at 570 nm using an ELISA reader (Model Wave XS2, BioTek, USA). The concentration of compounds resulting in 50% cell death (IC<sub>50</sub>) was determined from the respective dose–response curves.

## 2.4.2. Antibacterial Activity

The antibacterial activity of Schiff base compounds (C1–C11) was evaluated against two representative bacterial strains: *Staphylococcus aureus* ATCC 12600 and *Escherichia coli* ATCC 11175, which were chosen as standard models for Gram-positive and Gram-negative bacteria, respectively. The activity was assessed by determining the minimum inhibitory concentration (MIC) of each compound using the broth microdilution method.

Broth micro-dilution method was performed for the determination of minimum inhibitory concentrations (MICs) according to the standard protocols recommended by CLSI (Clinical Laboratory Standards Institute). MIC was defined as the lowest concentration of each tested compound required to inhibit visible bacterial growth. Two-fold serial dilutions of each compound were prepared in a concentration range of 0.001–4 mM in sterile micro-dilution trays containing Mueller–Hinton broth medium. Bacterial suspensions were prepared from freshly cultured cells in sterile normal saline and adjusted to 0.5 McFarland standard turbidity, then further diluted (1:100) with sterile Mueller–Hinton broth (MHB) immediately before inoculation into the trays containing the serial dilutions of each compound. Thus, each concentration of the compounds was tested against approximately  $0.5\text{--}1 \times 10^6$  bacterial cells. The 96-well plates were incubated at 37 °C for 24 h. Resazurin was used as a growth indicator, 4 µL of a 4 mg/mL stock solution in sterile distilled water was added to each well. Pinkish wells indicated bacterial growth, whereas blue wells showed growth inhibition by the tested compounds. Ampicillin and Tetracycline were used as a standard antibiotic control.<sup>140</sup>

## 2.5. Molecular Docking Studies

Molecular docking studies were performed using PyRx software (version 0.8), which utilizes AutoDock Vina as the docking engine. The 3D crystal Structure of human Tryptophan 2,3-dioxygenase was retrieved from the Protein Data Bank (PDB) (PDB ID. 6YPP) with a resolution of 2.40 Å, R-Value Work of 0.191, and R-Value Free of 0.237) <https://doi.org/10.2210/pdb6PYY/pdb>. The protein structure was prepared using PyMOL by removing water molecules and the co-crystallized ligand 3-(5-fluoro-1H-indol-3-yl)pyrrolidine-2,5-dione. The synthesized compounds were used in this study, and their chemical structures were drawn using Chem3D software. (version 23.1.1.3). Following energy minimization, these ligands and protein were converted to PDBQT format within PyRx. Docking was carried out using a grid box encompassing the active site of the protein with dimensions of [x = 25.0, y = 25.0, z = 25.0 Å, and exhaustiveness = 8]. Binding affinities were expressed in kcal/mol, and the most favorable docking poses were selected based on the lowest binding energy values. Protein–ligand interactions were further visualized and analyzed using Discovery Studio Visualizer (version 25.1.0.24284) and PyMOL software (version 3.1.6.1).<sup>141</sup>

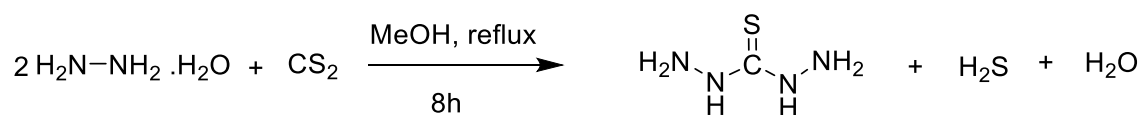
# CHAPTER THREE

### 3. Results and Discussion

#### 3.1. Thiocarbohydrazide (A)

##### 3.1.1. The synthetic strategy

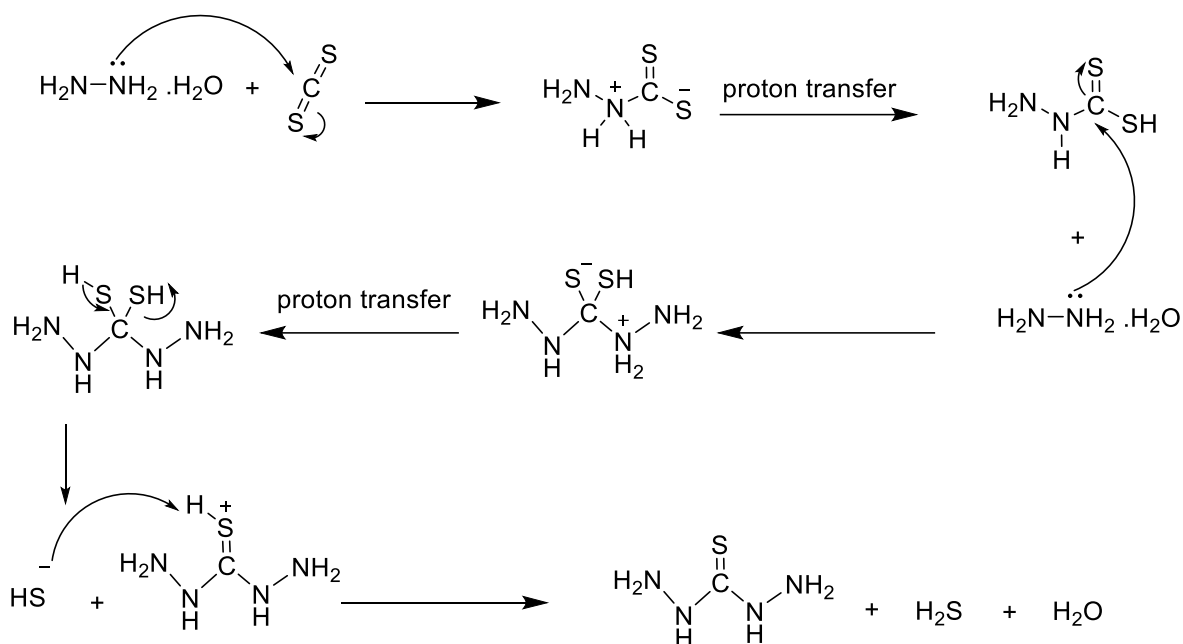
The protocol involved adding 80% hydrazine hydrate (20 g, 0.4 mol) to a round-bottom flask. Subsequently, (6.0 g, 0.08 mol) of carbon disulfide was slowly added over 60 minutes. Afterward, 120 mL of methanol was added, and the reaction mixture was refluxed for 8 hours until completion<sup>136</sup> (Scheme 3.1).



Scheme 3.1: Synthesis of thiocarbohydrazide (A)

##### 3.1.2. The proposed mechanism

The proposed mechanism of the reaction involves nucleophilic attacks of hydrazine on the electrophilic carbon atom of CS<sub>2</sub>. The first nucleophilic attack generates dithiocarbazate as an intermediate, which undergoes a second nucleophilic attack by another hydrazine molecule. Subsequent proton transfer converts the thiolate group into -SH, which is eliminated as H<sub>2</sub>S, to produce the stable product, thiocarbohydrazide<sup>136,142</sup> (Scheme 3.2).

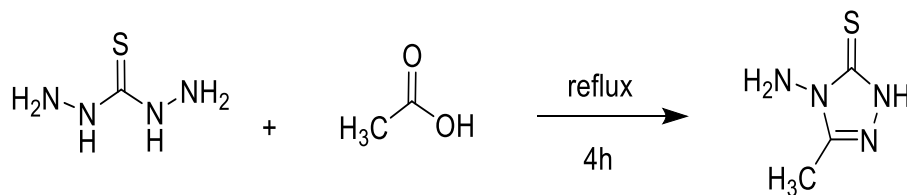


**Scheme 3.2:** The proposed mechanism of the synthesis of thiocarbohydrazide (A)

## 3.2. 4-amino-5-methyl-2,4-dihydro-1*H*-1,2,4-triazole-3-thione (B)

### 3.2.1. The synthetic strategy

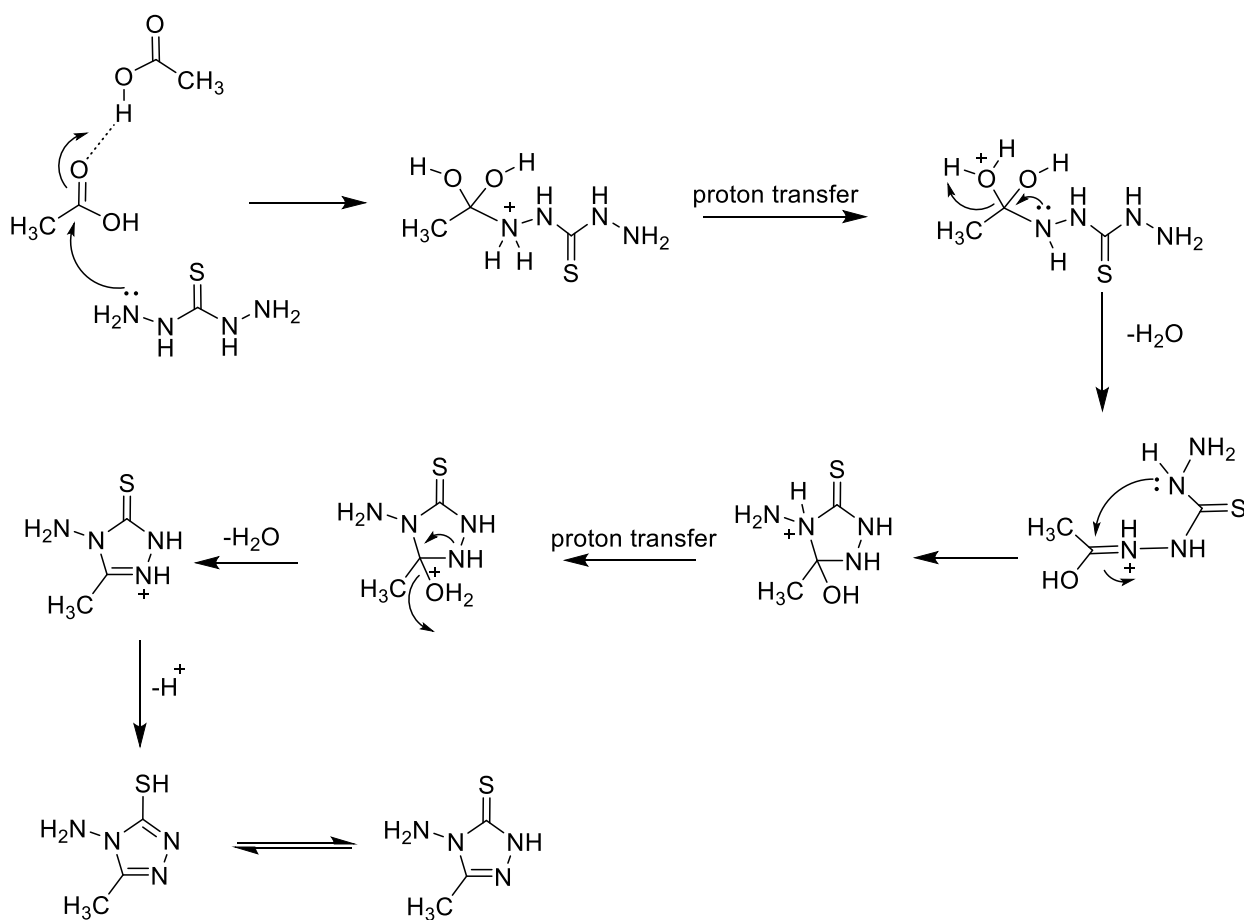
The protocol involves the addition of (1g , 0.0094 mol) thiocarbohydrazide (A) to a round-bottomed flask containing 6ml of glacial acetic acid. The mixture was heated under reflux for 4 h until the reaction was completed<sup>137</sup> (Scheme 3.3).



**Scheme 3.3:** Synthesis of 4-amino-5-methyl-3*H*-1,2,4-triazole-3-thione (B)

### 3.2.2. The proposed mechanism

The proposed reaction mechanism involves partial protonation of acetic acid in the acidic medium, which activates the carbonyl carbon, increasing its electrophilicity and making it susceptible to nucleophilic attack. Thiocarbohydrazone then reacts with the carbonyl group to form thiocarbohydrazone as an intermediate, which undergoes intramolecular nucleophilic attack by the adjacent nitrogen, inducing cyclization to form a five-membered ring. Subsequent dehydration produces 4-amino-5-methyl-2,4-dihydro-3*H*-1,2,4-triazole-3-thione (Scheme 3.4).



**Scheme 3.4: The proposed mechanism of Synthesis 4-amino-5-methyl-3*H*-1,2,4-triazole-3-thione (B)**

### 3.2.3. Spectroscopic characterization of 4-amino-5-methyl-2,4-dihydro-3H-1,2,4-triazole-3-thione (B).

The structure of the synthesized compound was confirmed based on spectroscopic techniques, including IR,  $^1\text{H}$  NMR, and  $^{13}\text{C}$  NMR spectra. The spectral data obtained were consistent with those reported in the related literature.<sup>143,144</sup>

The IR spectrum of this compound shows absorption bands in (3269–3113)  $\text{cm}^{-1}$ , which belong to the N–H stretching vibrations, and the bands at (2947)  $\text{cm}^{-1}$  are attributed to the aliphatic C–H stretching vibrations. A band at (1628)  $\text{cm}^{-1}$  indicates the presence of the C=N stretching vibration, while the N-H bending vibration appeared at (1575)  $\text{cm}^{-1}$ , and a band at (1319)  $\text{cm}^{-1}$  confirms the presence of the C=S stretching vibration.

The  $^1\text{H}$  NMR spectrum of the compound displays three characteristic singlets at  $\delta$  13.41, 5.52, and 2.23 ppm, which are assigned to the protons of the NH,  $\text{NH}_2$ , and  $\text{CH}_3$  groups, respectively. The presence of these signals confirms the formation of the desired compound.

$^{13}\text{C}$  NMR spectrum of the compound exhibits three distinct signals at  $\delta$  165.9, 149.6, and 10.9 ppm, corresponding to the carbon atoms of the C=S, C–NH, and  $\text{CH}_3$  groups, respectively. These signals further confirm the structure of the synthesized compound.

**4-amino-5-methyl-2,4-dihydro-3H-1,2,4-triazole-3-thione (B):** white crystals, m.p. 192-194°C; IR (KBr): 3269 and 3177 ( $\text{NH}_2$ ), 3113 (N-H), 2947 ( $\text{CH}_3$ ), 1628 (C=N), 1576 (N-H bending vibration) 1319 (C=S)  $\text{cm}^{-1}$ ;  $^1\text{H}$ -NMR (400 MHz,  $\text{DMSO-d}_6$ ): ppm  $\delta$  13.41(s, 1H, NH), 5.52 (s, 2H,  $\text{NH}_2$ ), 2.23 (s, 3H,  $\text{CH}_3$ );  $^{13}\text{C}$ -NMR (100 MHz,  $\text{DMSO-d}_6$ ): ppm  $\delta$  165.9 (C=S), 149.6 (C=N), 10.9 ( $\text{CH}_3$ ).

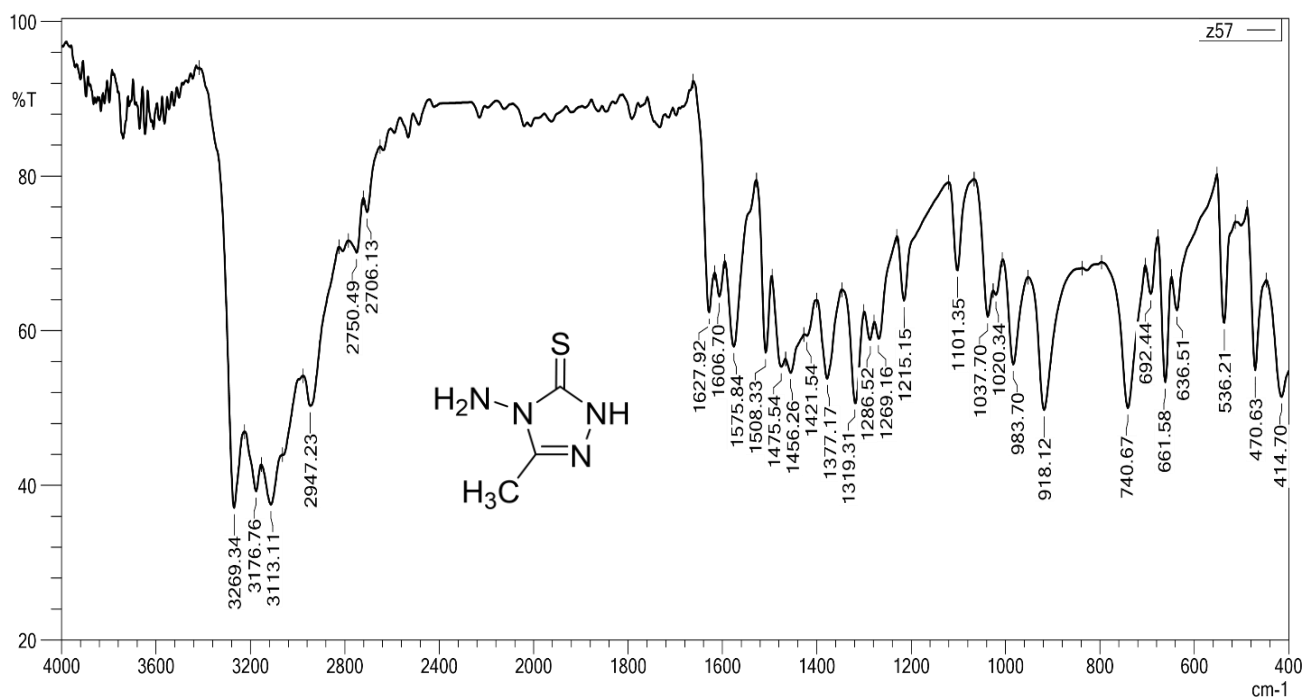


Figure (3.1): IR Spectrum of the compound B

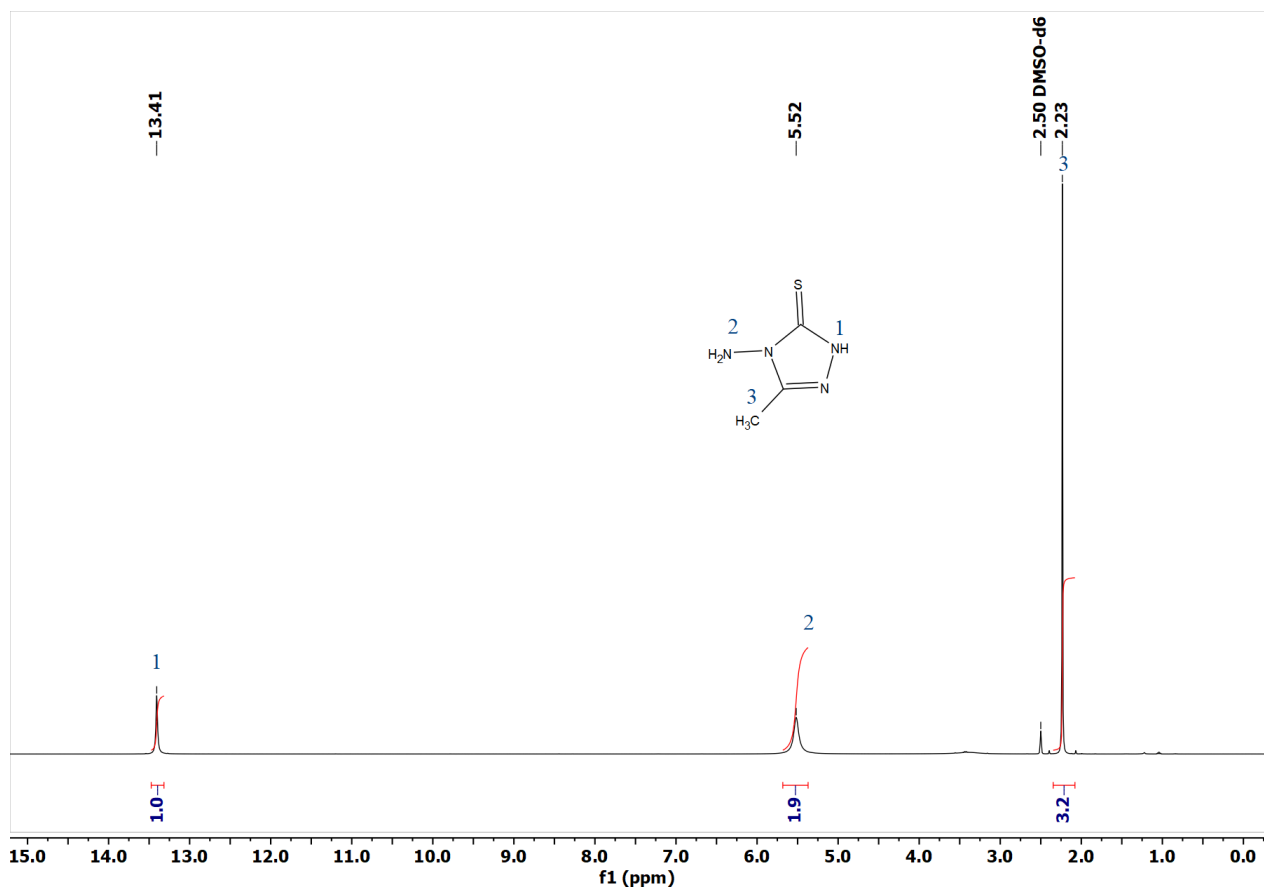


Figure (3.2): <sup>1</sup>H NMR Spectrum of the compound B

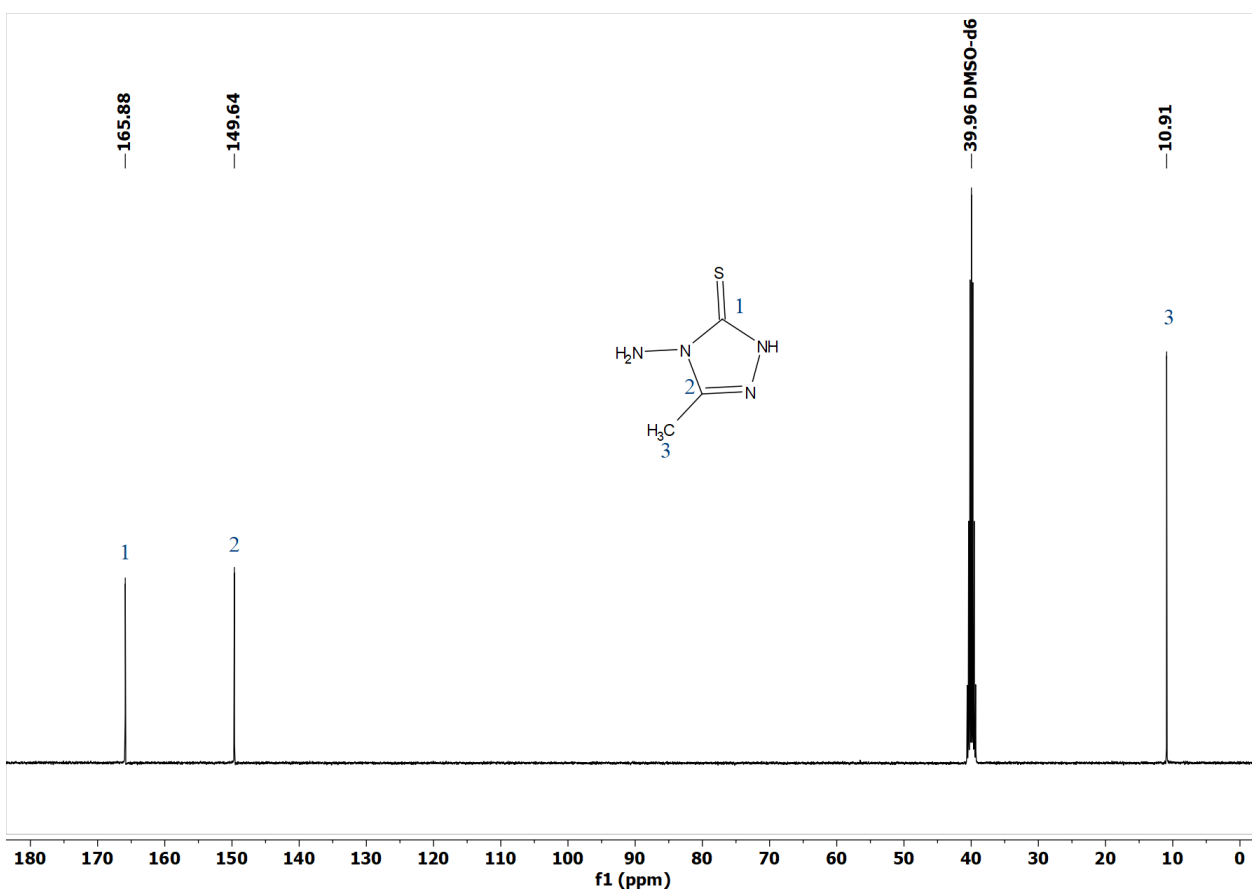
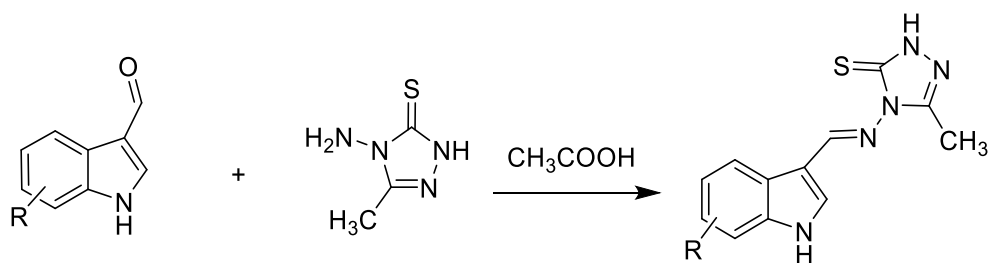


Figure (3.3):  $^{13}\text{C}$ NMR Spectrum of the compound B

### 3.3. Schiff Bases (C1-C11)

#### 3.3.1. The synthetic strategy

The protocol involves treating 4-Amino-3-methyl-1,2,4-triazole-3-thione (B) (0.004 mol) with various substituted indole-3-carboxaldehydes (0.004 mol) in a flask containing glacial acetic acid (22 mL). The mixture was heated under reflux for 30 minutes to 3 hours until the reaction was completed<sup>138</sup> (Scheme 3.5).

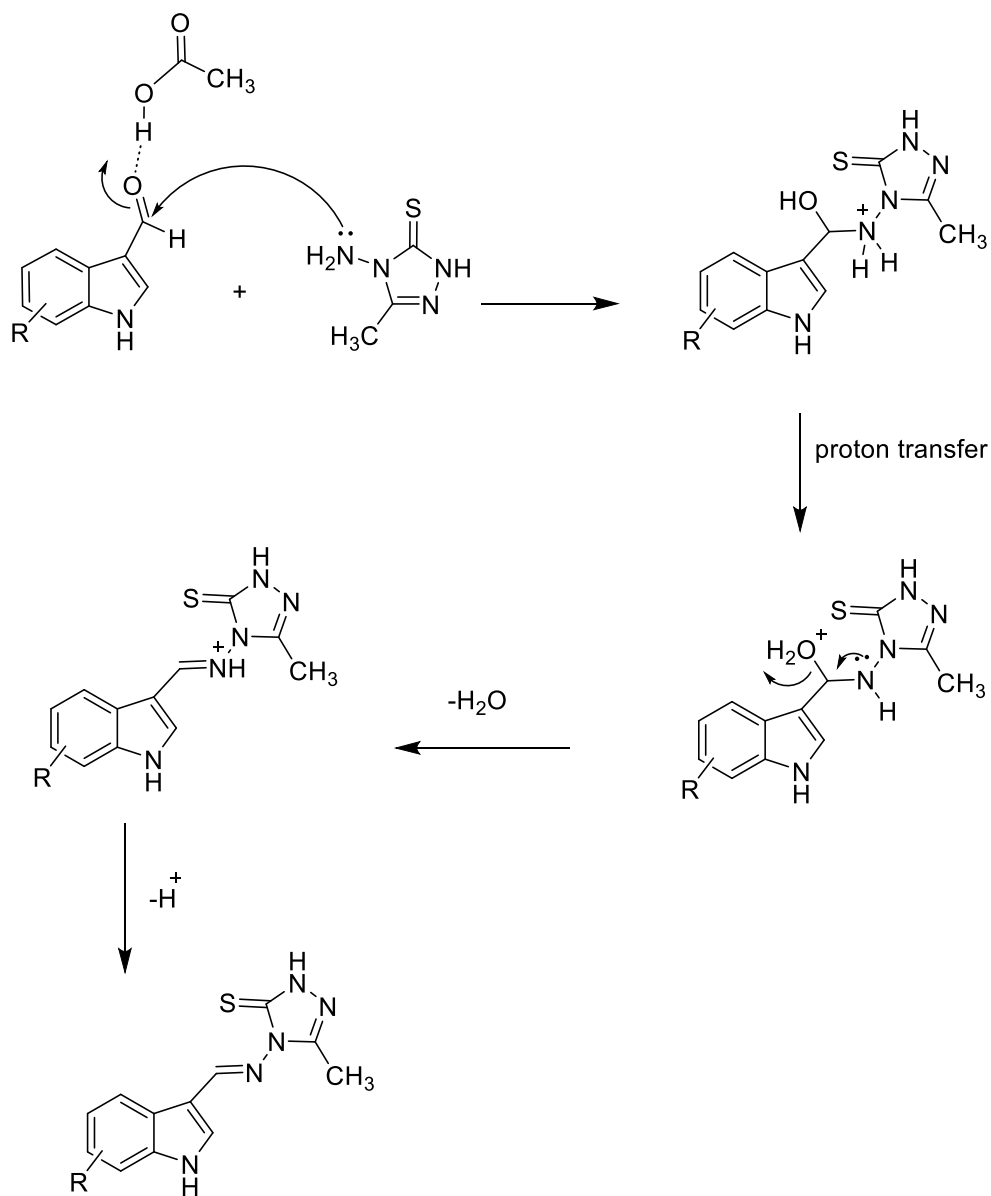


R=H, 6-Cl, 5-Cl, 5-Br, 6-Br, 6-F, 5-F, 4-F, 7-NO<sub>2</sub>, 5-MeO, 5-CN

**Scheme 3.5: Synthesis of Schiff bases (C1-C11)**

### 3.3.2. The proposed mechanism

The proposed reaction mechanism involves the activation of aromatic aldehydes (substituted indole-3-carboxaldehydes) through hydrogen bonding between the hydrogen atom of the acetic acid molecule and the carbonyl oxygen atom of the aldehydes, thereby increasing the electrophilicity of the carbonyl carbon. Subsequently, the nucleophilic addition of 4-amino-5-methyl-2,4-dihydro-3H-1,2,4-triazole-3-thione (a primary amine) to the carbonyl compound occurs, forming a tetrahedral intermediate known as a carbinolamine. This is followed by the elimination of a water molecule, leading to the formation of a Schiff base<sup>145</sup> (Scheme 3.6).



**Scheme 3.6: Mechanism of Synthesis of Schiff bases**

### 3.3.3. Spectroscopic characterization of Schiff bases (C1-C11)

The IR spectrum exhibits a strong band in the region (3251–3369)  $\text{cm}^{-1}$ , which belongs to the N–H stretching vibrations of the heterocyclic rings. The bands in the region (3097–3101)  $\text{cm}^{-1}$  represent the aromatic C–H stretching vibrations, while those at (3049–3057)  $\text{cm}^{-1}$  correspond to the C–H stretching vibrations of the imine group. The bands at (2926–2933)  $\text{cm}^{-1}$  are attributed to the aliphatic C–H stretching vibrations. A strong band at (1606–1595)  $\text{cm}^{-1}$  indicates the presence of the C=N stretching vibration, bands that at (1585–1564)  $\text{cm}^{-1}$  belong to the N–H bending vibrations, whereas the band at (1502–1510)  $\text{cm}^{-1}$  is assigned to the aromatic C=C stretching vibrations. The C–N stretching vibration appears in the region (1427–1433)  $\text{cm}^{-1}$ , and a band at (1300–1310)  $\text{cm}^{-1}$  confirms the presence of the C=S stretching vibration.

The  $^1\text{H}$  NMR spectrum of the compound displays distinct signals. Two singlets at  $\delta$  (13.58-13.66) and (11.9-12.59) ppm are assigned to the –NH protons of the triazole and indole rings, respectively, while a singlet at  $\delta$  (9.66-9.91) ppm corresponds to the CH=N proton of the imine. signals in the region  $\delta$  6.89–8.55 ppm are attributed to the aromatic protons. Finally, a singlet at  $\delta$  2.33- 2.40 ppm is assigned to the –CH<sub>3</sub> group. These signals confirm the presence of the expected functional groups in the synthesized compound.

The  $^{13}\text{C}$ -NMR spectra of all synthesized compounds were in agreement with the proposed structures. The disappearance of the aldehydic carbon signal and the appearance of a new peak at  $\delta$  148-149 ppm confirm the formation of the imine (C=N) group. Signals in the aromatic region ( $\delta$  110–150 ppm) correspond to the carbons of the indole and triazole rings. Quaternary carbons appear at  $\delta$  161–162 ppm, while methyl group carbon appear at  $\delta$  11 ppm. In fluoro-substituted derivatives (C6, C7, and C8), clear  $^{13}\text{C}$ – $^{19}\text{F}$  coupling was observed: the directly bonded carbon showed a strong one-bond coupling ( $J_{\text{C-F}} \approx 233\text{-}245$  Hz), while the ortho, meta,

and para carbons exhibited weaker long-range couplings. The nitrile-substituted compound (C10) displayed a signal at  $\delta$  104.2 ppm for the nitrile carbon ( $C\equiv N$ ), and the methoxy derivative (C11) showed a singlet at  $\delta$  55.7 ppm due to the  $O-CH_3$  group. All compounds exhibited a peak at  $\delta$  11–12 ppm assigned to the methyl group on the triazole ring ( $CH_3$ ).

The HSQC analysis was performed on compounds C1 and C9. The HSQC (Heteronuclear Single Quantum Coherence) spectrum was used to determine the direct one-bond correlations between hydrogen and carbon atoms in the synthesized compounds. In this technique, signals corresponding to NH protons and quaternary carbons were absent because they do not possess directly attached hydrogen atoms. Only protonated carbons, including  $CH$ ,  $CH_2$ , and  $CH_3$  groups, appeared in the HSQC spectrum, which facilitated the assignment of the proton–carbon correlations and supported the structural elucidation of the compounds

In addition, the high-resolution mass spectrometry (HRMS) analysis gave an exact molecular ion peak that matched the calculated mass of the proposed molecular formula, thereby providing strong confirmation of the molecular weight and overall structure.<sup>138,146</sup>

**4-(((1H-indol-3-yl)methylene)amino)-5-methyl-2,4-dihydro-3H-1,2,4-triazole-3-thione(C1):** White powder, Yield (92%), mp 280–282°C; IR(KBr): 3310, 1574 (N-H), 3098 (C-H(Ar)), 3049 (C-H(imine)), 2926 (C-H(aliph)), 1597(C=N), 1504.48 (C=C(Ar)), 1427 (C-N), 1300 (C=S)  $cm^{-1}$ ;  $^1H$ -NMR (400 MHz, DMSO- $d_6$ ): ppm  $\delta$ 13.60 (s, 1H, NH(triazole)), 12.04 (s, 1H, NH(indole)), 9.67 (s, 1H, imine), 8.19 (d, 1H,  $J=7.5$  Hz, Ar-H), 8.14 (d, 1H,  $J=2.9$  Hz, Ar-H), 7.52 (d, 1H,  $J=5$  Hz, Ar-H), 7.25 (m, 2H, Ar-H), 2.36 (s, 3H,  $CH_3$ );  $^{13}C$ -NMR (100 MHz, DMSO- $d_6$ ): ppm  $\delta$  161.8 (C=S), 161.6 (C=N) triazole, 148.5 (C=N) imine, 137.8 (Ar-C), 135.8 (Ar-CH), 124.7 (Ar-C), 123.7 (Ar-CH), 122.5 (Ar-CH), 122.0 (Ar-CH), 122.8 (Ar-CH), 110.4

(Ar-C), 11.33 (CH<sub>3</sub>); HRMS(ESI<sup>+</sup>) *m/z*: (M+H<sup>+</sup>) Calcd. for C<sub>12</sub>H<sub>12</sub>N<sub>5</sub>S<sup>+</sup> 258.0813, Found 258.0813

**4-(((6-chloro-1H-indol-3-yl)methylene)amino)-5-methyl-2,4-dihydro-3H-1,2,4-triazole-3-thione (C2):** Pale orange powder, Yield (84%), m.p. 303-305°C; IR (KBr): 3354, 1570 (N-H), 3100 (C-H(Ar)), 3049 (C-H(imine)), 2932 (C-H(aliph.)), 1597 (C=N), 1503 (C=C(Ar)), 1414 (C-N), 1302 (C=S) cm<sup>-1</sup>; <sup>1</sup>H-NMR (DMSO-d<sub>6</sub>, 400 MHz): ppm δ 13.62 (s, 1H, NH(triazole)), 12.12 (s, 1H, NH(indole)), 9.71 (s, 1H, imine), 8.18 (m, 2H, Ar-H), 7.57 (d, 1H, J=1.3 Hz, Ar-H), 7.25 (dd, 1H, J<sub>1</sub>=8.4 Hz, J<sub>2</sub>=1.6 Hz, Ar-H), 2.36 (s, 3H, CH<sub>3</sub>); <sup>13</sup>C-NMR (DMSO-d<sub>6</sub>, 100 MHz) : ppm δ 161.6 (C=S), 161.2(C=N)triazole, 148.5 (C=N)imine, 138.3 (Ar-C), 136.6 (Ar-CH), 128.3 (Ar-C), 123.8 (Ar-C), 123.4 (Ar-CH), 122.3 (Ar-CH), 112.6 (Ar-CH), 110.5 (Ar-C), 11.3 (CH<sub>3</sub>); HRMS(ESI<sup>+</sup>) *m/z*: (M+H<sup>+</sup>) Calcd. for C<sub>12</sub>H<sub>11</sub>ClN<sub>5</sub>S<sup>+</sup> 292.0424, Found 292.0421.

**4-(((5-chloro-1H-indol-3-yl)methylene)amino)-5-methyl-2,4-dihydro-3H-1,2,4-triazole-3-thione(C3):** pale orange powder, Yield (97%), m.p. 300-302°C; IR (KBr): 3281, 1574 (N-H), 3098 (C-H(Ar)), 3049 (C-H(imine)), 2930 (C-H(aliph.)), 1597 (C=N), 1504 (C=C(Ar)), 1413 (C-N), 1298 (C=S) cm<sup>-1</sup>; <sup>1</sup>H-NMR (DMSO-d<sub>6</sub>, 400 MHz): ppm δ 13.61 (s, 1H, NH(triazole)), 12.21 (s, 1H, NH(indole)), 9.67 (s, 1H, imine), 8.21 (s, 1H, Ar-H), 8.15 (s, 1H, Ar-H), 7.55 (d, 1H, J=8.6, Ar-H), 7.29 (d, 1H, J=8.6 Hz, Ar-H), 2.37 (s, 3H, CH<sub>3</sub>); <sup>13</sup>C-NMR (DMSO-d<sub>6</sub>, 100 MHz) : ppm δ 161.7 (C=S), 161.6 (C=N)triazole, 148.4 (C=N)imine, 137.0 (Ar-C), 136.3 (Ar-CH), 126.6 (Ar-C), 125.8 (Ar-C), 123.7 (Ar-CH), 121.5 (Ar-CH), 114.5 (Ar-CH), 110.0 (Ar-C), 11.3 (CH<sub>3</sub>); HRMS(ESI<sup>+</sup>) *m/z*: (M+H<sup>+</sup>) Calcd. for C<sub>12</sub>H<sub>11</sub>ClN<sub>5</sub>S<sup>+</sup> 292.0424, Found 292.0420.

**4-(((5-bromo-1H-indol-3-yl)methylene)amino)-5-methyl-2,4-dihydro-3H-1,2,4-triazole-3-thione (C4):** off white powder, Yield (86%), m.p. 288-292°C; IR (KBr): 3370, 1568 (N-H), 3100 (C-H(Ar)), 3042 (C-H(imine)), 2928 (C-H(aliph.)), 1595 (C=N), 1501 (C=C(Ar)), 1427 (C-N), 1288 (C=S)  $\text{cm}^{-1}$ ;  $^1\text{H-NMR}$  (DMSO- $\text{d}_6$ , 400 MHz): ppm  $\delta$  13.62 (s, 1H, NH(triazole)), 12.22 (s, 1H, NH(indole)), 9.66 (s, 1H, imine), 8.30 (s, 1H, Ar-H), 8.20 (s, 1H, Ar-H), 7.50 (d, 1H,  $J=8.6$  Hz, Ar-H), 7.40 (d, 1H,  $J=8.6$  Hz, Ar-H), 2.36 (s, 3H,  $\text{CH}_3$ );  $^{13}\text{C-NMR}$  (DMSO- $\text{d}_6$ , 100 MHz): ppm  $\delta$  161.69 (C=S), 161.66 (C=N)triazole, 148.4 (C=N)imine, 136.8 (Ar-C), 136.6 (Ar-CH), 126.4 (Ar-C), 126.3(Ar-C), 124.6 (Ar-CH), 114.9 (Ar-CH), 114.6 (Ar-CH), 109.9 (Ar-C), 11.3( $\text{CH}_3$ ); HRMS(ESI $^+$ )  $m/z$ : ( $\text{M}+\text{H}^+$ ) Calcd. for  $\text{C}_{12}\text{H}_{11}\text{BrN}_5\text{S}^+$  335.9919, Found 335.9919.

**4-(((6-bromo-1H-indol-3-yl)methylene)amino)-5-methyl-2,4-dihydro-3H-1,2,4-triazole-3-thione(C5):** yellow powder, Yield (89%), m.p. 300-304°C; IR (KBr): 3358, 1564 (N-H), 3102 (C-H(Ar)), 3049 (C-H(imine)), 2934 (C-H(aliph.)), 1595 (C=N), 1503 (C=C(Ar)), 1414 (C-N), 1304 (C=S)  $\text{cm}^{-1}$ ;  $^1\text{H-NMR}$  (DMSO- $\text{d}_6$ , 400 MHz): ppm  $\delta$  13.61 (s, 1H, NH(triazole)), 12.12 (s, 1H, NH(indole)), 9.72 (s, 1H, imine), 8.17 (d, 1H,  $J=2.6$ , Ar-H), 8.11 (d, 1H,  $J=8.5$  Hz, Ar-H), 7.72 (d, 1H,  $J=1.0$  Hz, Ar-H), 7.37 (dd, 1H,  $J_1=8.6$  Hz,  $J_2=1.4$  Hz, Ar-H), 2.36 (s, 3H,  $\text{CH}_3$ );  $^{13}\text{C-NMR}$  (DMSO- $\text{d}_6$ , 100 MHz): ppm  $\delta$  161.6 (C=S), 161.2 (C=N)triazole, 148.5 (C=N)imine, 138.7 (Ar-C), 136.4 (Ar-CH), 124.9 (Ar-C), 124.1 (Ar-C), 123.7 (Ar-CH), 116.3 (Ar-CH), 115.5 (Ar-CH), 110.5 (Ar-C), 11.3 ( $\text{CH}_3$ ); HRMS(ESI $^+$ )  $m/z$ : ( $\text{M}+\text{H}^+$ ) Calcd. for  $\text{C}_{12}\text{H}_{11}\text{BrN}_5\text{S}^+$  335.9919, Found 335.9920.

**4-(((4-fluoro-1H-indol-3-yl)methylene)amino)-5-methyl-2,4-dihydro-3H-1,2,4-triazole-3-thione(C6):** pale yellow powder, Yield (48%), m.p. 266-268°C; IR (KBr): 3331, 1578 (N-H), 3100 (C-H(Ar)), 3050 (C-H(imine)), 2928 (C-H(aliph.)), 1603 (C=N), 1505 (C=C(Ar)), 1424 (C-N), 1300 (C=S)  $\text{cm}^{-1}$ ;  $^1\text{H-NMR}$  (DMSO- $d_6$ , 400 MHz): ppm  $\delta$  13.62 (s, 1H, NH(triazole)), 12.38 (s, 1H, NH(indole)), 9.91 (s, 1H, imine), 8.25 (d, 1H,  $J=2.7$  Hz, Ar-H), 7.36 (d, 1H,  $J=8.1$ , Ar-H), 7.22 (m, 1H, Ar-H), 6.96 (m, 1H, Ar-H), 2.33 (s, 3H,  $\text{CH}_3$ );  $^{13}\text{C-NMR}$  (DMSO- $d_6$ , 100 MHz): ppm  $\delta$  162.4 (C=S), 160.5 (C=N)triazole, 158.3 and 155.9 (d,  $J_1=246.6$  Hz, Ar-C), 149.5 (C=N)imine, 140.9 (d,  $J_4=11$  Hz, Ar-C), 132.3 (Ar-CH), 124.8 (d,  $J_5=7.65$  Hz, Ar-CH), 115.1 (d,  $J_2=20.7$  Hz, Ar-C), 110.4 (d,  $J_7=3.4$  Hz, Ar-CH), 109.1 (d,  $J_6=3.6$  Hz, Ar-C), 108.0 (d,  $J_3=19.5$  Hz, Ar-CH), 12.04 ( $\text{CH}_3$ ); HRMS(ESI $^+$ )  $m/z$ : ( $\text{M}+\text{H}^+$ ) Calcd. for  $\text{C}_{12}\text{H}_{11}\text{FN}_5\text{S}^+$  276.0719, Found 276.0714.

**4-(((5-fluoro-1H-indol-3-yl)methylene)amino)-5-methyl-2,4-dihydro-3H-1,2,4-triazole-3-thione(C7):** pale yellow powder, Yield (84%), m.p. 302-306°C; IR (KBr): 3252, 1578 (N-H), 3098 (C-H(Ar)), 3051 (C-H(imine)), 2928 (C-H(aliph.)), 1601 (C=N), 1503 (C=C(Ar)), 1433 (C-N), 1300 (C=S)  $\text{cm}^{-1}$ ;  $^1\text{H-NMR}$  (DMSO- $d_6$ , 400 MHz): ppm  $\delta$  13.60 (s, 1H, NH(triazole)), 12.13 (s, 1H, NH(indole)), 9.69 (s, 1H, imine), 8.21 (d, 1H,  $J=2.8$  Hz, Ar-H), 7.85 (dd, 1H,  $J_1=9.5$  Hz,  $J_2=2.1$  Hz, Ar-H), 7.53 (m, 1H, Ar-H), 6.13 (m, 1H, Ar-H), 2.37 (s, 3H,  $\text{CH}_3$ );  $^{13}\text{C-NMR}$  (DMSO- $d_6$ , 100 MHz): ppm  $\delta$  161.6 (C=S), 161.5 (C=N)triazole, 159.9 and 157.6 (d,  $J_1=234.4$  Hz, Ar-C), 148.5 (C=N)imine, 137.2 (Ar-CH), 134.4 (Ar-C), 125.0 (d,  $J_4=10.9$  Hz, Ar-CH), 114.1 (d,  $J_5=10$  Hz, Ar-C), 112.0 (d,  $J_2=26$  Hz, Ar-CH), 110.5 (d,  $J_6=4.2$  Hz, Ar-C), 107.3 (d,  $J_3=24$  Hz, Ar-CH), 11.3 ( $\text{CH}_3$ ); HRMS(ESI $^+$ )  $m/z$ : ( $\text{M}+\text{H}^+$ ) Calcd. for  $\text{C}_{12}\text{H}_{11}\text{FN}_5\text{S}^+$  276.0719, Found 276.0715.

**4-(((6-fluoro-1H-indol-3-yl)methylene)amino)-5-methyl-2,4-dihydro-3H-1,2,4-triazole-3-thione (C8):** pale yellow powder, Yield (67%), m.p. 306-308°C; IR (KBr): 3362, 1585 (N-H), 3102 (C-H(Ar)), 3051 (C-H(imine)), 2932 (C-H(aliph.)), 1601 (C=N), 1504 (C=C(Ar)), 1420 (C-N), 1304 (C=S)  $\text{cm}^{-1}$ ;  $^1\text{H-NMR}$  (DMSO- $\text{d}_6$ , 400 MHz): ppm  $\delta$  13.60 (s, 1H, NH(triazole)), 12.07 (s, 1H, NH(indole)), 9.69 (s, 1H, imine), 8.17 (m, 2H, Ar-H), 7.32 (dd, 1H,  $J_1=9.5$  Hz,  $J_2=1.6$  Hz, Ar-H), 7.10 (t, 1H,  $J=9.9$  Hz, Ar-H), 2.36 (s, 3H,  $\text{CH}_3$ );  $^{13}\text{C-NMR}$  (DMSO- $\text{d}_6$ , 100 MHz) : ppm  $\delta$  161.6 (C=S), 161.3 (C=N)triazole, 161.2 and 158.9 (d,  $J_1=237.2$  Hz, Ar-C), 148.5 (C=N)imine, 137.9 (d,  $J_4=12.9$  Hz, Ar-C), 136.4(d,  $J_6=2.3$  Hz, Ar-C), 123.7 (d,  $J_5=10.2$  Hz, Ar-CH), 121.4 (Ar-CH), 110.5(Ar-c), 110.3 (d,  $J_3=23.7$  Hz, Ar-CH), 99.1 (d,  $J_2=25.7$  Hz, Ar-CH), 11.3 ( $\text{CH}_3$ ); HRMS(ESI $^+$ )  $m/z$ : (M+H $^+$ ) Calcd. for  $\text{C}_{12}\text{H}_{11}\text{FN}_5\text{S}^+$  276.0719 Found 276.0718.

**5-methyl-4-(((7-nitro-1H-indol-3-yl)methylene)amino)-2,4-dihydro-3H-1,2,4-triazole-3-thione (C9):** yellow powder, Yield (80%), m.p. 288-291°C; IR (KBr): 3347, 1477 (N-H), 3100 (C-H(Ar)), 3058 (C-H(imine)), 2934 (C-H(aliph.)), 1607 (C=N), 1541 (C=C(Ar)), 1510, 1319 (N=O), 1404 (C-N), 1284(C=S)  $\text{cm}^{-1}$ ;  $^1\text{H-NMR}$  (DMSO- $\text{d}_6$ , 400 MHz): ppm  $\delta$  13.66 (s, 1H, NH(triazole)), 12.59 (s, 1H, NH(indole)), 9.90 (s, 1H, imine), 8.64 (d, 1H,  $J=7.8$  Hz, Ar-H), 8.28 (d, 1H,  $J=2.6$  Hz, Ar-H), 8.20 (d, 1H,  $J=7.9$  Hz, Ar-H), 7.43 (t, 1H,  $J=7.9$  Hz, Ar-H), 2.39 (s, 3H,  $\text{CH}_3$ );  $^{13}\text{C-NMR}$  (DMSO- $\text{d}_6$ , 100 MHz) : ppm  $\delta$  161.6 (C=S), 160.5 (C=N)triazole, 148.6 (C=N)imine, 138.0 (Ar-CH), 133.6 (Ar-C), 130.7 (Ar-CH), 130.0(Ar-C), 128.4 (Ar-C), 121.9 (Ar-CH), 120.6 (Ar-CH), 111.6 (Ar-C), 11.4 ( $\text{CH}_3$ ); HRMS (ESI $^+$ )  $m/z$ : (M+H $^+$ ) Calcd. for  $\text{C}_{12}\text{H}_{11}\text{O}_2\text{N}_6\text{S}^+$  303.0664, Found 303.0662

**3-(((3-methyl-5-thioxo-1,5-dihydro-4H-1,2,4-triazol-4-yl)imino)methyl)-1H-indole-5-carbonitrile (C10):** yellow powder, Yield (98%), m.p. 208-309°C; IR (KBr): 3256, 1576 (N-H), 3098 (C-H(Ar)), 3051 (C-H(imine)), 2932 (C-H(aliph.)), 2224 (C≡N), 1599(C=N), 1504 (C=C(Ar)), 1431 (C-N), 1300 (C=S) cm<sup>-1</sup>; <sup>1</sup>H-NMR (DMSO-d<sub>6</sub>, 400 MHz): ppm δ 13.64 (s, 1H, NH(triazole)), 12.49 (s, 1H, NH(indole)), 9.80 (s, 1H, imine), 8.55 (s, 1H, Ar-H), 8.35 (d, 1H, J=2.2 Hz, Ar-H), 7.70 (d, 1H, J=8.3 Hz, Ar-H), 7.64 (d, 1H, J=8.3 Hz, Ar-H), 2.40 (s, 3H, CH<sub>3</sub>); <sup>13</sup>C-NMR (DMSO-d<sub>6</sub>, 100 MHz): ppm δ 161.6 (C=S), 160.8 (C=N)triazole, 148.6 (C=N)imine, 139.7 (Ar-C), 137.7 (Ar-CH), 127.4 (Ar-C), 126.6 (Ar-C), 124.4 (Ar-CH), 120.7 (Ar-CH), 114.3 (Ar-CH), 110.9 (Ar-C), 104.2 (C≡N), 11.4 (CH<sub>3</sub>); HRMS(ESI<sup>+</sup>) *m/z*: (M+H<sup>+</sup>) Calcd. for C<sub>13</sub>H<sub>11</sub>N<sub>6</sub>S<sup>+</sup> 283.0766, Found 283.0766

**4-(((5-methoxy-1H-indol-3-yl)methylene)amino)-5-methyl-2,4-dihydro-3H-1,2,4-triazole-3-thione (C11):** pale yellow powder, Yield (53%), m.p. 260-363°C; IR (KBr): 3232, 1574 (N-H), 3102 (C-H(Ar)), 3063 (C-H(imine)), 2940 (C-H(aliph.)), 1599 (C=N), 1528 (C=C(Ar)), 1483 (C-O), 1443 (C-N), 1282 (C=S) cm<sup>-1</sup>; <sup>1</sup>H-NMR (DMSO-d<sub>6</sub>, 400 MHz): ppm δ 13.58 (s, 1H, NH(triazole)), 11.91 (s, 1H, NH (indole )), 9.71 (s, 1H, imine), 8.06 (s, 1H, Ar-H), 7.69 (s, 1H, Ar-H), 7.40 (d, 1H, J=8.3 Hz, Ar-H), 6.90 (d, 1H, J=8.3 Hz, Ar-H), 3.80 (s, 3H, CH<sub>3</sub>), 2.38 (s, 3H, CH<sub>3</sub>); <sup>13</sup>C-NMR (DMSO-d<sub>6</sub>, 100 MHz): ppm δ 161.6 (C=S), 161.4 (C=N)triazole, 155.6 (Ar-C), 148.5 (C=N)imine, 135.8 (Ar-CH), 132.6 (Ar-C), 125.4 (Ar-C), 113.5 (Ar-CH), 113.4 (Ar-CH), 110.2 (Ar-C), 104.4 (Ar-CH), 55.7 (CH<sub>3</sub>), 11.3 (CH<sub>3</sub>); HRMS(ESI<sup>+</sup>) *m/z*: (M+H<sup>+</sup>) Calcd. for C<sub>13</sub>H<sub>14</sub>ON<sub>5</sub>S<sup>+</sup> 288.0919, Found 288.0916

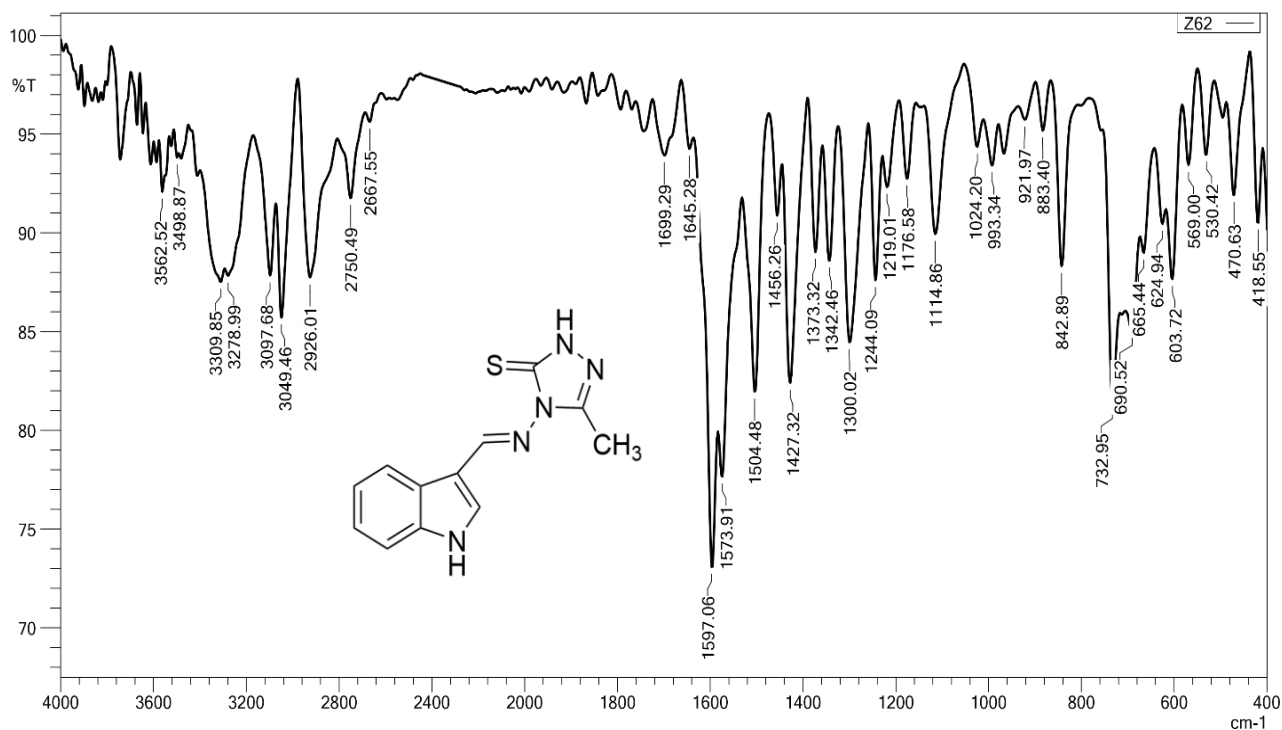


Figure (3.4): IR Spectrum of the compound C1

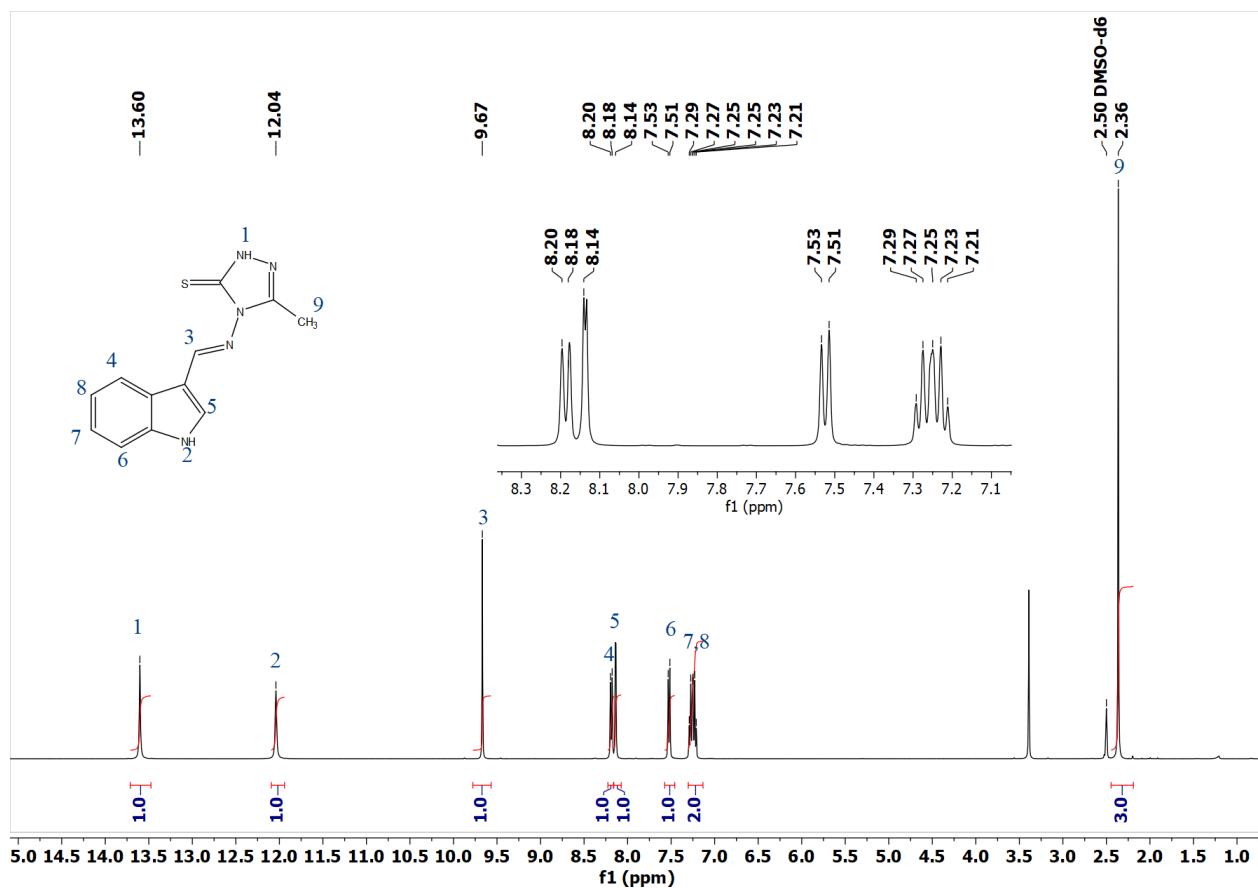


Figure (3.5): <sup>1</sup>H NMR Spectrum of the compound C1

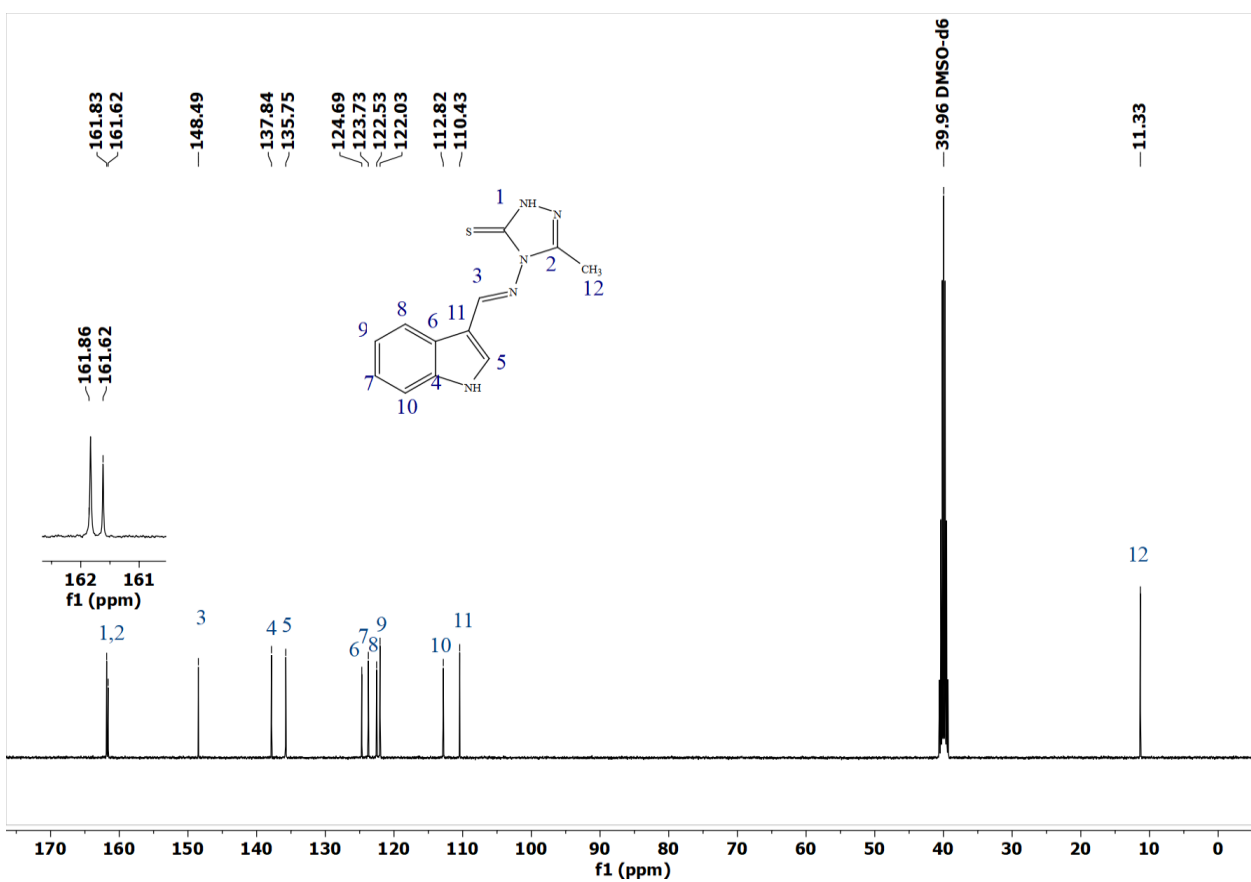


Figure (3.6):  $^{13}\text{C}$ NMR Spectrum of the compound C1

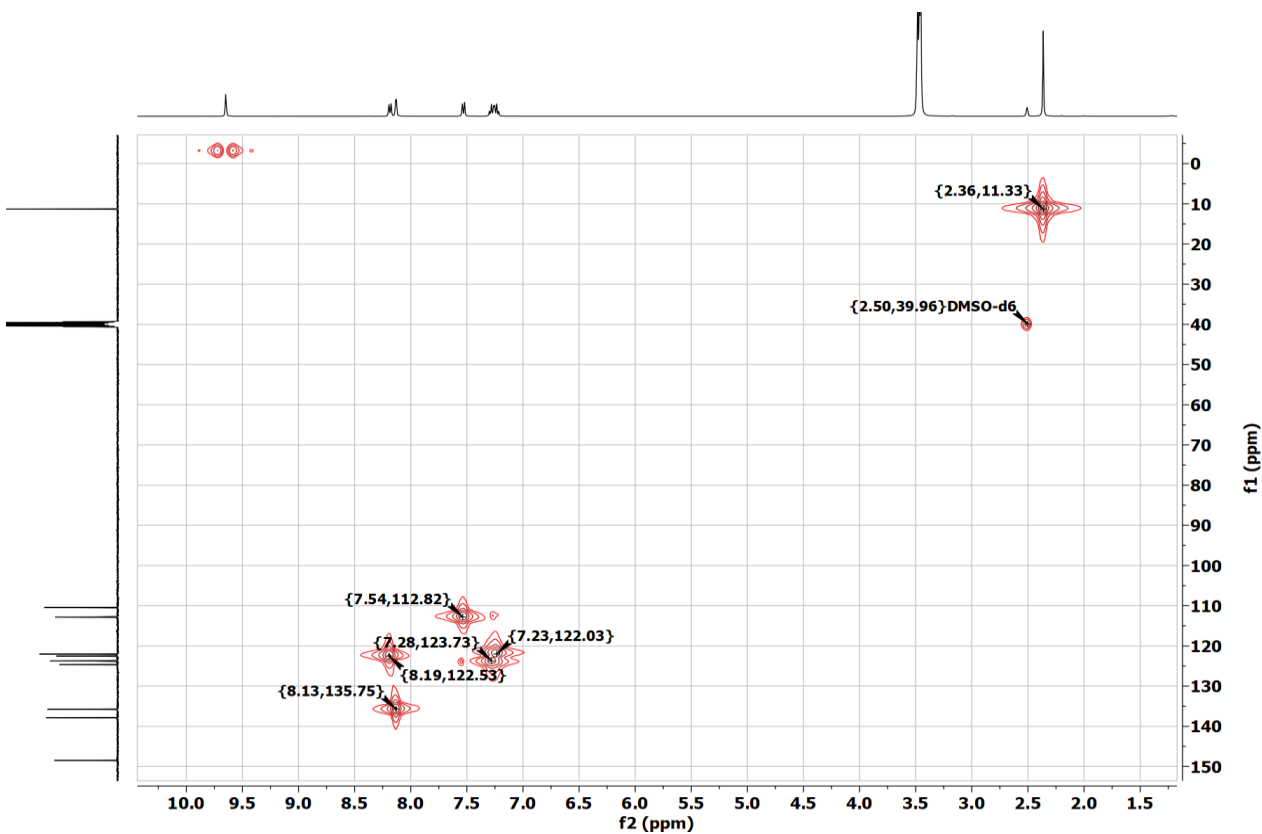


Figure (3.7): HSQC Spectrum of the compound C1

UAM\_Z62\_20251119164754 #18-24 RT: 0.14-0.19 AV: 3 SB: 4 0.01-0.08 NL: 4.53E7  
T: FTMS + p ESI Full ms [100.0000-1000.0000]

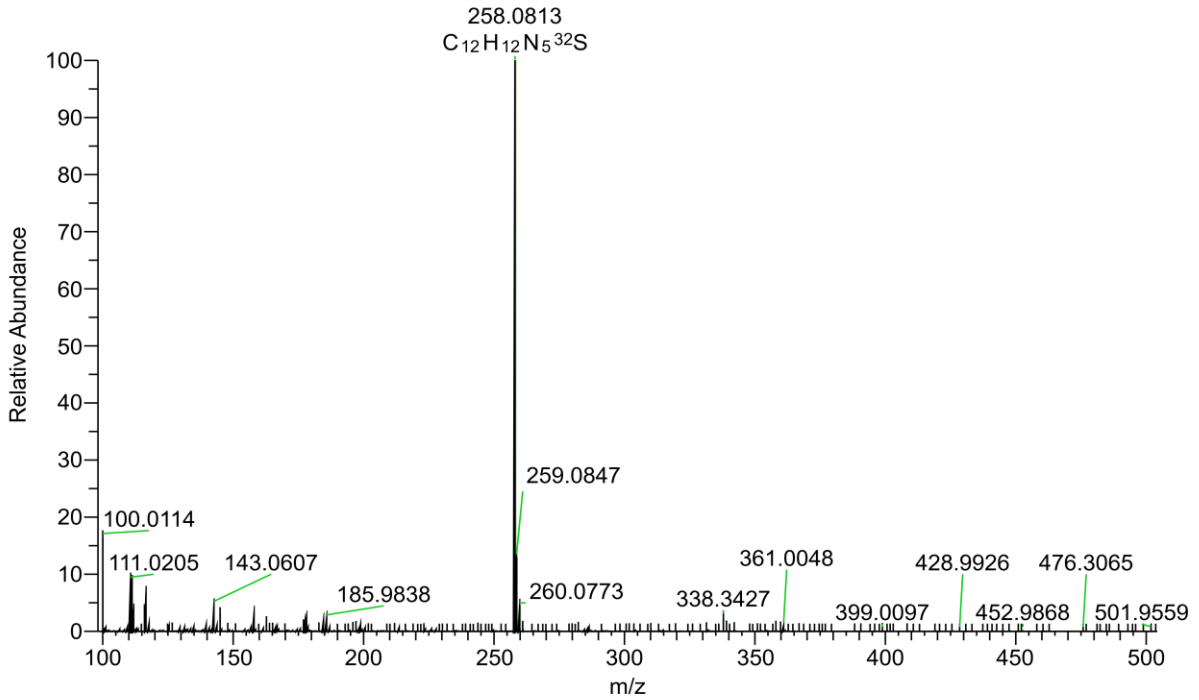


Figure (3.8): Mass Spectrum (ESI) of the compound C1

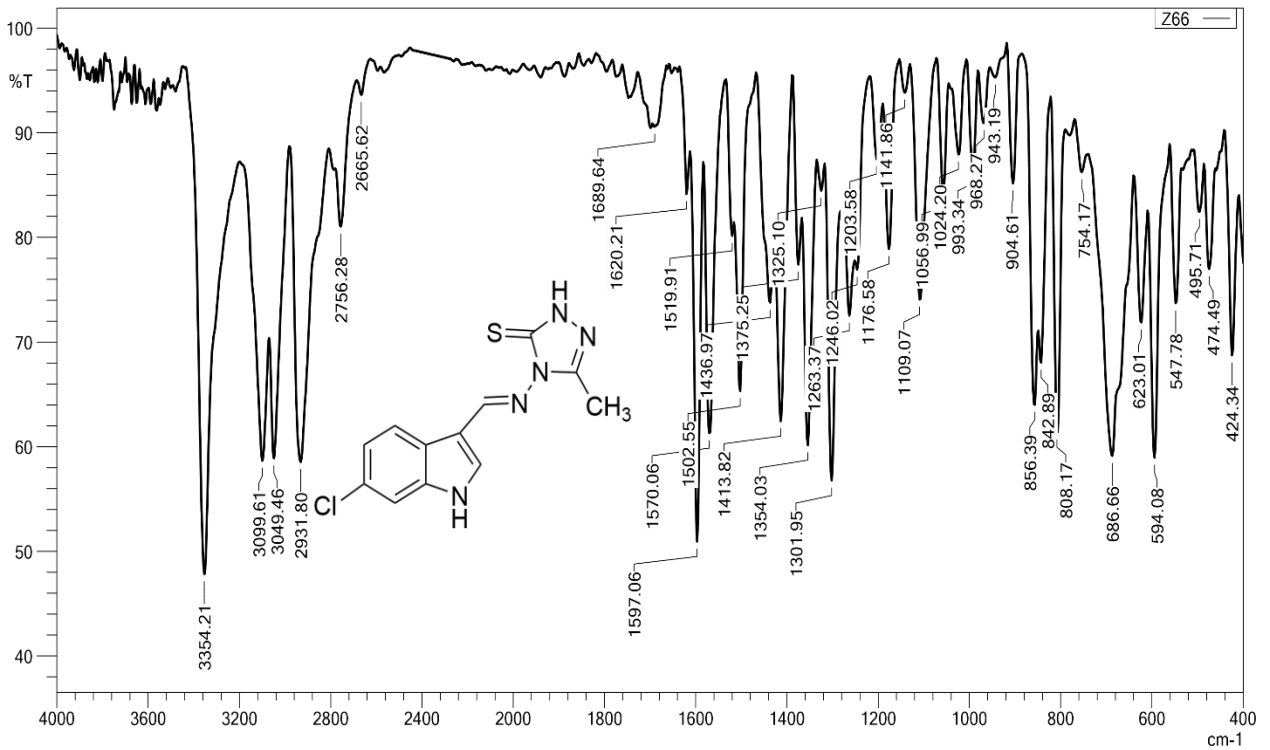


Figure (3.9): IR Spectrum of the compound C2

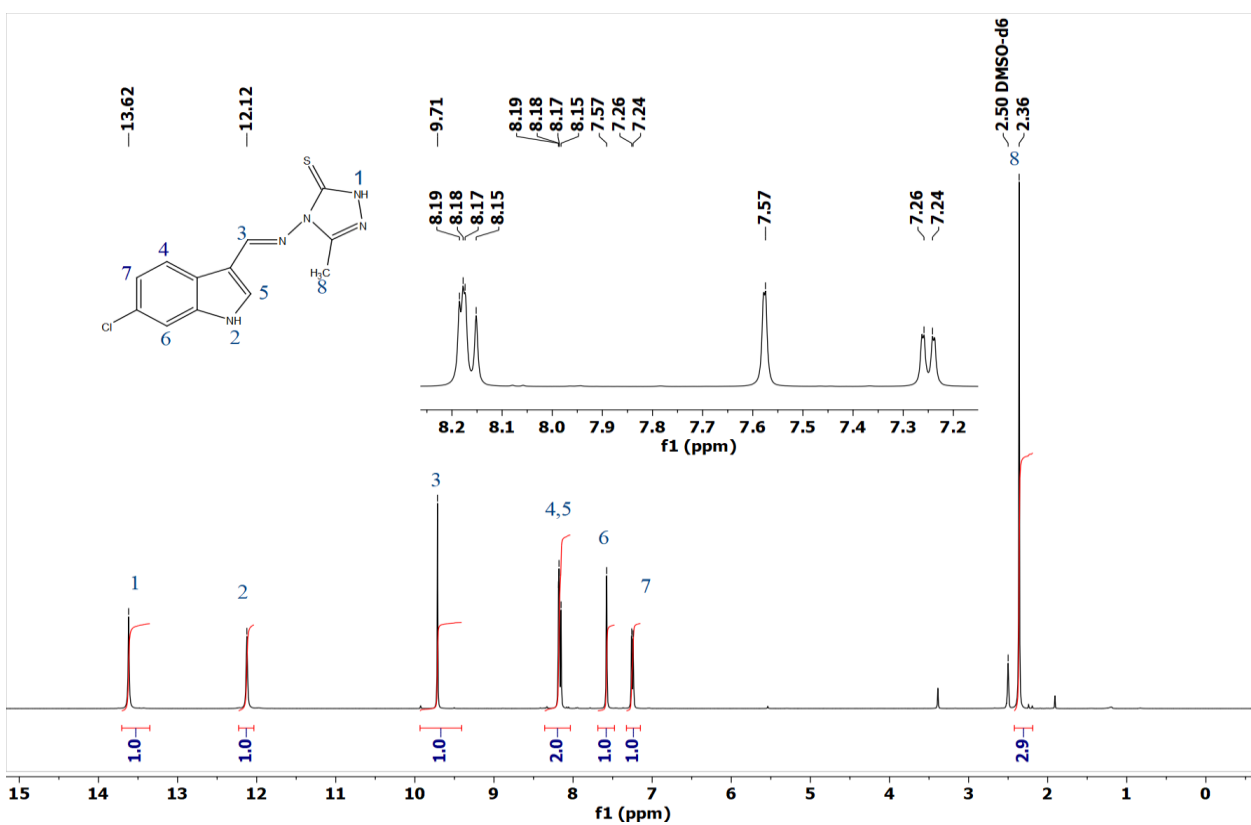


Figure (3.10): <sup>1</sup>H NMR Spectrum of the compound C2

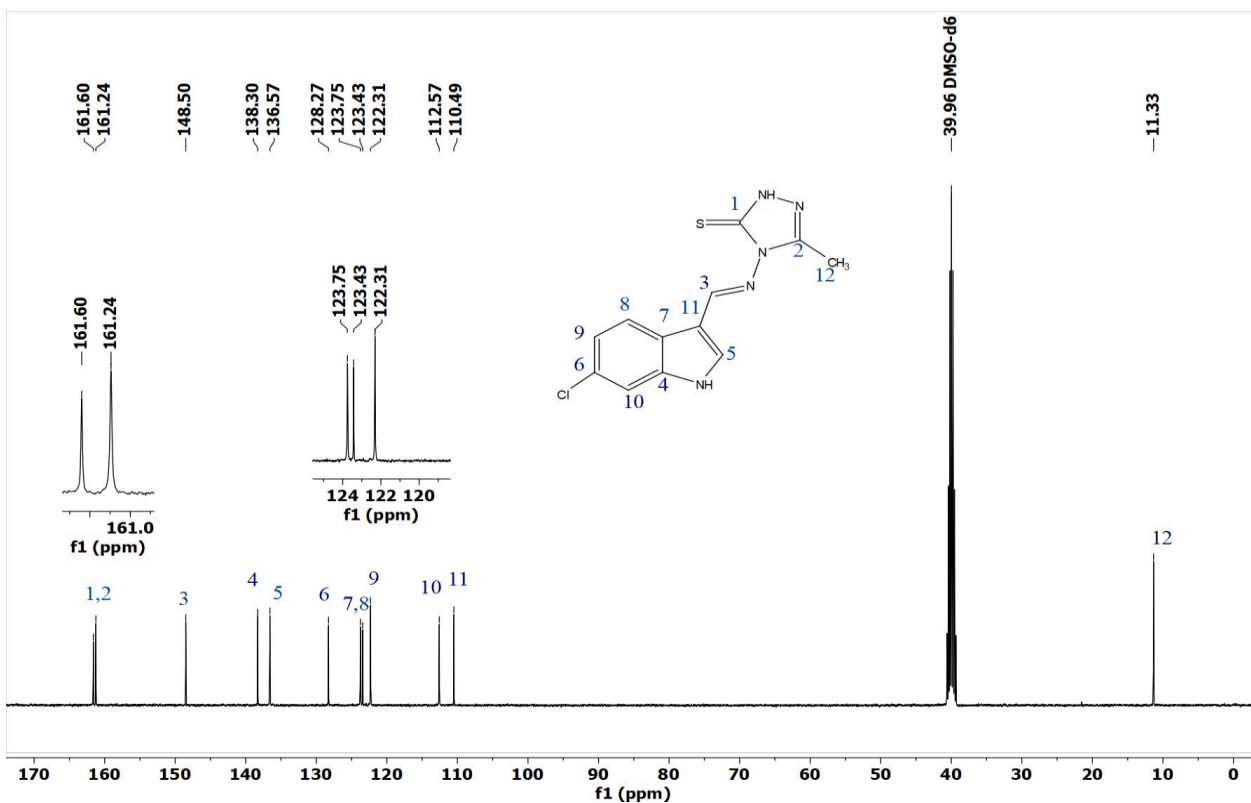


Figure (3.11): <sup>13</sup>C NMR Spectrum of the compound C2

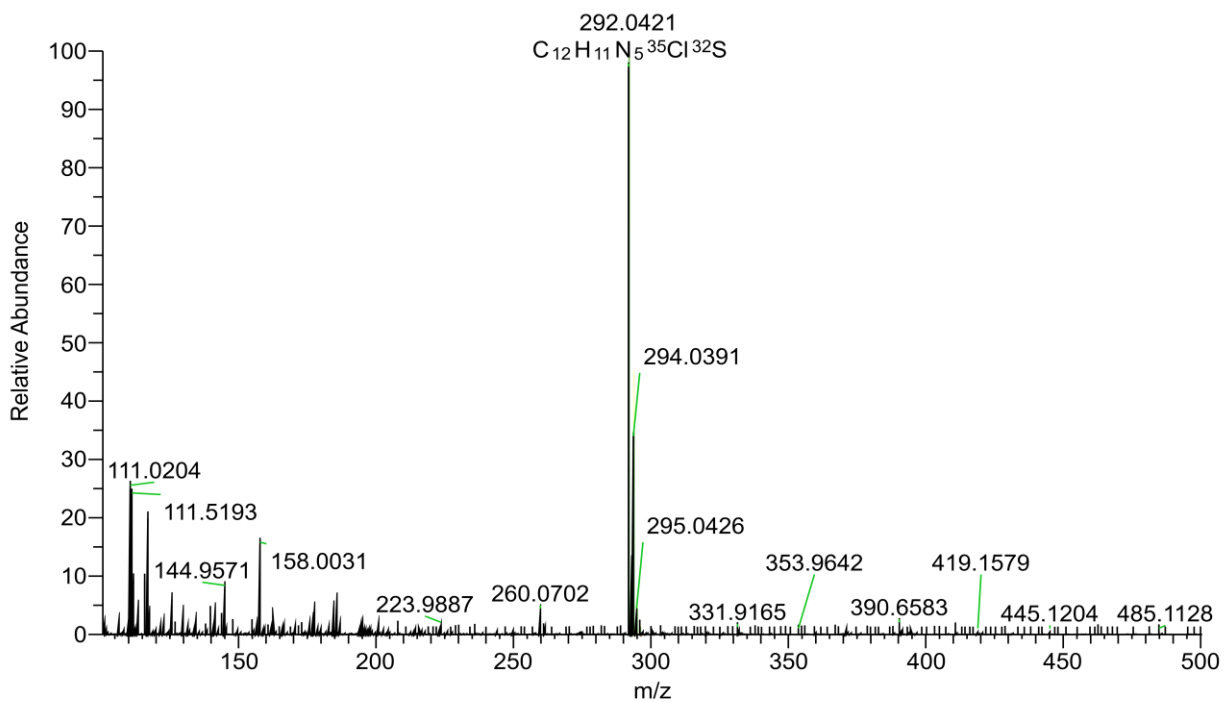


Figure (3.12): Mass Spectrum (ESI) of the compound C2

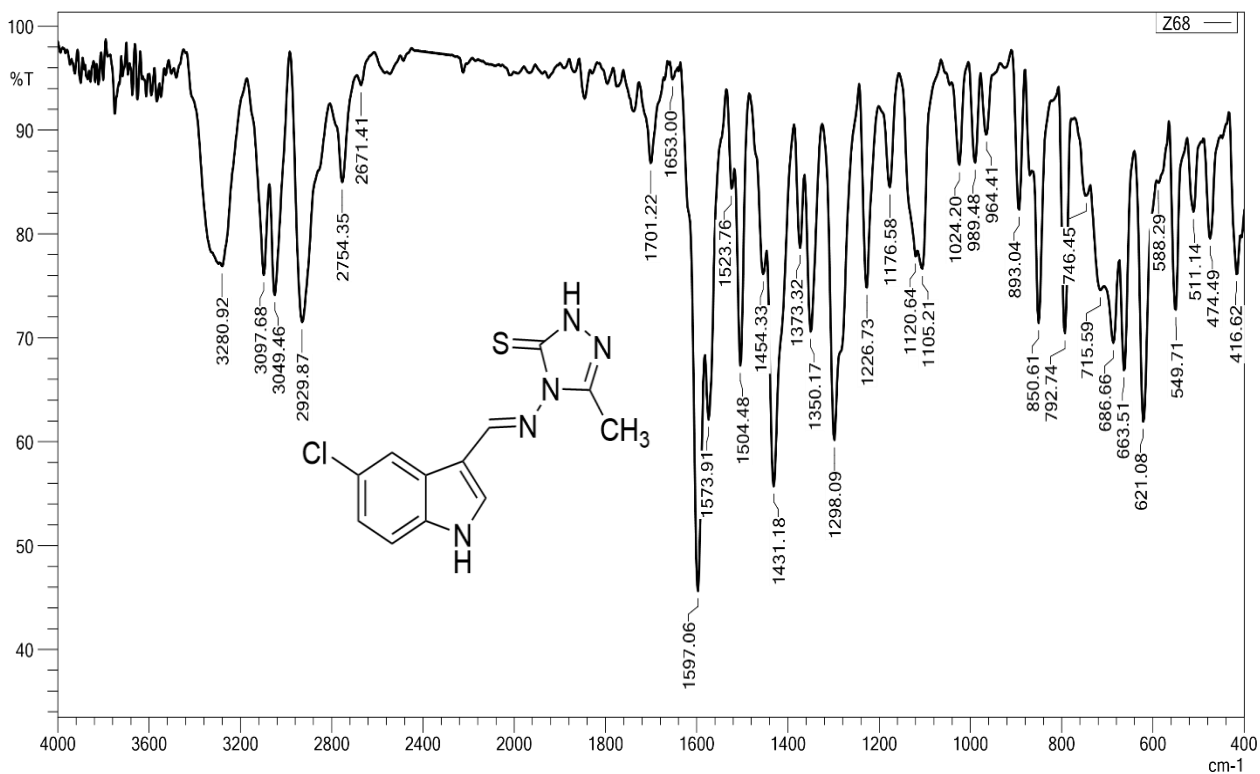


Figure (3.13): IR Spectrum of the compound C3

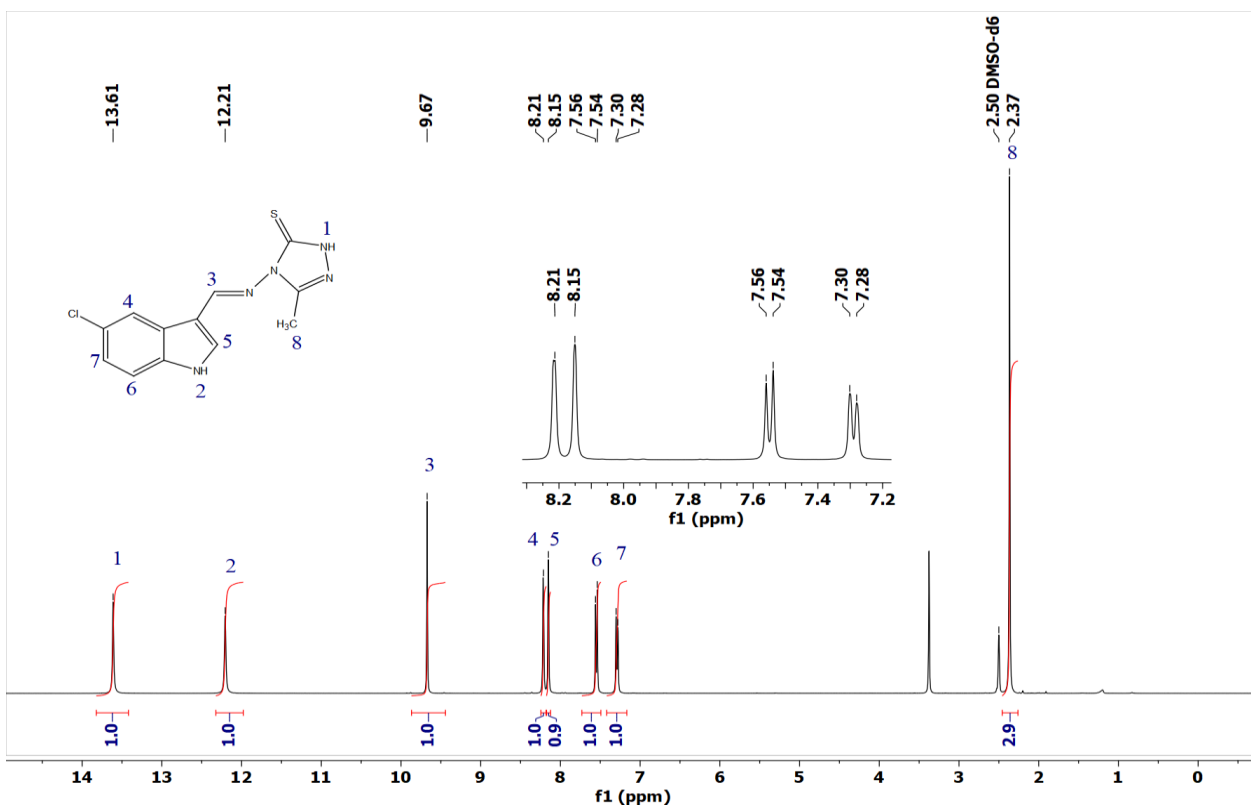


Figure (3.14):  $^1\text{H}$ NMR Spectrum of the compound C3

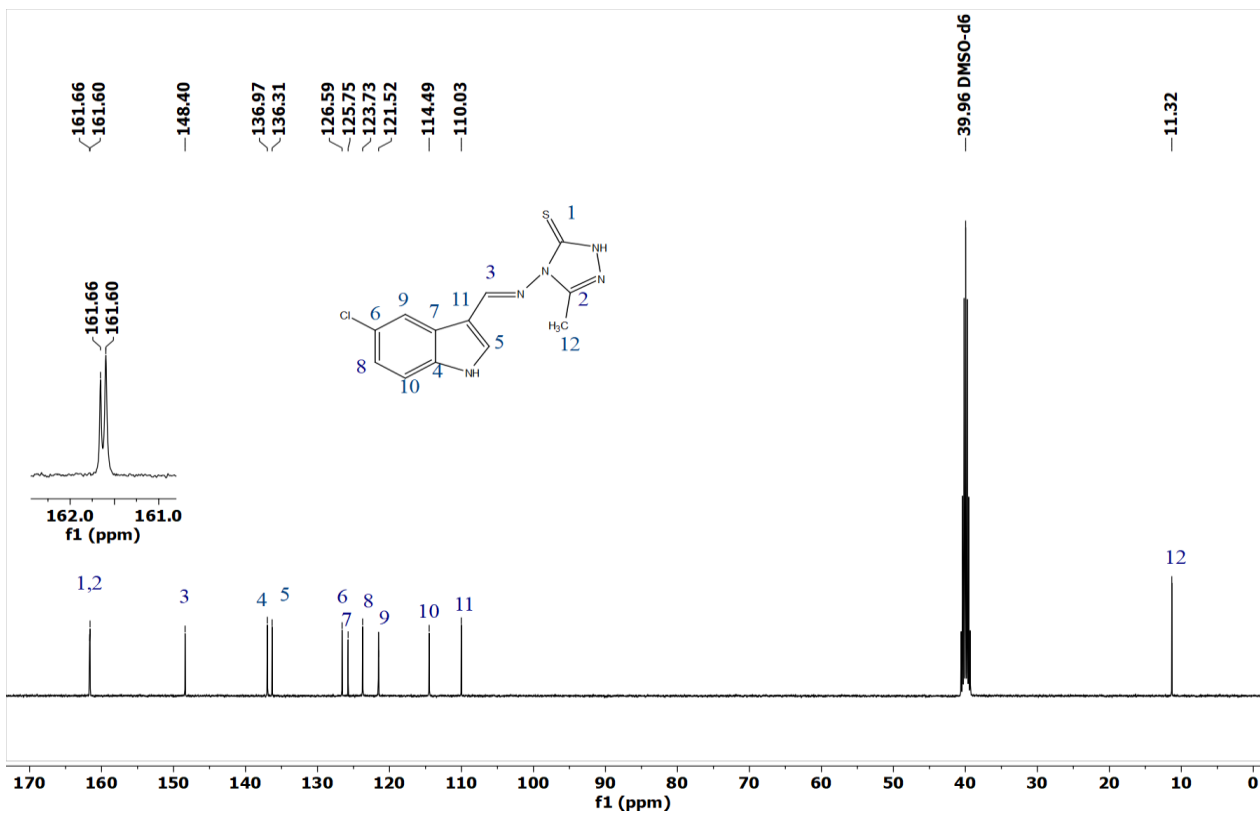


Figure (3.15):  $^{13}\text{C}$ NMR Spectrum of the compound C3

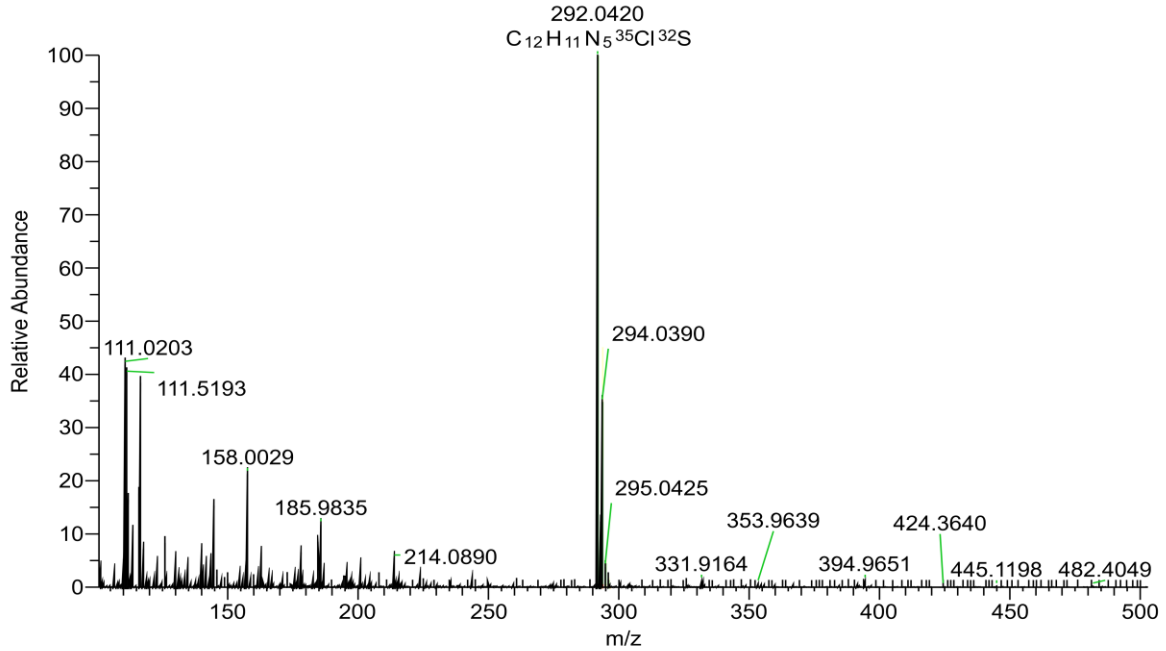


Figure (3.16): Mass Spectrum (ESI) of the compound C3

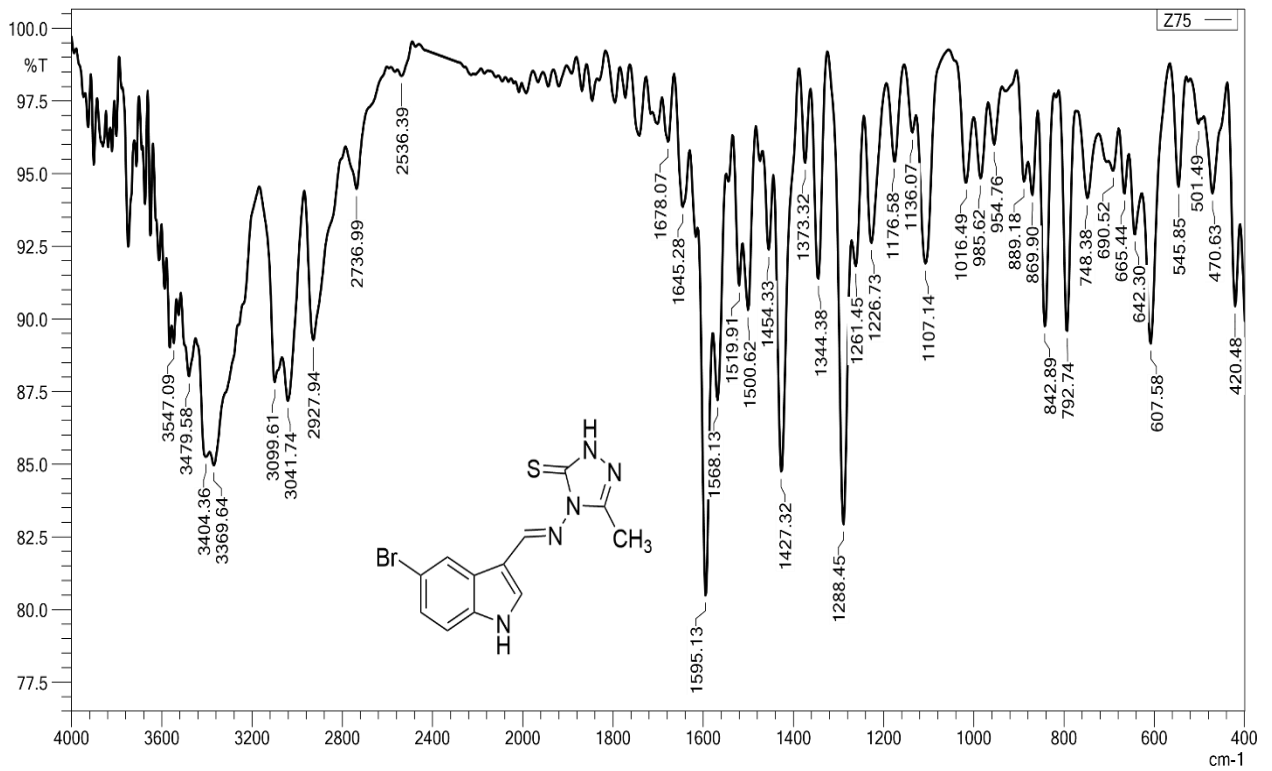
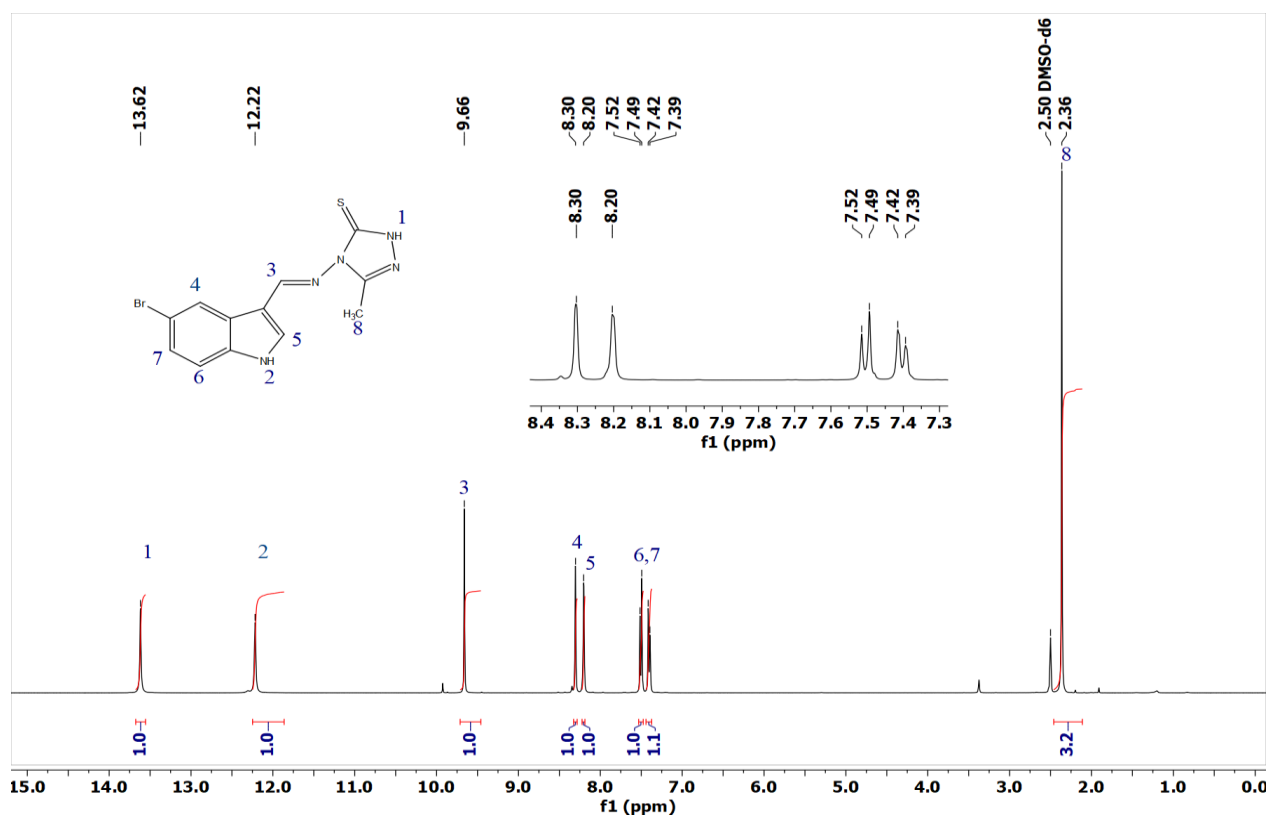
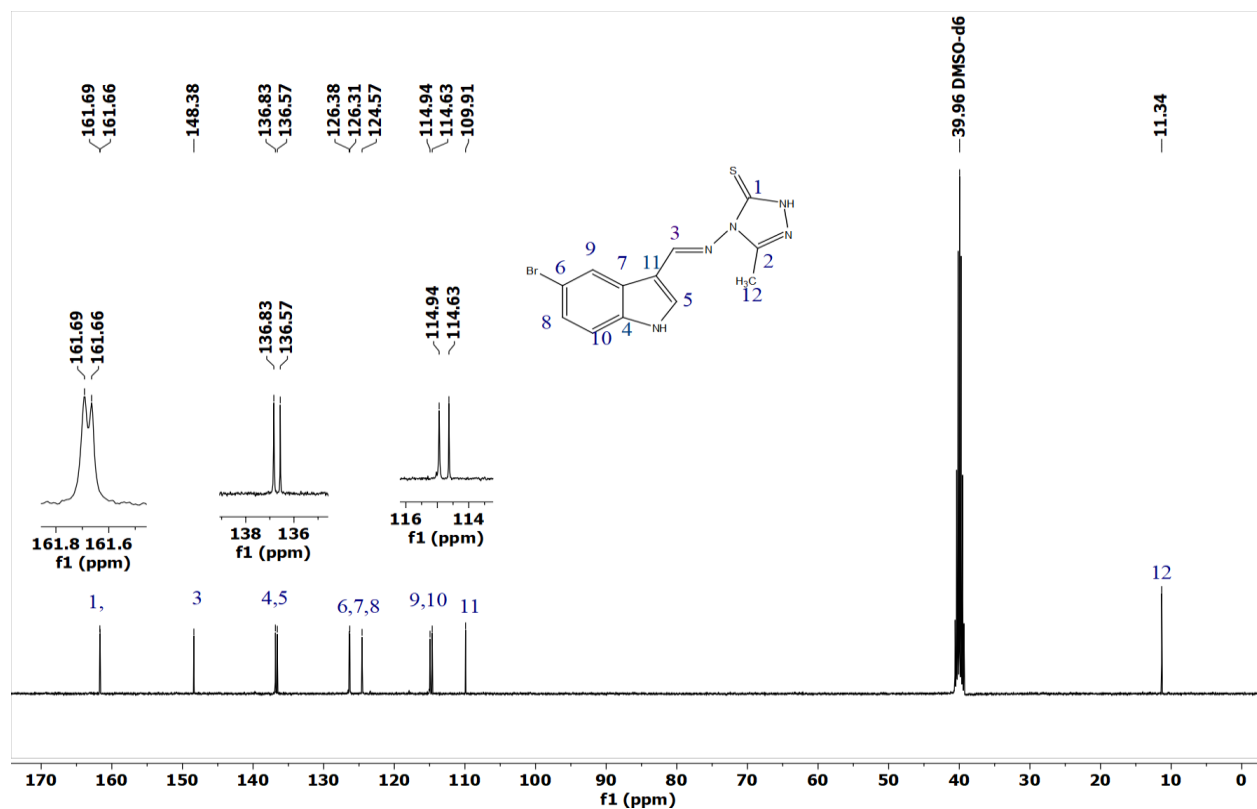


Figure (3.17): IR Spectrum of the compound C4



**Figure (3.18):  $^1\text{H}$ NMR Spectrum of the compound C4**



**Figure (3.19):  $^{13}\text{C}$ NMR Spectrum of the compound C4**

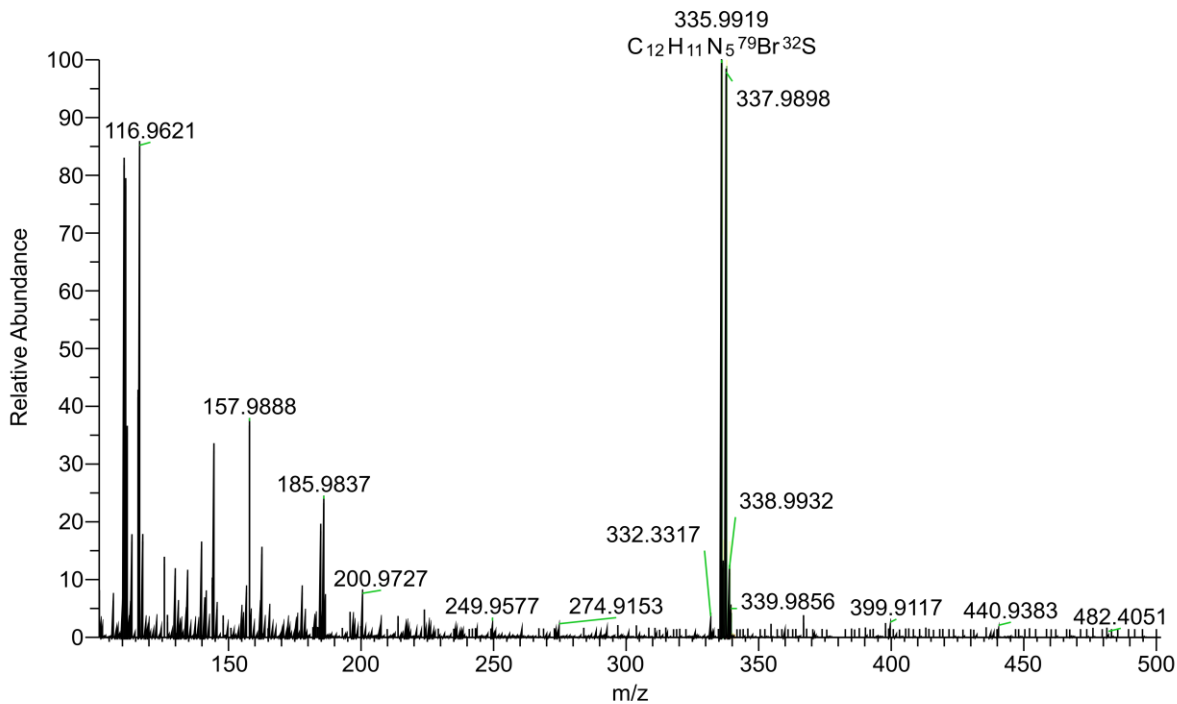


Figure (3.20): Mass Spectrum (ESI) of the compound C4

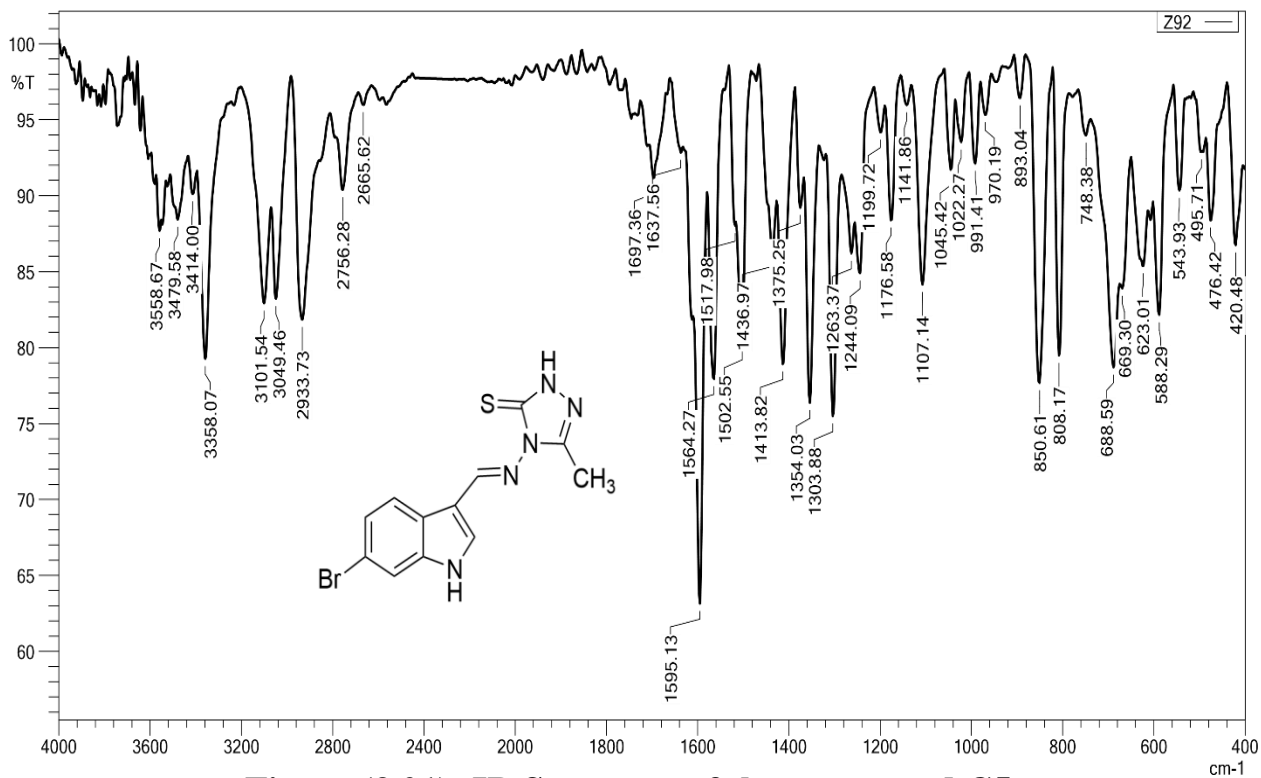
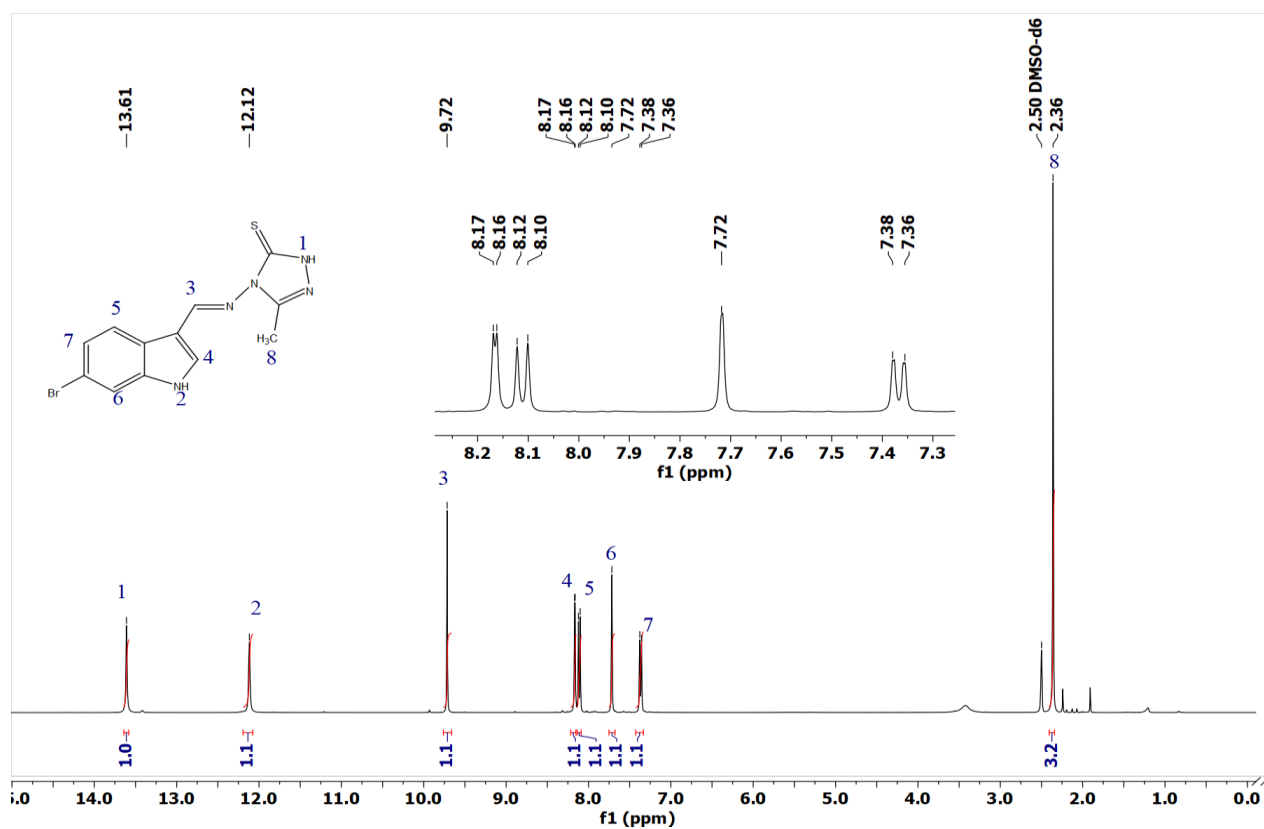
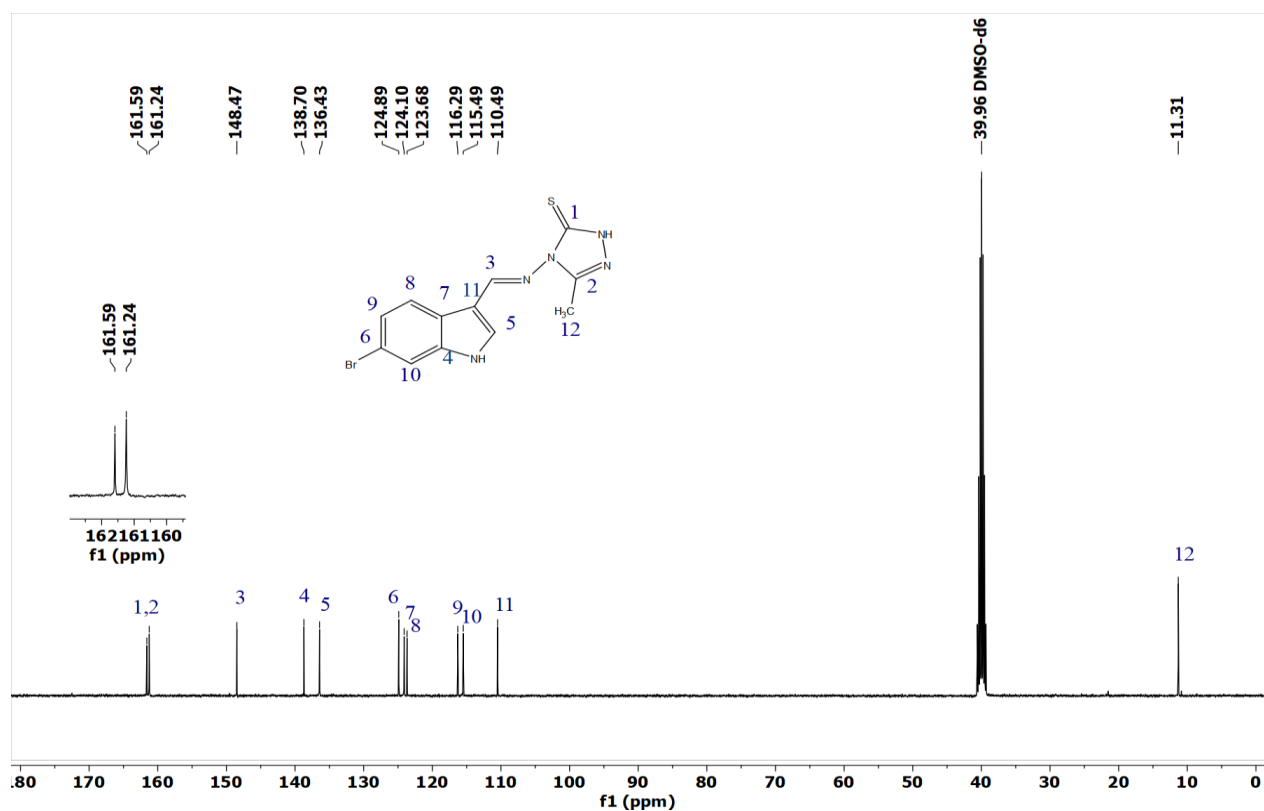


Figure (3.21): IR Spectrum of the compound C5



**Figure (3.22): <sup>1</sup>H NMR Spectrum of the compound C5**



**Figure (3.23): <sup>13</sup>C NMR Spectrum of the compound C5**

UAM\_Z92 #19-27 RT: 0.14-0.21 AV: 5 SB: 5 0.01-0.08 NL: 7.71E6  
T: FTMS + p ESI Full ms [100.0000-1000.0000]

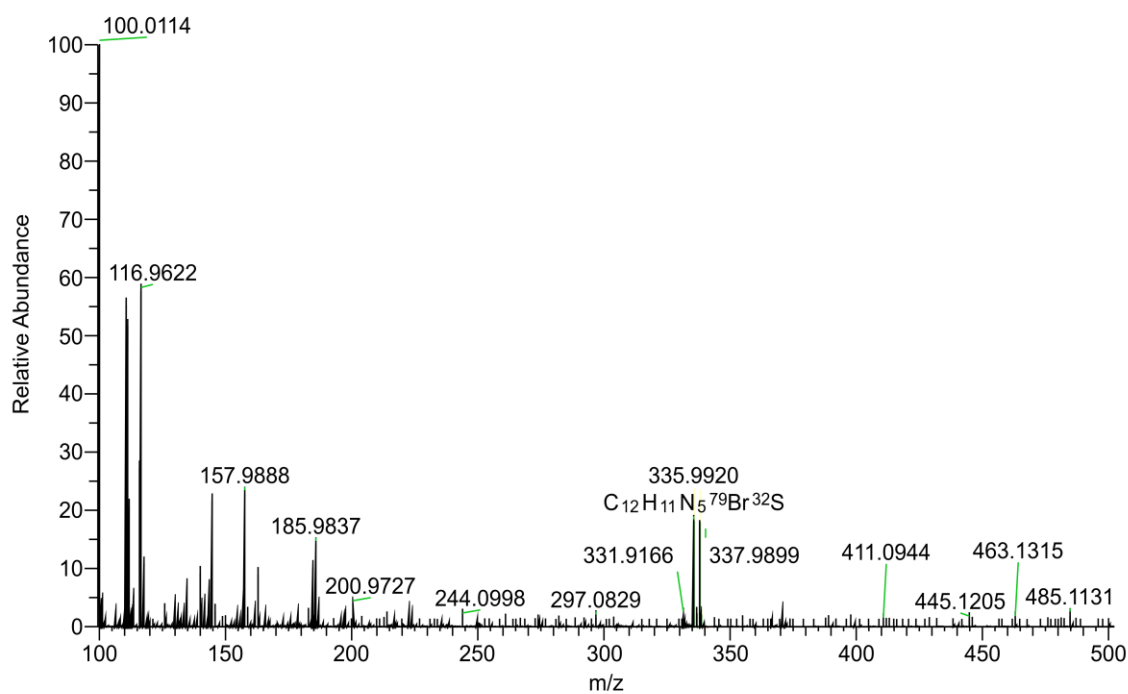


Figure (3.24): Mass Spectrum (ESI) of the compound C5

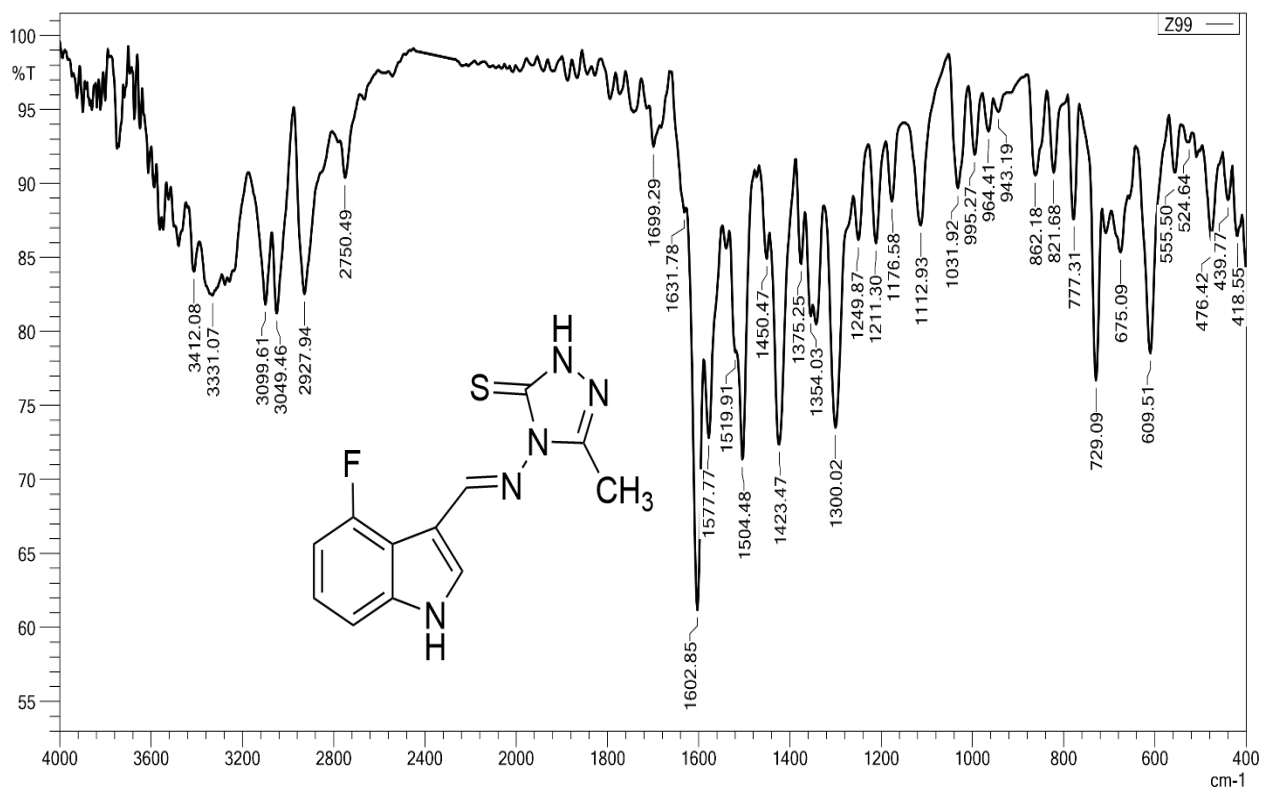
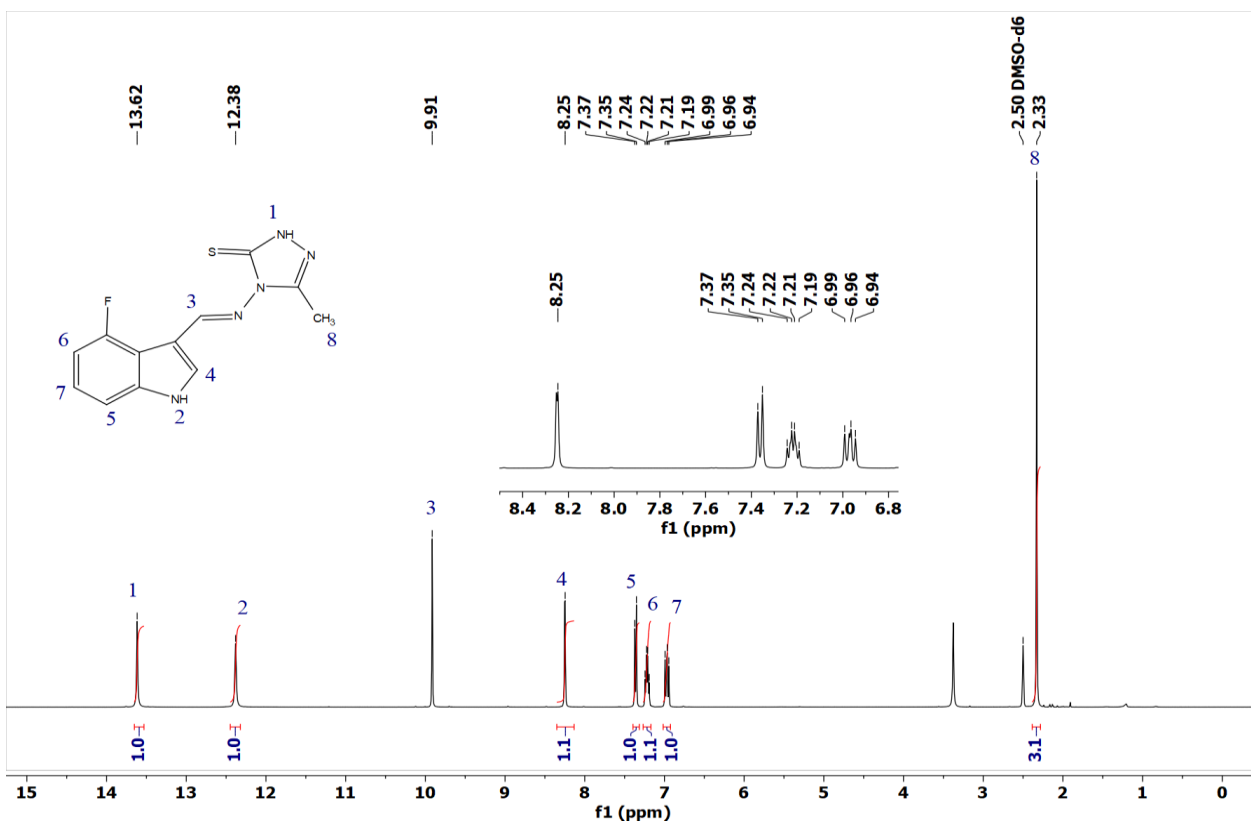
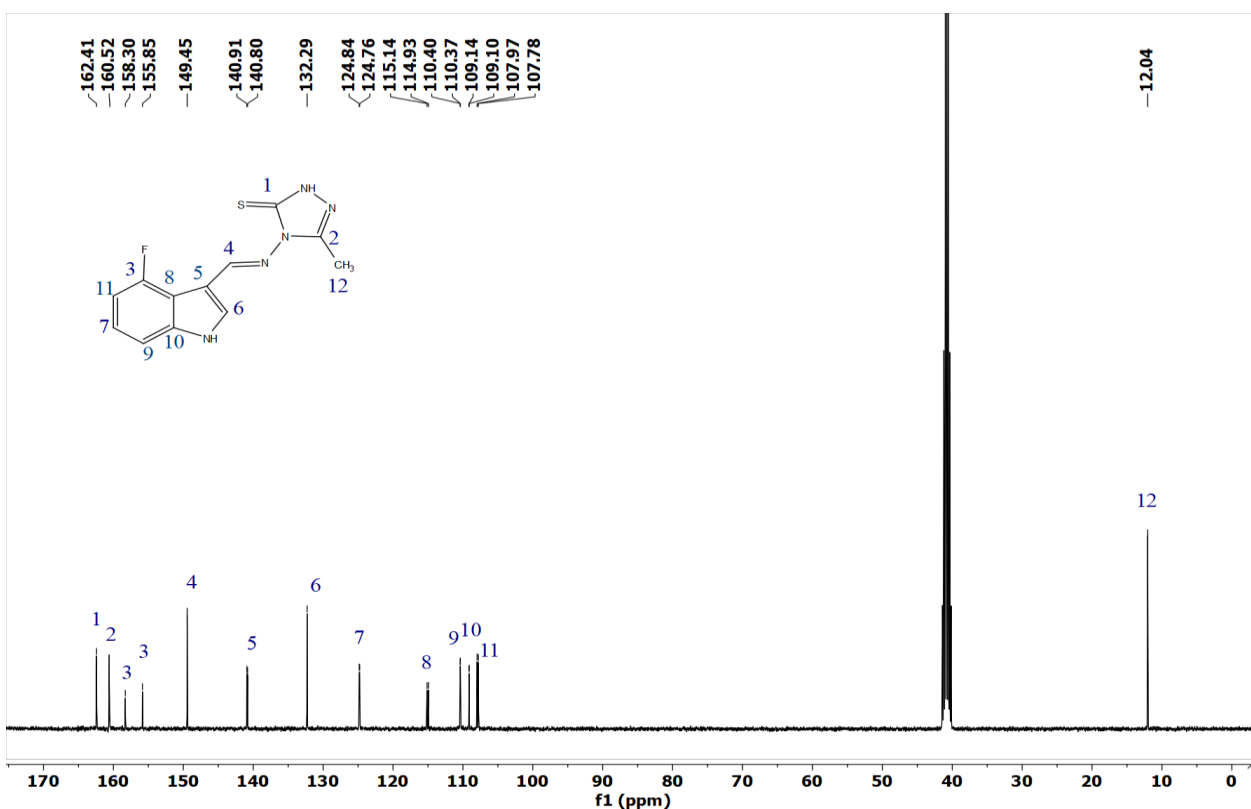


Figure (3.25): IR Spectrum of the compound C6



**Figure (3.26): <sup>1</sup>H NMR Spectrum of the compound C6**



**Figure (3.27): <sup>13</sup>C NMR Spectrum of the compound C6**

UAM\_Z99\_20251119175305 #18-27 RT: 0.13-0.2 AV: 5 SB: 5 0.01-0.08 NL: 1.64E8  
T: FTMS + p ESI Full ms [100.0000-1000.0000]

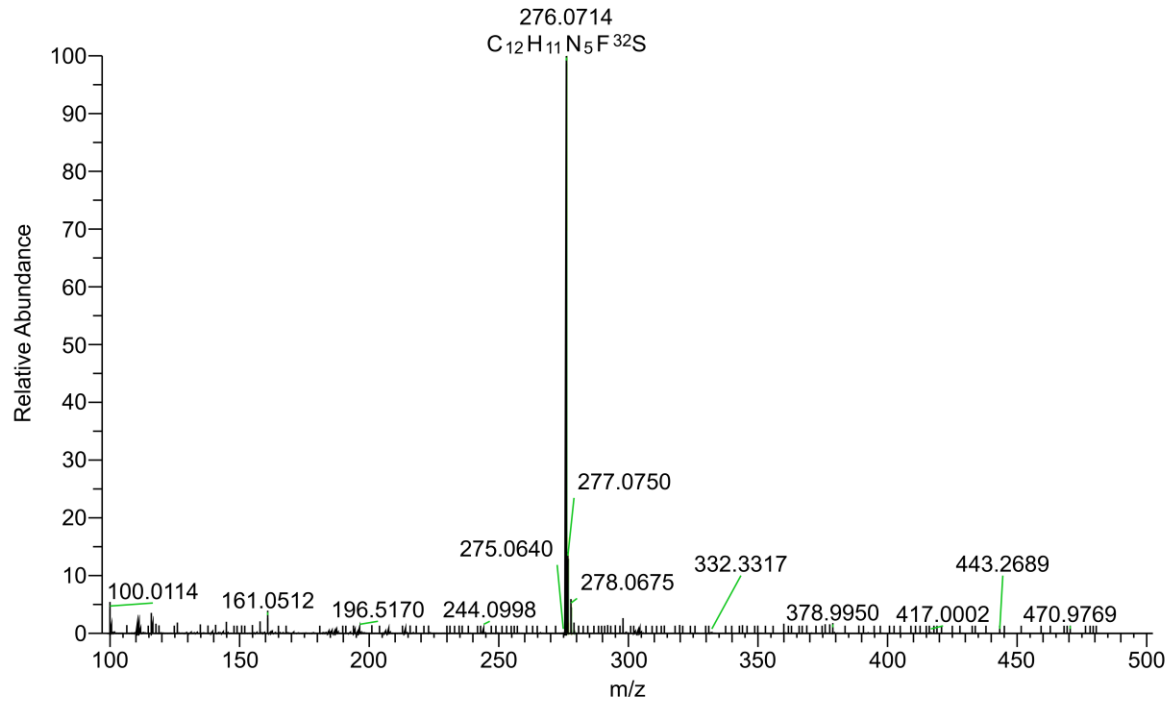


Figure (3.28): Mass Spectrum (ESI) of the compound C6

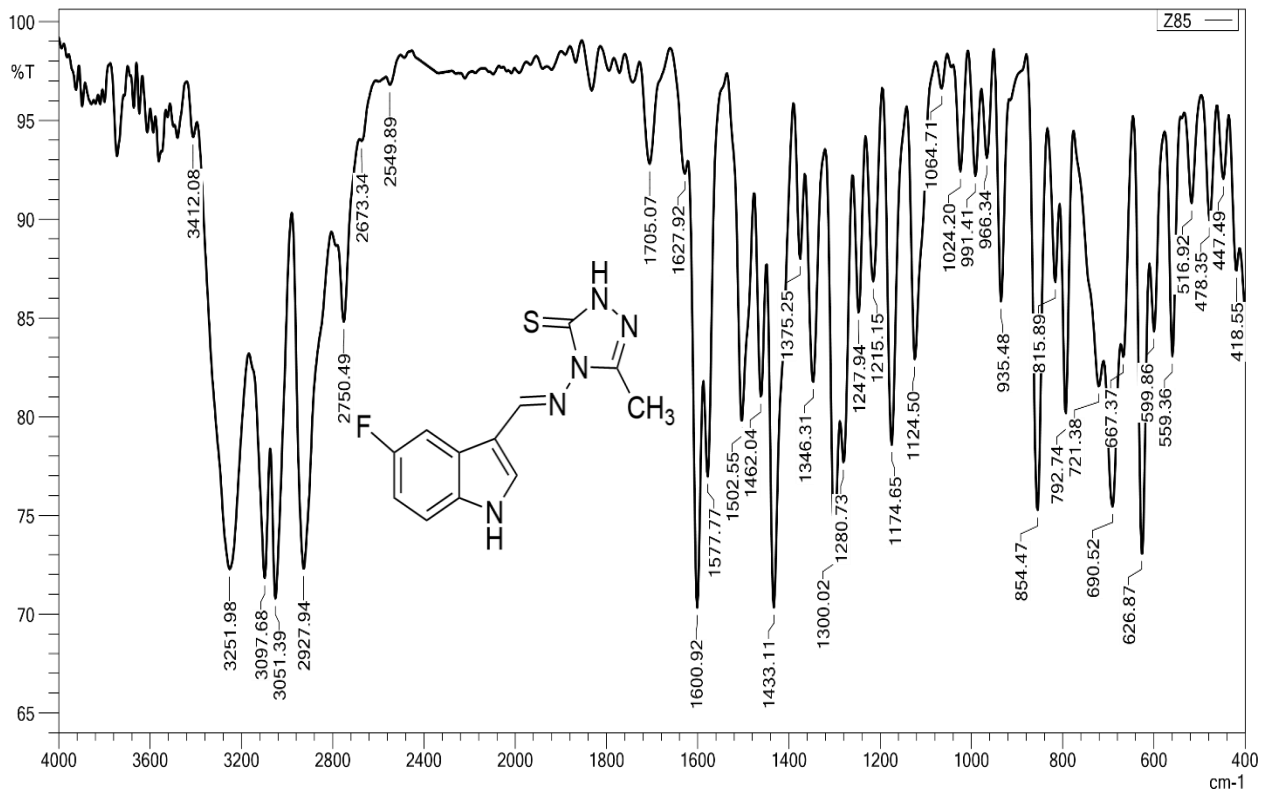


Figure (3.29): IR Spectrum of the compound C7

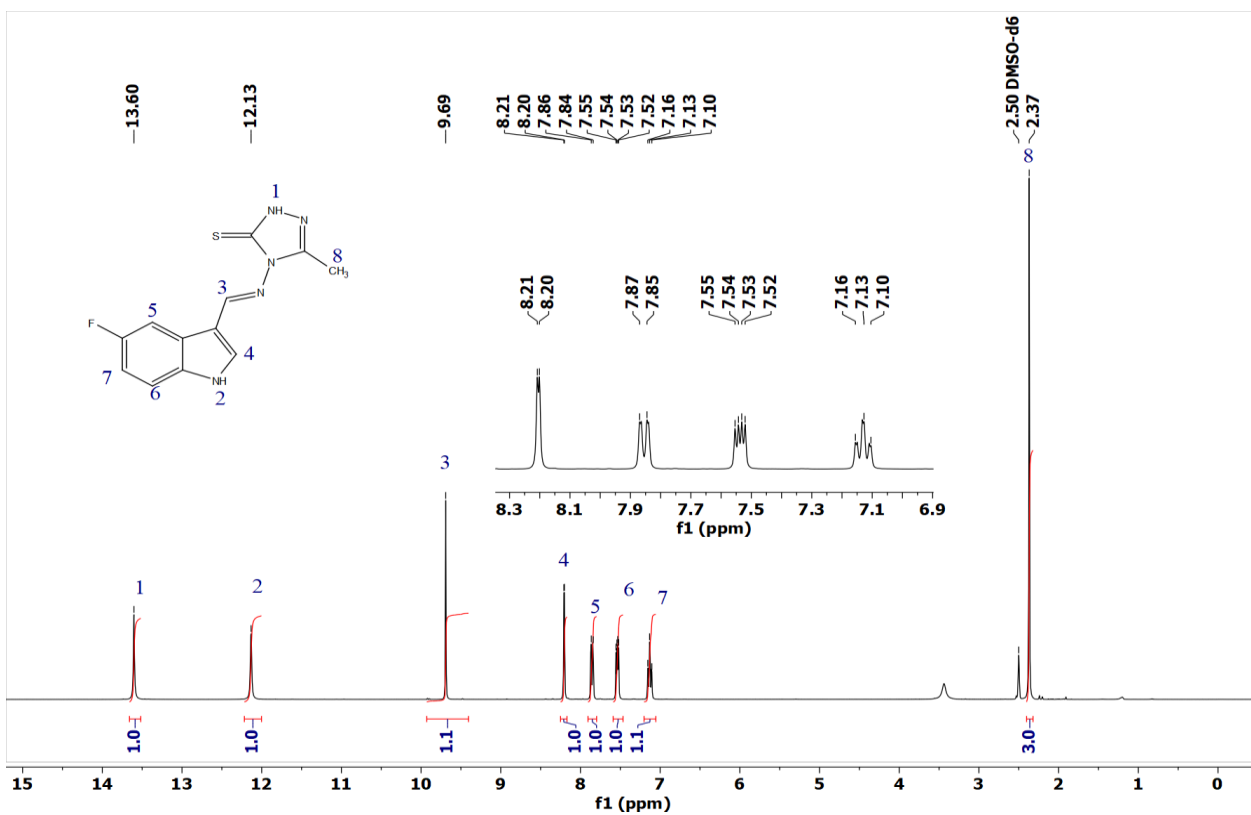


Figure (3.30):  $^1\text{H}$ NMR Spectrum of the compound C7

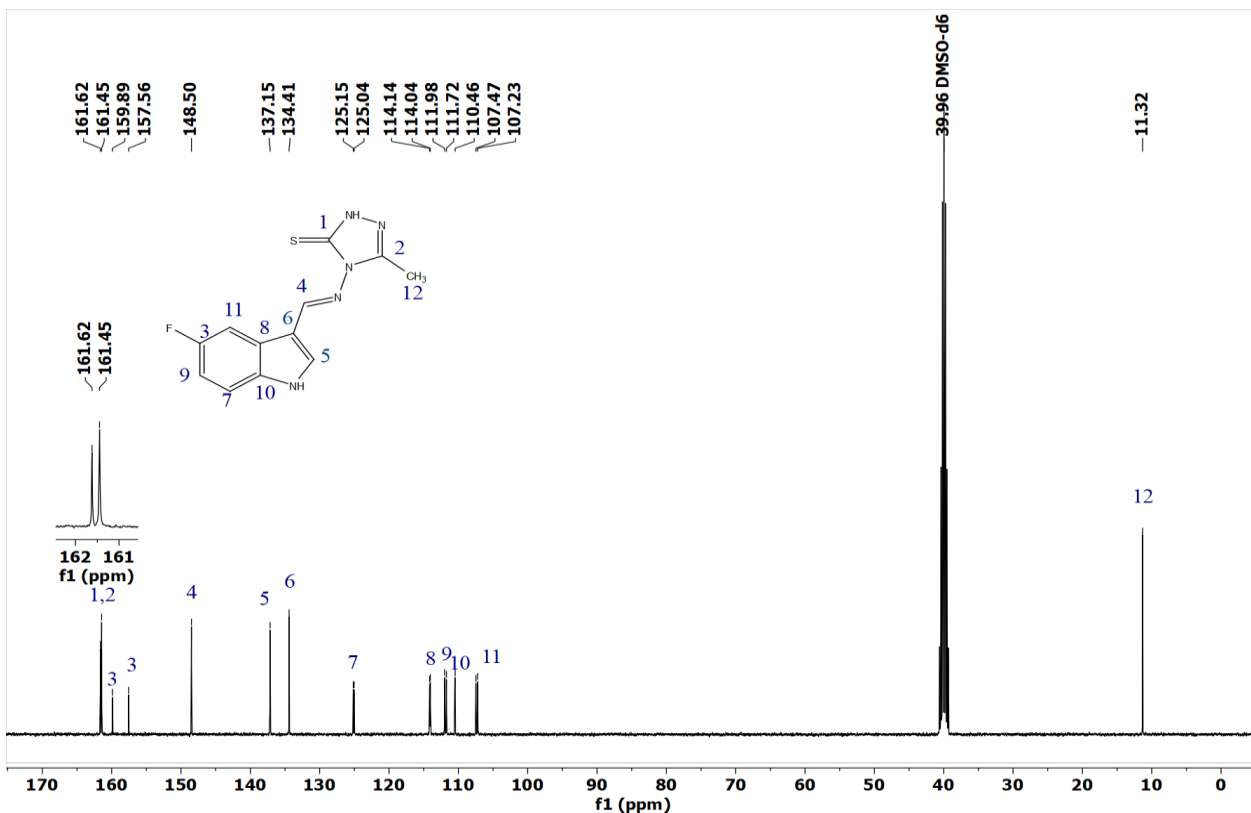


Figure (3.31):  $^{13}\text{C}$ NMR Spectrum of the compound C7

UAM\_Z85 #18-26 RT: 0.13-0.2 AV: 4 SB: 5 0.01-0.08 NL: 7.46E6  
T: FTMS + p ESI Full ms [100.0000-1000.0000]

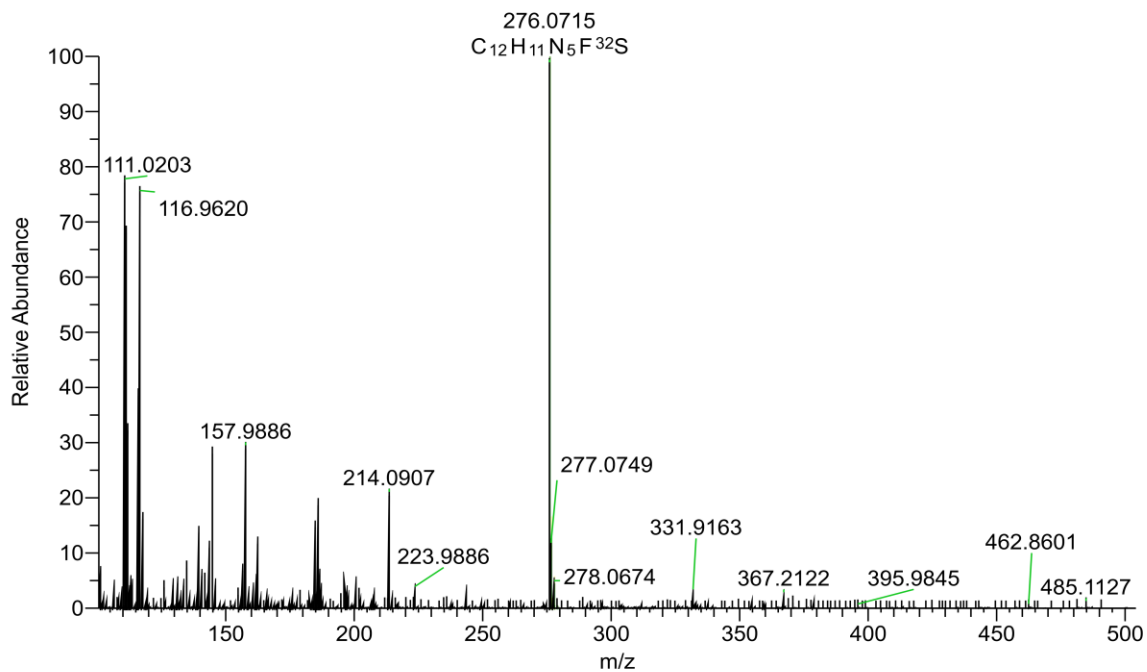


Figure (3.32): Mass Spectrum (ESI) of the compound C7

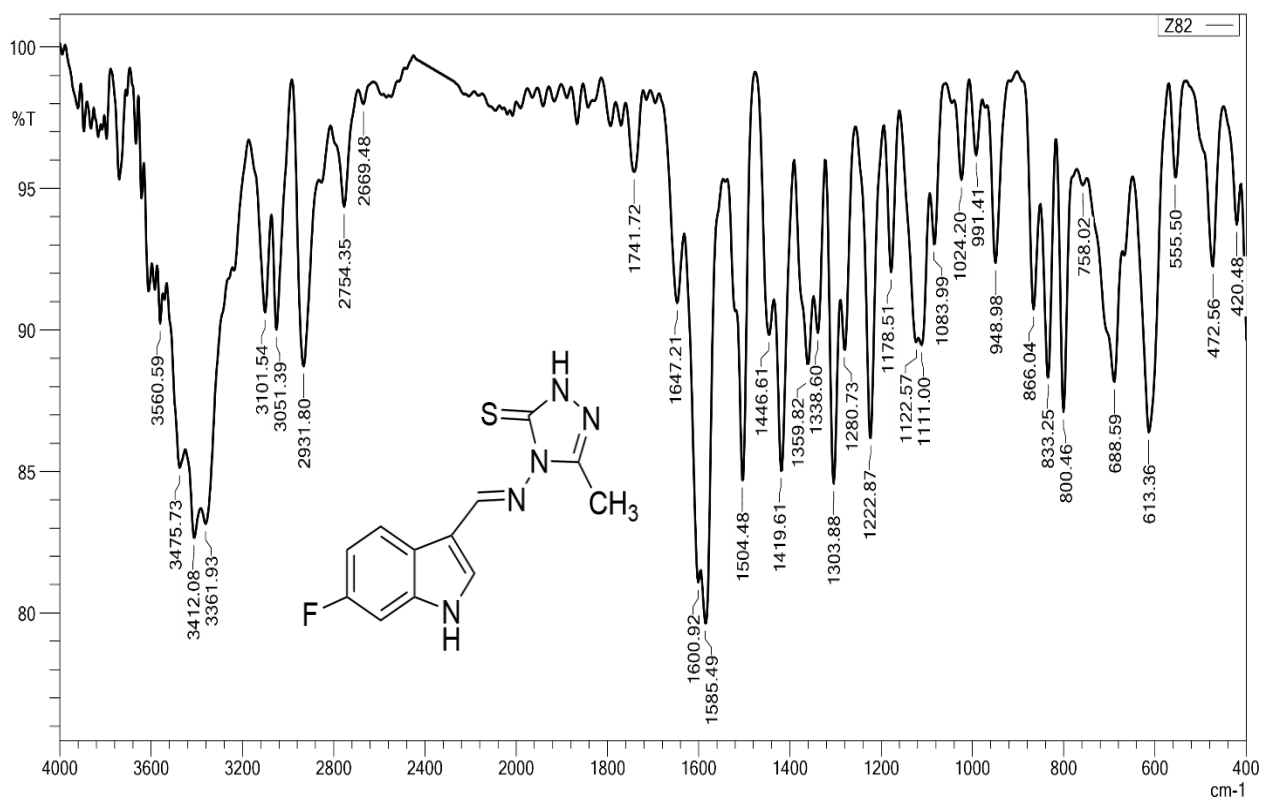
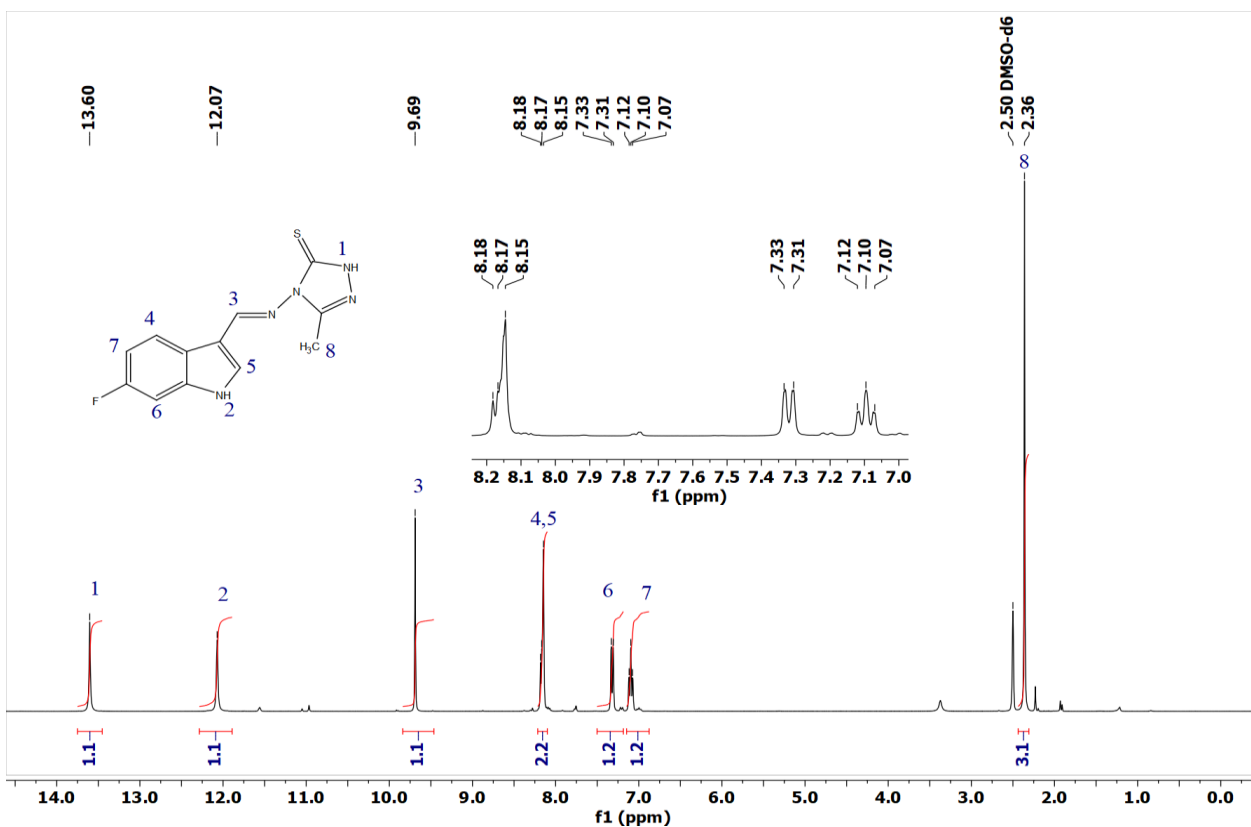
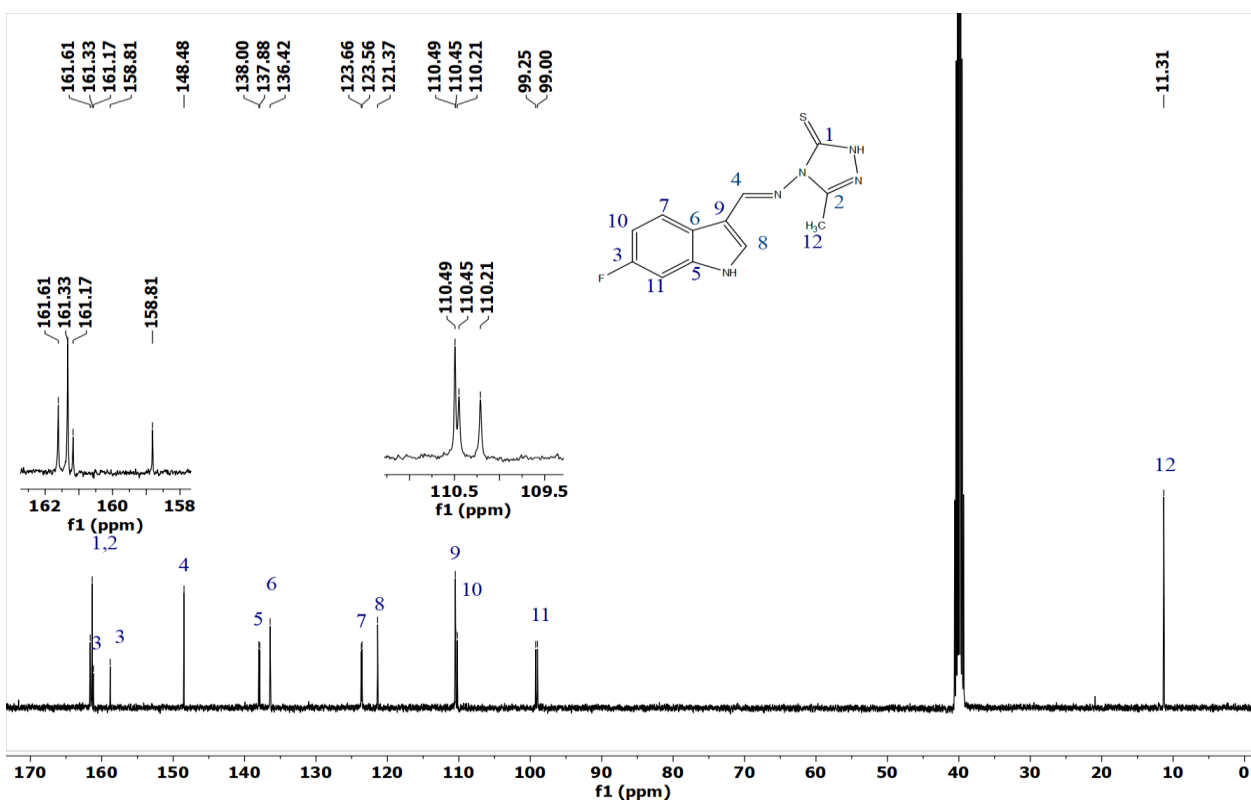


Figure (3.33): IR Spectrum of the compound C8



**Figure (3.34):  $^1\text{H}$ NMR Spectrum of the compound C8**



**Figure (3.35):  $^{13}\text{C}$ NMR Spectrum of the compound C8**

UAM\_Z82 #19-27 RT: 0.14-0.2 AV: 5 SB: 5 0.01-0.08 NL: 1.16E7  
T: FTMS + p ESI Full ms [100.0000-1000.0000]

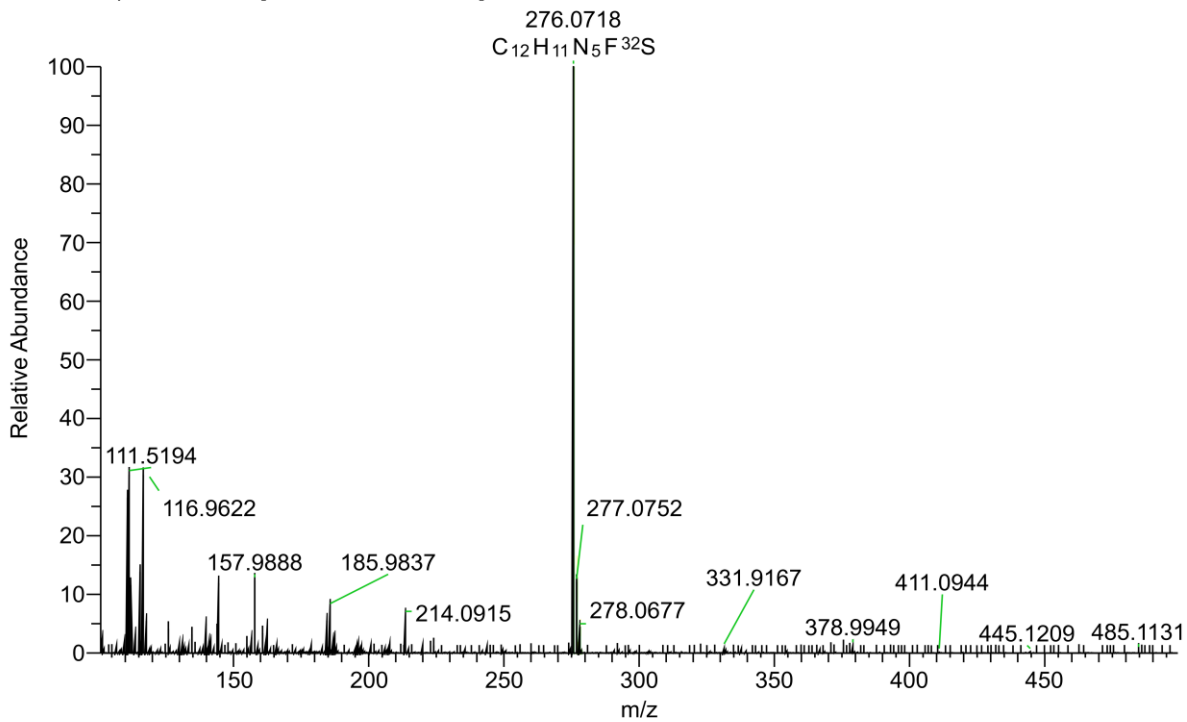


Figure (3.36): Mass Spectrum (ESI) of the compound C8

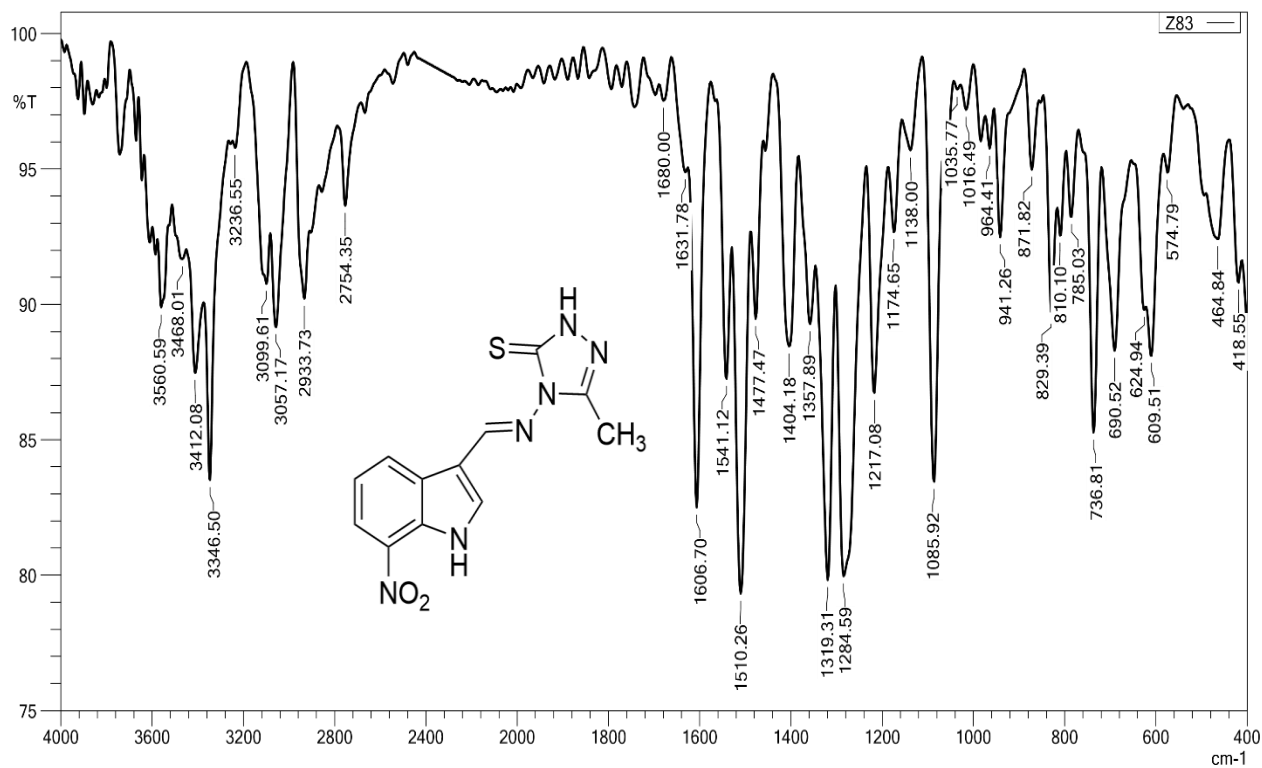


Figure (3.37): IR Spectrum of the compound C9

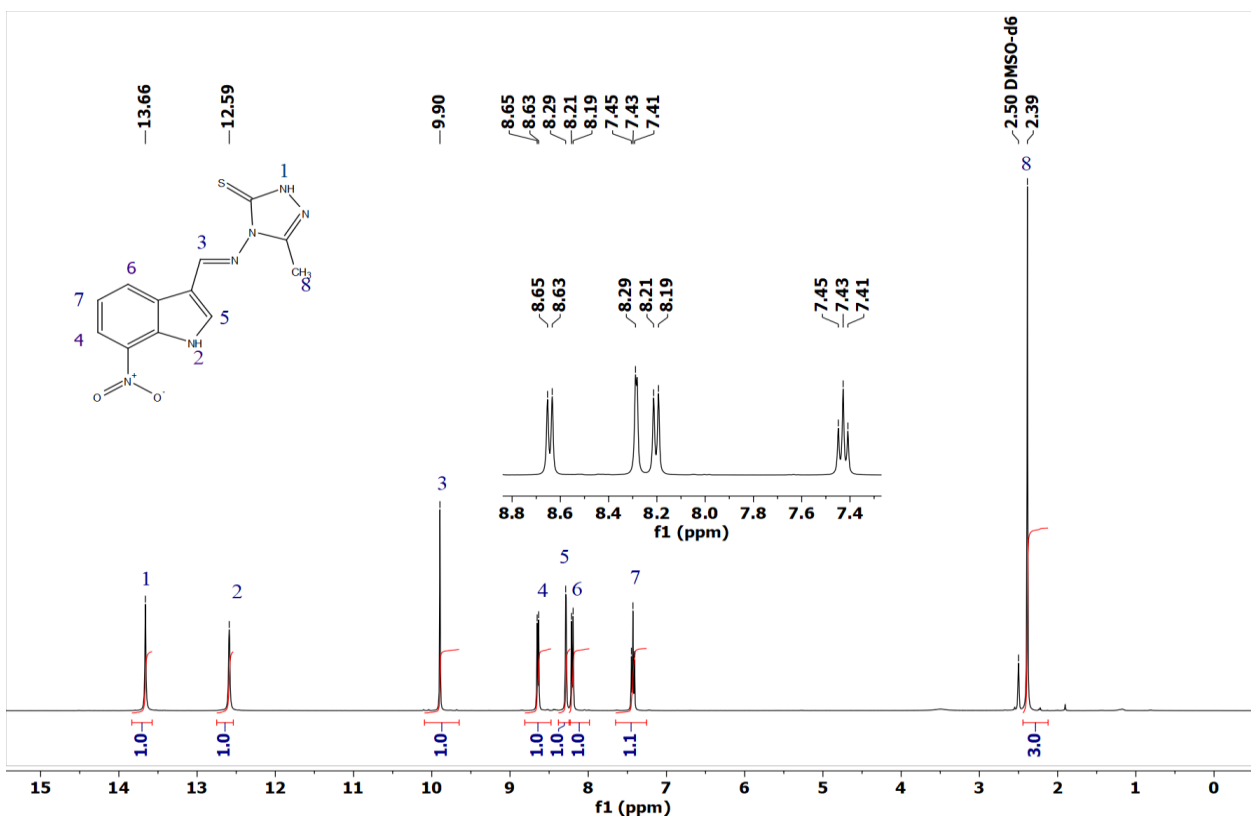


Figure (3.38):  $^1\text{H}$ NMR Spectrum of the compound C9

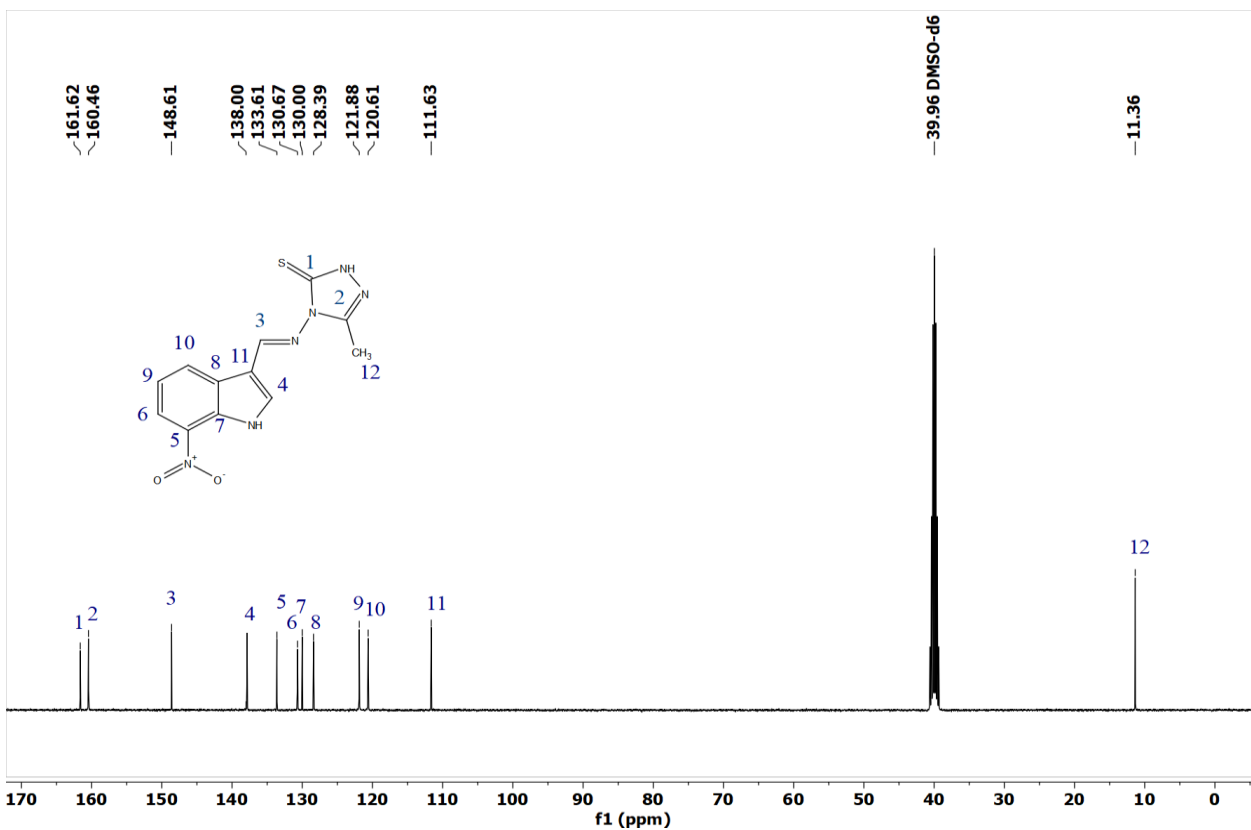


Figure (3.39):  $^{13}\text{C}$ NMR Spectrum of the compound C9

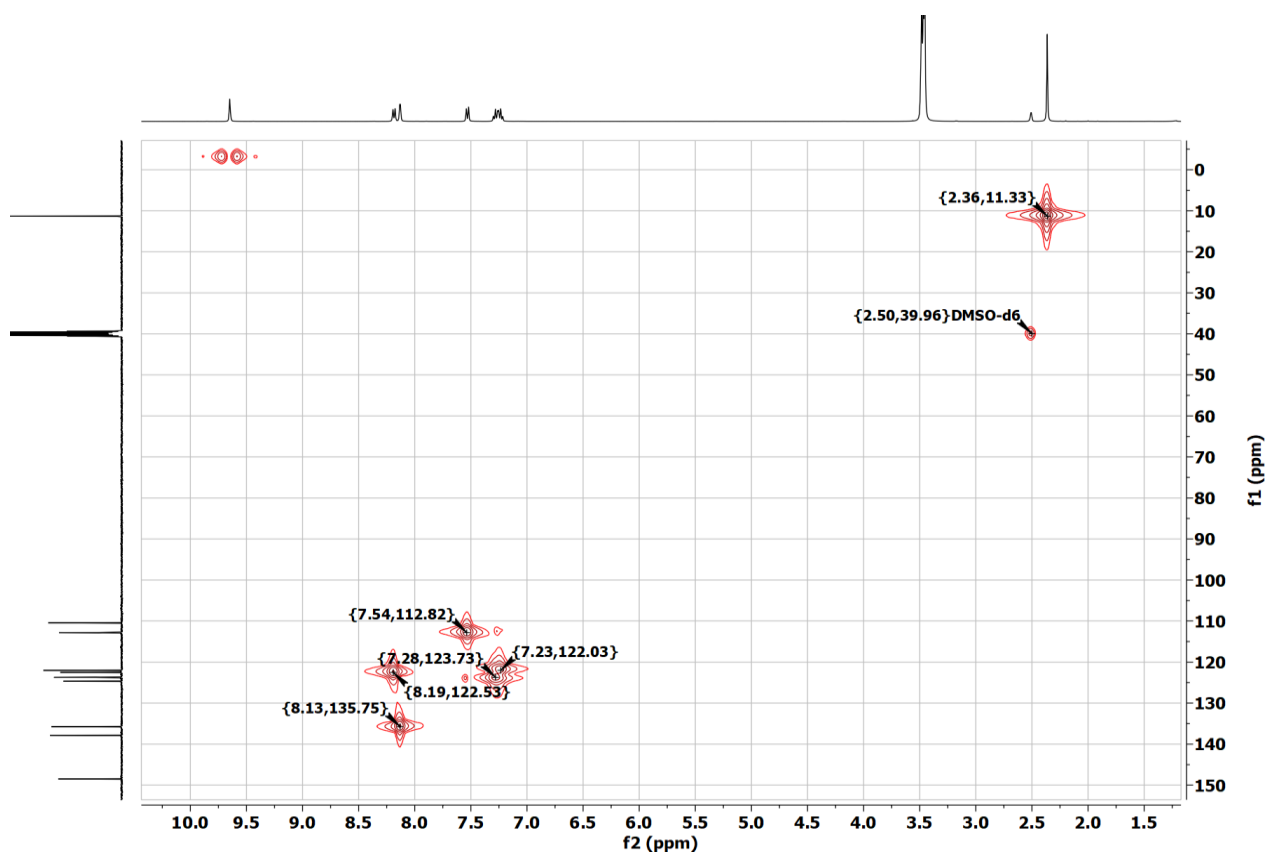


Figure (3.40): HSQC Spectrum of the compound C9

UAM\_Z83 #18-27 RT: 0.13-0.2 AV: 5 SB: 5 0.01-0.08 NL: 6.79E6  
 T: FTMS + p ESI Full ms [100.0000-1000.0000]

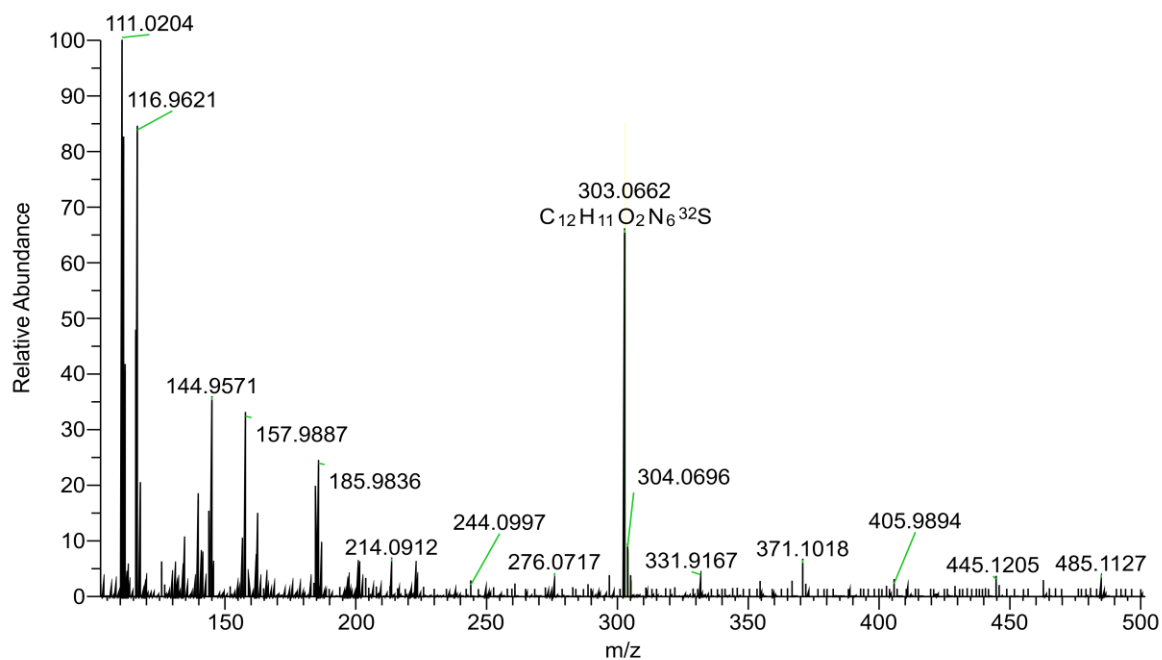


Figure (3.41): Mass Spectrum (ESI) of the compound C9

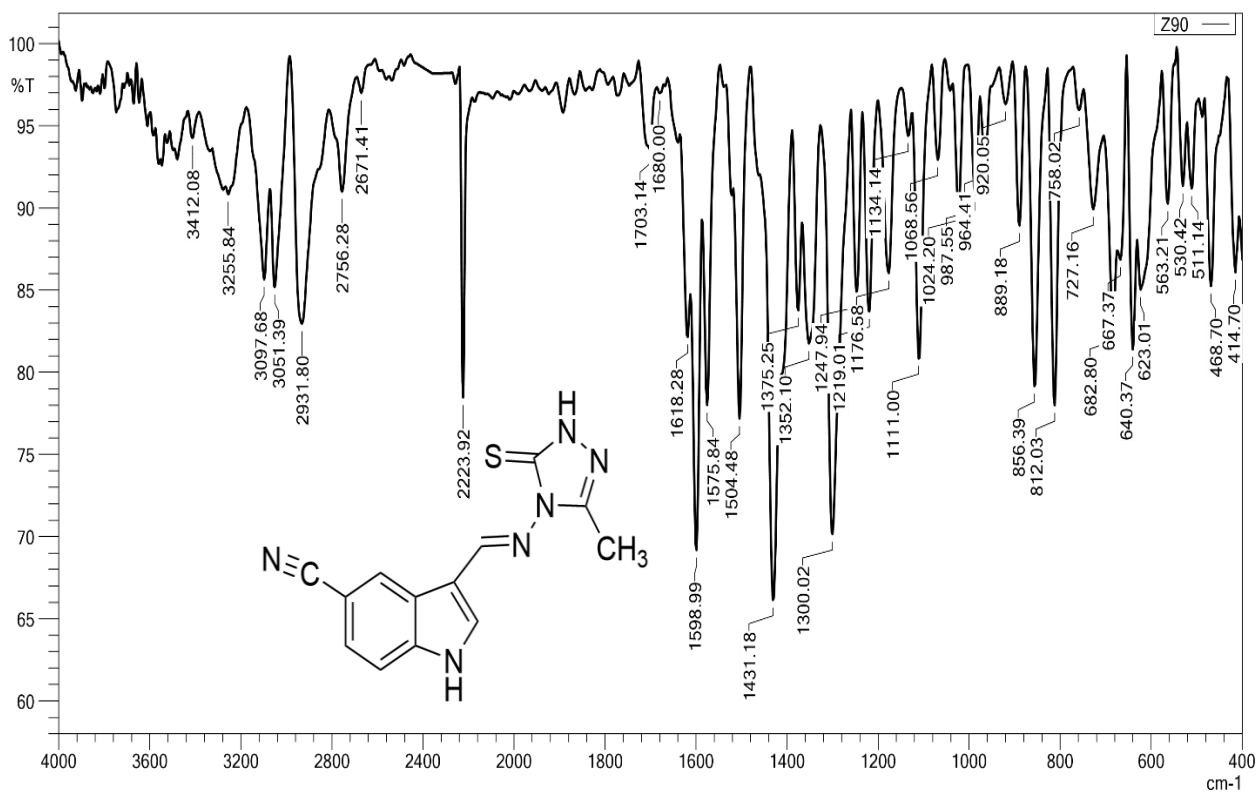


Figure (3.42): IR Spectrum of the compound C10

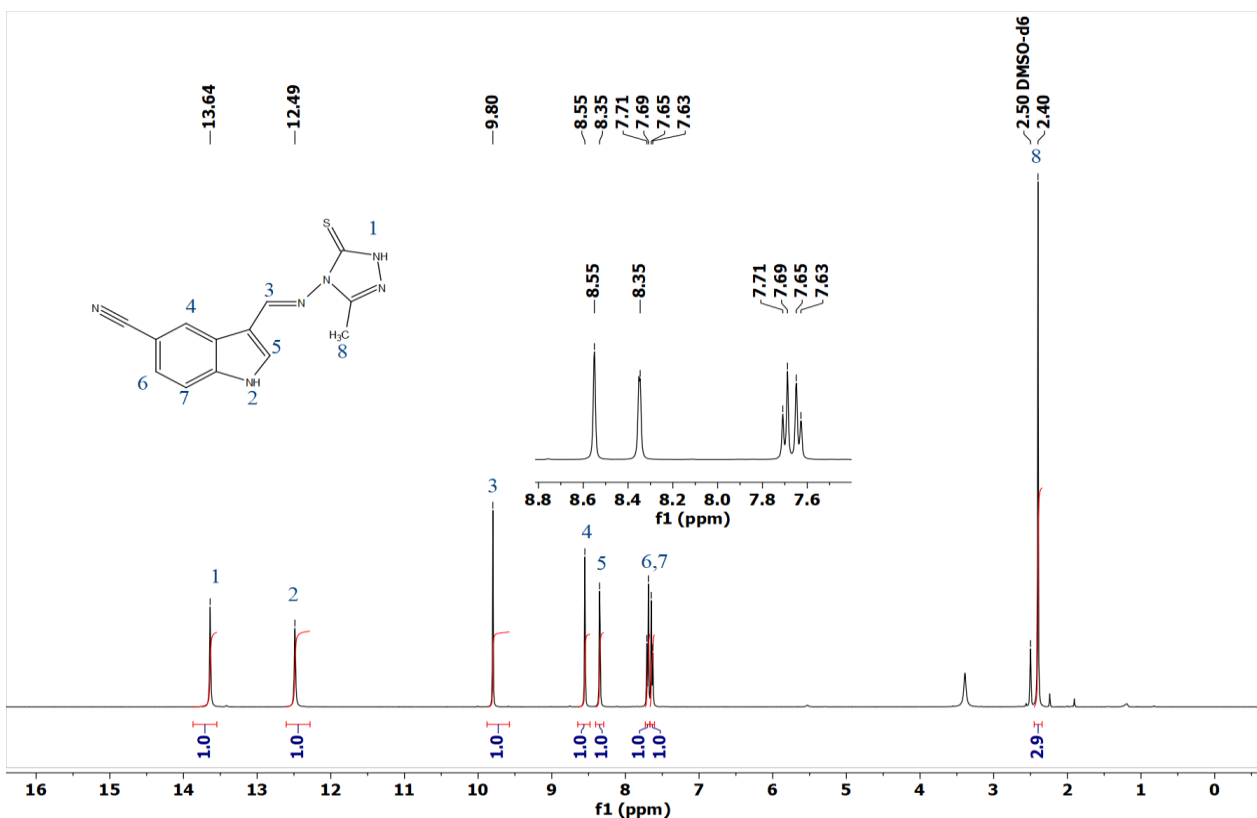


Figure (3.43): <sup>1</sup>H NMR Spectrum of the compound C10

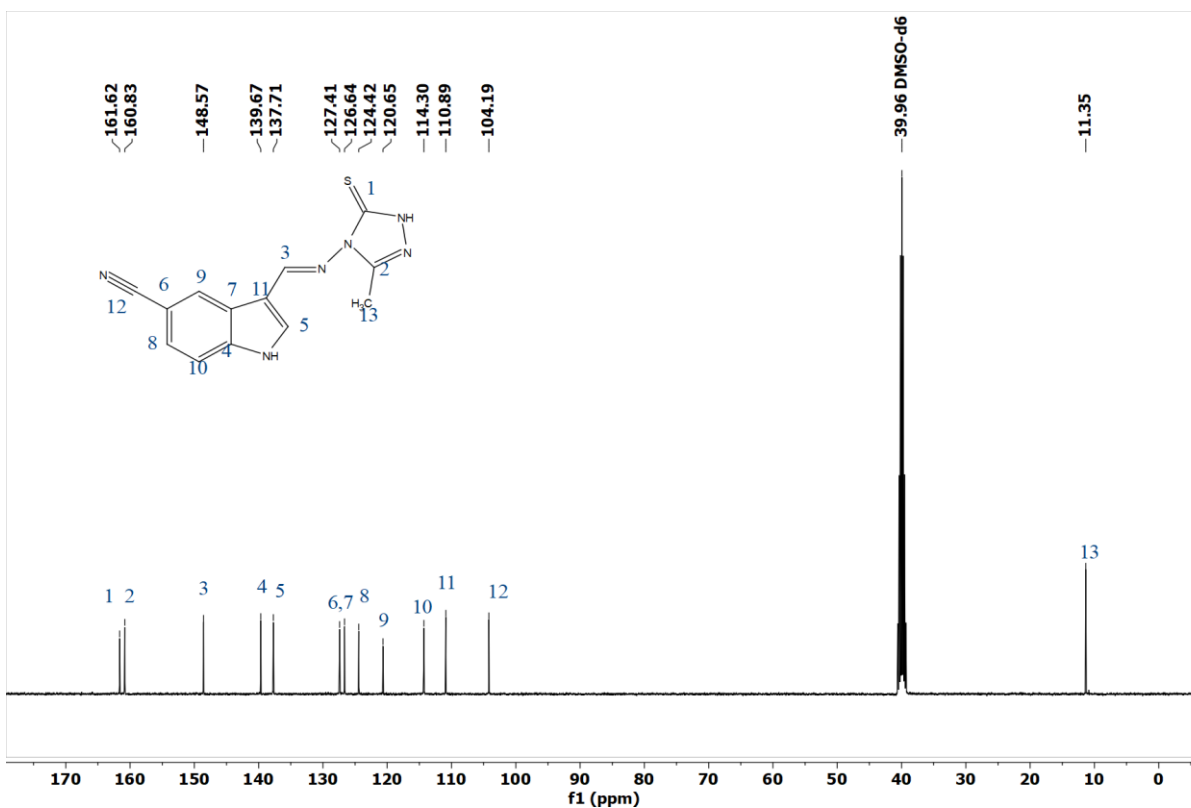
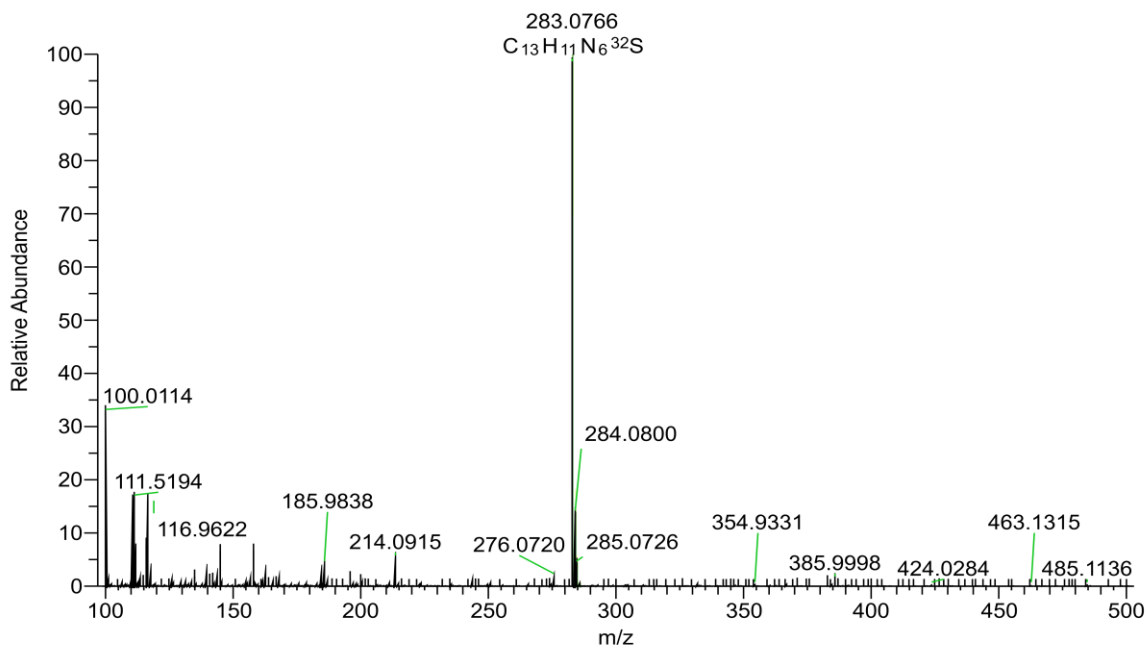


Figure (3.44): <sup>13</sup>CNMR Spectrum of the compound C10

UAM\_Z90 #18-26 RT: 0.14-0.2 AV: 4 SB: 5 0.01-0.08 NL: 1.70E7  
T: FTMS + p ESI Full ms [100.0000-1000.0000]



Figure(3.45): Mass Spectrum (ESI) of the compound C10

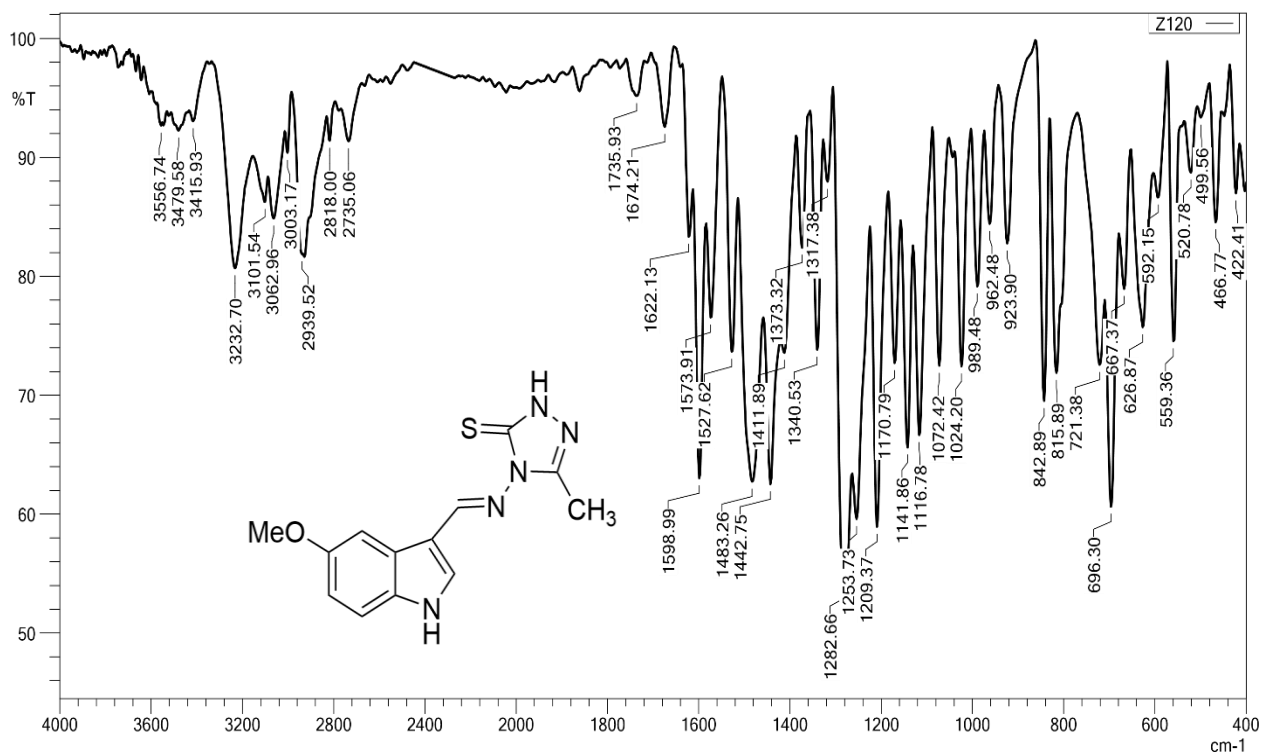


Figure (3.46): IR Spectrum of the compound C11

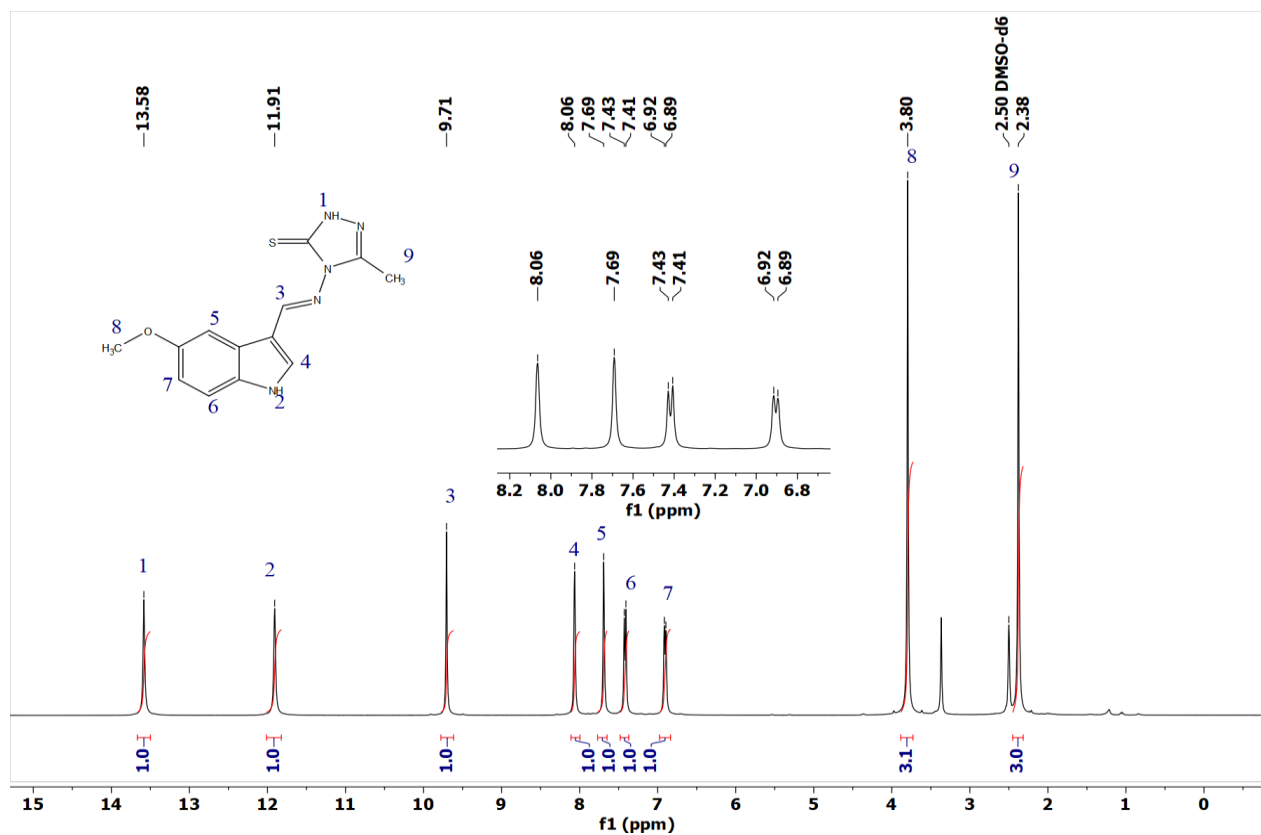


Figure (3.47): <sup>1</sup>H NMR Spectrum of the compound C11

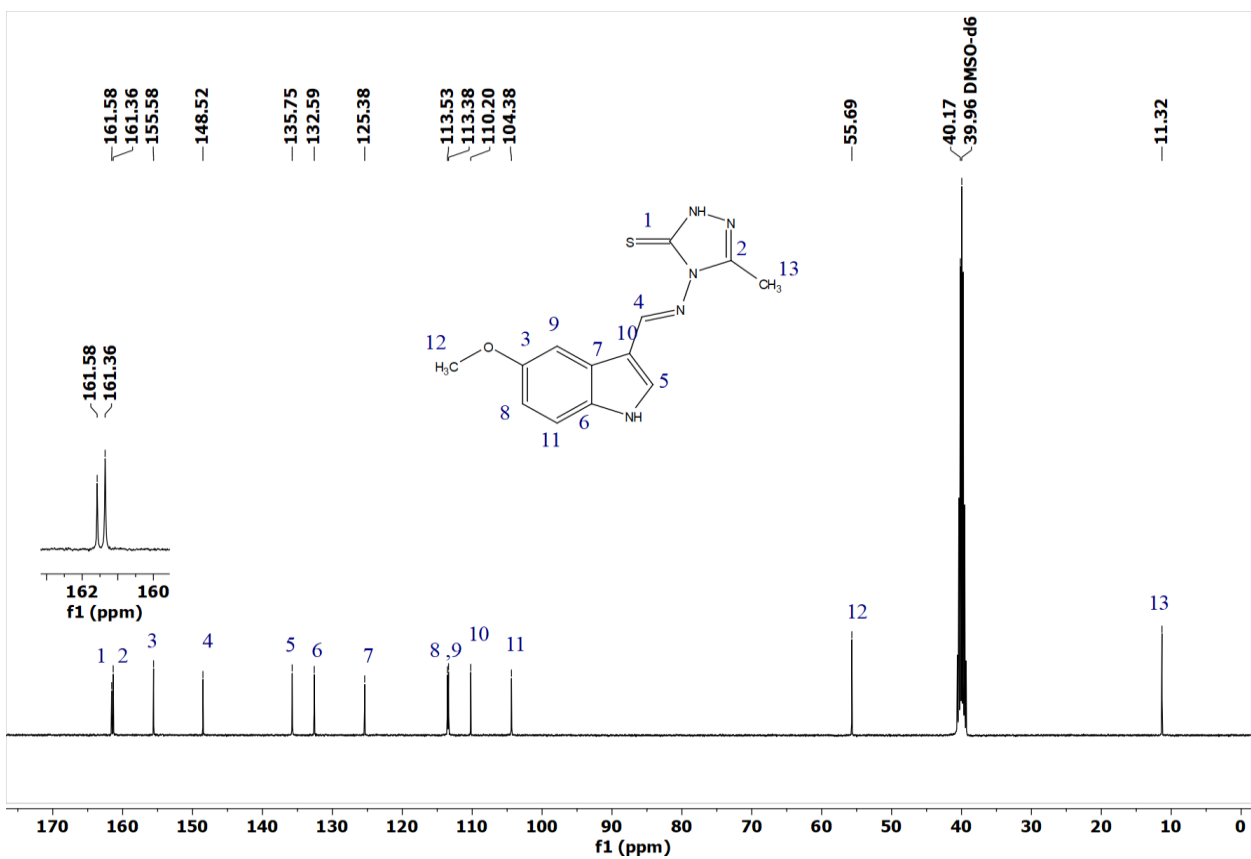
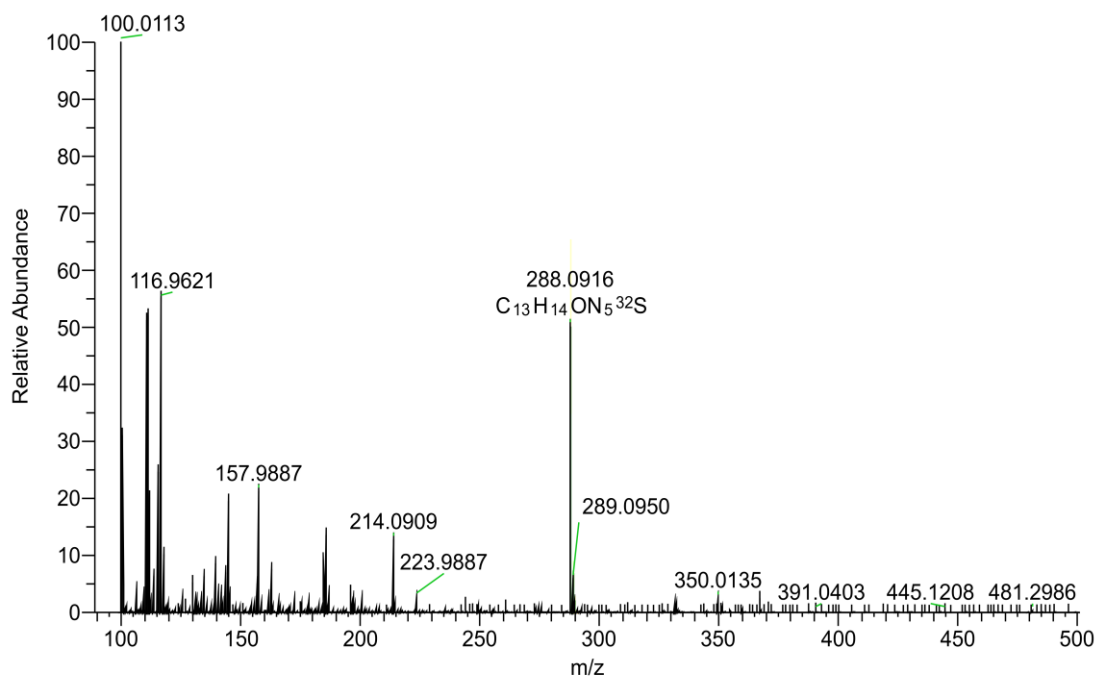


Figure (3.48):  $^{13}\text{C}$ NMR Spectrum of the compound C11

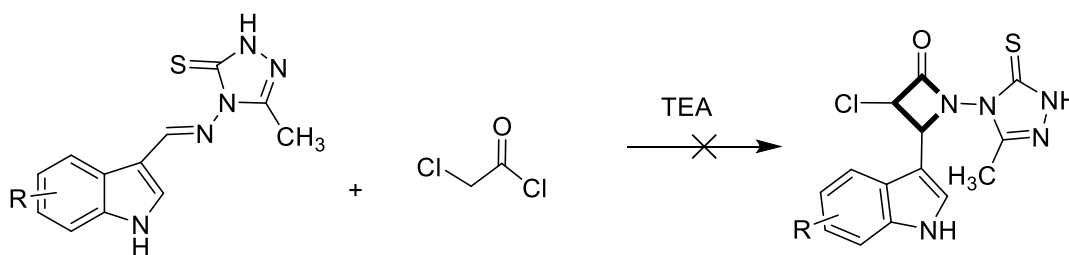
UAM\_Z120 #19-27 RT: 0.14-0.21 AV: 5 SB: 5 0.01-0.08 NL: 5.59E6  
T: FTMS + p ESI Full ms [100.0000-1000.0000]



Figure(3.49): Mass Spectrum (ESI) of the compound C11

### 3.4. Attempted Synthesis of $\beta$ -Lactam Derivative

After synthesizing the Schiff base and confirming its spectroscopically, the next step involved attempting to cyclize the Schiff base to obtain the corresponding  $\beta$ -lactam using chloroacetyl chloride in the presence of TEA as a base, with dioxane as the solvent. Based on the structural features of the synthesized Schiff base, it was anticipated that the imine functionality could undergo intramolecular ring closure under these conditions<sup>147,148</sup> (Scheme 3.7)



**Scheme 3.7: Attempted Synthesis of  $\beta$ -Lactam**

However, despite several trials, the cyclization attempts did not yield the desired  $\beta$ -lactam product. Different reaction parameters were systematically modified, including increasing the molar equivalents of chloroacetyl chloride and triethylamine, changing the reaction temperature, and using other solvents such as DMF and THF.

The unsuccessful outcome can be attributed to several intrinsic factors related to the Schiff base obtained in the previous step. These include possible steric hindrance around the imine group, insufficient nucleophilic reactivity necessary for ring closure, and the inherent instability of the transition state required to form the highly strained  $\beta$ -lactam ring.

### **3.4. Biological activity**

#### **3.4.1. The cytotoxic activity of the synthesized compounds (C1-C11)**

The cytotoxic activity of the synthesized Schiff base compounds was evaluated against the human liver cancer cell line (HepG2) using the MTT assay. The  $IC_{50}$  value is considered a key indicator of the inhibitory efficiency of biological and biochemical materials, where lower  $IC_{50}$  values represent higher cytotoxic potency. The experimental results demonstrated that all tested compounds exhibited weak cytotoxic effects toward HepG2 cells. Most compounds showed  $IC_{50}$  values exceeding 100  $\mu\text{g/mL}$ , while only a single derivative (C2) displayed an  $IC_{50}$  value of 98.95  $\mu\text{g/mL}$ . In comparison, doxorubicin, used as a reference drug, exhibited strong cytotoxic activity with an  $IC_{50}$  value of 1.16  $\mu\text{g/mL}$ .

The relatively low cytotoxic activity of the synthesized compounds may be attributed to several physicochemical and structural factors. Primarily, their limited aqueous solubility could have markedly reduced their bioavailability in the culture medium. Insufficient solubility likely restricted the diffusion of the molecules toward the cellular membrane, thereby decreasing their effective intracellular concentration and subsequent interaction with biological targets. Additionally, the structural characteristics of the molecules, including the electronic distribution and steric properties of the indole and triazole rings, may impede binding to key molecular targets involved in cancer cell survival and proliferation. Such structural constraints are often critical in determining the cytotoxic potency of small molecules, while being chemically interesting, requires further structural optimization to enhance biological activity. Potential strategies could include the introduction of hydrophilic substituents to improve solubility or functional groups designed to enhance membrane permeability and target affinity, which could increase cellular uptake and cytotoxic efficiency.

**Table 3.1: In vitro anticancer screening of the compound(C1-C11)**

<b>Compound</b>	<b>IC<sub>50</sub> (µg/mL)</b>
C1	291.46
C2	98.95
C3	153.30
C4	136.74
C5	705.23
C6	486.35
C7	434.71
C8	367.56
C9	267.41
C10	332.08
C11	241.19
Doxorubicin	1.16

**Table 3.2: Growth inhibition (%) of HepG2 cells at different concentrations**

Sample ID	C1						HepG2 24h			
Concentration (µg/mL)	7.4		22.22		66.66		200		600	
absorption at 570 nm	0.434	0.479	0.398	0.438	0.319	0.350	0.300	0.233	0.209	0.239
Viability (%)	84.44	93.19	77.43	85.21	62.06	68.09	58.37	45.33	40.66	46.50
Average Viability (%)	88.81		81.32		65.08		51.85		43.58	
Standard Deviation (±)	6.19		5.50		4.26		9.22		4.13	

Sample ID	C2						HepG2 24h			
Concentration (µg/mL)	7.4		22.22		66.66		200		600	
absorption at 570 nm	0.470	0.402	0.377	0.336	0.303	0.308	0.180	0.179	0.160	0.128
Viability (%)	91.44	78.21	73.35	65.37	58.95	59.92	35.02	34.82	31.13	24.90
Average Viability (%)	84.82		69.36		59.44		34.92		28.02	
Standard Deviation (±)	9.35		5.64		0.69		0.14		4.40	

Sample ID	C3						HepG2 24h			
Concentration (µg/mL)	7.4		22.22		66.66		200		600	
absorption at 570 nm	0.487	0.433	0.352	0.362	0.303	0.315	0.211	0.203	0.195	0.212
Viability (%)	94.75	84.24	68.48	70.43	58.95	61.28	41.05	39.49	37.94	41.25
Average Viability (%)	89.49		69.46		60.12		40.27		39.59	
Standard Deviation (±)	7.43		1.38		1.65		1.10		2.34	

Sample ID	C4						HepG2 24h			
Concentration (µg/mL)	7.4		22.22		66.66		200		600	
absorption at 570 nm	0.418	0.443	0.404	0.409	0.335	0.283	0.200	0.217	0.211	0.124
Viability (%)	81.32	86.19	78.60	79.57	65.18	55.06	38.91	42.22	41.05	24.12
Average Viability (%)	83.75		79.09		60.12		40.56		32.59	
Standard Deviation (±)	3.44		0.69		7.15		2.34		11.97	

Sample ID	C5						HepG2 24h			
Concentration (µg/mL)	7.4		22.22		66.66		200		600	
absorption at 570 nm	0.445	0.506	0.437	0.462	0.414	0.375	0.339	0.352	0.240	0.251
Viability (%)	85.25	96.93	83.72	88.51	79.31	71.84	64.94	67.43	45.98	48.08
Average Viability (%)	91.09		86.11		75.57		66.19		47.03	
Standard Deviation (±)	8.26		3.39		5.28		1.76		1.49	

Sample ID	C6						HepG2 24h			
Concentration (µg/mL)	7.4		22.22		66.66		200		600	
absorption at 570 nm	0.463	0.452	0.417	0.412	0.357	0.389	0.327	0.332	0.234	0.218
Viability (%)	88.70	86.59	79.89	78.93	68.39	74.52	62.64	63.60	44.83	41.76
Average Viability (%)	87.64		79.41		71.46		63.12		43.30	
Standard Deviation (±)	1.49		0.68		4.33		0.68		2.17	

Sample ID	C7						HepG2 24h			
Concentration (µg/mL)	7.4		22.22		66.66		200		600	
absorption at 570 nm	0.454	0.463	0.422	0.405	0.396	0.352	0.333	0.304	0.286	0.211
Viability (%)	88.33	90.08	82.10	78.79	77.04	68.48	64.79	59.14	55.64	41.05
Average Viability (%)	89.20		80.45		72.76		61.96		48.35	
Standard Deviation (±)	1.24		2.34		6.05		3.99		10.32	

Sample ID	C8						HepG2 24h			
Concentration (µg/mL)	7.4		22.22		66.66		200		600	
Absorption at 570 nm	0.467	0.453	0.413	0.409	0.329	0.317	0.249	0.303	0.283	0.214
Viability (%)	90.86	88.13	80.35	79.57	64.01	61.67	48.44	58.95	55.06	41.63
Average Viability (%)	89.49		79.96		62.84		53.70		48.35	
Standard Deviation (±)	1.93		0.55		1.65		7.43		9.49	

Sample ID	C9						HepG2 24h			
Concentration (µg/mL)	7.4		22.22		66.66		200		600	
Absorption at 570nm	0.487	0.456	0.379	0.353	0.346	0.306	0.276	0.287	0.209	0.224
Viability (%)	94.75	88.72	73.74	68.68	67.32	59.53	53.70	55.84	40.66	43.58
Average Viability (%)	91.73		71.21		63.42		54.77		42.12	
Standard Deviation (±)	4.26		3.58		5.50		1.51		2.06	

Sample ID	C10						HepG2 24h			
Concentration (µg/mL)	7.4		22.22		66.66		200		600	
absorption at 570 nm	0.444	0.480	0.387	0.428	0.331	0.328	0.295	0.286	0.246	0.206
Viability (%)	86.38	93.39	75.29	83.27	64.40	63.81	57.39	55.64	47.86	40.08
Average Viability (%)	89.88		79.28		64.11		56.52		43.97	
Standard Deviation (±)	4.95		5.64		0.41		1.24		5.50	

Sample ID	C11						HepG2 24h			
Concentration (µg/mL)	7.4		22.22		66.66		200		600	
absorption at 570 nm	0.474	0.516	0.432	0.433	0.329	0.376	0.262	0.275	0.175	0.223
Viability (%)	90.80	98.85	82.76	82.95	63.03	72.03	50.19	52.68	33.52	42.72
Average Viability (%)	94.83		82.85		67.53		51.44		38.12	
Standard Deviation (±)	5.69		0.14		6.37		1.76		6.50	

Sample ID	Doxorubicin HCl						HepG2 24h			
Concentration (µg/mL)	0.073		0.22		0.66		2		6	
absorption at 570 nm	0.513	0.521	0.431	0.371	0.315	0.311	0.291	0.230	0.194	0.198
Viability (%)	86.07	87.42	72.32	62.25	52.85	52.18	48.83	38.59	32.55	33.22
Average Viability (%)	86.74		67.28		52.52		43.71		32.89	
Standard Deviation (±)	0.95		7.12		0.47		7.24		0.47	

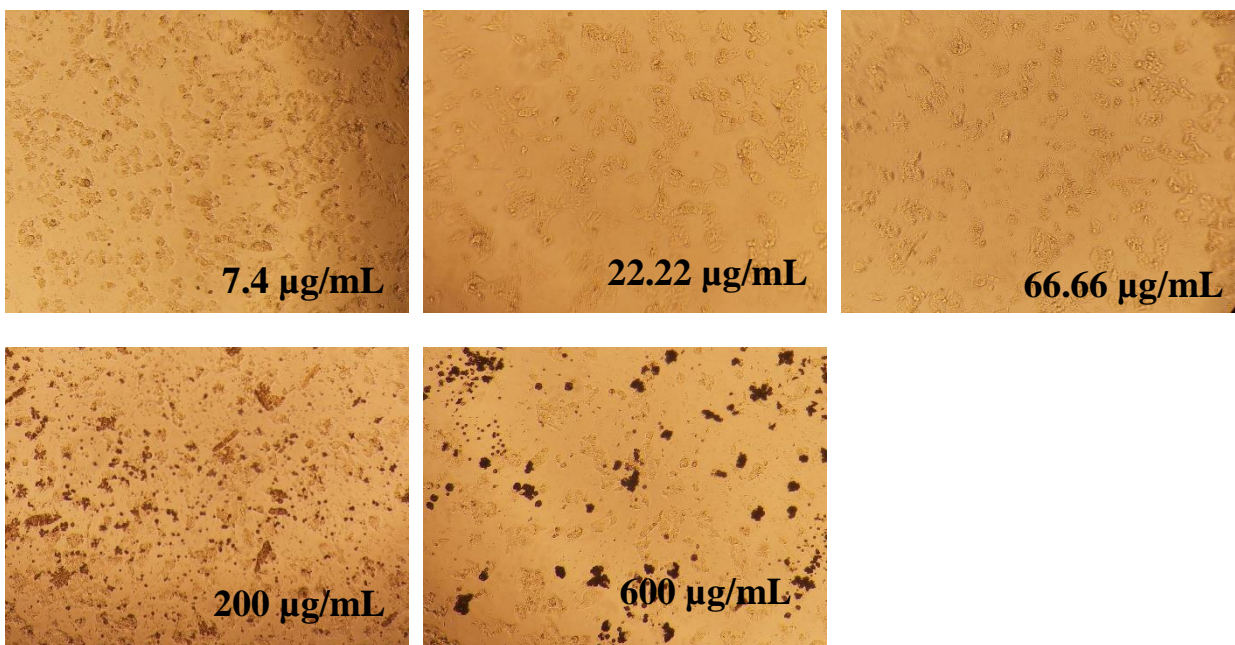


**Figure 3.50: MTT image of compound C1 against HepG2 cells**

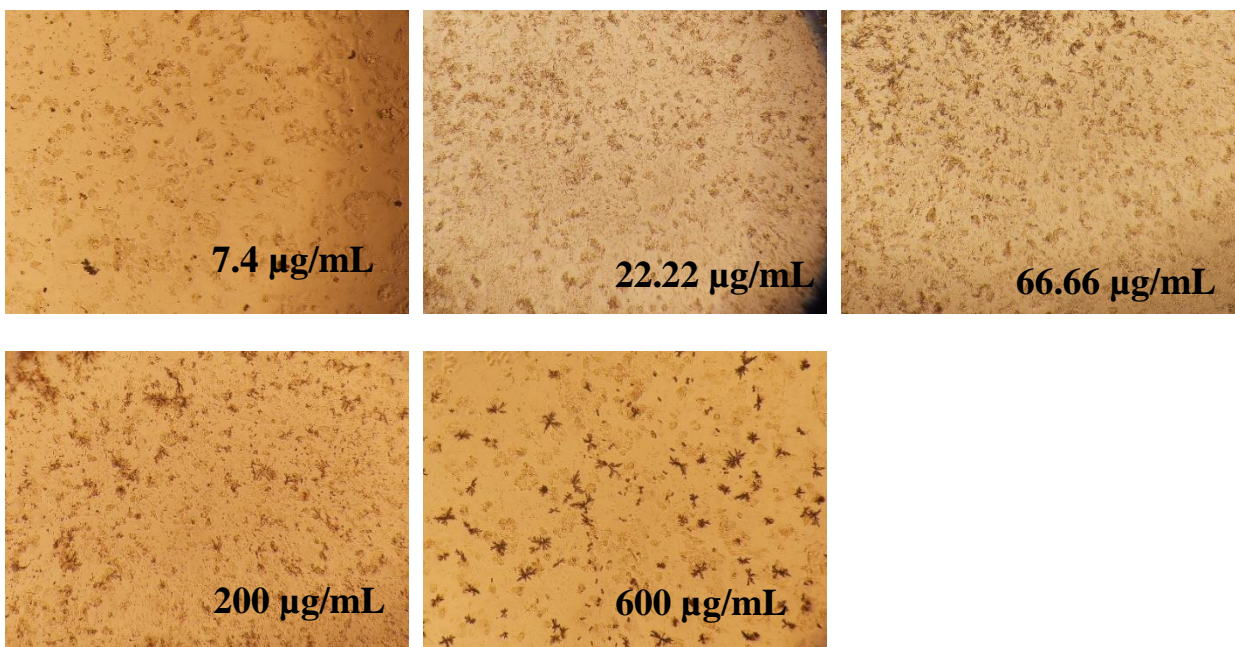


**Figure 3.51: MTT image of compound C2 against HepG2 cells.**

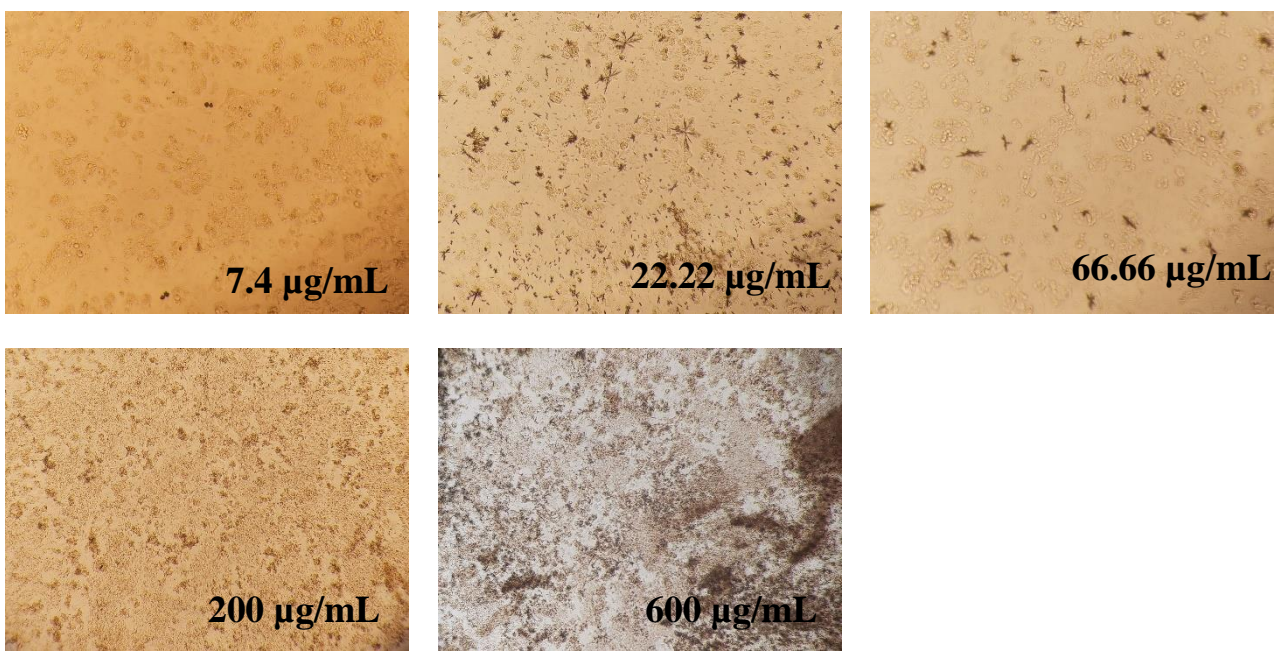


**Figure 3.52: MTT image of compound C3 against HepG2 cells**

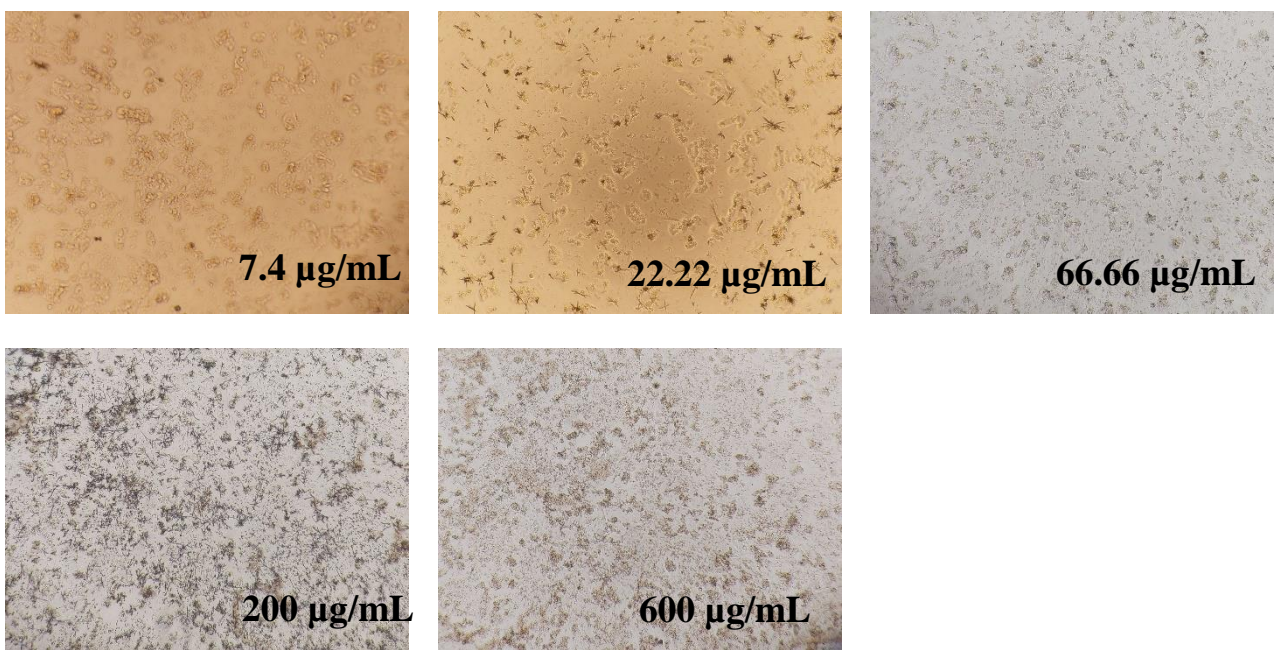


**Figure 3.53: MTT image of compound C4 against HepG2 cells**

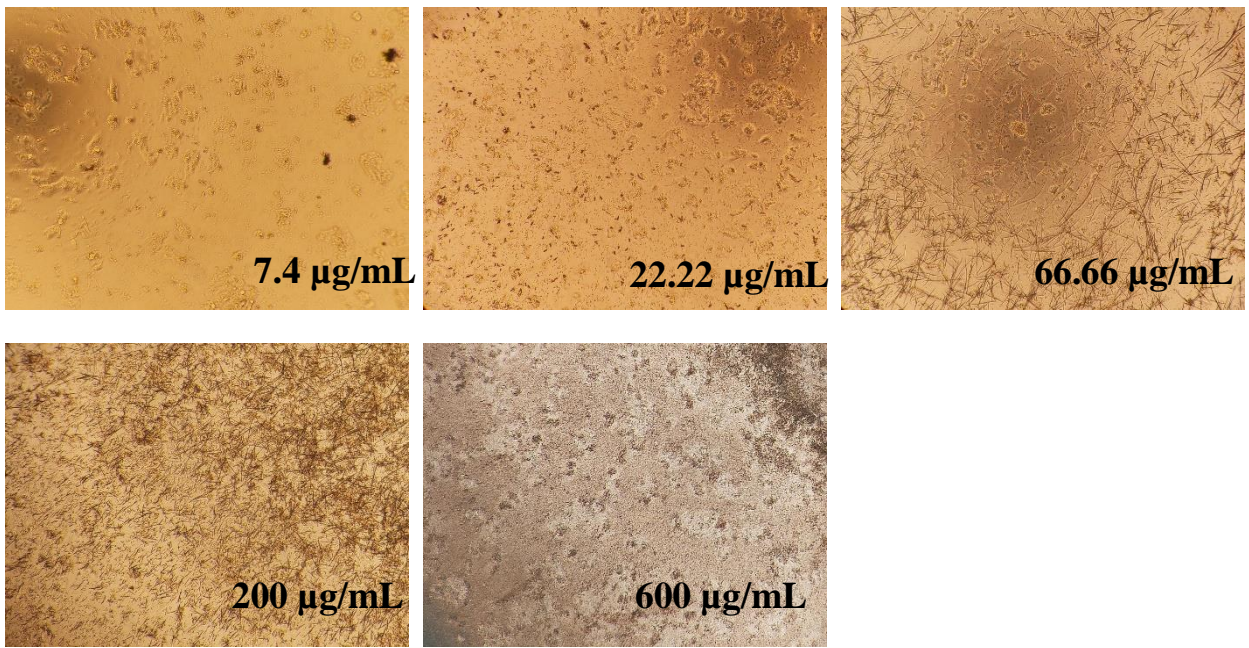


**Figure 3.54: MTT image of compound C5 against HepG2 cells**

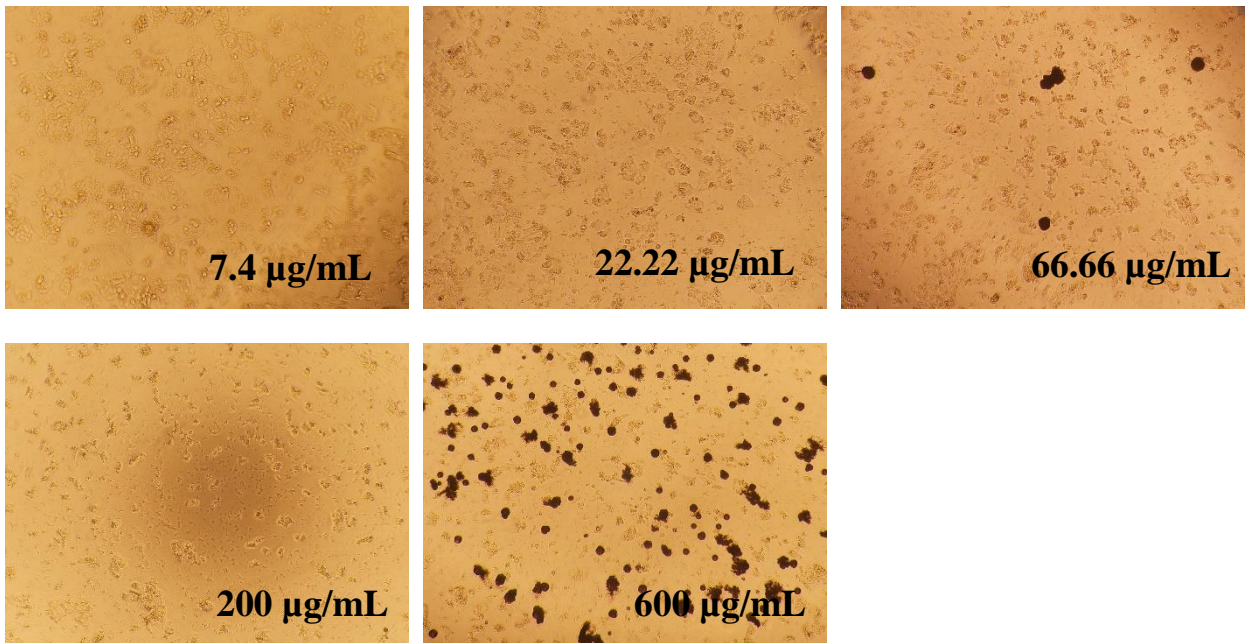


**Figure 3.55: MTT image of compound C6 against HepG2 cells**

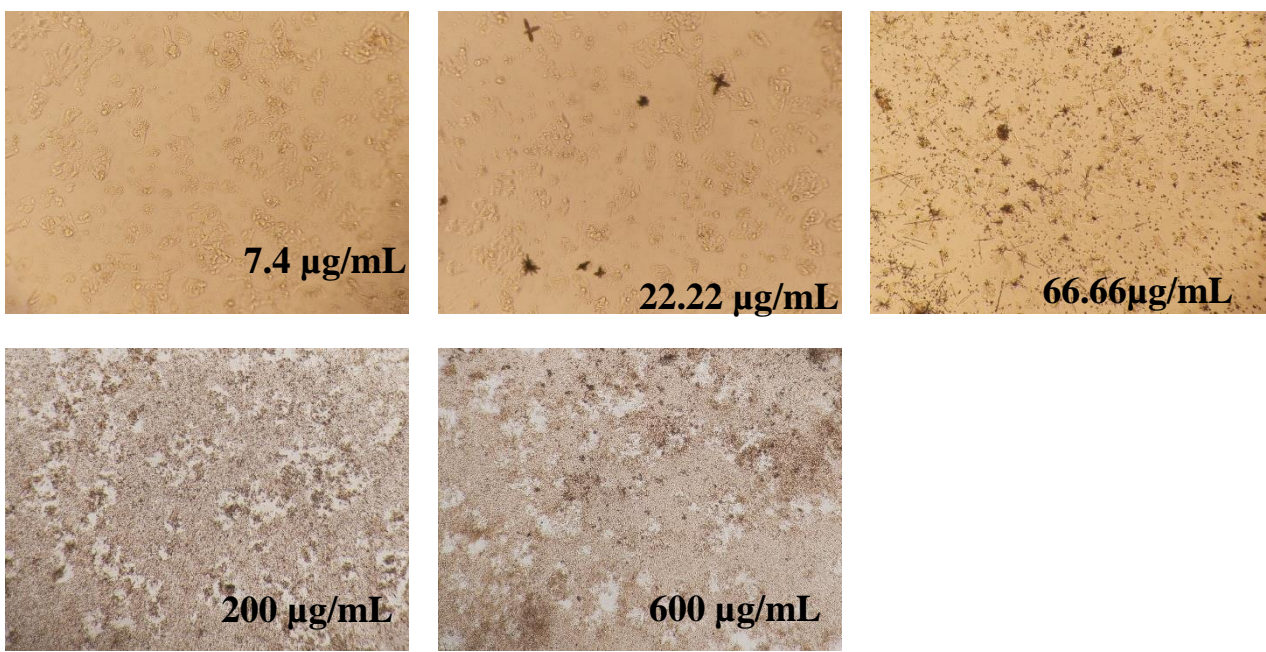


**Figure 3.56: MTT image of compound C7 against HepG2 cells**

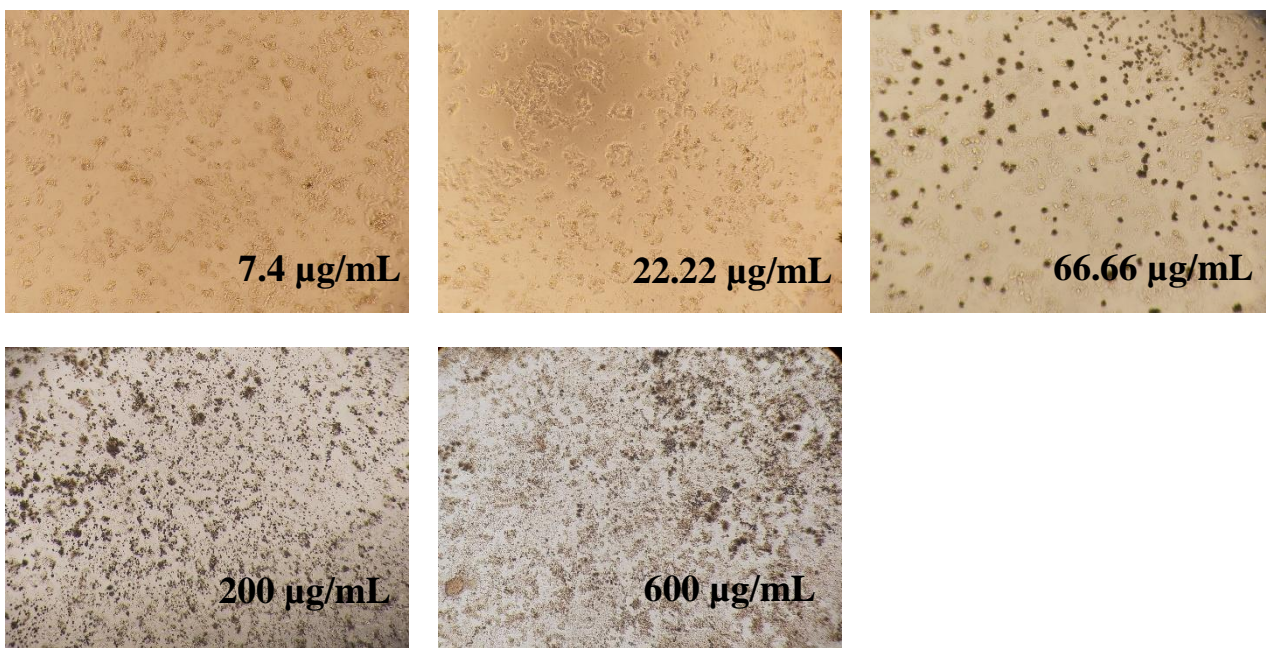


**Figure 3.57: MTT image of compound C8 against HepG2 cells**

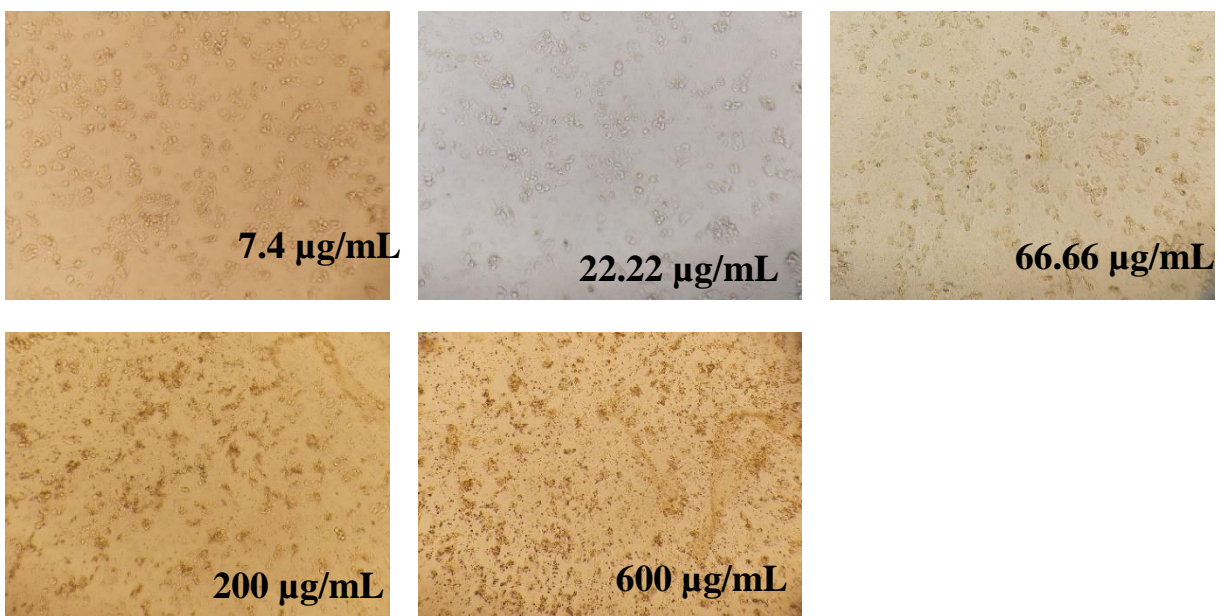


**Figure 3.58: MTT image of compound C9 against HepG2 cells**

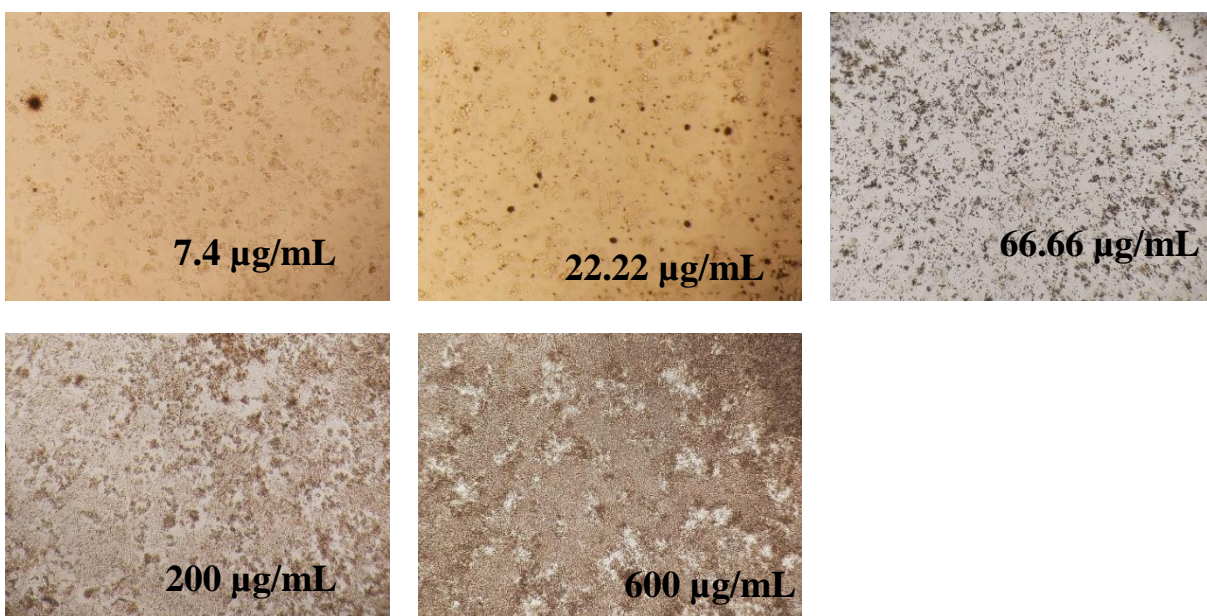


**Figure 3.59: MTT image of compound C10 against HepG2 cells**

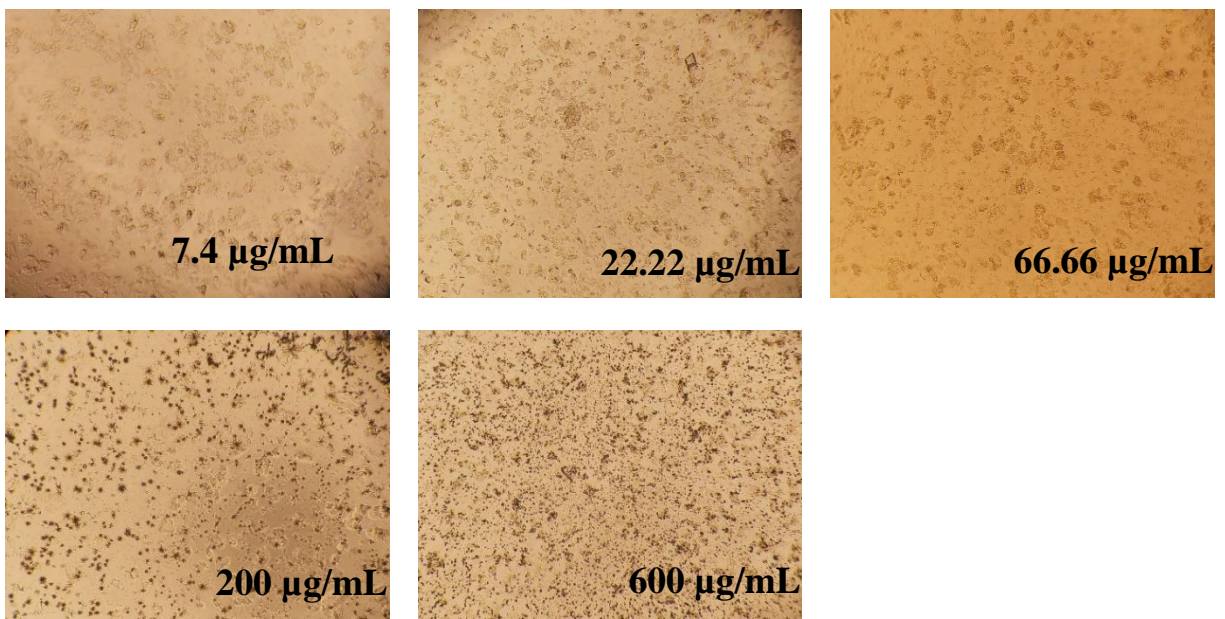


**Figure 3.60: MTT image of compound C11 against HepG2 cells**

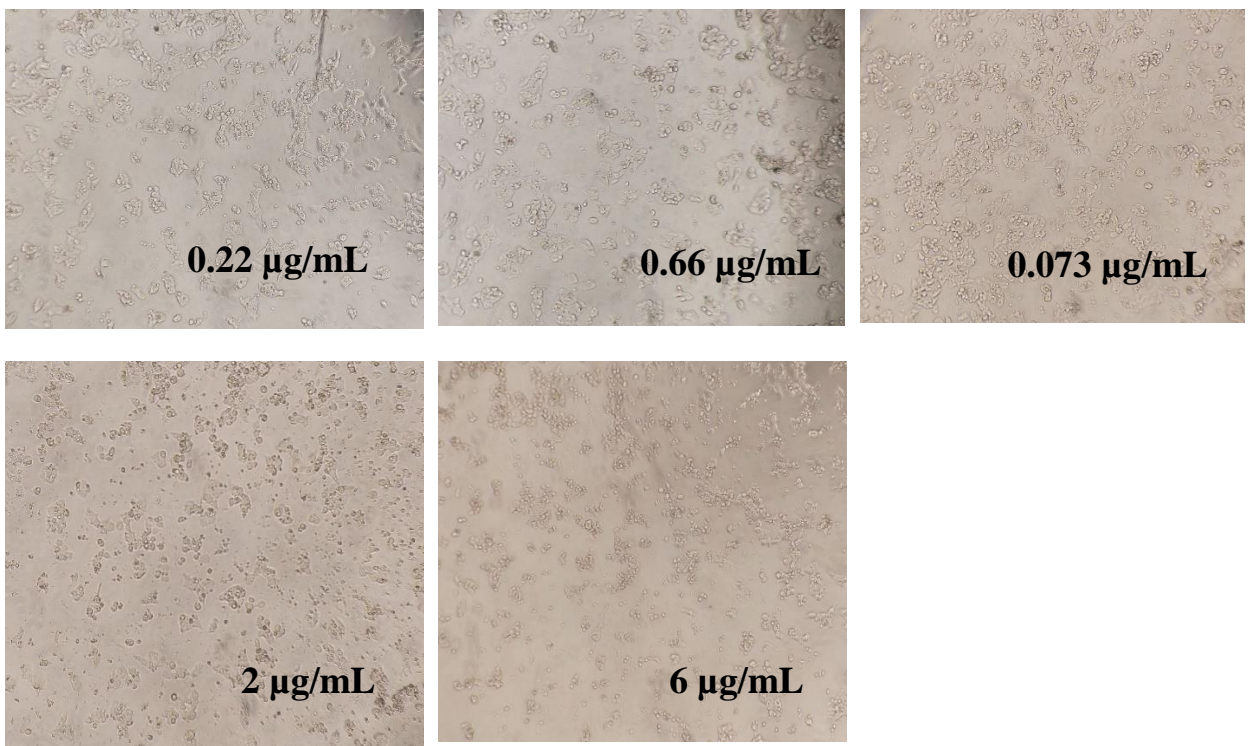


**Figure 3.61: MTT image of doxorubicin against HepG2 cells**

### 3.4.2. Antibacterial activity

The continuous emergence of antibiotic-resistant bacterial strains has created a serious global health concern, emphasizing the urgent need for new antimicrobial agents with novel chemical structures and mechanisms of action.<sup>149</sup> Heterocyclic systems containing nitrogen and sulfur atoms, such as indole, triazole, and thione derivatives, have attracted great interest due to their potential biological activities, including antibacterial, antifungal, and anticancer effects. Therefore, evaluating the antibacterial potential of the newly synthesized compounds represents an important step in assessing their pharmacological relevance.<sup>150</sup>

In the present study, the synthesized compounds were evaluated against *Staphylococcus aureus* ATCC12600 and *Escherichia coli* ATCC11175 using the microdilution method. The obtained results revealed that all compounds exhibited weak antibacterial activity, with minimum inhibitory concentration (MIC) values ranging from 1000 to 2000  $\mu\text{M}$ . Among them, compounds (C6, C8, and C10) showed slightly better inhibition toward *S. aureus* (MIC = 1000  $\mu\text{M}$ ), while all compounds displayed poor activity against *E. coli* (MIC = 2000  $\mu\text{M}$ ).

This difference may indicate that Gram-positive bacteria are more sensitive to the tested compounds compared with Gram-negative strains, which is most likely due to the structural variation in their cell walls. The outer membrane of Gram-negative bacteria acts as an additional permeability barrier that restricts the entry of large or polar molecules.<sup>151</sup>

When compared with the standard antibiotics Ampicillin (AMP) and Tetracycline (TET), which were tested under identical conditions. The reference drugs exhibited significantly lower MIC values, confirming their much higher antibacterial effectiveness. Specifically, Ampicillin showed MIC values of 250  $\mu\text{M}$  and 315  $\mu\text{M}$  against *Staphylococcus aureus* ATCC12600 and *Escherichia coli* ATCC11175,

respectively, while Tetracycline displayed MICs of 1000  $\mu\text{M}$  and 2500  $\mu\text{M}$  for the same strains, which are significantly lower than those of the tested compounds.

The weak antibacterial activity of the synthesized compounds can be primarily attributed to its structural rigidity and limited aqueous solubility. Despite containing polar groups, the rigid structure likely hinders membrane penetration and reduces effective concentration at bacterial targets. In comparison, ampicillin and tetracycline are smaller and more flexible molecules, which facilitates diffusion through bacterial membranes and results in higher antibacterial activity.

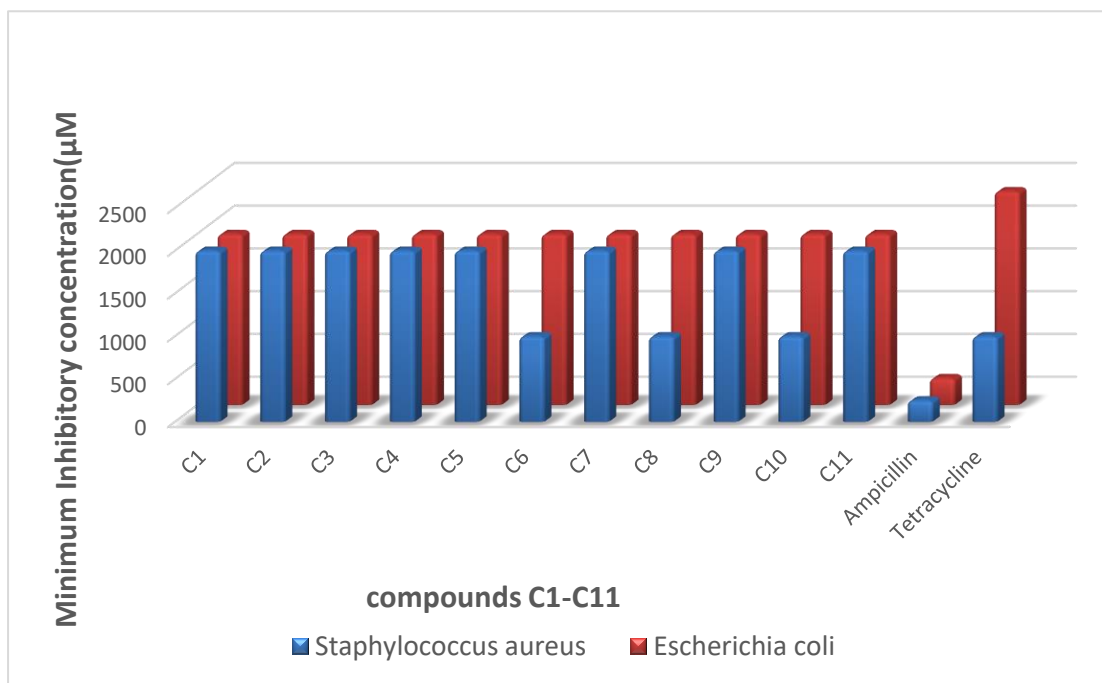


**Figure 3.62: Graph illustrating the MIC values of (C1-C11) against *Escherichia coli* and *Staphylococcus aureus***

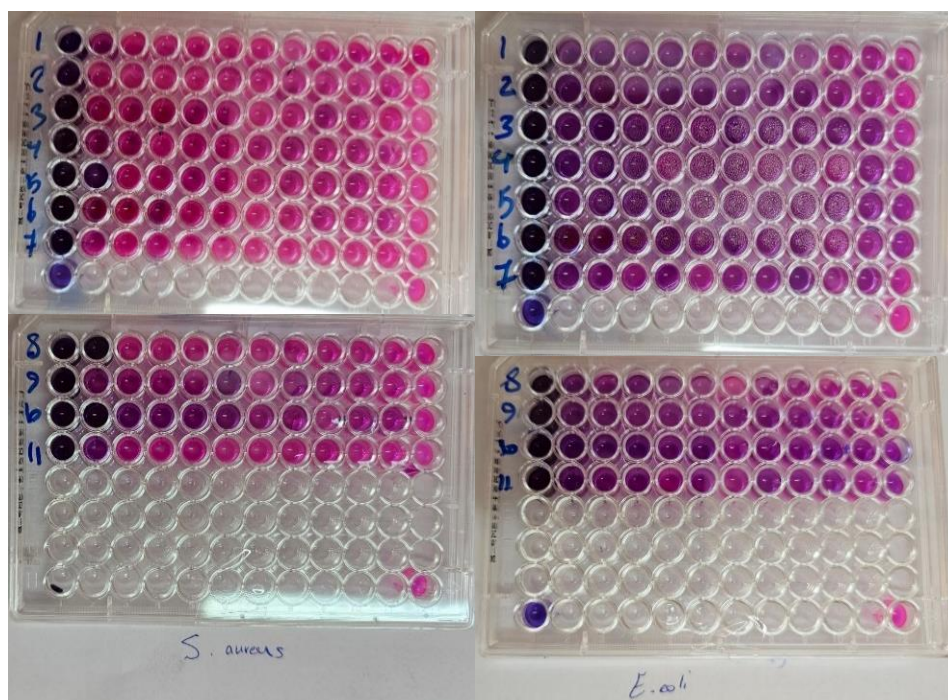


**Figure 3.63:** Images of MIC produced by C1-C11 against *Escherichia coli* and *Staphylococcus aureus*

### 3.5. Molecular Docking Studies

TDO2 was selected as the molecular target for the docking study because its natural substrate, L-tryptophan, contains an indole ring, which is also a core structural feature of the synthesized compounds. Since indole plays a key role in the recognition and binding of tryptophan within the TDO2 active site, it was hypothesized that the indole-containing synthesized derivatives may exhibit favorable interactions with this enzyme.<sup>131</sup> Therefore, evaluating their binding affinities toward TDO2 provides valuable insights into their potential biological relevance and possible inhibitory activity.

The molecular docking results revealed that all synthesized compounds (C1–C11) exhibited notable binding affinities toward the target protein, with docking scores ranging from -7.9 to -8.8 kcal/mol, in comparison with the co-crystallized ligand

3-(5-fluoro-1H-indol-3-yl)pyrrolidine-2,5-dione which showed a binding affinity of -8.4 kcal/mol, forming stable hydrogen bonds with key active-site residues such as Glu80, Ala150, Ser151, and HEM401.

Among the designed compounds, C2 demonstrated the highest binding affinity (-8.8 kcal/mol), indicating stronger predicted interactions than the reference ligand. This compound formed multiple hydrogen bonds with crucial residues (Glu80, Ala150, Ser151) at short distances (2.1–2.9 Å), suggesting a stable and compact ligand–protein complex. Similarly, (C1, C6, and C9) also exhibited docking scores (-8.6 kcal/mol each), maintaining strong interactions with the same residues within the active pocket.

On the other hand, (C3, C7, and C11) displayed comparatively lower binding affinities (-7.9 kcal/mol) and longer hydrogen-bond distances, reflecting weaker stabilization within the binding site. (C10) showed a score (-8.3 kcal/mol) close to that of the reference ligand, confirming its good binding potential.

Compound (C2) was the best in the docking study, and this finding is in good agreement with the MTT assay results, in which it exhibited the highest inhibitory activity among the tested derivatives. Such consistency between computational and biological data reinforces the assumption that enhanced binding affinity is closely associated with increased cytotoxic potency.

Overall, these findings indicate that several of the newly synthesized derivatives, particularly (C2), could exhibit stronger binding efficiency than the native ligand. Their favorable binding energies and interaction patterns highlight them as promising candidates for further biological and pharmacological evaluation.

**Table 3.3: Molecular docking results of compounds (C1-C11)**

<b>Compound</b>	<b>Binding affinity kcal/mol</b>	<b>Interaction</b>	<b>Distance(A°)</b>
<b>C1</b>	-8.6	H-bonds NH(indole)-Ala 150	2.9
		Pi-Pi Indole -HEM 401	5.80
		Indole -Phe72	6.23
		PI-Alkyl Indole-Leu147	3.74
<b>C2</b>	-8.8	H-bonds NH(triazole) -Glu80	2.1
		NH(indole)-Ala150	2.9
		Pi-sigma Indole -Ser151	4.45
		Imine-His76	4.67
		Pi-Pi Indole -HEM 401	5.91
		PI-Alkyl Indole-Leu147	3.64
<b>C3</b>	-7.9	Pi-sigma Indole -Ser151	4.57
		Imine-His76	4.95
		Pi-Pi Indole -HEM 401	6.55
		Indole -Phe72	4.81
		PI-Alkyl Indole-Leu147	4.95
		Indole -Lie73	4.40
<b>C4</b>	-8.1	H-bonds NH(indole) -Glu80	2
		NH(triazole)-Ala150	2.9
		Pi-sigma Indole -Ser151	4.57
		Imine-His76	4.24
		Pi-Pi Indole -HEM 401	3.70
		PI-Alkyl Indole -Ile73	4.22
		H-bonds NH(triazole) -Glu80	2.2

<b>C5</b>	-8.2	NH(indole)-Ala150 Pi-sigma Indole -Ser151 Indole -HEM 401 PI-Alkyl Indole -Leu147	2.9 4.52 3.59 4.20
<b>C6</b>	-8.6	H-bonds NH(triazole) -Glu80 NH(indole)-Ala150 Florine-His67 Pi-sigma Indole -Ser151 PI-Alkyl Indole-Leu147 Florin -HEM 401	2.2 3.0 2.4 4.39 3.62 3.96
<b>C7</b>	-7.9	H-bonds NH(indole) -Glu80 thione-Gly152 PI-Alkyl Triazole-Ala150 Indole-Leu147	2.0 2.7 4.42 4.43
<b>C8</b>	-8	H-bonds NH(triazole) -Glu80 NH(indole)-Ala150 Pi-sigma Indole -HEM 401 Indole -Ser151 PI-Alkyl Indole-Leu147	2.2 2.9 3.61 4.54 5.62
<b>C9</b>	-8.6	H-bonds NH(triazole) -Glu80 NH(indole)-Ala150 Nitro-The342 Pi-Pi Indole-HEM 401 PI-Alkyl Indole-Leu147	2.0 2.9 2.0 3.77 3.92
<b>C10</b>	-8.3	H-bonds NH(indole) -Glu80 NH(triazole)-Ala150 Pi-sigma	2.1 2.9

		Indole-HEM 401 Triazole-Ser151 PI-Alkyl Indole-Leu147	3.72 4.59  5.75
<b>C11</b>	-7.9	H-bonds NH(indole) -Glu80 NH(triazole)-Ala150 Pi-sigma Indole-HEM 401 Triazole-Ser151 PI-Alkyl Indole-Leu147	2.0 2.9  3.67 4.56  5.70
<b>3-(5-fluoro-1H-indol-3-yl)pyrrolidine-2,5-dione</b>	-8.4	H-bonds Florine-Thr342 Pi-Pi Indole-HEM 401	3.2  4.78

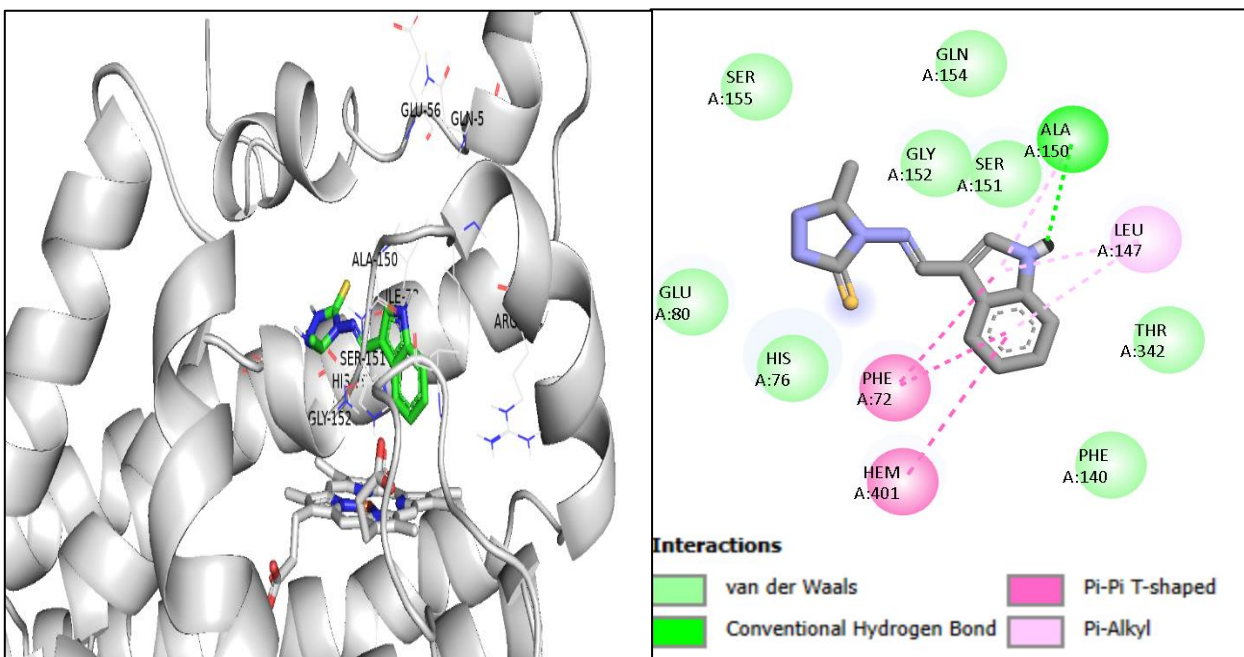


**Figure 3.64: Binding mode of compound C1 with TDO2 and its 2D schematic interaction**

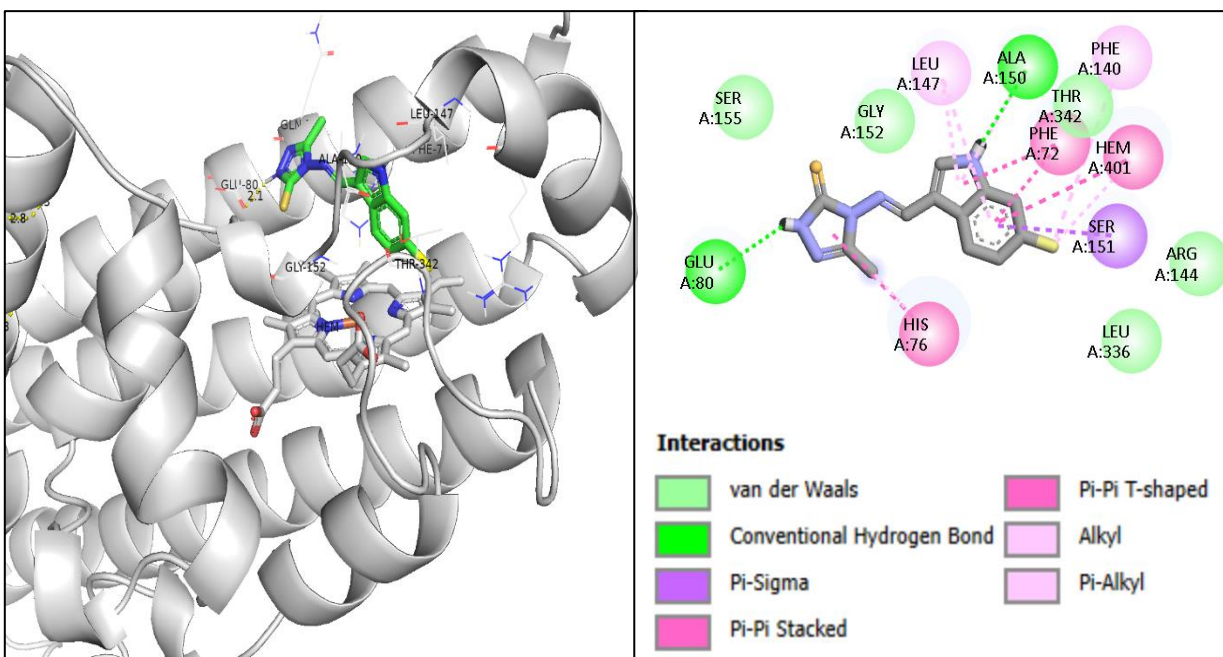


**Figure 3.65: Binding mode of compound C2 with TDO2 and its 2D schematic interaction**

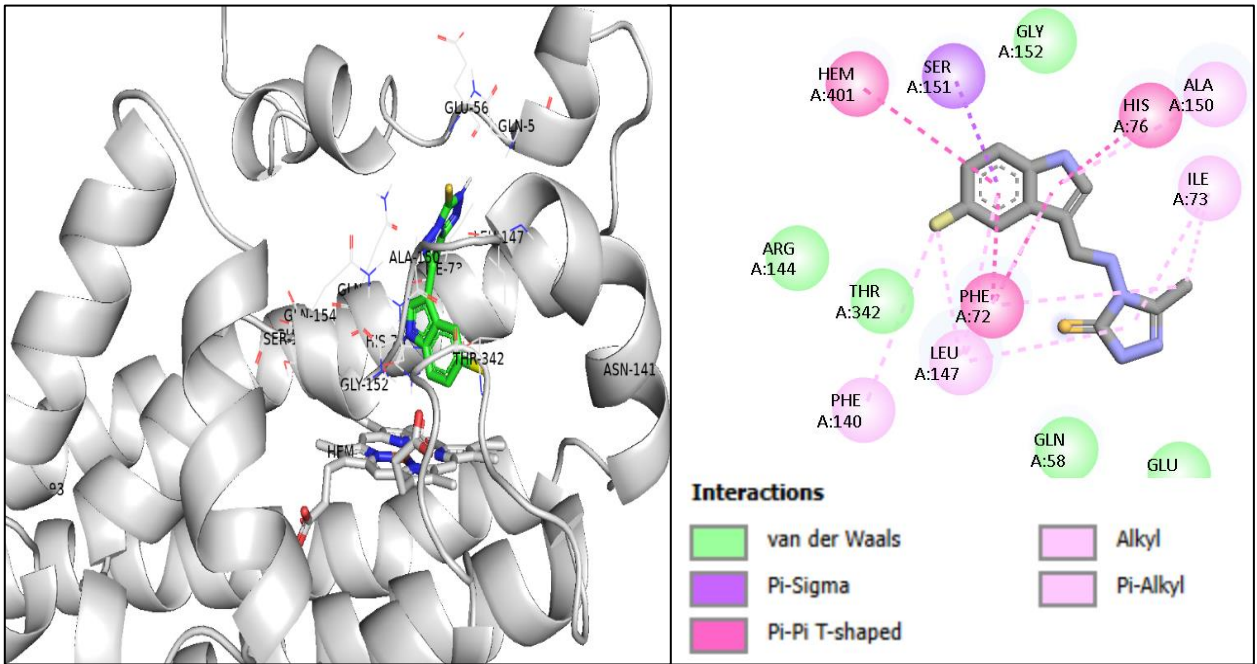


**Figure 3.66: Binding mode of compound C3 with TDO2 and its 2D schematic interaction**

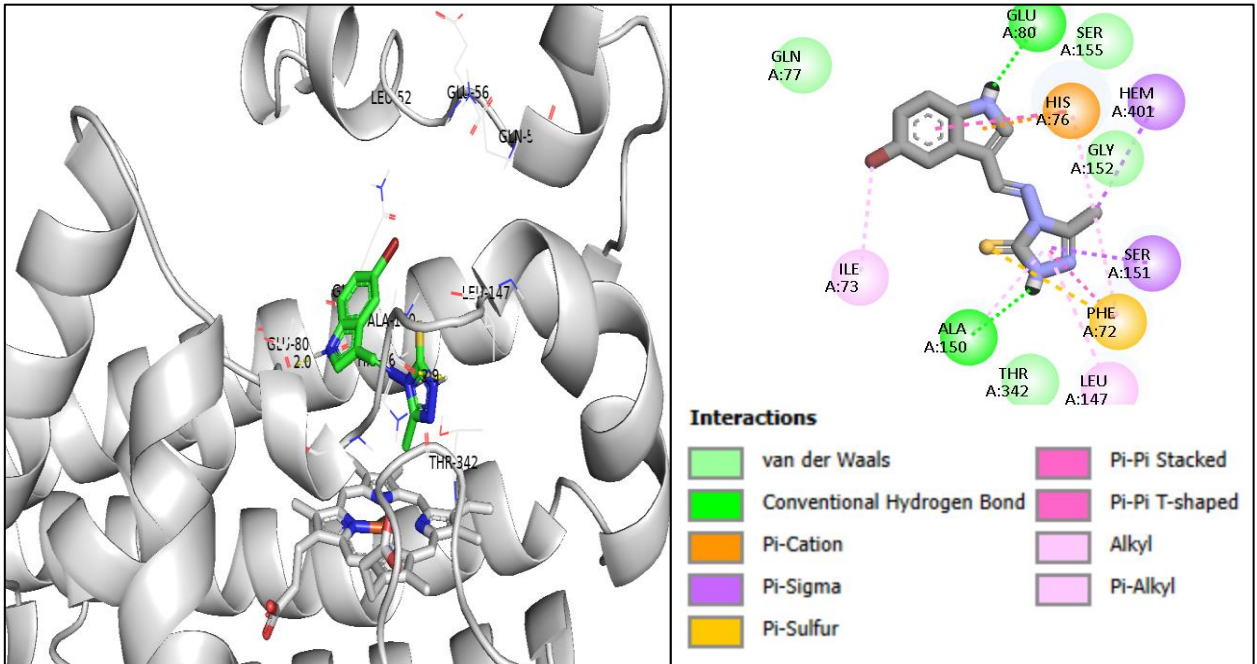


**Figure 3.67: Binding mode of compound C4 with TDO2 and its 2D schematic interaction**

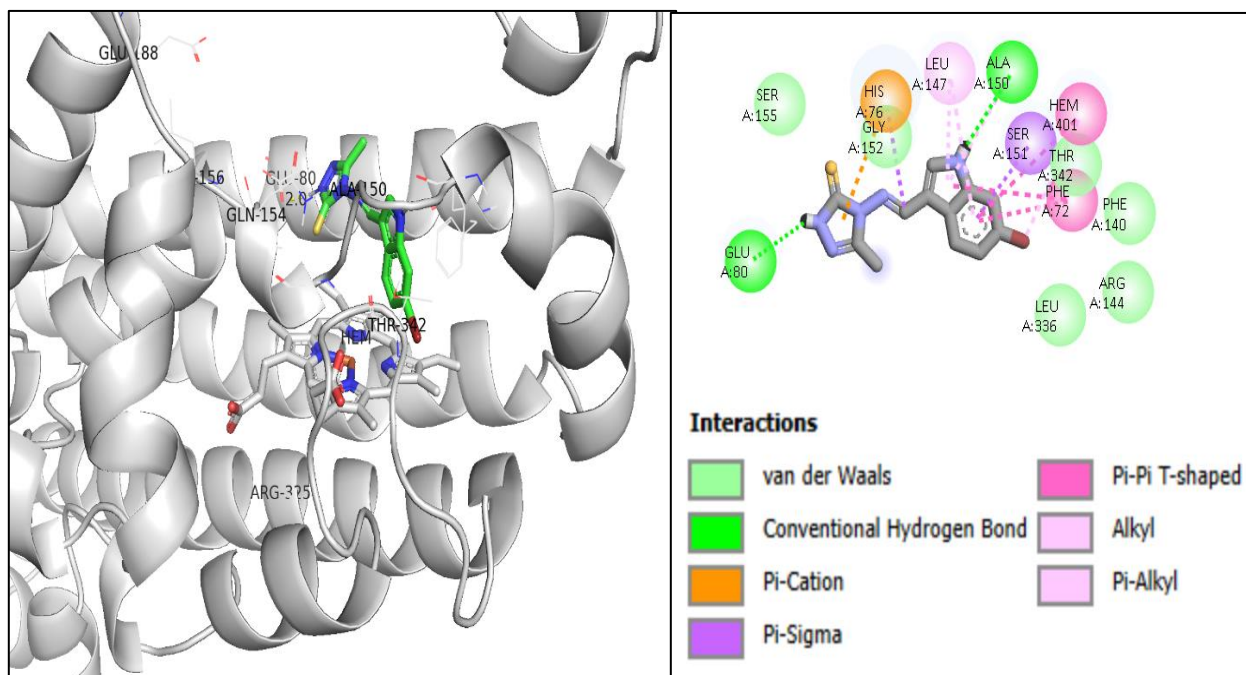


**Figure 3.68: Binding mode of compound C5 with TDO2 and its 2D schematic interaction**

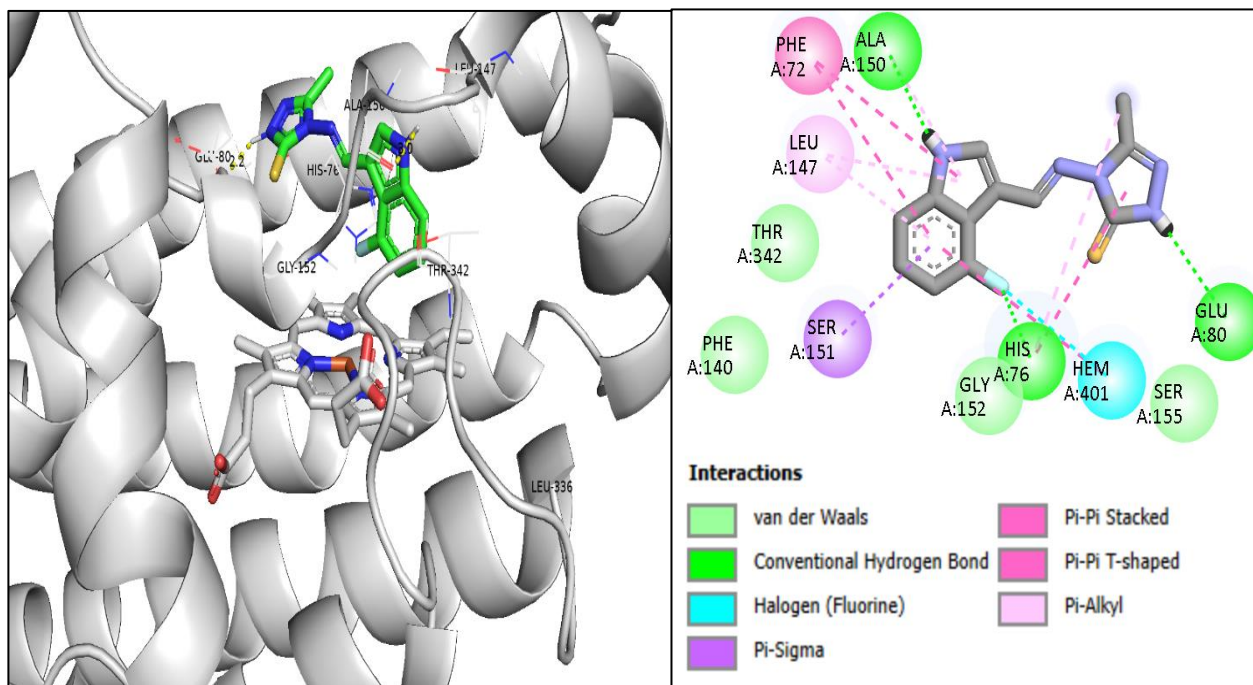


**Figure 3.69: Binding mode of compound C6 with TDO2 and its 2D schematic interaction**

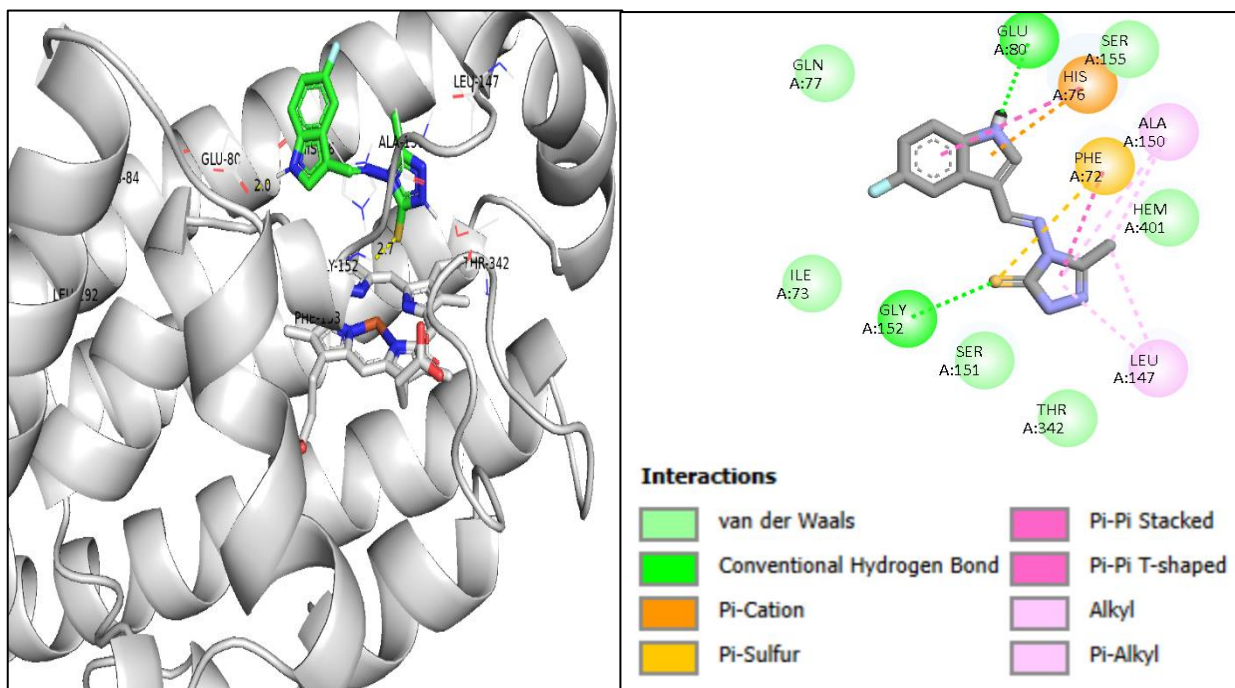


**Figure 3.70: Binding mode of compound C7 with TDO2 and its 2D schematic interaction.**

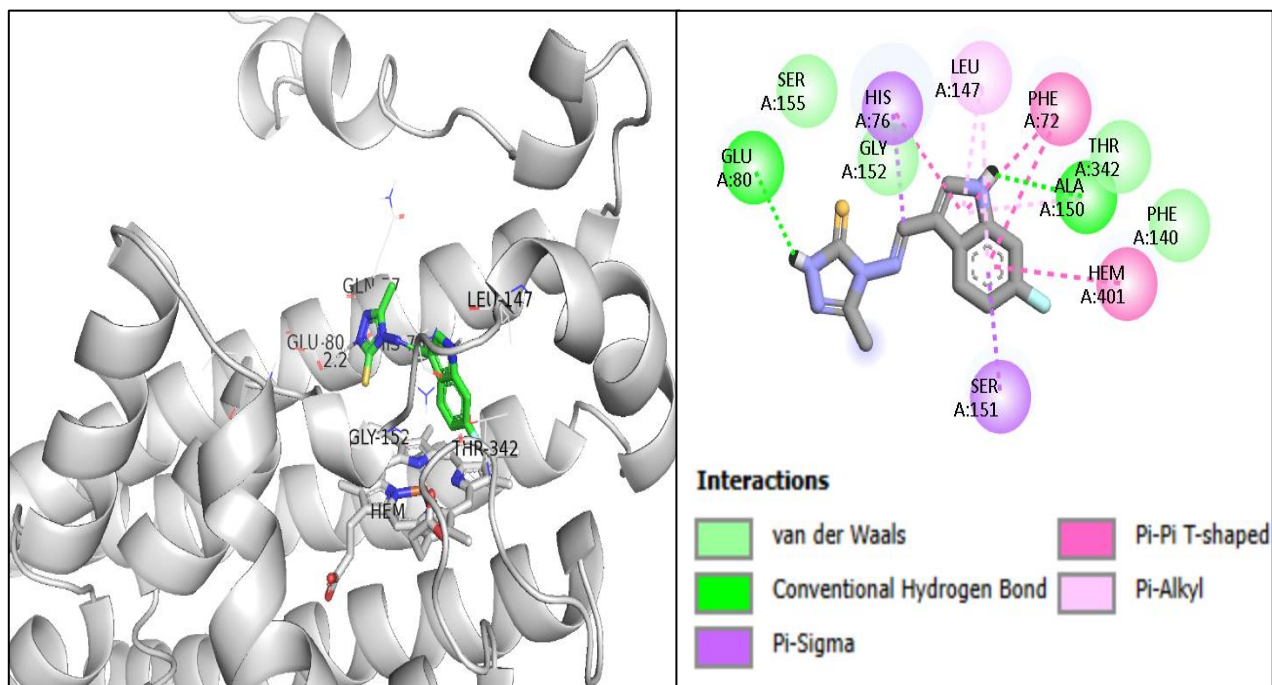


**Figure 3.71 : Binding mode of compound C8 with TDO2 and its 2D schematic interaction.**

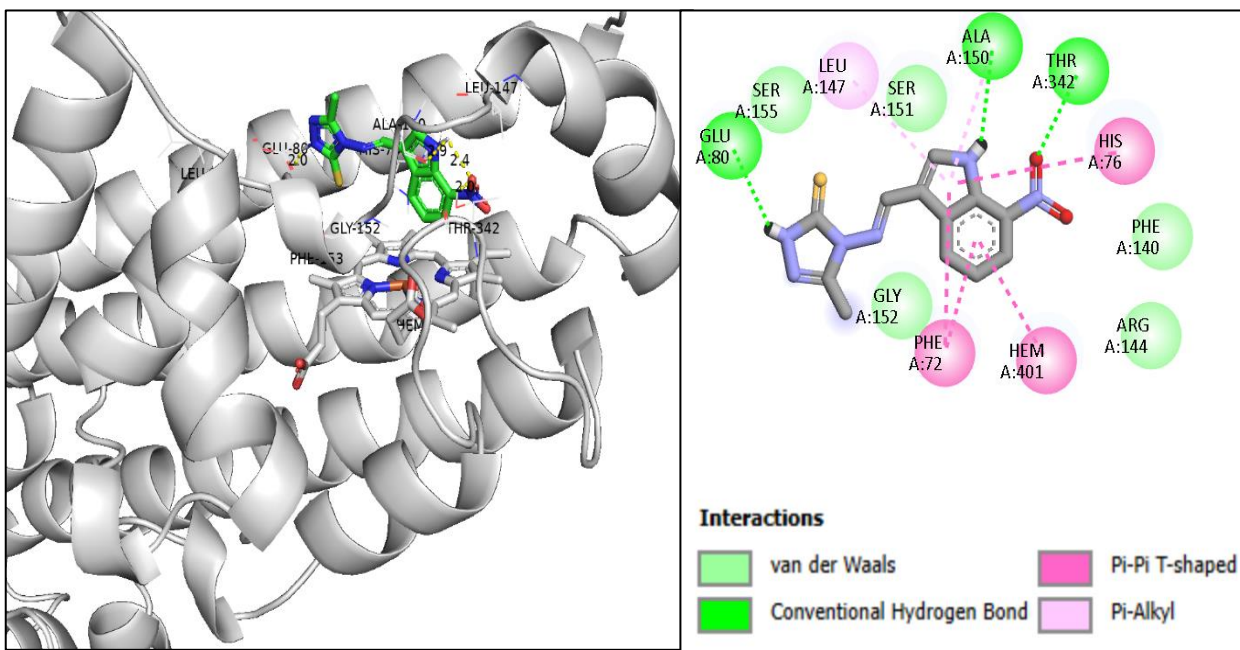


**Figure 3.72: Binding mode of compound C9 with TDO2 and its 2D schematic interaction.**

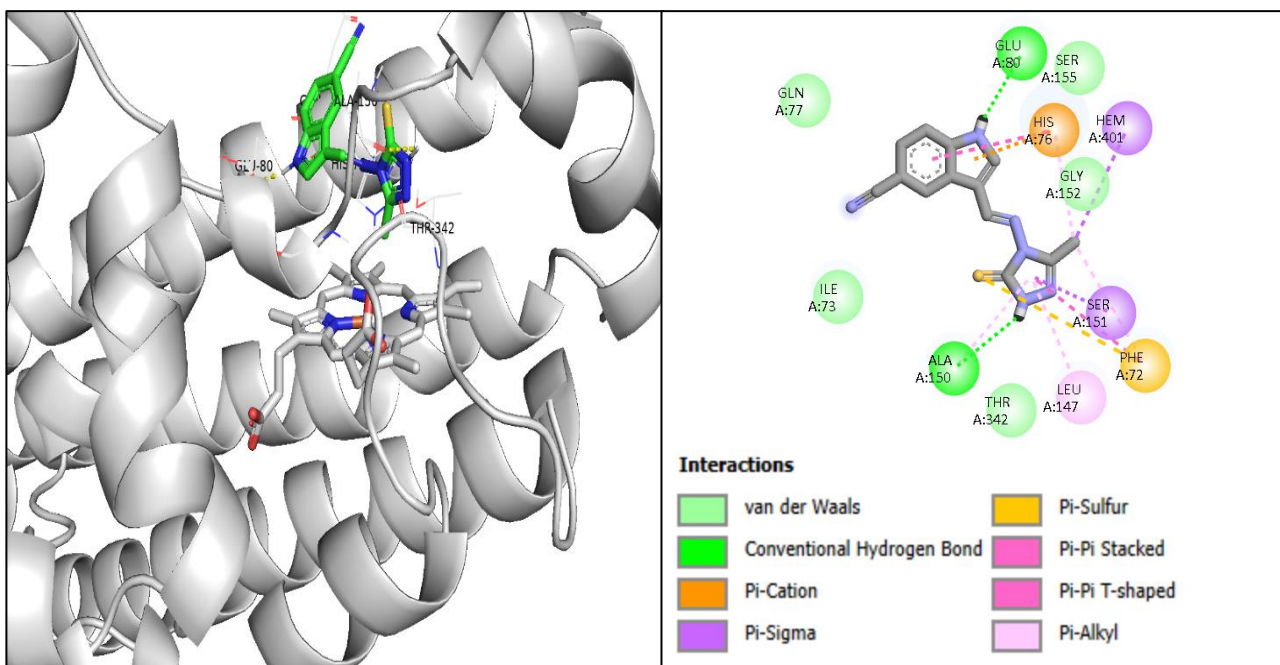


**Figure 3.73: Binding mode of compound C10 with TDO2 and its 2D schematic interaction**

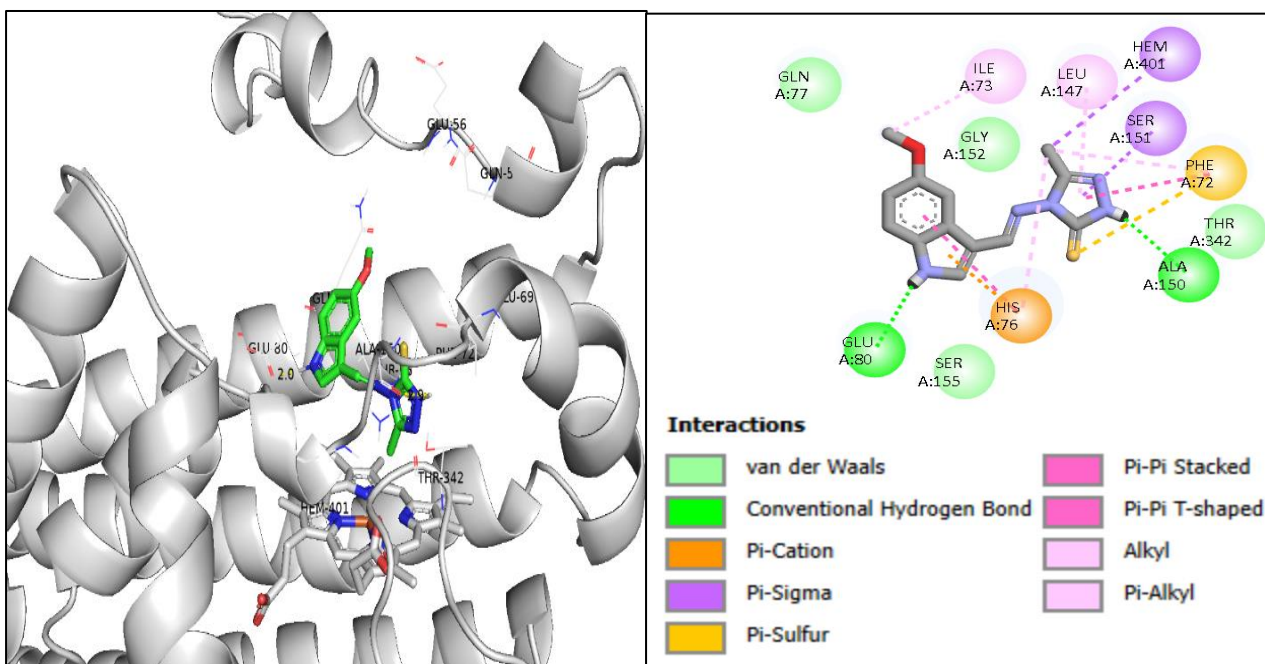


**Figure 3.74: Binding mode of compound C11 with TDO2 and its 2D schematic interaction.**

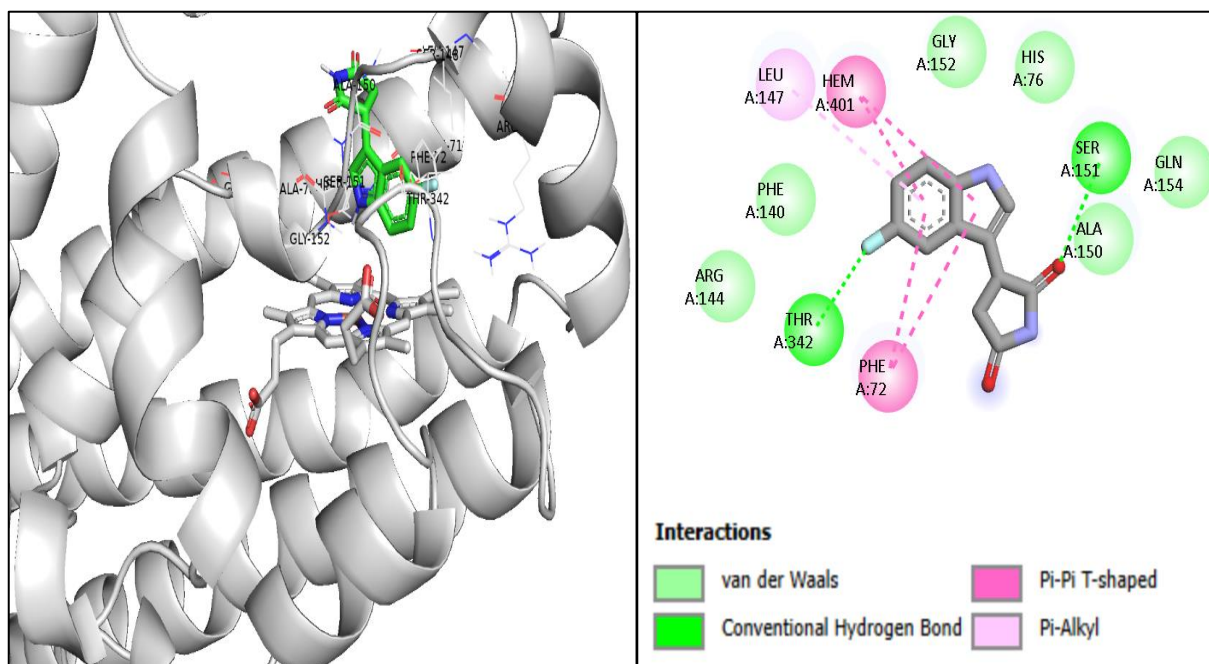


**Figure 3.75: Binding mode of 3-(5-fluoro-1H-indol-3-yl)pyrrolidine-2,5-dione with TDO2 and its 2D schematic interaction**

### 3.6. Conclusions

1. A new series of indole bearing triazole-3-thione derivatives were synthesized and their structures were characterized using FTIR, <sup>1</sup>HNMR, <sup>13</sup>CNMR, and HRMS spectrometry.
2. The biological evaluation revealed that the synthesized compounds exhibited weak to moderate anticancer activity against the human liver cancer cell line (HepG2).
3. The antibacterial screening indicated that the prepared compounds showed weak antibacterial activity against the tested bacterial strains.
4. Molecular docking studies against tryptophan 2,3-dioxygenase (TDO2) demonstrated favorable binding interactions, which supported the experimental biological result

### **3.7. Recommendations**

1. Preparation of new derivatives of 4-amino-1,2,4-triazole-3-thione by replacing the methyl group with various substituted groups, and studying the effects of their steric and electronic properties.
2. Utilize the synthesized Schiff base and its azomethine group as a versatile scaffold for the synthesis of heterocyclic compounds.
3. Evaluate the synthesized compounds against TDO2 using enzymatic assays to validate the docking predictions and identify the most potent inhibitors.
4. Perform molecular dynamics simulations to study the stability and dynamics of Schiff base–TDO2 interactions, which can guide further structural optimization.

## REFERENCES

1. Devkota K, Pathak G, Shakya B. Synthesis and evaluation of Schiff bases of 4-amino-5-(chlorine substituted phenyl)-4H-1, 2, 4-triazole-3-thione as antimicrobial agents. *J Nepal Chem Soc.* 2020;41(1):26-35.
2. Dayan, Franck E Vincent, Armelle C Romagni, Joanne G Allen, Stacy N Duke, Stephen O Duke, Mary V Bowling, John J Zjawiony, Jordan K. Amino-and urea-substituted thiazoles inhibit photosynthetic electron transfer. *J Agric Food Chem.* 2000;48(8):3689-3693.
3. Huang W, Yang GF. Microwave-assisted, one-pot syntheses and fungicidal activity of polyfluorinated 2-benzylthiobenzothiazoles. *Bioorg Med Chem.* 2006;14(24):8280-8285.
4. Ling S, Xin Z, Qing Z, Jian-Bing L, Zhong J, Jian-Xin F. Synthesis, Structure, and Biological Activity of Novel 1 H-1, 2, 4-Triazol-1-yl-thiazole Derivatives. *Synth Commun.* 2007;37(2):199-207.
5. Temple C, Montgomery JA. *Triazoles 1, 2, 4, Volume 37.* Vol 37. John Wiley & Sons; 2009.
6. Shneine JK, Alaraji YH. Chemistry of 1, 2, 4-Triazole: A Review Article. *Int J Sci Res.* 2016;5(3):1411-1423.
7. Kotelevskii S, Prezhdo O. Aromaticity indices revisited: Refinement and application to certain five-membered ring heterocycles. *Tetrahedron.* 2001;57:5715-5729.
8. Obot I, Johnson A. Ab initio, DFT and TD-DFT electronic absorption spectra investigations on 3,5-diamino-1,2,4-triazole. *Comput Chem.* 2012.
9. Ozimiński WP, Dobrowolski JC, Mazurek AP. DFT studies on tautomerism of C5-substituted 1,2,3-triazoles. *J Mol Struct.* 2003;651-653:697-704.

10. D'souza A, Venuprasad KD, Nayak P, Poonacha LK. A Review Article on Triazoles and its Pharmacological Activities. *J Pharm Res Int*. 2021;33(43A SE-Review Article):309-317.
11. Pinto D, Santos CMM, Silva AMS. Advanced NMR techniques for structural characterization of heterocyclic structures. *Recent Res Dev Heterocycl Chem*. 2007;37(661):397-475.
12. Gao F, Wang T, Xiao J, Huang G. Antibacterial activity study of 1,2,4-triazole derivatives. *Eur J Med Chem*. 2019;173:274-281.
13. Yazdani M, Edraki N, Badri R, Khoshneviszadeh M, Irajli A, Firuzi O. Multi-target inhibitors against Alzheimer disease derived from 3-hydrazinyl 1,2,4-triazine scaffold containing pendant phenoxy methyl-1,2,3-triazole: Design, synthesis and biological evaluation. *Bioorg Chem*. 2019;84:363-371.
14. Timur İ, Kocyigit ÜM, Dastan T, Sandal S, Ceribasi AO, Taslimi P, Gulcin I, Koparir M, Karatepe M, Çiftci M. In vitro cytotoxic and in vivo antitumoral activities of some aminomethyl derivatives of 2,4-dihydro-3H-1,2,4-triazole-3-thiones—Evaluation of their acetylcholinesterase and carbonic anhydrase enzymes inhibition profiles. *J Biochem Mol Toxicol*. 2019;33(1):e22239.
15. Ziyaev AA, Sasmakov SA, Toshmurodov TT, Abdurakhmanov JM, Ikramov SA, Khasanov S Sh., Ashirov ON, Ziyaeva MA, Begimqulova DB. Synthesis and Biological Activity of 5-Substituted-2,4-dihydro-1,2,4-triazole-3-thiones and Their Derivatives. *Organics*. 2025;6(3):41.
16. Kaproń B, Łuszczki JJ, Płazińska A, Siwek A, Karcz T, Gryboś AC, Nowak G, Makuch-Kocka A, Walczak K, Langner E, Szalast K, Marciniak S, Paczkowska M, Cielecka PJ, Ciesla LM, Plech T. Development of the 1,2,4-triazole-based anticonvulsant drug candidates acting on the voltage-gated sodium channels. Insights from in-vivo, in-vitro, and in-silico studies. *Eur J*

*Pharm Sci.* 2019;129:42-57.

17. Küçükgülzel İ, Tatar E, Küçükgülzel ŞG, Rollas S, De Clercq E. Synthesis of some novel thiourea derivatives obtained from 5-[(4-aminophenoxy)methyl]-4-alkyl/aryl-2,4-dihydro-3H-1,2,4-triazole-3-thiones and evaluation as antiviral/anti-HIV and anti-tuberculosis agents. *Eur J Med Chem.* 2008;43(2):381-392.
18. Plech T, Kaproń B, Łuszczki JJ, Paneth A, Siwek A, Kołaczkowski M, Żołnierek M, Nowak G. Studies on the anticonvulsant activity of 4-alkyl-1,2,4-triazole-3-thiones and their effect on GABAergic system. *Eur J Med Chem.* 2014;86:690-699.
19. Łuszczki JJ, Plech T, Wujec M. Effect of 4-(4-bromophenyl)-5-(3-chlorophenyl)-2,4-dihydro-3H-1,2,4-triazole-3-thione on the anticonvulsant action of different classical antiepileptic drugs in the mouse maximal electroshock-induced seizure model. *Eur J Pharmacol.* 2012;690(1):99-106.
20. Hassan AA, Mohamed NK, Aly AA, Tawfeek HN, Bräse S, Nieger M. Eschenmoser-Coupling Reaction Furnishes Diazenyl-1,2,4-triazole-5(4H)-thione Derivatives. *ChemistrySelect.* 2019;4(2):465-468.
21. SUN XH, TAO Y, LIU YF, CHEN B. Synthesis and Biological Activities of Substituted Triazolethione Schiff Base. *Chinese J Chem.* 2007;25(10):1573-1576.
22. Hanif M, Hassan M, Rafiq M, Abbas Q, Ishaq A, Shahzadi S, Seo SY, Saleem M. Microwave-Assisted Synthesis, In Vivo Anti-Inflammatory and In Vitro Anti-Oxidant Activities, and Molecular Docking Study of New Substituted Schiff Base Derivatives. *Pharm Chem J.* 2018;52(5):424-437.
23. Ibrahim DA, Al-Wahaibi LH, Abu-Melha HM. Synthesis and Biochemical Evaluation of Novel Coumarin Derivatives as Anticancer and Anti-HIV

Inhibitors Targeting CDK2. *Chemotherapy*. 2017;6(244):2.

24. Wang BL, Liu XH, Zhang XL, Zhang JF, Song HB, Li ZM. Synthesis, Structure and Biological Activity of Novel 1,2,4-Triazole Mannich Bases Containing a Substituted Benzylpiperazine Moiety. *Chem Biol Drug Des*. 2011;78(1):42-49.
25. Cartwright DDJ, Clark BAJ, McNab H. Gas-phase pyrolysis of 4-amino-3-allylthio-1,2,4-triazoles: a new route to [1,3]thiazolo[3,2-b][1,2,4]triazoles. *J Chem Soc Perkin Trans 1*. 2001;(4):424-428.
26. Awad LF, Ashry ESHE. Synthesis and conformational analysis of seco C-nucleosides and their diseco double-headed analogues of the 1,2,4-triazole, 1,2,4-triazolo[3,4-b]1,3,4-thiadiazole. Parts of this work were presented at 19th International Carbohydrate Symposium, San Diego, C. *Carbohydr Res*. 1998;312(1):9-22.
27. Carmelo J. Rizzo. The chemical linkage between monomer units in nucleic acids 341 is a phosphodiester 174. *Org Chem Lect*. 2008:174-186.
28. Reddy TRK, Li C, Guo X, Fischer PM, Dekker L V. Design, synthesis and SAR exploration of tri-substituted 1,2,4-triazoles as inhibitors of the annexin A2–S100A10 protein interaction. *Bioorg Med Chem*. 2014;22(19):5378-5391.
29. Vainilavicius P, Smicius R, Jakubkiene V, Tumkevicius S. Synthesis of 5-(6-Methyl-2,4-dioxo-1,2,3,4-tetrahydro-3-pyrimidinyl)-methyl-4-amino-1,2,4-triazole-3-thione and its Reactions with Polyfunctional Electrophiles. *Monatshefte für Chemie/Chemical Mon*. 2001;132(7):825-831.
30. L-Soud YA, Al-Masoudi ANA. A new class of dihaloquinolones bearing N'-aldehydoglycosylhydrazides, mercapto-1,2,4-triazole, oxadiazoline and amino ester precursors: synthesis and antimicrobial activity. *J Braz Chem Soc*. 2003;14:790-796.

31. Cansiz A, Koparir M, Demirdağ A. Synthesis of some new 4,5-substituted-4H-1,2,4-triazole-3-thiol derivatives. *Molecules*. 2004;9(4):204-212.
32. Wajda-Hermanowicz K, Pieniżczak D, Zatajska A, Wróbel R, Drabent K, Ciunik Z. A Study on the Condensation Reaction of 4-Amino-3,5-dimethyl-1,2,4-triazole with Benzaldehydes: Structure and Spectroscopic Properties of Some New Stable Hemiaminals. *Molecules*. 2015;20(9):17109-17131.
33. Keskin E, Uzgoren-Baran A. Synthesis and characterization of novel 1,2,4-triazole-3-thione Schiff bases compounds containing tetrahydrocarbazole moiety. *J Mol Struct*. 2025;1322:140616.
34. Shaker RM, Aly AA. Recent trends in the chemistry of 4-amino-1, 2, 4-triazole-3-thiones. *Phosphorus Sulfur Silicon Relat Elem*. 2006;181(11):2577-2613.
35. Kolodina AA, Lesin A V, Nelyubina Y V. Ring formation and ring opening reactions of a dihydrothiadiazine cycle fused to 1,2,4-triazole. *Mendeleev Commun*. 2008;18(5):253-254.
36. Farghaly AH. Synthesis, reactions and antimicrobial activity of some new indolyl-1, 3, 4-oxadiazole, triazole and pyrazole derivatives. *J Chinese Chem Soc*. 2004;51(1):147-156.
37. El-masry AH, Fahmy HH, Ali Abdelwahed SH. Synthesis and antimicrobial activity of some new benzimidazole derivatives. *molecules*. 2000;5(12):1429-1438.
38. Badr SMI, Barwa RM. Synthesis of some new [1,2,4]triazolo[3,4-b][1,3,4]thiadiazines and [1,2,4]triazolo[3,4-b][1,3,4] thiadiazoles starting from 5-nitro-2-furoic acid and evaluation of their antimicrobial activity. *Bioorg Med Chem*. 2011;19(15):4506-4512.

39. Cao L, Zhang L, Cui P. Synthesis of 3-(3-Alkyl-5-thioxo-1H-4, 5-dihydro-1, 2, 4-triazol-4-yl) aminocarbonylchromones. *Chem Heterocycl Compd.* 2004;40(5):635-640.
40. Plech T, Wujec M, Kosikowska U, Malm A, Rajtar B, Polz-Dacewicz M. Synthesis and in vitro activity of 1,2,4-triazole-ciprofloxacin hybrids against drug-susceptible and drug-resistant bacteria. *Eur J Med Chem.* 2013;60:128-134.
41. Küçükgülzel Ş.G, Çıkla S, Pelin. Recent advances bioactive 1,2,4-triazole-3-thiones. *European Journal of Medicinal Chemistry.* 2015;97:830-870.
42. Hassan GS, El-Messery SM, Al-Omary FAM, Al-Rashood ST, Shabayek MI, Abulfadl YS, Habib El-Sayed E, El-Hallouty SM, Fayad W, Mohamed KM, El-Menshawi, Bassem S, El-Subbagh, Hussein I. Nonclassical antifolates, part 4. 5-(2-Aminothiazol-4-yl)-4-phenyl-4H-1,2,4-triazole-3-thiols as a new class of DHFR inhibitors: Synthesis, biological evaluation and molecular modeling study. *Eur J Med Chem.* 2013;66:135-145.
43. Lipkus AH, Yuan Q, Lucas KA, Funk SA, Bartelt WF, Schenck RJ, Trippe AJ. Structural Diversity of Organic Chemistry. A Scaffold Analysis of the CAS Registry. *J Org Chem.* 2008;73(12):4443-4451.
44. Kaushik NK, Kaushik N, Attri P, Kumar N, Kim CH, Verma AK, Choi EH. Biomedical importance of indoles. *Molecules.* 2013;18(6):6620-6662.
45. Won C, Shen X, Mashiguchi K, Zheng Z, Dai X, Cheng Y, Kasahara H, Kamiya Y, Chory J, Zhao Y. Conversion of tryptophan to indole-3-acetic acid by TRYPTOPHAN AMINOTRANSFERASES OF ARABIDOPSIS and YUCCAs in Arabidopsis. *Proc Natl Acad Sci.* 2011;108(45):18518-18523.
46. Zhang MZ, Mulholland N, Beattie D, Irwin D, Gu Yu-C, Chen Q, Yang G-Fu Clough J. Synthesis and antifungal activity of 3-(1, 3, 4-oxadiazol-5-yl)-

- indoles and 3-(1, 3, 4-oxadiazol-5-yl) methyl-indoles. *Eur J Med Chem.* 2013;63:22-32.
47. Young SN. How to increase serotonin in the human brain without drugs. *J psychiatry Neurosci JPN.* 2007;32(6):394.
48. Diss LB, Robinson SD, Wu Y, Fidalgo S, Yeoman MS, Patel BA. Age-related changes in melatonin release in the murine distal colon. *ACS Chem Neurosci.* 2013;4(5):879-887.
49. Takada Y, Bhardwaj A, Potdar P, Aggarwal BB. Nonsteroidal anti-inflammatory agents differ in their ability to suppress NF- $\kappa$ B activation, inhibition of expression of cyclooxygenase-2 and cyclin D1, and abrogation of tumor cell proliferation. *Oncogene.* 2004;23(57):9247-9258.
50. Chan TA, Morin PJ, Vogelstein B, Kinzler KW. Mechanisms underlying nonsteroidal antiinflammatory drug-mediated apoptosis. *Proc Natl Acad Sci.* 1998;95(2):681-686.
51. Taber DF, Tirunahari PK. Indole synthesis: a review and proposed classification. *Tetrahedron.* 2011;67(38):7195-7210.
52. Blackburn RS, Bechtold T, John P. The development of indigo reduction methods and pre-reduced indigo products. *Color Technol.* 2009;125(4):193-207.
53. Smith BJ, Liu R. A theoretical investigation of indole tautomers. *J Mol Struct THEOCHEM.* 1999;491(1-3):211-222.
54. Dubnikova F, Lifshitz A. Isomerization of indole. Quantum chemical calculations and kinetic modeling. *J Phys Chem A.* 2001;105(14):3605-3614.
55. Lakhdar S, Westermaier M, Terrier F, et al. Nucleophilic reactivities of indoles. *J Org Chem.* 2006;71(24):9088-9095.

56. Bandini M, Eichholzer A. Catalytic functionalization of indoles in a new dimension. *Angew Chemie Int Ed.* 2009;48(51):9608-9644.
57. de Sa Alves FR, Barreiro EJ, Manssour Fraga CA. From nature to drug discovery: the indole scaffold as a 'privileged structure.' *Mini Rev Med Chem.* 2009;9(7):782-793.
58. Shimazaki Y, Yajima T, Takani M, Yamauchi O. Metal complexes involving indole rings: Structures and effects of metal–indole interactions. *Coord Chem Rev.* 2009;253(3-4):479-492.
59. Pelkey ET, Barden TC, Gribble GW. Nucleophilic addition reactions of 2-nitro-1-(phenylsulfonyl)indole. A new synthesis of 3-substituted-2-nitroindoles. *Tetrahedron Lett.* 1999;40(43):7615-7619.
60. Yadav JS, Reddy BVS, Krishna AD, Swamy T. InBr<sub>3</sub>-catalyzed sulfonation of indoles: a facile synthesis of 3-sulfonyl indoles. *Tetrahedron Lett.* 2003;44(32):6055-6058.
61. Hofmann M, Hampel N, Kanzian T, Mayr H. Electrophilic Alkylations in Neutral Aqueous or Alcoholic Solutions. *Angew Chemie Int Ed.* 2004;43(40):5402-5405.
62. MURAKAMI Y. Chemistry of Indoles : New Reactivities of Indole Nucleus and Its Synthetic Application. *YAKUGAKU ZASSHI.* 1999;119(1):35-60.
63. Takeuchi Y, Tarui T, Shibata N. A novel and efficient synthesis of 3-fluorooxindoles from indoles mediated by selectfluor. *Org Lett.* 2000;2(5):639-642.
64. Kirschning A, Yusubov MS, Yusubova RY, Chi KW, Park JY. M-Iodosylbenzoic acid - A convenient recyclable reagent for highly efficient aromatic iodinations. *Beilstein J Org Chem.* 2007;3:1-5.

65. Ansari N, Taylor M, Söderberg B. Syntheses of three naturally occurring polybrominated 3,3'-bi-1H-indoles. *Tetrahedron Lett.* 2017;58.
66. Exlonk Gil A, Hadad CZ. Reaction Mechanism and Effect of Substituent in Direct Bromination of Indoles. *ChemistrySelect.* 2023;8(35):e202302032.
67. Wang Z, Jimenez LS. A total synthesis of ( $\pm$ )-Mitomycin K. Oxidation of the mitosene C9-9a double bond by (hexamethylphosphoramide)oxodiperoxomolybdenum (VI) ( $\text{MoO}_5 \cdot \text{HMPA}$ ). *Tetrahedron Lett.* 1996;37(34):6049-6052.
68. Xu J, Liang L, Zheng H, Chi YR, Tong R. Green oxidation of indoles using halide catalysis. *Nat Commun.* 2019;10(1):1-11.
69. Kukuljan L, Kranjc K, Perdih F. Synthesis and Structural Evaluation of 5-Methyl-6-acetyl Substituted Indole and Gramine. *Acta Chim Slov.* 2016;63(4).
70. Dai H, Li J, Li T. Efficient and practical synthesis of mannich bases related to gramine mediated by zinc chloride. *Synth Commun.* 2006;36(13):1829-1835.
71. Dadashpour S, Emami S. Indole in the target-based design of anticancer agents: A versatile scaffold with diverse mechanisms. *Eur J Med Chem.* 2018;150:9-29.
72. Reyaz HM, Roohi M-ud-d, Taha UW, Mohammad OD, Abdul JS, Bashir L, Chawla P, Mubashir HM. Indole: A privileged heterocyclic moiety in the management of cancer. *Curr Org Chem.* 2021;25(6):724-736.
73. Honore S, Pasquier E, Braguer D. Understanding microtubule dynamics for improved cancer therapy. *Cell Mol Life Sci.* 2005;62(24):3039-3056.
74. Lu Y, Chen J, Wang J, Li C, Ahn S, Barrett CM, Dalton JT, Li W, Miller DD. Design, synthesis, and biological evaluation of stable colchicine binding site tubulin inhibitors as potential anticancer agents. *J Med Chem.* 2014;57(17):7355-7366.

75. Mirzaei H, Shokrzadeh M, Modanloo M, Ziar A, Riazi GH, Emami S. New indole-based chalconoids as tubulin-targeting antiproliferative agents. *Bioorg Chem.* 2017;75:86-98.
76. Zhou Y, Duan K, Zhu L, Liu Z, Zhang C, Yang L, Li M, Zhang H, Yang, X. Synthesis and cytotoxic activity of novel hexahydropyrrolo[2,3-b]indole imidazolium salts. *Bioorg Med Chem Lett.* 2016;26(2):460-465.
77. Leneva IA, Russell RJ, Boriskin YS, Hay AJ. Characteristics of arbidol-resistant mutants of influenza virus: Implications for the mechanism of anti-influenza action of arbidol. *Antiviral Res.* 2009;81(2):132-140.
78. Boriskin Y, Leneva I, Pecheur EI, Polyak S. Arbidol: A Broad-Spectrum Antiviral Compound that Blocks Viral Fusion. *Curr Med Chem.* 2008;15(10):997-1005.
79. Romero DL, Olmsted RA, Poel TJ, Morge RA, Biles C, Keiser BJ, Kopta, LA, Friis JM, Hosley JD, Stefanski KJ, Wishka DG, Evans DB, Morris J, Stehle RG, Sharma SK, Yagi Y, Voorman RL, Adams WJ, Tarpley W G, Thomas, RC. Targeting Delavirdine/Ateviridine Resistant HIV-1: Identification of (Alkylamino)piperidine-Containing Bis(heteroaryl)piperazines as Broad Spectrum HIV-1 Reverse Transcriptase Inhibitors. *J Med Chem.* 1996;39(19):3769-3789.
80. Yu F, Lu L, Du L, Zhu X, Debnath AK, Jiang S. Approaches for identification of HIV-1 entry inhibitors targeting gp41 pocket. *Viruses.* 2013;5(1):127-149.
81. Sanna G, Madeddu S, Giliberti G, Piras S, Struga M, Wrzosek M, Kubiak-Tomaszewska G, Koziol AE, Savchenko O, Lis T, Stefanska J, Tomaszewski P, Skrzycki M, Szulczyk D. Synthesis and biological evaluation of novel indole-derived thioureas. *Molecules.* 2018;23(10):1-17.
82. Sayed M, Kamal El-Dean AM, Ahmed M, Hassanien R. Synthesis of some

- heterocyclic compounds derived from indole as antimicrobial agents. *Synth Commun.* 2018;48(4):413-421.
83. Di Matteo V, Esposito E. Biochemical and Therapeutic Effects of Antioxidants in the Treatment of Alzheimers Disease, Parkinsons Disease, and Amyotrophic Lateral Sclerosis. *Curr Drug Targets CNS Neurol Disord.* 2003;2:95-107.
  84. Rao V, Balachandran BP. Role of Oxidative Stress and Antioxidants in Neurodegenerative Diseases. *Nutr Neurosci.* 2002;5:291-309.
  85. Gurer-Orhan H, Karaaslan C, Ozcan S, Firuzi O, Tavakkoli M, Saso L, Suzen S. Novel indole-based melatonin analogues: Evaluation of antioxidant activity and protective effect against amyloid  $\beta$ -induced damage. *Bioorg Med Chem.* 2016;24(8):1658-1664.
  86. Silveira CC, Mendes SR, Soares JR, Victoria FN, Martinez DM, Savegnago L. Synthesis and antioxidant activity of new C-3 sulfenyl indoles. *Tetrahedron Lett.* 2013;54(36):4926-4929.
  87. BAYTAŞ S, Kapcak E, ÇOBAN T, Özbilge H. Synthesis and antioxidant and antimicrobial evaluation of novel 4-substituted-1H-1, 2, 4-triazole derivatives. *Turkish J Chem.* 2012;36(6):867-884.
  88. Li YY, Wu HS, Tang L, Li, Feng CR, Yu JH, Li Y, Yang YS, Yang B, He QJ. The potential insulin sensitizing and glucose lowering effects of a novel indole derivative in vitro and in vivo. *Pharmacol Res.* 2007;56(4):335-343.
  89. Kajal A, Bala S, Kamboj S, Sharma N, Saini V. Schiff bases: a versatile pharmacophore. *J Catal.* 2013;2013(1):893512.
  90. Pradhan A, Kumar A. A review: an overview on synthesis of some Schiff bases and there metal complexes with anti-microbial activity. *Chem Process Eng Res.* 2015;35:84-86.

91. Chaurasia M, Tomar D, Chandra S. BSA Binding Studies of Co (II), Ni (II) and Cu (II) Metal Complexes of Schiff base Derived from 2-hydroxy-4-methoxybenzaldehyde and 2-amino-6-methylbenzothiazole. *Egypt J Chem.* 2019;62(2):357-372.
92. Hossain MS, Roy PK, Zakaria CM, Kudrat-E-Zahan M. Selected Schiff base coordination complexes and their microbial application: A review. *Int J Chem Stud.* 2018;6(1):19-31.
93. Mishra N, Kumar Dm. Coordination chemistry of Schiff base tin complexes. *Russ J Coord Chem.* 2014;40(6):343-357.
94. Silva CM, da Silva DLd, Modolo L V, et al. Schiff bases: A short review of their antimicrobial activities. *J Adv Res.* 2011;2(1):1-8.
95. Zoubi W Al, Al-Hamdani AAS, Ko YG. Schiff bases and their complexes: Recent progress in thermal analysis. *Sep Sci Technol.* 2017;52(6):1052-1069.
96. Przybylski P, Huczynski A, Pyta K, Brzezinski B, Bartl F. Biological Properties of Schiff Bases and Azo Derivatives of Phenols. *Curr Org Chem.* 2009;13(2):124-148.
97. Sathe BS, Jaychandran E, Jagtap VA, Sreenivasa GM. Synthesis characterization and anti-inflammatory evaluation of new fluorobenzothiazole schiff's bases. *Int J Pharm Res Dev.* 2011;3(3):164-169.
98. Sondhi SM, Singh N, Kumar A, Lozach O, Meijer L. Synthesis, anti-inflammatory, analgesic and kinase (CDK-1, CDK-5 and GSK-3) inhibition activity evaluation of benzimidazole/benzoxazole derivatives and some Schiff's bases. *Bioorg Med Chem.* 2006;14(11):3758-3765.
99. Pandey A, Rajavel R, Chandraker S, Dash D. Synthesis of Schiff Bases of 2-amino-5-aryl-1, 3, 4-thiadiazole and Its Analgesic, Anti-Inflammatory and

Anti-Bacterial Activity. *J Chem.* 2012;9(4):2524-2531.

100. Chandramouli C, Shivanand MR, Nayanbhai TB, Bheemachari B, Udupi RH. Synthesis and biological screening of certain new triazole Schiff bases and their derivatives bearing substituted benzothiazole moiety. *J Chem Pharm Res.* 2012;4(2):1151-1159.
101. Chinnasamy RP, Sundararajan R, Govindaraj S. Synthesis, characterization, and analgesic activity of novel schiff base of isatin derivatives. *J Adv Pharm Technol Res.* 2010;1(3):342-347.
102. Mounika K, Pragathi A, Gyanakumari C. Synthesis characterization and biological activity of a Schiff base derived from 3-ethoxy salicylaldehyde and 2-amino benzoic acid and its transition metal complexes. *J Sci Res.* 2010;2(3):513.
103. Venkatesh P. Synthesis, characterization and antimicrobial activity of various schiff bases complexes of Zn(II) and Cu(II) ions. *Asian J Pharm Hea Sci.* 2011;1:8-11.
104. Chaubey AK, Pandeya SN. Synthesis & anticonvulsant activity (Chemo Shock) of Schiff and Mannich bases of Isatin derivatives with 2-Amino pyridine (mechanism of action). *Int J PharmTech Res.* 2012;4(4):590-598.
105. Aboul-Fadl T, Mohammed FAH, Hassan EAS. Synthesis, antitubercular activity and pharmacokinetic studies of some Schiff bases derived from 1-alkylisatin and isonicotinic acid hydrazide (INH). *Arch Pharm Res.* 2003;26(10):778-784.
106. Miri R, Razzaghi-asl N, Mohammadi MK. QM study and conformational analysis of an isatin Schiff base as a potential cytotoxic agent. *J Mol Model.* 2013;19(2):727-735.

107. Ali SMM, Azad MAK, Jesmin M, Ahsan S, Rahman MM, Khanam JA, Islam MN, Shahriar SMS. In vivo anticancer activity of vanillin semicarbazone. *Asian Pac J Trop Biomed.* 2012;2(6):438-442.
108. Wei D, Li N, Lu G, Yao K. Synthesis, catalytic and biological activity of novel dinuclear copper complex with Schiff base. *Sci China Ser B.* 2006;49(3):225-229.
109. Avaji PG, Kumar CHV, Patil SA, Shivananda KN, Nagaraju C. Synthesis, spectral characterization, in-vitro microbiological evaluation and cytotoxic activities of novel macrocyclic bis hydrazone. *Eur J Med Chem.* 2009;44(9):3552-3559.
110. Venugopala KN, Jayashree BS. Synthesis of carboxamides of 2'-amino-4'-(6-bromo-3-coumarinyl) thiazole as analgesic and antiinflammatory agents. *Indian J Heterocycl Chem.* 2003;12(4):307-310.
111. Vashi K, Naik HB. Synthesis of novel Schiff base and azetidinone derivatives and their antibacterial activity. *J Chem.* 2004;1(5):272-275.
112. Ershad S, Sagathforoush LA, Karim-nezhad G, Kangari S. Electrochemical behavior of N2SO Schiff-base Co (II) complexes in non-aqueous media at the surface of solid electrodes. *Int J Electrochem Sci.* 2009;4(6):846-854.
113. Jarrahpour A, Khalili D, De Clercq E, Salmi C, Brunel JM. Synthesis, antibacterial, antifungal and antiviral activity evaluation of some new bis-Schiff bases of isatin and their derivatives. *Molecules.* 2007;12(8):1720-1730.
114. El-Shafiey ZA. Synthesis, spectroscopic characterization, thermal investigation and antimicrobial activity of S, O and N-donor heterocyclic Schiff base ligands and their Co (II), Cd (II), Hg (II), Fe (III) and UO<sub>2</sub> (II) metal complexes. *Egypt J Chem.* 2010;53(1):137-162.

115. Qin W, Long S, Panunzio M, Biondi S. Schiff Bases: A Short Survey on an Evergreen Chemistry Tool. *Molecules*, 2013;12264-12289.
116. Cornils B. Houben-Fischer nitrile synthesis. In: *Catalysis from A to Z*. ; 2020.
117. Ayoob AI, Sadeek GT, Saleh MY. Synthesis and Biologically Activity of Novel 2-Chloro-3-Formyl-1, 5-Naphthyridine Chalcone Derivatives. *J Chem Heal Risks*. 2022;12(1).
118. Al-Thakafy NT, Al-Enizzi MS, Saleh MY. Synthesis of new Organic reagent by Vilsmeier–Haack reaction and estimation of pharmaceutical compounds (Mesalazine) containing aromatic amine groups. *Egypt J Chem*. 2022;65(6):685-697.
119. Cebeci YU, Bayrak H, Şirin Y. Synthesis of novel Schiff bases and azol-β-lactam derivatives starting from morpholine and thiomorpholine and investigation of their antitubercular, antiurease activity, acetylcholinesterase inhibition effect and antioxidant capacity. *Bioorg Chem*. 2019;88:102928.
120. Shady AA, Abu Bakr SM, Khidre MD. Synthesis of Various Schiff Bases Containing Isoxazole Ring and Their Applications with Thioglycollic Acid and Diverse Phosphorus Reagents. *J Heterocycl Chem*. 2017;54(1):71-79.
121. Fayyadh K. Synthesis , Characterization and Spectroscopic Study of Some Heterocyclic Synthesis , Characterization and Spectroscopic Study of Some Heterocyclic Compounds ( 2 , 3-Dihydroquinazolin , Dzetidin-2-one ) Derived from Schiff Bases and Evaluation Their Bacte. 2020;(January).
122. Yadav M, Sharma S, Devi J. Designing, spectroscopic characterization, biological screening and antioxidant activity of mononuclear transition metal complexes of bidentate Schiff base hydrazones. *J Chem Sci*. 2021;133.
123. Singh A, Gogoi H, Barman P, Guha A. Novel Thioether Schiff base Transition

- metal complexes: Design, Synthesis, Characterization, Molecular docking, Computational, Biological, and Catalytic Studies. *Appl Organomet Chem.* 2022;36.
124. Dhingra N, Singh JB, Singh HL. Synthesis, spectroscopy, and density functional theory of organotin and organosilicon complexes of bioactive ligand containing nitrogen, sulfur donor atoms as antimicrobial agents: in-vitro and in-silico studies. *Dalt Trans.* 2022;51.
125. Kitchen DB, Decornez H, Furr JR, Bajorath J. Docking and scoring in virtual screening for drug discovery: methods and applications. *Nat Rev Drug Discov.* 2004;3(11):935-949.
126. Meng XY, Zhang HX, Mezei M, Cui M. Molecular docking: a powerful approach for structure-based drug discovery. *Curr Comput Aided Drug Des.* 2011;7(2):146-157.
127. Amaro RE, Baudry J, Chodera J, Demir Ö, McCammon JA, Miao Y, Smith JC. Ensemble Docking in Drug Discovery. *Biophys J.* 2018;114(10):2271-2278.
128. Carlson HA. Protein flexibility and drug design: how to hit a moving target. *Curr Opin Chem Biol.* 2002;6(4):447-452.
129. Abagyan R, Totrov M. High-throughput docking for lead generation. *Curr Opin Chem Biol.* 2001;5(4):375-382.
130. Agu PC, Afiukwa CA, Orji OU, Ezech EM, Ofoke IH, Ogbu CO, Ugwuja EI, Aja PM. Molecular docking as a tool for the discovery of molecular targets of nutraceuticals in diseases management. *Sci Rep.* 2023;13(1):13398.
131. Van Baren N, Van den Eynde BJ. Tryptophan-Degrading Enzymes in Tumoral Immune Resistance. *Front Immunol.* 2016;Volume 6-.
132. Ye Z, Yue L, Shi J, Shao M, Wu T. Role of IDO and TDO in Cancers and

- Related Diseases and the Therapeutic Implications. *J Cancer*. 2019;10(12):2771-2782.
133. Abdel-Magid AF. Targeting the Inhibition of Tryptophan 2,3-Dioxygenase (TDO-2) for Cancer Treatment. *ACS Med Chem Lett*. 2017;8(1):11-13.
134. Garg S, Oran A, Wajchman J, Sasaki S, Maris CH, Kapp JA, Jacob J. Erratum: Genetic tagging shows increased frequency and longevity of antigen-presenting, skin-derived dendritic cells in vivo. *Nat Immunol*. 2003;4(10):1037.
135. Prendergast GC, Malachowski WJ, Mondal A, Scherle P, Muller AJ. Chapter Four - Indoleamine 2,3-Dioxygenase and Its Therapeutic Inhibition in Cancer. In: Galluzzi LBTIR of C and MB, ed. Vol 336. Academic Press; 2018:175-203.
136. Omwoma S. New Synthetic Pathways for Thiocarbohydrazide and Salicylaldehyde Azine Compounds. *Asian J Chem Scinces*. 2017;3:1-8.
137. Sen AK, Singh RN, Handa RN, Dubey SN, Squattrito PJ. A structural comparison of some amine- and thione-substituted triazoles. *J Mol Struct*. 1998;470(1):61-69.
138. Mashayekhi V, Haj Mohammad Ebrahim Tehrani K, Amidi S, Kobarfard F. Synthesis of Novel Indole Hydrazone Derivatives and Evaluation of Their Antiplatelet Aggregation Activity. *Chem Pharm Bull*. 2013;61(2):144-150.
139. Pawar CD, Chavan SL, Pawar UD, Pansare DN, Deshmukh S V, Shinde DB. Synthesis, anti-proliferative activity, SAR, and kinase inhibition studies of thiazol-2-yl- substituted sulfonamide derivatives. *J Chinese Chem Soc*. 2019;66(3):257-264.
140. Yao J, Moellering R. Antibacterial Agents. In: Murray PR, Baron EJ, Jorgensen JH, Landry ML, Pfaller MA, eds. *Manual of Clinical Microbiology*.

Washington, DC: ASM Press; 2007:1077-1113.

141. Sari S, Tomek P, Leung E, Reynisson J. Discovery and Characterisation of Dual Inhibitors of Tryptophan 2,3-Dioxygenase (TDO2) and Indoleamine 2,3-Dioxygenase 1 (IDO1) Using Virtual Screening. *Molecules*. 2019;24(23).
142. Jangale A, Kumavat P, Wagh Y, Tayade Y, Mahulikar P, Dalal D. ChemInform Abstract: Green Process Development for the Synthesis of Aliphatic Symmetrical N,N'-Disubstituted Thiourea Derivatives in Aqueous Medium. *Synth Commun*. 2015;45.
143. Smičius R, Burbuliene MM, Jakubkiene V, Udrenaite E, Vainilavičius P. Convenient way to 5-substituted 4-amino-2,3-dihydro-4H-1,2,4-triazole-3-thiones. *J Heterocycl Chem*. 2007;44(2):279-284.
144. Fateev I V, Sasmakov SA, Abdurakhmanov JM. Synthesis of Substituted 1,2,4-Triazole-3-Thione Nucleosides Using E. coli Purine Nucleoside Phosphorylase. *Biomolecules*. 2024;14(7).
145. Meena R, Fahmi N, Kumari A, Meena P, Sharma N. Schiff Bases and Their Metal Complexes: Synthesis, Structural Characteristics and Applications. In: Akitsu T, ed. IntechOpen; 2023.
146. Linciano P, Gianquinto E, Montanari M, Maso L, Bellio P, Cebrián-Sastre E, Celenza G, Blázquez J, Cendron L, Spyraakis F, Tondi D. 4-Amino-1,2,4-triazole-3-thione as a Promising Scaffold for the Inhibition of Serine and Metallo- $\beta$ -Lactamases. *Pharmaceuticals (Basel)*. 2020;13(3).
147. A YUC, B HB, A YŞ. Synthesis of novel Schiff bases and azol- $\beta$ -lactam derivatives starting from morpholine and thiomorpholine and investigation of their antitubercular, antiurease activity, acetylcholinesterase inhibition effect and antioxidant capacity. *Bioorg Chem*. 2019;88(April):102928.

148. Srivastava K, Prakash R, Singh RB, Srivastava A, Vishnoi R kumar. SYNTHESIS, CHARACTERIZATION AND ANTIBACTERIAL EVALUATION OF NOVEL B- LACTAM AND THIAZOLIDIN-4-ONE DERIVATIVES HAVING THIADIAZINYL RING. *Bull Pharm Sci Assiut Univ.* 2023;46(1):203-216.
149. Tabbi A, Kaplancikli ZA, Tebbani D, Yurttas L, Cantürk Z, Atli Ö, Baysal M, Turan-Zitouni G. Synthesis of novel thiazolylpyrazoline derivatives and evaluation of their antimicrobial activities and cytotoxicities. *Turkish J Chem.* 2016;40(4):641-654.
150. Boraiei ATA, Sarhan AAM, Yousuf S, Barakat A. Synthesis of a New Series of Nitrogen/Sulfur Heterocycles by Linking Four Rings: Indole; 1,2,4-Triazole; Pyridazine; and Quinoxaline. *Molecules.* 2020;25(3).
151. Zgurskaya HI, Rybenkov V V. Permeability barriers of Gram-negative pathogens. *Ann N Y Acad Sci.* 2020;1459(1):5-18.

## الجزء الخامس

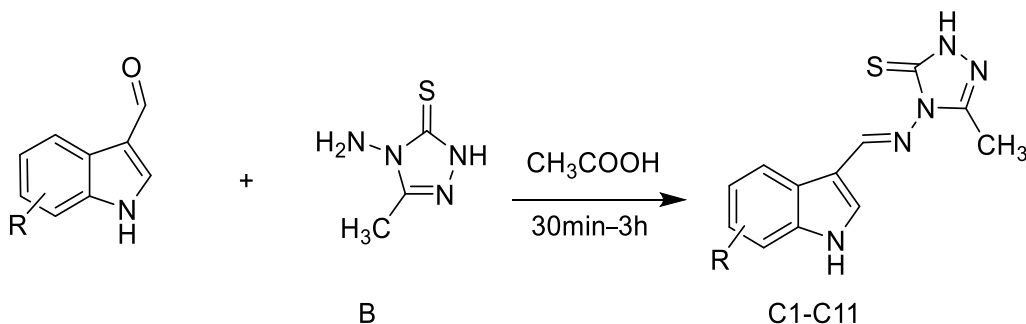
تم دراسة الالتحام الجزيئي (Molecular Docking) باستخدام برنامج PyRx والذي يعتمد على AutoDock vina كمحرك رئيسي لعمليات الالتحام ، وكذلك تم استخدام برنامج pymol لتحضير البروتين واطهار نتائج الالتحام.

هدفت هذه الدراسة الى تقييم قابلية ارتباط المركبات المحضرة بأنزيم تربتوفان-3و2-ديوكسيجيناز (TDO2) والذي يعد احد الانزيمات الرئيسية في مسار الكينورينين، ويتواجد بصورة اساسية في الكبد وكما يعد هذا الانزيم هدفا علاجيا مهما في علاج السرطان نظرا لدوره في تعزيز التهرب المناعي للخلايا السرطانية والمساهمة في تقدم المرض.

واظهرت نتائج الالتحام الجزيئي قيم ارتباط جيدة وتفاعلات قوية وكانت هذه النتائج متوافقة مع الفعالية البايولوجية للمركبات المدروسة.

### الجزء الثالث

يشمل هذا الجزء تحضير قواعد شيف جديدة من خلال تفاعل 4-أمينو-5-ميثيل-2,4-ديهيدرو-3H-1,2,4-تريازول-3-ثيون (B) مع اندول-3-كاربوكسيلديهايد المعوض بمجاميع معوضة مختلفة، وذلك تحت ظروف حامضية باستخدام حامض الخليك الثلجي كمذيب. وقد تم الحصول على نواتج بحصيلة جيدة تتراوح بين (48-98%) بفترة زمنية قصيرة وتم تأكيد التراكيب الكيميائية للمركبات المحضرة باستخدام تقنيات FTIR, <sup>1</sup>HNMR, <sup>13</sup>CNMR, .HRMS.



### الجزء الرابع

تم تقييم النشاط المضاد للمركبات المحضرة (C1-C11) ضد خلايا سرطان الكبد البشرية HepG2. اذ اظهرت النتائج هذه المركبات تمتلك فعالية ضعيفة مقارنة بالدواء القياسي المضاد للسرطان (doxorubicin)، الذي اظهر سمية خلوية عالية .

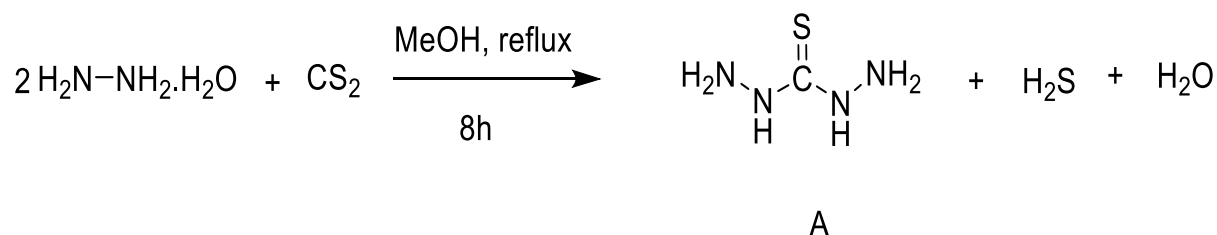
بالإضافة الى ذلك، تم اختبار النشاط المضاد للبكتريا باستخدام التركيز المثبط الأدنى (MIC) ضد بكتيريا *Staphylococcus aureus* و *Escherichia coli* و اظهرت النتائج ان هذه المركبات تمتلك نشاطاً ضعيفاً، حيث تراوحت قيم MIC بين (1000-2000)  $\mu$ M

## الخلاصة

تتضمن هذه الدراسة تحضير وتشخيص وتقييم الفعالية البايولوجية لمشتقات جديدة من الترايزول-3-ثايون الحاوية على الاندول. تنقسم هذه الدراسة الى خمسة اجراء كما هو موضع ادناه .

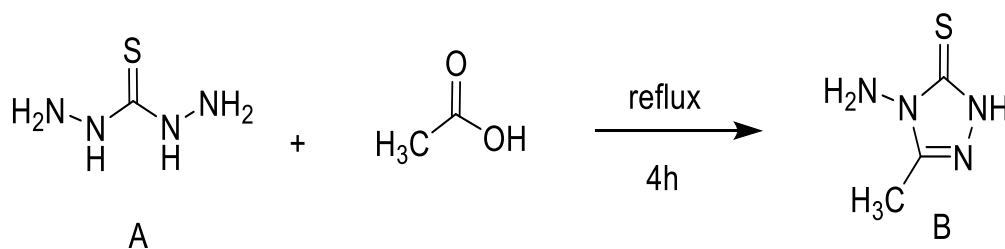
### الجزء الاول

يشمل هذا الجزء تحضير الثايوكاربوهيدراز ايد (A) من خلال تفاعل الهيدرازين هايدريت (80%) مع ثاني كبريتيد الكربون (CS<sub>2</sub>) بوجود الميثانول كمذيب وتحت ظروف الارتجاع. بعد ذلك، تم تنقية الناتج باستخدام اعادة البلورة وبحصيلة جيدة بلغت (83%)



### الجزء الثاني

يتضمن تخليق 4-أمينو-5-ميثيل-2,4-ديهيدرو-3H-1,2,4-تريازول-3-ثايون (B) من خلال تخليق الثايوكاربوهيدراز ايد (A) المحضرفي الجزء الاول، مع حامض الخليك الثلجي تحت ظروف الارتجاع. تم استخدام اعادة البلورة للتنقية وبحصيلة معتدلة بلغت (44)، تم تأكيد التركيب الكيميائي للمركب بواسطة تقنيات التحليل الطيفي FTIR, <sup>1</sup>HNMR, <sup>13</sup>CNMR



جامعة ميسان

كلية العلوم

قسم الكيمياء



## تحضير والارساء الجزئي وتقييم الفعالية البايولوجية لبعض الترايازولات الجديدة الحاوية على الاندول

الرسالة

مقدمة الى كلية العلوم / جامعة ميسان

لأستيفاء متطلبات الحصول على درجة الماجستير في علوم الكيمياء

من قبل

**زينب محمد خالد**

بكالوريوس علوم كيمياء / جامعة ميسان 2019

بأشراف

**أ.م.د أسامة علي محسن**

**2026**